NEW CHIRAL CATALYSTS FOR THE ASYMMETRIC MUKAIYAMA-TYPE ALDOL REACTION

by

ORIN TEMPKIN

BA, Chemistry
Columbia College, 1988

Submitted to the Department of Chemistry
in Partial Fulfillment of the Requirements for the Degree of

Doctor of Philosophy
in Organic Chemistry
at the

Massachusetts Institute of Technology

February 1994

Signature of Author _____
Department of Chemistry
January 18, 1994

Certified by _____
Professor Satoru Masamune
Thesis Advisor

Accepted by _____
Professor Glenn A. Berchtold, Chairman
Departmental Committee on Graduate Students

This doctoral thesis has been examined by a Committee of the Department of Chemistry as follows:

Professor Glenn A. Berchtold _____
Chairman

Professor Satoru Masamune _____
Thesis Supervisor

Professor Gregory C. Fu _____

NEW CHIRAL CATALYSTS FOR THE ASYMMETRIC MUKAIYAMA-TYPE ALDOL REACTION

by

ORIN TEMPKIN

Submitted to the Department of Chemistry on January 18, 1994 in partial fulfillment of the requirements for the Degree of Doctor of Philosophy in Chemistry.

ABSTRACT

The asymmetric Mukaiyama aldol reaction of aldehydes with silyl ketene acetals is promoted by the chiral borane complexes of α-amino acid arenesulfonamides such as *N*-tosyl-L-valine. The reaction proceeds efficiently in the presence of *catalytic* amounts (10–20 mole percent) of the chiral Lewis acid when the ligand is derived from an α,α-*disubstituted* amino acid. The best stereoselection is obtained with ligand **A**, prepared from the commercially available amino acid α-methyl-DOPA, and ligand **B**, synthesized from

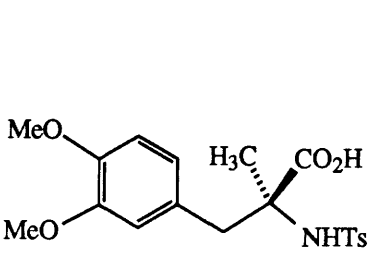

A

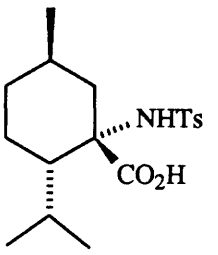

B

(–)-menthone in a sequence including a diastereoselective Bucherer–Bergs reaction. The stereochemistry of **B** was secured by an X-ray crystal structure. A survey of alkane- and arenesulfonyl groups for ligand **A** shows that *para*-substituted benzenesulfonamide derivatives offer the highest stereoselectivity in the Mukaiyama reaction; of these, the tosyl group provides the most consistent results. The borane complexes exhibit single broad peaks at +5–10 ppm in their proton-decoupled ^{11}B NMR spectra.

The chiral borane is formed by addition of BH_3·THF to the amino acid sulfonamide in propionitrile at 40–50 °C, and the catalytic aldol reaction is carried out at –78 °C. Slow addition of the aldehyde in propionitrile over 3–4 h to a mixture of the ketene acetal and the catalyst is essential for high enantioselection. The β-trimethylsiloxy esters initially obtained as major products are hydrolyzed to the corresponding β-hydroxy esters by treatment with dilute aqueous hydrochloric acid. The mechanism is interpreted in terms of a hypothetical catalytic cycle featuring a fast step (addition of the ketene acetal to the coordinated aldehyde) and a rate-limiting step (formation of the β-siloxy ester and regeneration of the catalyst).

In the presence of 20 mole percent of the chiral mediators derived from **A** and **B**, the Mukaiyama reaction of aldehydes with 1-trimethylsiloxy-1-ethoxy-2-methyl-1-propene provides β-hydroxy-α,α-dimethyl esters in high yields and with enantiomeric excesses (ee's) ranging from 84 to 96% for secondary aldehydes and >97% for primary aldehydes.

Under similar conditions, ketene acetals derived from phenyl acetate, *S*-ethyl ethanethioate, and *S*-*t*-butyl ethanethioate react with aldehydes to give β-hydroxy esters with 81–93% ee. Propionate-derived ketene acetals afford high yields of β-hydroxy-α-methyl esters enriched in the *anti* isomers, with *anti*:*syn* ratios of up to 94:6; these results represent the first example of the *anti* preference for the catalytic asymmetric Mukaiyama reaction. The enantiopurity of both diastereomers are high, the minor (*syn*) isomer especially being formed with high enantioselectivity (90–98% ee in eight examples). Ketene acetals derived from *O*-alkyl acetates and propionates generally provide lower enantioselection. For both ligands **A** and **B**, the sense of asymmetric induction in aldol reactions corresponds to *si*-face attack of the aldehyde.

In the presence of 20 mole percent of the chiral borane complex of **B** (or its *p*-nitrobenzenesulfonamide analogue) in *nitroethane* at –78 °C, the asymmetric Mukaiyama reaction of aldehydes with silyl enol ethers derived from methyl ketones affords β-hydroxy ketones in high yields and with 60 to 85% ee. In contrast to the reactions with ketene acetals, slow addition of the aldehyde is not essential for high enantioselectivity.

The chiral boranes derived from **A** and **B** (10–20 mole percent) catalyze the asymmetric Diels–Alder reaction of methacrolein and cyclopentadiene, giving the (*R*)-isomer of the *exo* cycloadduct (98:2 diastereoselectivity) in high yield and with a maximum of 76% ee (ligand **B**, THF, –78 °C). The catalysts do not, however, induce useful levels of asymmetry in allylation, imine addition, or Mukaiyama–Michael reactions.

The new results throughout compare favorably with recent literature reports from other groups, notably Mukaiyama's asymmetric Sn(II)-promoted and -catalyzed aldol reactions, Yamamoto's CAB-catalyzed Diels–Alder and aldol reactions, and Corey's oxazaborolidine-catalyzed reactions.

Thesis Supervisor: Dr. Satoru Masamune

Title: Arthur C. Cope Professor of Chemistry

Acknowledgments

I would first like to thank Professor Satoru Masamune for the privilege of working in his laboratories. I highly esteem the integrity of his approach to scientific problems, the unwaveringly high standards he maintains for research, and the breadth of his expertise. I have enjoyed working on a number of research projects—some successful and some not, but all challenging—under his supervision.

I am grateful to the Merck Manufacturing Division (MMD) for a fellowship including four years of generous support and a postdoctoral appointment. I particularly thank Dr. George Wildman of MMD for his confidence in me and for getting my career off to a promising start.

Thanks are also due to the MIT Department of Chemistry for teaching and research assistantships.

I have had the good fortune to work alongside several talented chemists, and some of their work is included in this thesis. Dr. Emma Parmee has been a superb collaborator and friend. It is a pleasure to acknowledge her contributions to the catalytic aldol project, which include synthesizing for the first time the ligands derived from 2-amino-2-phenylpropionic acid and α-methyl-DOPA, developing the slow addition procedure, performing several of the aldol reactions in Chapters Two and Three, and doing some of the work on boron derivatives and allylation reactions in Chapter Five. I am also grateful to Emma for proofreading this thesis. I admire the seemingly limitless enthusiasm and talent of Dr. Yaping Hong, who contributed to the propionate aldol reactions in Chapter Three and the assignment of absolute configurations. Dr. Atsushi Abiko performed portions of the exploratory work on the project and carried out the initial synthesis of the

ligand derived from menthone; Dr. Hironao Sajiki obtained some of the early results on ketone aldols in Chapter Four. Additional specific contributions are acknowledged in the text and references.

I also thank Dr. Scott Batcheller and Dr. Takeshi Tsumuraya for their assistance on the Group 14 organometallics project. Scott taught me a lot about air-sensitive techniques and kinetics experiments, and also increased my appreciation of the chemistry.

I am grateful to Ms. Janet MacLaughlin for keeping the details of our research group, financial and otherwise, in good order.

I thank Professors Dan Kemp, Rick Danheiser, and Barry Sharpless, and Ms. Melinda Cerny for a memorable year as a teaching assistant for 5.12 and 5.13 (1988–89).

I also thank Professor Thomas Katz of Columbia University for welcoming me into his laboratory and encouraging me to go to graduate school. Thanks also to Professor Leonard Fine for allowing me to teach as an undergraduate and for arranging a summer job at Cyanamid.

Special thanks to Dr. Ken Barr, who has been a great friend from the very beginning. It was particularly fun TA'ing, writing the Chemistry Department Christmas Shows, and teaching a course in organic chemistry for high school students with Ken.

Over the last few years, I have enjoyed many a movie and concert with Pam England, a good friend and an outstanding scientist. I appreciate her honesty and integrity.

I have had many baymates during my time in the Masamune group, but the best one was Dr. Craig Zimmerman. It was great fun talking about chemistry, music, movies and Howard Stern.

Graduate school was difficult, but going through the flames alongside fellow classmates and Masamune group members Sandy Filla (almost Dr.!) and Dr. Sam Gerritz made it a lot easier. They both have fine senses of humor.

A curtain call and a round of applause go to my friends in the Shakespeare Ensemble at MIT. My work with the Ensemble was an excellent balance to everything

else, and my life at MIT would have suffered without it—the good memories are plentiful. I would especially like to thank Kermit Dunkelberg and Kim Mancuso for the experience.

I would also like to thank Chris Crowley, Natalya Eliashberg, Michael Fenter, Andrea Leszek, Jonathan Nash, Brian Rought, Debbie Wells, and Ryun Yu. Finally, I thank my parents, Florence and Gerald Tempkin, and my brother, Adam Tempkin, for their encouragement and moral support.

To my teachers

HORAM EXPECTA VENIET

--inscription, Columbia University sundial

In youth my wings were strong and tireless,
But I did not know the mountains.
In age I knew the mountains
But my weary wings could not follow my vision—
Genius is wisdom and youth.

--Edgar Lee Masters,
Spoon River Anthology

Ain't it fun

--Stiv Bators

Table of Contents

New Chiral Catalysts for the Asymmetric Mukaiyama-type Aldol Reaction

Chapter One

The Mukaiyama-type Aldol Reaction

1.1 Introduction

From the time of its discovery in the mid-nineteenth century[1], the aldol reaction has occupied a prominent position among the techniques available to the organic chemist for the formation of carbon-carbon single bonds. The chemical literature[2] of the late 1970s

Figure 1.1 Chiral Boron and Titanium Enolates

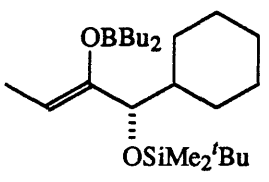

1-1
Masamune, 1981[3]

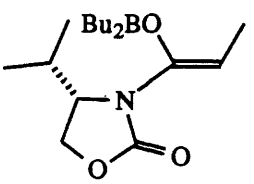

1-2
Evans, 1981[4]

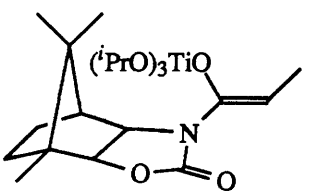

1-3
Thornton, 1991[5]

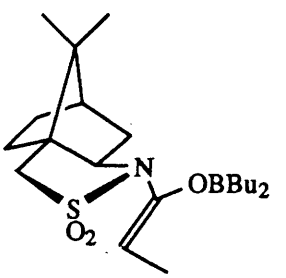

1-4
Oppolzer, 1990[6]

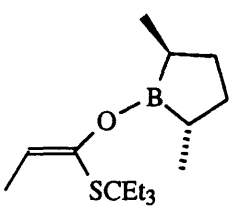

1-5
Masamune, 1986[7]

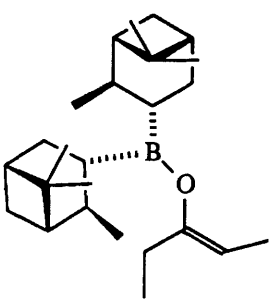

1-6
Paterson, 1987[8]

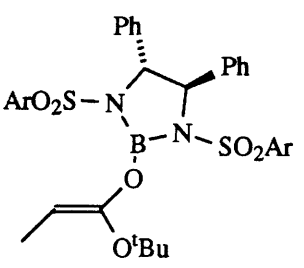

1-7
Corey, 1990[9]
Ar= 3,5-bis(trifluoro-methyl)phenyl

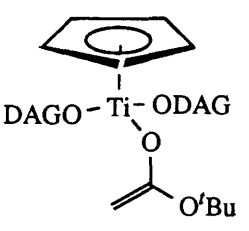

1-8
Duthaler, 1989[10]
DAGOH= diacetoneglucose

revealed a resurgence of interest in the aldol reaction, particularly in the context of the stereoselective synthesis of β-hydroxycarbonyl and β-hydroxy-α-methylcarbonyl units, structural fragments commonly embedded in polyketide-type natural products such as macrolides and polyether antibiotics. Several research groups including that of Masamune dedicated their efforts to the development of asymmetric aldol and allylation reactions as

Scheme 1.1 Examples of Asymmetric Aldol Reactions

I. "Internal" Chiral Reagent

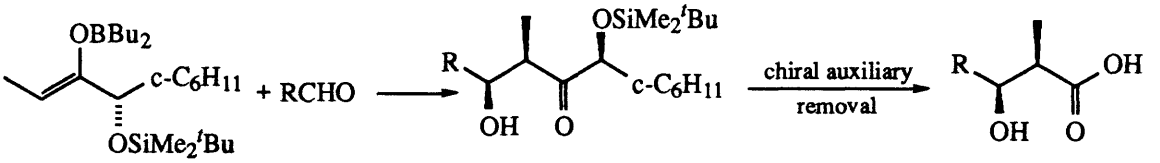

chiral boron enolate

II. "External" Chiral Reagent

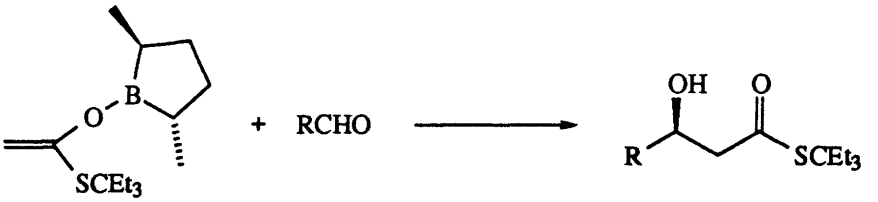

chiral boron enolate

III. Lewis Acid-Catalyzed Mukaiyama Aldol Reaction

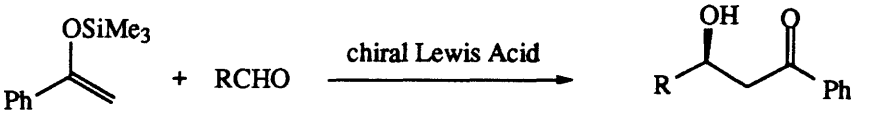

achiral silyl enol ether

approaches to the general problems of acyclic stereoselection and fragment coupling in natural product synthesis, and in the 1980s new reagents for diastereoselective and enantioselective nucleophilic addition to carbonyl groups began to appear[11]. Some of the noteworthy reagents designed for asymmetric aldol reactions are shown in Figure 1.1. These chiral enolates, derived from esters of acetic and propionic acid as well as from ketones, exhibit high facial selectivities in their reactions with aldehydes. The enolates may

be divided into two broad classes, that of "internal" chiral reagents[12] (**1-1–1-4**) and "external" chiral reagents[12] (**1-5–1-8**), providing aldol products that respectively contain or do not contain the chiral moiety of the reagent in addition to newly formed stereogenic centers (Scheme 1.1, Cases I and II). The "external" reagents are advantageous as they directly give the desired aldol products without need of a second step for removal of the chiral auxiliary.

Acyclic stereoselection continues to capture the attention of workers in the field of asymmetric synthesis. In 1989 we began to examine the asymmetric Mukaiyama-type aldol reaction of achiral aldehydes and silyl enolates as an alternative route to optically active β-hydroxy ketones and esters (Scheme 1.1, Case III). Catalysis of this reaction by a chiral Lewis acid would represent a significant advance over the existing reagent-based methodology, and our progress towards the development of this process is the subject of this thesis. Before undertaking a detailed discussion of new results, an introduction to earlier work on the Mukaiyama reaction is in order and occupies the rest of this chapter.

1.2 The Mukaiyama Aldol Reaction: General Features

The discovery of the Lewis acid-mediated reaction of trialkylsilyl enolates with aldehydes by Mukaiyama[13] in 1973 is a milestone in the evolution of the directed aldol reaction (Scheme 1.2). Silyl enol ethers, or silyl enolates derived from ketones, are

Scheme 1.2 General Mukaiyama-type Aldol Reaction

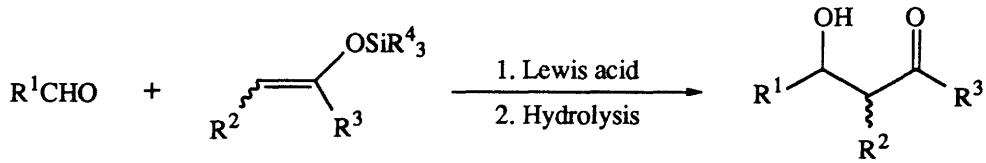

generally not sufficiently nucleophilic to undergo addition to unactivated aldehydes[14]; in this important respect they differ from lithium, boron, and titanium enolates[2]. However, Mukaiyama and co-workers found that in the presence of a Lewis acid, the aldol reaction

giving β-hydroxy ketones proceeded cleanly, regiospecifically, and in high yield at -78 °C in methylene chloride. The best yields were achieved using titanium tetrachloride ($TiCl_4$) as the Lewis acid, but other metal salts such as tin(IV) chloride ($SnCl_4$), aluminum chloride ($AlCl_3$), and boron trifluoride etherate ($BF_3{\cdot}OEt_2$) promoted the reaction effectively. Mukaiyama also investigated the performance of substoichiometric quantities of promoter and found that as little as 0.13 equivalent of $TiCl_4$, relative to aldehyde (1 equivalent), was sufficient to drive the reaction in only slightly (ca. 10%) lower yield than the stoichiometric case. Although this result merited only a few sentences in the original report, it laid the groundwork for future catalytic modifications of the reaction.

Silyl enolates derived from esters, thioesters, ketones, and aldehydes are all viable

Figure 1.2 Typical Silyl Ketene Acetals and Silyl Enol Ethers

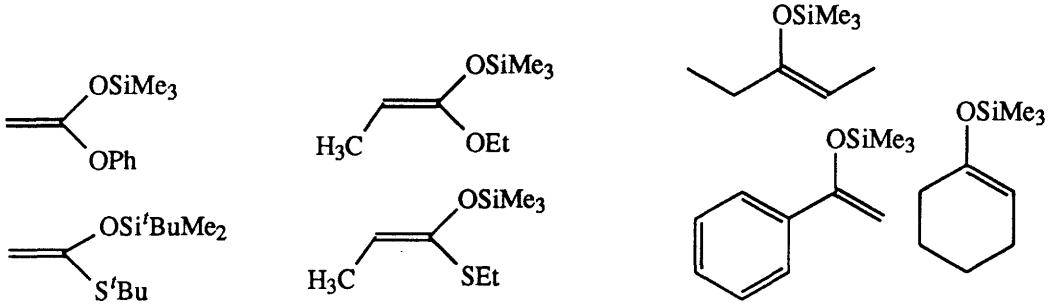

Ketene acetals derived from acetates.

Ketene acetals derived from propionates.

Silyl enol ethers derived from ethyl, methyl, and cyclic ketones.

nucleophiles in the Mukaiyama aldol reaction (Figure 1.2). In the first two cases, the enolates are termed silyl ketene acetals, and their Lewis acid-mediated reaction with aldehydes to give β-hydroxy esters[15] provides a mild alternative to the Reformatsky reaction (Scheme 1.3). The concurrent development of methods for the regio- and stereoselective synthesis of silyl enol ethers and ketene acetals has resulted in numerous applications of the Mukaiyama reaction to the synthesis of natural products.[16] The most common method for the synthesis of these isolable and stable enolate equivalents is the

trapping of lithium enolates, generated under conditions of either kinetic or thermodynamic

Scheme 1.3 Aldol Reaction of a Silyl Ketene Acetal

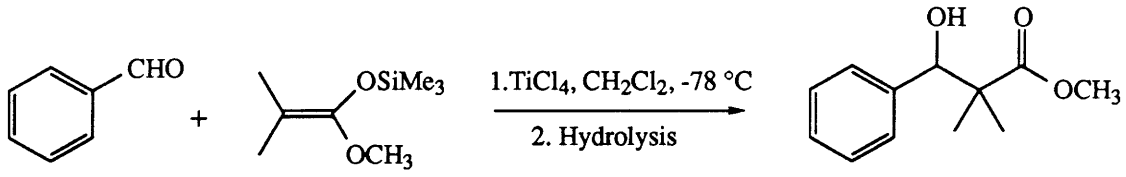

control, with a trialkylsilyl chloride.[17] For example, either regioisomer of the trimethylsilyl enol ether derived from 2-methylcyclohexanone is accessible (Scheme 1.4).[17c] Coupling of the two unique silyl enol ethers shown below with benzaldehyde gives rise to structurally isomeric β-hydroxy ketones. The importance of regioselectivity in the synthesis of silyl enol ethers derived from unsymmetrically substituted ketones is obvious,

Scheme 1.4 Synthesis of Silyl Enol Ethers from Unsymmetrical Ketones

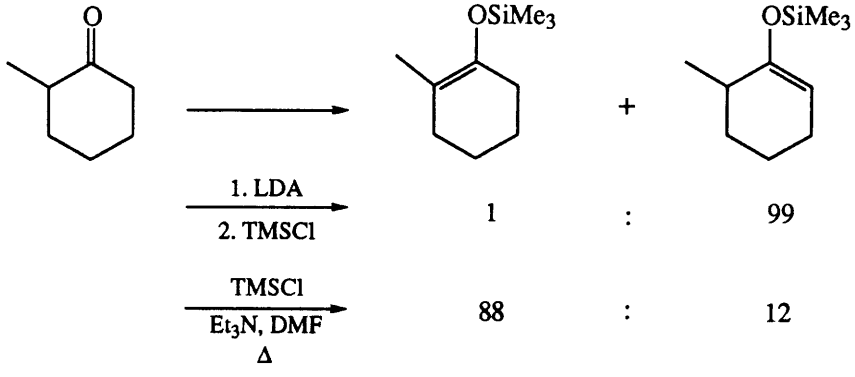

and a variety of satisfactory methods, such as the 1,4-hydrosilylation of α,β-unsaturated ketones[18] and the use of hindered lithium dialkylamide bases[19], have been developed for this purpose.

1.3 Mechanism

Although the mechanism of the Mukaiyama reaction is by no means definitively established, two mechanistic alternatives are usually considered.[13,20] In the first (mechanism A, Scheme 1.5), the aldehyde is activated toward nucleophilic attack by

coordination to the Lewis acid, followed by addition of the silyl enol ether, giving intermediate **1-9**. The formation of a complex between a Lewis acid and a carbonyl group is a fundamental process in organic chemistry[21], and it has been known for some time that such an interaction increases the electrophilic reactivity of the carbonyl carbon; in recent years, complexes between aldehydes and Lewis acids such as $TiCl_4$, $BF_3{\cdot}OEt_2$, and

Scheme 1.5 Proposed Mechanism A: Aldehyde Activation

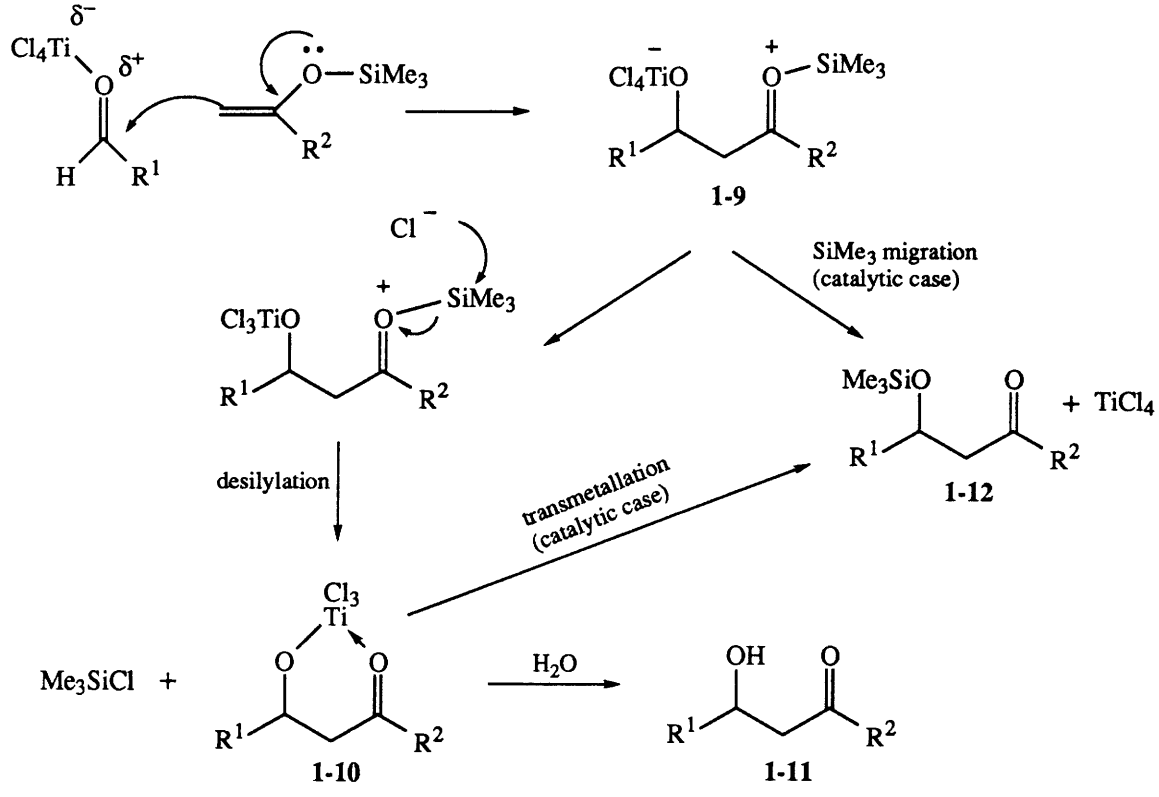

$SnCl_4$ have been isolated and characterized by X-ray crystallography and NMR spectroscopy.[21] Attack of a chloride ion on silicon in **1-9** gives trimethylsilyl chloride (TMSCl), and the aldol product is intercepted as its trichlorotitanium salt, or titanium aldolate **1-10**. The formation of a six-membered titanium chelate intermediate presumably inhibits a retro-aldol pathway.[13] Hydrolysis of the reaction mixture at this point would furnish the desired free hydroxy ketone **1-11**. In the case of a catalytic reaction, the intermediate **1-10** would undergo transmetallation with TMSCl to give the silyl ether **1-12** of the hydroxy ketone and the regenerated Lewis acid catalyst; another possibility for

catalytic turnover is intramolecular silyl migration in **1-9**. The silyl ether **1-12** is isolable and may be converted to **1-11** upon mild acid hydrolysis.

A second mechanistic extreme for the Mukaiyama reaction involves activation of the silyl enol ether by formation of a titanium enolate, **1-13**, and TMSCl (Scheme 1.6).[20] This new enolate would react with an aldehyde to provide the intermediate titanium aldolate (**1-10**) described above, and as before, a catalytic variant is possible. Accumulated

Scheme 1.6 Proposed Mechanism B: Silyl Enolate Activation

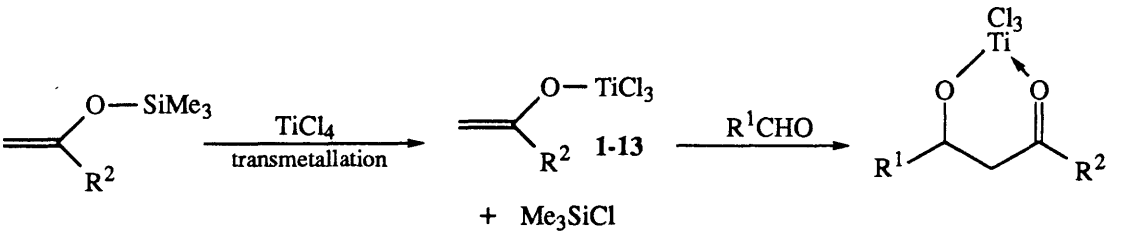

evidence suggests that, at least in the case of TiCl4, the reaction proceeds by the first mechanism involving Lewis acid activation of the aldehyde, *not* by formation of a titanium enolate.[20] For example, Nakamura and Kuwajima[22] showed that aldol reactions of authentic trichlorotitanium enolates gave a different stereochemical outcome from the TiCl4-mediated reaction of silyl enol ethers.

1.4 Stereochemistry

This section explores some of the stereochemical nuances of the Mukaiyama reaction, beginning with a note on terminology. The two possible stereoisomers of a silyl

Scheme 1.7 Silyl Enolate Stereochemistry

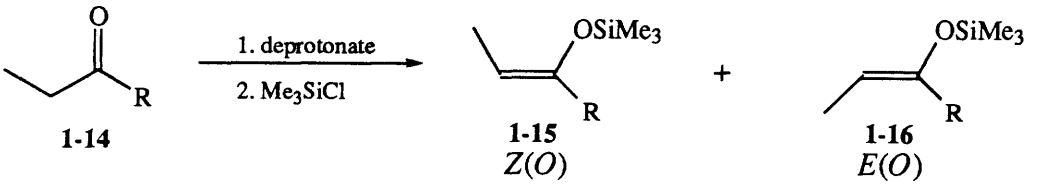

enolate derived from the deprotonation and *O*-silylation of a carbonyl compound, for example, **1-15** and **-16** from **1-14**, are given the descriptors *Z*(*O*) and *E*(*O*) as shown in Scheme 1.7.[11,23] The -OSiMe3 substituent on C(1) always takes the higher priority regardless of R: for example, the two compounds shown below would have opposite assignments under the conventional *E*/*Z* nomenclature due to a change in sequence rule priority with sulfur. The newer system places both structures in the *E*(*O*) category and

E, or *E*(*O*) *Z*, or *E*(*O*)

establishes their stereochemical relationship unambiguously. Silyl enol ethers or ketene acetals enriched in either the *E*(*O*) or *Z*(*O*) isomers may be prepared under various reaction conditions (Scheme 1.8).[17]

Scheme 1.8 Synthesis of *Z*(*O*)- and *E*(*O*)-enriched Silyl Enolates

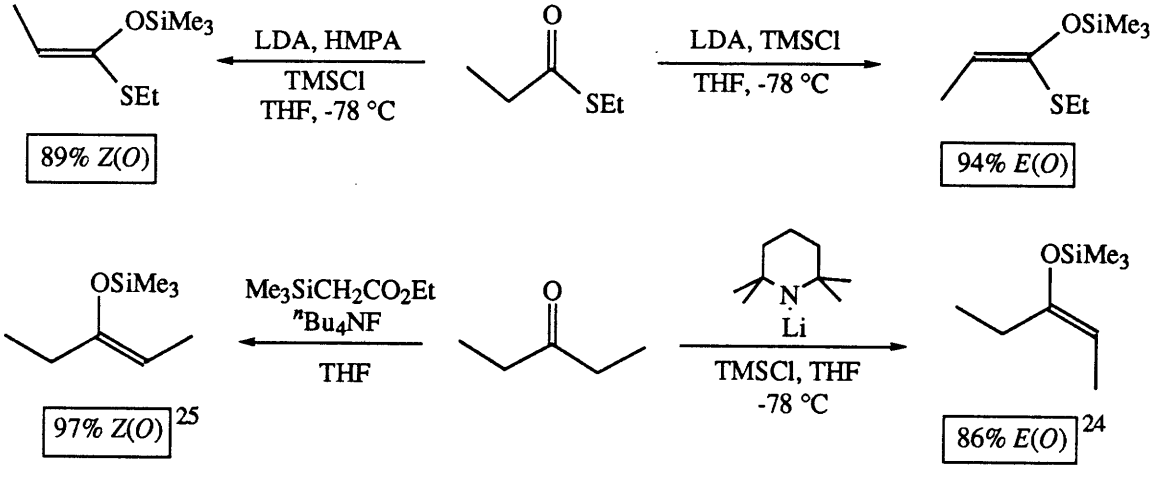

The aldol reaction of a prochiral silyl enolate with a prochiral aldehyde furnishes a pair of racemic diastereomers, and the terms *syn* and *anti* are used to express the relative stereochemistry of the substituents on the aldol products in accord with the convention introduced by Masamune (Scheme 1.9).[23] These replace the older corresponding terms

erythro and *threo* which have their origins in carbohydrate chemistry and are confusing in the present context.

Scheme 1.9 *Syn* and *Anti* Aldol Diastereomers

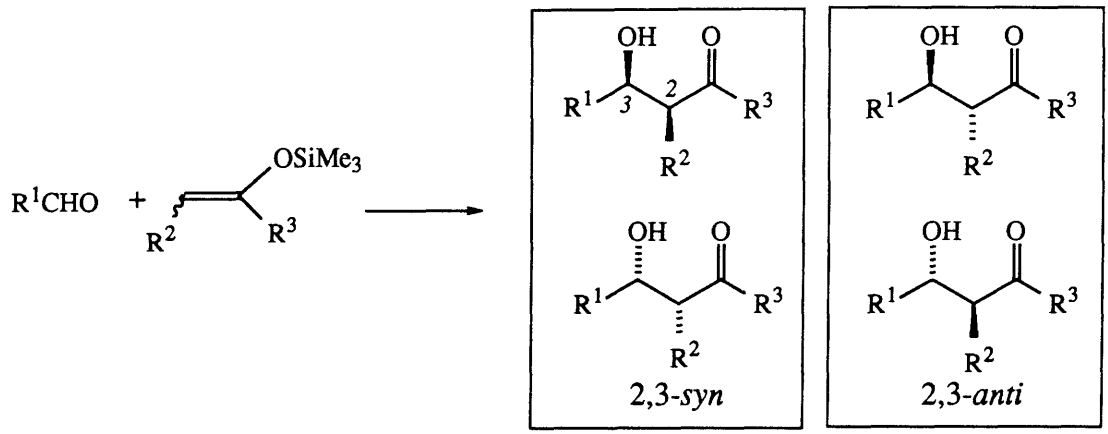

The reactions of silyl enol ethers or ketene acetals with aldehydes generally proceed with low levels of simple diastereoselection in the presence of a stoichiometric amount of a Lewis acid such as $TiCl_4$, $BF_3{\cdot}OEt_2$, or $SnCl_4$.[20,24] The *anti/syn* ratios typically range from 25/75 to 80/20 depending on the specific silyl enolate, aldehyde and Lewis acid.[20] Diastereoselectivities in excess of 90/10, frequently favoring the *anti* isomers, are obtainable in some cases with selected substrates and carefully chosen reaction conditions; these examples have been comprehensively reviewed.[2,20] Many new mediators and catalysts for the Mukaiyama reaction continue to be reported, each exhibiting distinctive stereoselectivity. These reagents range from the ordinary to the exotic and include trityl salts[26], cationic zirconium complexes[27], lanthanide triflates[28], bismuth trichloride[29], and clay montmorillonites[30].

Diastereoselection in the Mukaiyama aldol reaction is frequently interpreted in terms of "open" or acyclic extended transition state structures[20,31] in which no intimate contact exists between the Lewis acid and the silyl enolate, a model that provides the best rationale for a large body of stereochemical results (Figure 1.3). The acyclic transition state is sharply distinguished from the six-membered, chelated, Zimmerman–Traxler-type "closed" transition state which governs the stereochemical course of directed aldol reactions

involving Group I, II, and III metal enolates.[2,11] For aldol processes proceeding via this pericyclic mechanism, the kinetic stereoselection is generally related to the enolate geometry, with *E(O)* enolates giving *anti* aldols and *Z(O)* enolates giving *syn* aldols predominantly. This paradigm does not typically apply to the reactions of silyl enol ethers.

Figure 1.3 Acyclic Extended vs. Cyclic Transition State Structures

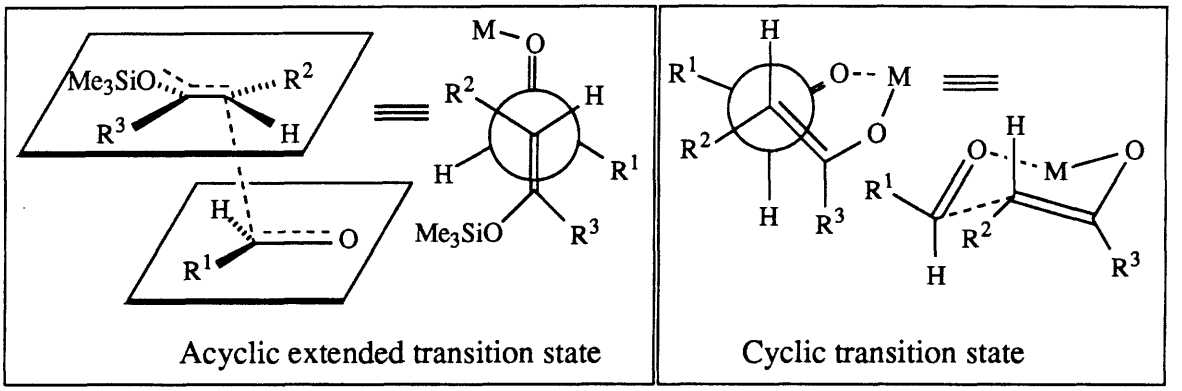

Acyclic transition states are also invoked in the fluoride ion-catalyzed reactions of silyl enol ethers and aldehydes studied by Kuwajima, Nakamura and Noyori[22,32], as well as the related reaction of silyl enol ethers with acetals catalyzed by trimethylsilyl triflate (TMSOTf), investigated by Noyori.[31] In contrast to the *anti*-selective aldol reactions described earlier, these reactions exhibit moderate to excellent *syn* selectivity; moreover, this preference is observed *regardless of the geometry—E(O) or Z(O)—of the silyl enol ether*. The stereoconvergent behavior is explained as follows (Scheme 1.10): in the reaction of either the *E(O)* or the *Z(O)* silyl enol ether and an aldehyde, the *anti* transition states are disfavored because of nonbonded gauche interactions between R^1 and R^2.[31] Note that in this model, (1) the two oxygen atoms are given maximum separation, and (2) the R^1/R^2 interaction determines the diastereoselectivity, but the outcome would be expected to change if the R^1/R^3 interaction (for the *Z(O)* isomer in the *syn* transition state), the R^2/M interaction (for either *syn* transition state), or the R^1/-OSiMe3 interaction (for the *E(O)* isomer in the *syn* transition state) becomes more significant.[20]

Scheme 1.10 Rationale for Stereoconvergent Aldol Reactions

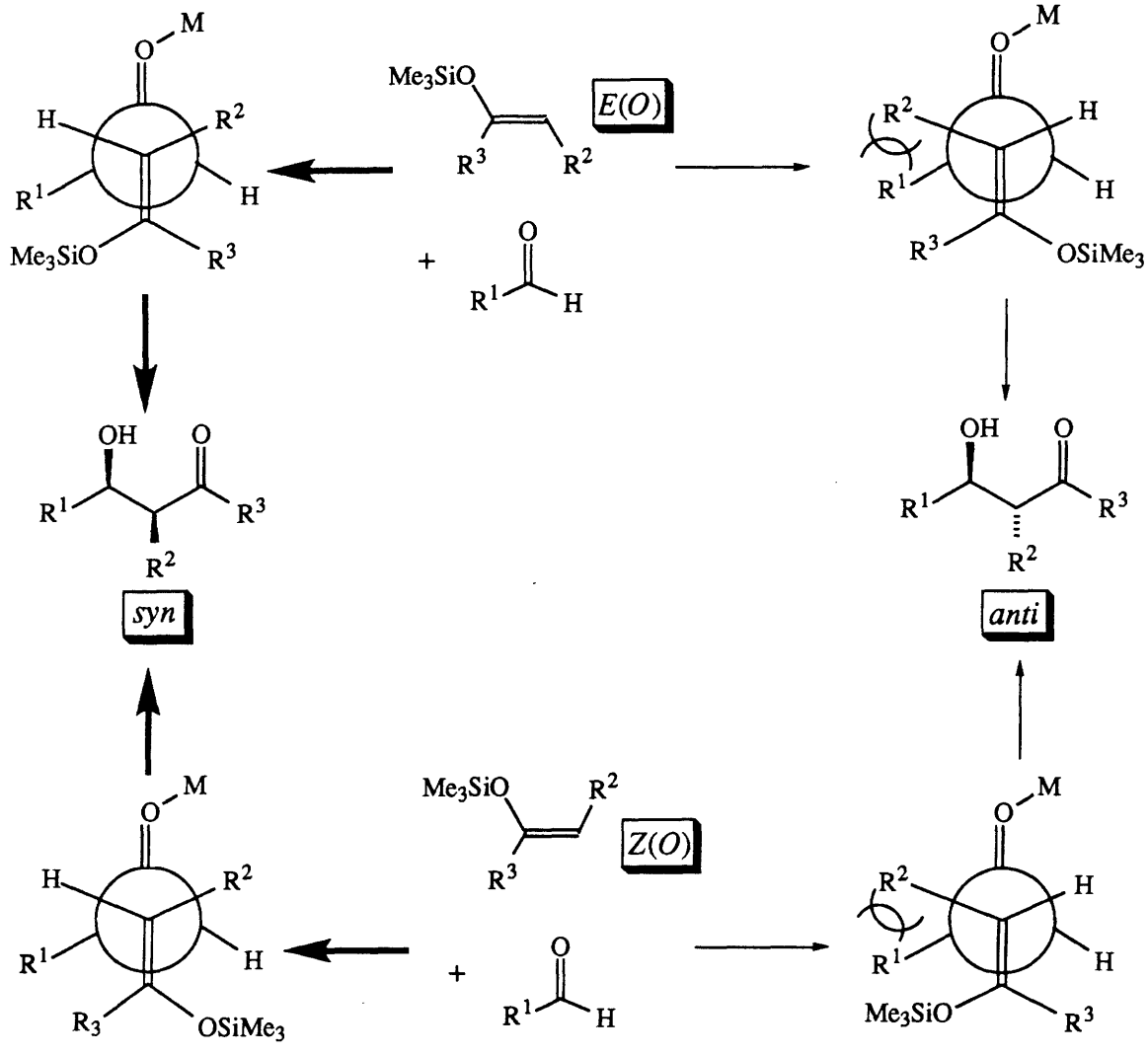

1.5 Asymmetric Mukaiyama Aldol Reactions

In the mid-1980s, several groups reported asymmetric versions of the Mukaiyama reaction.[20] The first approaches involved chiral aldehydes or chiral silyl enol ethers (ketene acetals), or a combination of the two (double asymmetric synthesis). Three ketene acetals that function as chiral templates in substrate-controlled, TiCl4-mediated aldol reactions are shown in Figure 1.4. These "internal"[12] chiral reagents, derived from ephedrine and camphor, gave aldol products with high enantio- and diastereoselectivities but the attachment and removal of the chiral auxiliaries was an obvious drawback to synthetic efficiency.

Figure 1.4 Chiral Ketene Acetals

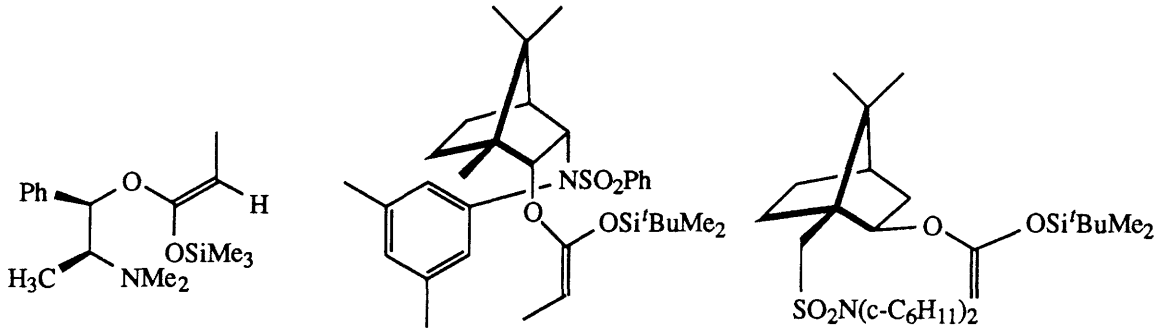

Gennari, 1985[33] Helmchen, 1985[34] Oppolzer, 1986[35]

A more powerful approach was the introduction of a *chiral Lewis acid* as an "external"[12] promoter for the asymmetric aldol reaction of achiral silyl enol ethers (ketene acetals) and achiral aldehydes. The first broadly applicable chiral Lewis acid for this purpose came from the work of Mukaiyama and Kobayashi[36]: in the presence of a chiral

Table 1.1 Tin(II) Triflate-Promoted Asymmetric Aldol Reactions of Acetate-Derived Ketene Acetals (Selected Results)[36a]

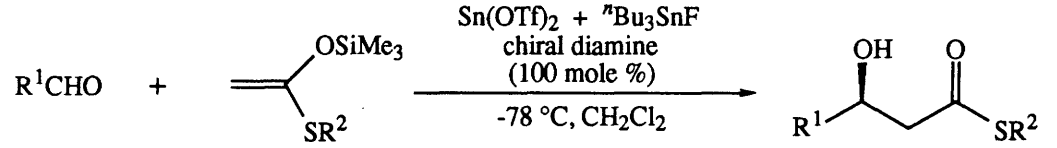

R^1	R^2	Chiral Diamine	Yield/ %	ee/ % (config.)
Ph	Et	A	52	92 (*S*)
Ph	Et	B	78	82 (*S*)
Ph	^{t}Bu	B	73	86 (*S*)
$PhCH_2CH_2$	^{t}Bu	B	71	85
$PhCH_2CH_2$	Et	A	50	81
^{t}Bu	Et	B	90	>98

A= 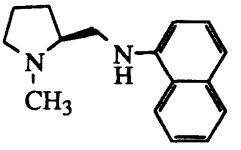

B= 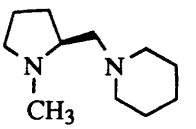

promoter triad consisting of tin(II) triflate, a proline-derived chiral diamine, and tributyltin fluoride (or dibutyltin diacetate), the trimethylsilyl ketene acetals of *S*-alkyl ethanethioates and propanethioates reacted with aldehydes in methylene chloride at -78 °C to give β-hydroxy thioesters in good yields and with high enantioselectivities and *syn* diastereoselectivities (Tables 1.1 and 1.2). The product thioesters are amenable to further synthetic transformation and are thus attractive intermediates.

Table 1.2 Tin(II) Triflate-Promoted Asymmetric Aldol Reactions of Propionate-Derived Ketene Acetals (Selected Results)[36a]

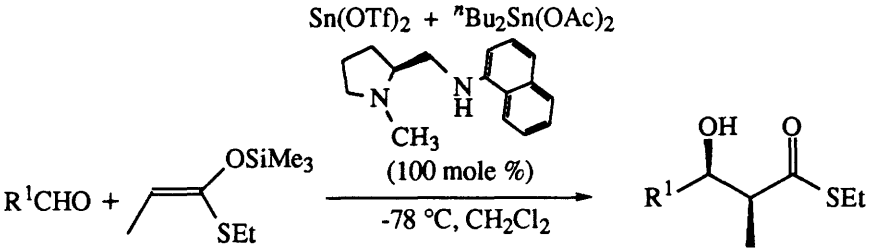

R^1	Yield /%	*syn* : *anti*	ee/ %
Ph	85	100 : 0	>98
$CH_3(CH_2)_6$	90	100 : 0	>98
c-C_6H_{11}	90	100 : 0	>98
^{i}Pr	70	100 : 0	>98
(*E*)-PhCH=CH	91	100 : 0	>98
2-furyl	92	100 : 0	>98

In some previously reported asymmetric aldol reactions with acetate-derived metal enolates, the enantioselectivities have been low.[37] This new reaction provided the adducts of acetic acid derivatives (in the form of ethanethioate ketene acetals) and aldehydes with high enantiomeric excesses (Table 1.1). The chiral promoter also gave spectacular results in the reaction of achiral *E*(*O*) propanethioate ketene acetals with aldehydes (Table 1.2), furnishing β-hydroxy-α-methyl esters with near-perfect enantioselection and *syn* diastereoselection (*syn/anti*= 100:0, *syn* aldol >98% ee). The reaction worked well with aromatic, α,β-unsaturated, straight-chain, and branched aldehydes.

The putative transition state[36] shown in Figure 1.5, in which coordination of the chiral diamine to tin(II) triflate produces a rigid asymmetric environment, provides a

Figure 1.5 Proposed Transition State for the Tin(II)-Promoted Aldol Reaction

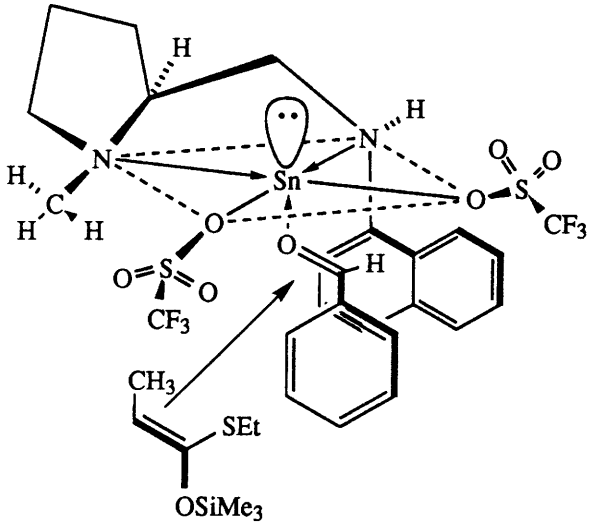

plausible explanation of the source of the enantioselectivity. The conformation of this complex is controlled by an interplay of the pyrrolidyl, naphthylamino, and triflate substituents. The aldehyde coordinates to a vacant site on tin(II), and in the resulting five-coordinate complex, the *re*-face of the aldehyde is well shielded from nucleophilic attack. This sense of asymmetric induction is consistent in the reported reactions.

Proton and tin nuclear magnetic resonance studies of the chiral promoter pointed to a mechanism involving activation of the aldehyde carbonyl group by the Lewis acid, and not tin enolate formation.[36a] The observation that a mixture of tin(II) triflate, chiral diamine, and tributyltin fluoride or dibutyltin diacetate was completely soluble in dichloromethane, whereas the tin(II) and tin(IV) compounds alone were only sparingly soluble, suggested to Mukaiyama the formation of a ternary complex such as **1-17** or **1-18** which acted as the Lewis acid. The peaks in the ^{119}Sn NMR spectrum corresponding to the Sn(II) and Sn(IV) nuclei in the complex were distinct from those of the individual compounds. The authors hypothesized a "double activation" mechanism in which the diamine-coordinated tin(II) triflate activates an aldehyde toward nucleophilic attack, and

simultaneously, the electronegative fluoride or acetate group on tin(IV) activates the ketene acetal by interaction with the silicon atom.[36a] The inclusion of one full equivalent of the tin(IV) compound was also essential for high enantioselectivity, but the reasons for this were not elucidated.

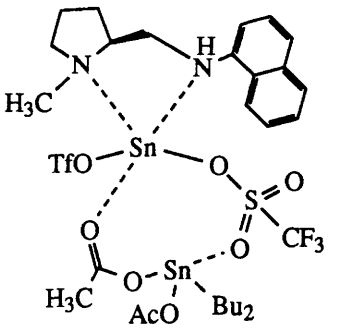

1-17

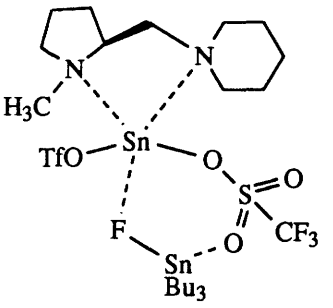

1-18

1.6 Catalytic Asymmetric Mukaiyama Aldol Reactions

Very recently a *catalytic* version of the tin(II) triflate system was introduced by the same workers.[38] The reaction conditions described above were modified as follows: (1) the aldehyde and ketene acetal (1 equivalent of each) were added slowly (over 3–4.5 h) to a solution of preformed diamine/tin(II)triflate complex (*0.2 equivalent*), (2) propionitrile was used as the solvent instead of methylene chloride, and (3) the tin(IV) compound was omitted. The results were not as uniformly excellent as in the case of the chiral promoter, but the stereoselectivities and yields were still very high (Table 1.3).

The catalytic reaction probably proceeds via the cycle shown in Scheme 1.11.[38] After reaction of the ketene acetal with the Lewis acid-activated aldehyde, transmetallation between tin(II) and TMSOTf must then follow for regeneration of the catalyst. The latter key step is likely rate limiting, and if the exchange does not proceed efficiently, the TMSOTf that accumulates will catalyze the aldol reaction without enantioselectivity. This problem is circumvented by two of the devices enumerated above: slow addition of the aldehyde and ketene acetal results in a low concentration of TMSOTf, and the more polar solvent propionitrile likely accelerates the transmetallation/turnover step. TMSOTf is

essentially consumed by transmetallation as it is formed, and the aldol product is obtained as its trimethylsilyl ether with high enantioselectivity.

Table 1.3 Tin(II)-Catalyzed Asymmetric Aldol Reaction (Selected Results)[38]

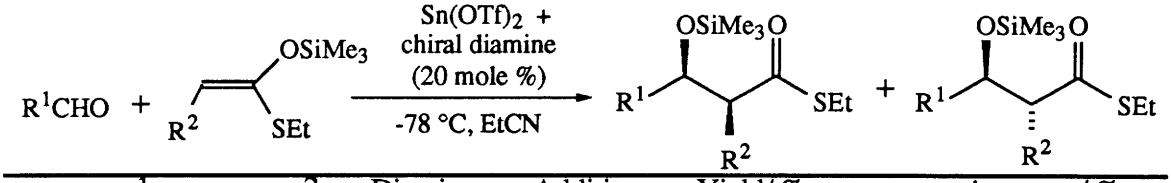

R^1	R^2	Diamine	Addition Time/ h	Yield/ %	*syn* : *anti*	ee/ %
$CH_3(CH_2)_6$	H	A	6	79	-	91
c-C_6H_{11}	H	A	4.5	81	-	92
Ph	CH_3	B	3	77	93:7	90
(*E*)-CH_3CH=CH	CH_3	B	3	76	96:4	93
$CH_3(CH_2)_6$	CH_3	B	4.5	80	100:0	>98
c-C_6H_{11}	CH_3	B	3	71	100:0	>98

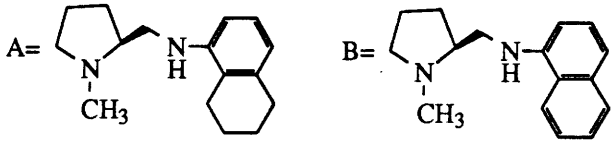

Scheme 1.11 Reaction Cycle for the Tin(II)-Catalyzed Asymmetric Aldol Reaction[38]

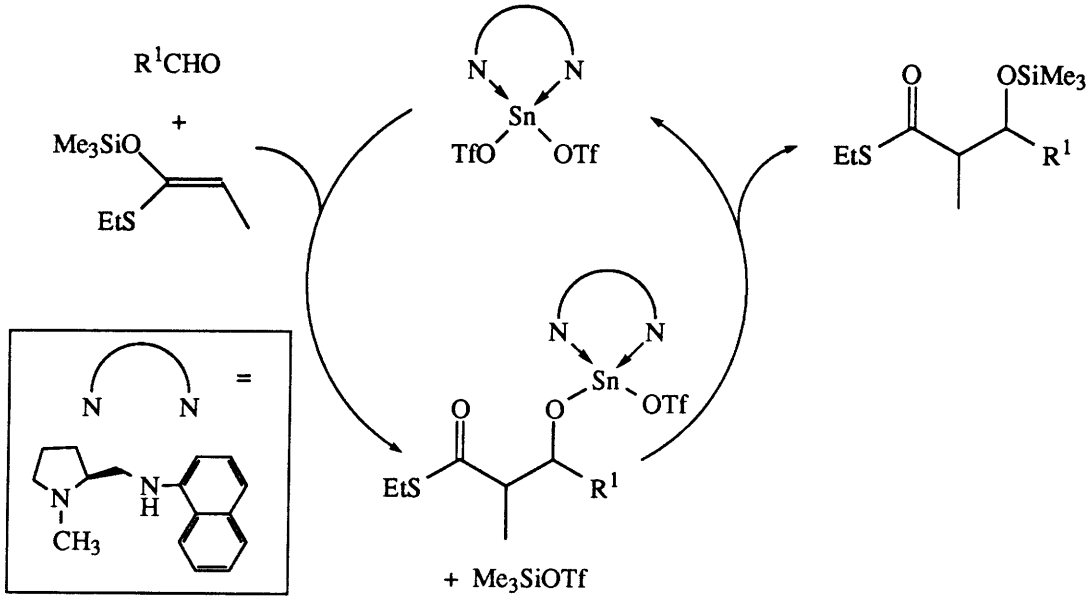

Two related contributions from the laboratories of Mukaiyama also deserve mention. Chiral Lewis acids with the suggested structures **1-19**[39] and **1-20**[40] also catalyzed the aldol reaction of silyl ketene acetals and aldehydes. Compound **1-19** was

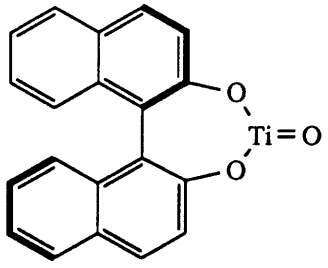

1-19

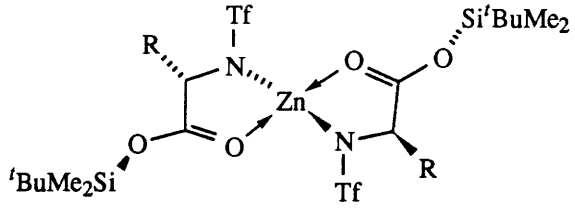

1-20a R= ^{i}Pr
1-20b R= CH_2Ph

derived from oxotitanium diisopropoxide and (*R*)-1,1′-bi-2-naphthol, a chiral ligand widely used in asymmetric synthesis. Initial studies[39] indicated a monomeric structure for **1-19**, but this assignment must await further confirmation, especially considering the paucity of compounds containing authentic titanium-oxygen double bonds.[41] The reaction of aldehydes with thioester-derived ketene acetals proceeded in the presence of 20 mole percent of complex **1-19** in toluene at low temperatures. Enantiomeric excesses of the aldol products ranged between 30–85% but surpassed 80% in only two examples involving α,β-unsaturated aldehydes. Although the enantioselectivities were not as high as those obtained with the tin(II) catalyst, they were far superior to the results of a related catalyst, **1-21**, reported earlier by Reetz.[42] The C_2-symmetric zinc(II) species **1-20a** and **b** catalyzed the aldol reaction of alkyl ester-derived ketene acetals and aldehydes in toluene.

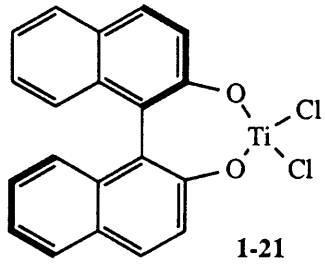

1-21

The yields of aldol products were high but the enantiomeric excesses exceeded 80% only with particularly reactive aldehydes such as Cl_3CCHO and Br_3CCHO.[40] Neither the structures nor the mode of action of catalysts **1-19**, **-20a**, and **-20b** were definitively established.

Another breakthrough came from the group of H. Yamamoto in 1991. This new method featured a chiral (acyloxy)borane (CAB) complex as a catalyst for the Mukaiyama condensation of silyl enol ethers, allowing the formation of β-hydroxy *ketones* in a highly diastereo- and enantioselective manner.[43] CAB, prepared in situ from L-tartaric acid derivative **1-22** and BH_3·THF complex in propionitrile at 0 °C, was assigned the structure **1-23** (Scheme 1.12).[44] The aldol reactions were conducted at -78 °C using 20 mole

Scheme 1.12 Formation of the Chiral (Acyloxy)Borane Catalyst

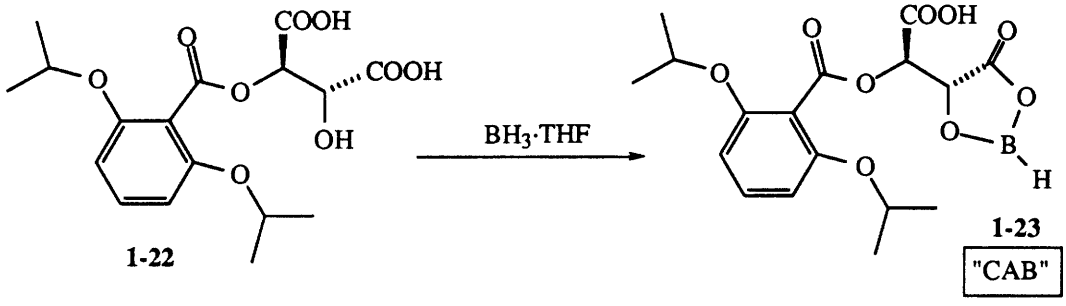

percent of the chiral borane, leading to high yields of the aldol product predominantly as the trimethylsilyl ether of the β-hydroxy ketone (Table 1.4). The sense of asymmetric induction was the same for all aldehydes examined (*re*-face attack), except when the ligand derived from D-tartaric acid was used to form the catalyst. *Syn* aldols were obtained with high diastereoselectivity regardless of the stereochemistry [*E*(*O*) or *Z*(*O*)] of the silyl enol ether (entries 4 and 5), a result that is consistent with the acyclic extended transition state mechanism postulated earlier (Section 1.4). The achievement of high asymmetric induction in aldol reactions of methyl ketones is a highly challenging task and the results in entries 1–3 are remarkable although the enantiomeric excesses are below 90%.

A follow-up paper by Yamamoto disclosed that the CAB species also catalyzed the Mukaiyama reaction of silyl ketene acetals (entries 6–10), particularly those derived from phenyl esters (entries 8–10).[44] Low to excellent diastereoselection and enantioselection were observed, with unsaturated aldehydes giving the best results (entry 10). The CAB Lewis acid is related to catalysts developed simultaneously in the Masamune group, and a discussion of its mode of action in the Mukaiyama reaction is deferred to Chapter Two.

Table 1.4 Selected CAB-Catalyzed Asymmetric Aldol Reactions[43,44]

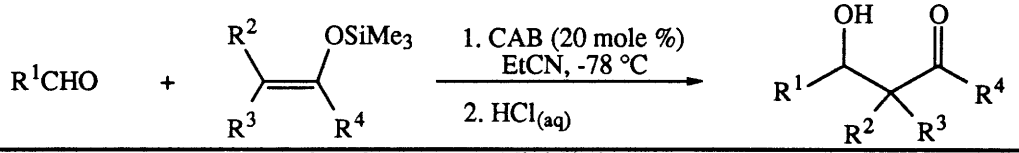

Entry	R^1	R^2, R^3, R^4	Yield/ %	*syn* : *anti*	ee/ % (config.)
1	$CH_3(CH_2)_3$	H, H, ^{n}Bu	70	-	80
2	Ph	H, H, Ph	98	-	85 (*R*)
3	(*E*)-PhCH=CH	H, H, Ph	88	-	83
4	Ph	H, CH_3, Et[a]	96	94:6	96 (*R*)[e]
5	Ph	CH_3, H, Et[b]	97	93:7	94 (*R*)[e]
6	Ph	H, H, OEt	63	-	84 (*R*)
7	Ph	H, CH_3, OEt[c]	51	50:50	61/47
8	Ph	H, CH_3, OPh[d]	83	79:21	92 (*R*)/6 (*R*)
9	$(CH_3)_2CH$	H, CH_3, OPh[d]	45	64:36	79/29
10	(*E*)-^{n}PrCH=CH	H, CH_3, OPh[d]	97	96:4	97[e]

[a]80/20 *E*(*O*)/*Z*(*O*) ratio. [b]14/86 *E*(*O*)/*Z*(*O*) ratio. [c]82/18 *E*(*O*)/*Z*(*O*) ratio. [d]>95/5 *E*(*O*)/*Z*(*O*) ratio. [e]ee of *syn* isomer.

The chiral Lewis acids presented in this chapter represent the most effective promoters and catalysts for the asymmetric Mukaiyama aldol reaction appearing in the literature through 1991; the selection is meant to be critical rather than exhaustive.[48] Several other chiral mediators have been reported (three are shown below) but these gave mediocre stereoselectivities, had limited application, or were less synthetically practical. A

discussion of our approach to the design of chiral Lewis acid catalysts for the Mukaiyama aldol reaction begins in Chaper Two.

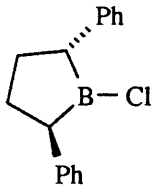

Promoter
Reetz, 1986[45]

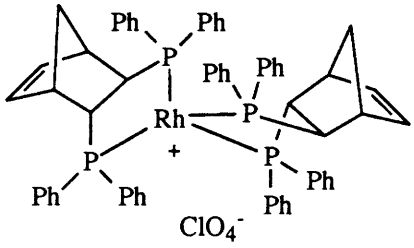

Catalyst
Reetz, 1987[46]

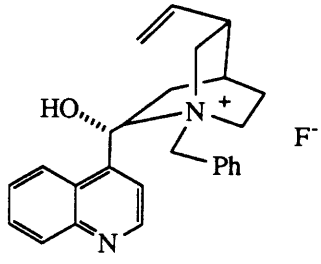

Catalyst
Shioiri, 1993[47]

Chapter Two

Discovery of New Catalysts for the Mukaiyama Aldol Reaction

2.1 Catalysis by Tin(IV) Compounds

In 1989, our search for new Lewis acid promoters and catalysts for the Mukaiyama reaction led us to examine tetravalent tin alkoxides and acetates.[49] These compounds, which previously had very limited application to organic synthesis[50], were potentially good Lewis acids and also might be prepared with optically active alkoxide ligands. The achiral

Scheme 2.1 Synthesis of Tin(IV) Alkoxides and Acetates

$$SnCl_4 + 4\,Et_2NH + 4\,ROH \xrightarrow[25\ ^\circ C]{\text{hexane}} Sn(OR)_4 + 4\,Et_2NH_2{}^+Cl^- \text{ (ref. 51)}$$

2-1 R= *t*-butyl
2-2 R= *t*-amyl

$$Sn(O^tBu)_4 \xrightarrow{\text{excess } {}^i\text{PrOH}} Sn(O^iPr)_4\cdot{}^i\text{PrOH} \xrightarrow{\text{distillation}} Sn(O^iPr)_4 \text{ (refs. 51,52)}$$

$$Ph_4Sn \xrightarrow[120\ ^\circ C]{AcOH,\ Ac_2O} Sn(OAc)_4 \text{ (ref. 53)}$$

$$Si(O^iPr)_4 + SnCl_4 \longrightarrow ({}^i\text{PrO})_2SnCl_2 \text{ (ref. 54)}$$

tin(IV) compounds initially studied were synthesized following literature procedures as shown in Scheme 2.1, and then tested as catalysts for the aldol reaction of benzaldehyde with the *t*-butyldimethylsilyl ketene acetal derived from ethyl acetate. Ten mole percent of the tin alkoxide **2-1** or **2-2** (relative to the amount of aldehyde) efficiently catalyzed the

reaction in CH_2Cl_2 at -78 °C, giving the *t*-butyldimethylsilyl ether of ethyl 3-hydroxy-3-phenylpropionate in high yield (Table 2.1, entries 1–3); tin(IV) acetate and diisopropoxytin dichloride were somewhat less effective catalysts and the aldol product was obtained in yields of less than 40% (entries 5–6).

Table 2.1 Activity of Tin(IV) Compounds in the Mukaiyama Reaction

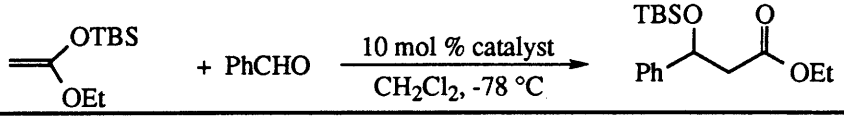

Entry	Catalyst	Reaction Time	Yield/ %
1	$Sn(O^tAmyl)_4$	50 min	90
2	$Sn(O^tAmyl)_4$	1 h 20 min	100
3	$Sn(O^tBu)_4$	1 h	92
4	$Sn(O^iPr)_4 \cdot {}^iPrOH$	7 h	60
5	$(^iPrO)_2SnCl_2$	2 h 30 min	36
6	$Sn(OAc)_4$	1 h	36

Mixtures of tin(IV) *t*-butoxide and the silyl ketene acetal in CD_2Cl_2 were analyzed by gas chromatography and low temperature ^1H NMR spectroscopy, and did not undergo transmetallation (tin enolate formation) between -78 °C and room temperature. *t*-Butyldimethyl-*t*-butoxysilane ($TBSO^tBu$), **2-3**, a compound expected to appear if

Scheme 2.2 Tin Enolate Formation Does Not Occur

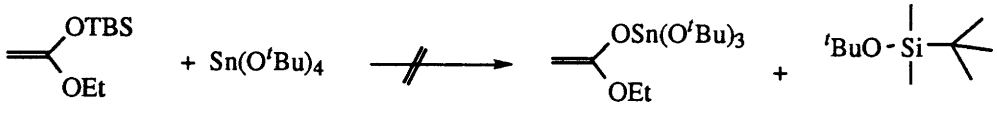

2-3

exchange between tin and silicon did indeed occur, was not observed (Scheme 2.2). This result, combined with the observation that $TBSO^tBu$ was likewise not detected in the aldol reaction mixture, suggested a carbonyl activation mechanism (Section 1.3) in which

regeneration of the catalyst proceeded by intramolecular silyl group migration (see Scheme 1.5).

The feasibility of substituting chiral alkoxide ligands for *t*-butoxide on the $Sn(O^tBu)_4$ catalyst and thereby obtaining an asymmetric tin(IV)-catalyzed aldol reaction was next investigated. Attempts to install optically active diols, such as 1,1´-bi-2-naphthol, stilbene diol, and diethyl tartrate by alcohol group exchange on $Sn(O^tBu)_4$ and $(^iPrO)_2SnCl_2$ met with difficulty, owing, in part, to the sensitivity of the starting compounds. The resulting tin species were poorly defined, and although catalysis of the aldol reaction was still achieved in several cases, the observed levels of enantioselection were negligible (≤ 10% ee). Because a satisfactory asymmetric Mukaiyama aldol process did not appear to be within reach using this methodology, the tin(IV) approach was ultimately abandoned.

2.2 Chiral Boranes from α-Amino Acids

A general strategy for the preparation of new chiral Lewis acids is the combination of ligands derived from inexpensive and readily available chiral sources, such as amino acids and carbohydrates, with sufficiently electropositive metallic or metalloidal species.

Scheme 2.3 Formation of a Borane Complex from *N*-Tosyl-(*S*)-Valine

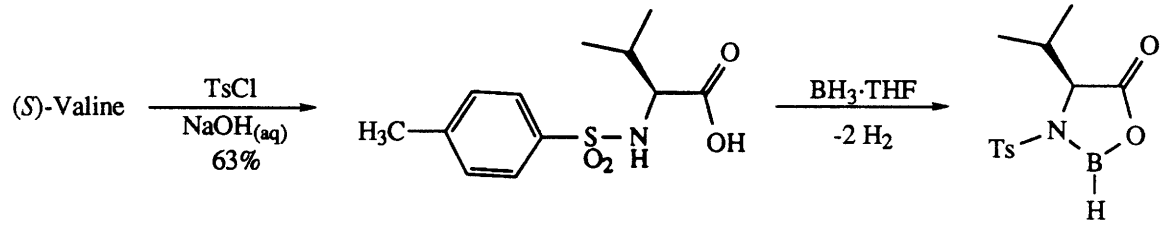

2-4

One family of Lewis acids that attracted our attention were those prepared from borane-tetrahydrofuran complex (BH_3·THF) and the arenesulfonamide derivatives of α-amino acids such as valine. These Lewis acids were recently identified as catalysts for asymmetric Diels-Alder reactions by Yamamoto[55] and independently by Helmchen[56] (see

Chapter Five). Addition of an equimolar amount of BH_3·THF to the *para*-toluenesulfonamide of (*S*)-valine in methylene chloride at room temperature results in the liberation of hydrogen and formation of a species provisionally assigned the structure **2-4** (Scheme 2.3). Borane is electrophilic and reacts rapidly with carboxylic acids via an acid–base reaction to give acyloxyboranes (the initial intermediates in the borane reduction of carboxylic acids[57]) and hydrogen gas. The proton on the sulfonamide nitrogen is also rendered acidic by the adjacent electron-withdrawing sulfonyl group.[58]

Application of amino acid-derived chiral boranes to the Mukaiyama aldol reaction led to an exciting discovery. The borane obtained from *N*-tosyl-(*S*)-valine and BH_3·THF efficiently promoted the highly enantioselective aldol condensation, shown in Scheme 2.4,

Scheme 2.4 Asymmetric Mukaiyama Reaction

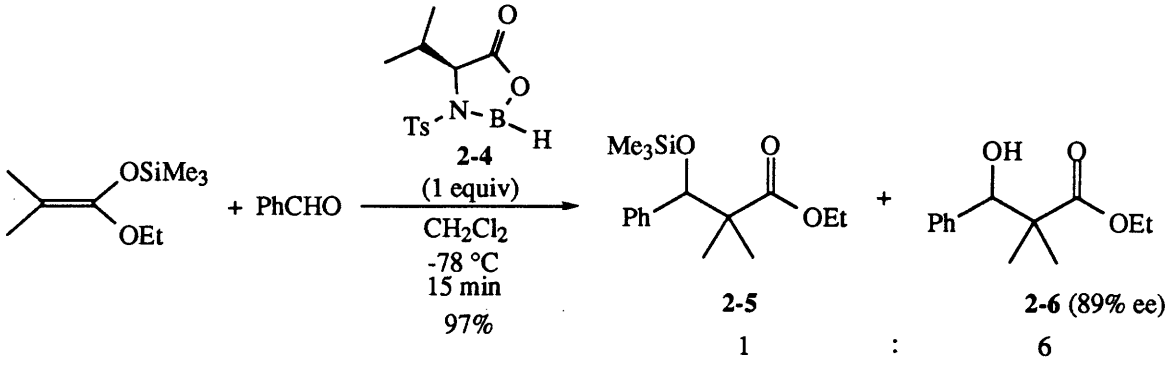

between benzaldehyde and the trimethylsilyl ketene acetal prepared from ethyl isobutyrate. This reaction, carried out at -78 °C in methylene chloride, was complete in about fifteen minutes and the product isolated at this stage, after a neutral aqueous workup, consisted of an approximately 6:1 ratio of the β-hydroxy ester **2-6** and its trimethylsilyl ether **2-5**; complete desilylation of the aldol products was accomplished by stirring with aqueous hydrochloric acid. Hydroxy ester **2-6** was thus obtained in nearly quantitative yield and, notably, with 89% ee. Ligands derived from other amino acids provided similar results (Table 2.2).

Interestingly, reaction mixtures allowed to stir for one to two days contained larger proportions of the trimethylsilyl ether **2-5**—in fact, after long reaction times this product was favored by a 2:1 ratio (Table 2.3). When the same aldol reaction was carried out in the presence of a *sub*stoichiometric amount (20 mole percent) of the Lewis acid, **2-6** was

Table 2.2 Aldol Reactions Promoted by Borane Complexes of Various Amino Acids

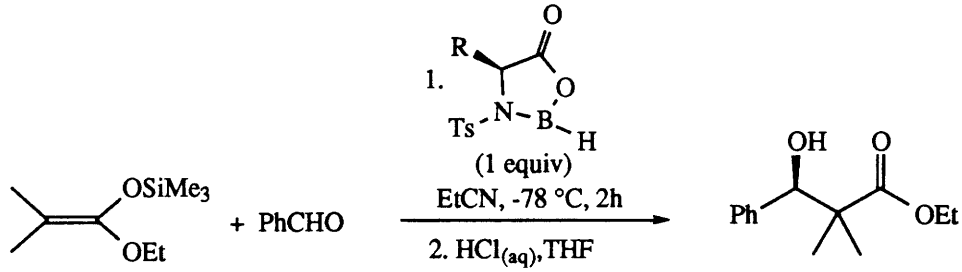

Entry	Amino Acid	Yield/ %	ee/ % (abs. config.)
1	L-valine (R= ^{i}Pr)	97	88 (*R*)
2	L-*tert*-leucine (R= ^{t}Bu)	86	88 (*R*)
3	L-leucine (R= ^{i}Bu)	75	75 (*R*)
4	L-isoleucine (R= ^{s}Bu)	90	74 (*R*)

Table 2.3 Effect of Reaction Conditions on Yield and Ratio of Aldol Products

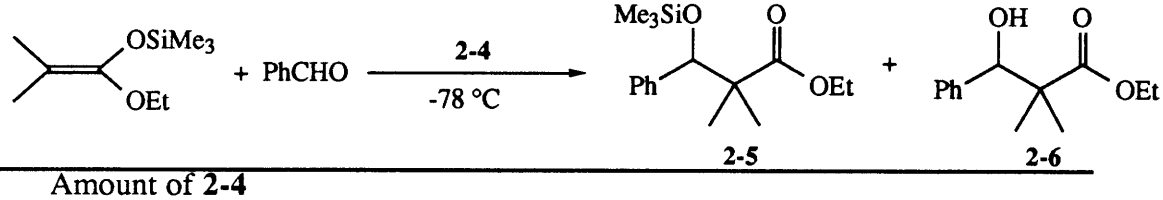

2-5 **2-6**

Amount of **2-4** / mole %	Reaction Time	Solvent	Yield	**2-5 : 2-6**
100	15 min	CH_2Cl_2	98%	1 : 6
100	17 h	CH_2Cl_2	94%	2 : 1
20	10 h	CH_2Cl_2	42%	1 : 4
20	14 h	EtCN	52%	1 : 1

obtained in 42% yield, with the hydroxy ester favored over silylated product by 4:1. This ratio changed to 1:1 and the yield increased slightly to 52% when propionitrile was used as the solvent instead of methylene chloride.

The hypothetical cycle shown in Scheme 2.5 accounts for the observations described above. Activation of the aldehyde by coordination to the boron atom of the Lewis acid **2-4** is followed by addition of the ketene acetal, providing zwitterion **2-7**.

Scheme 2.5 Hypothetical Reaction Cycle

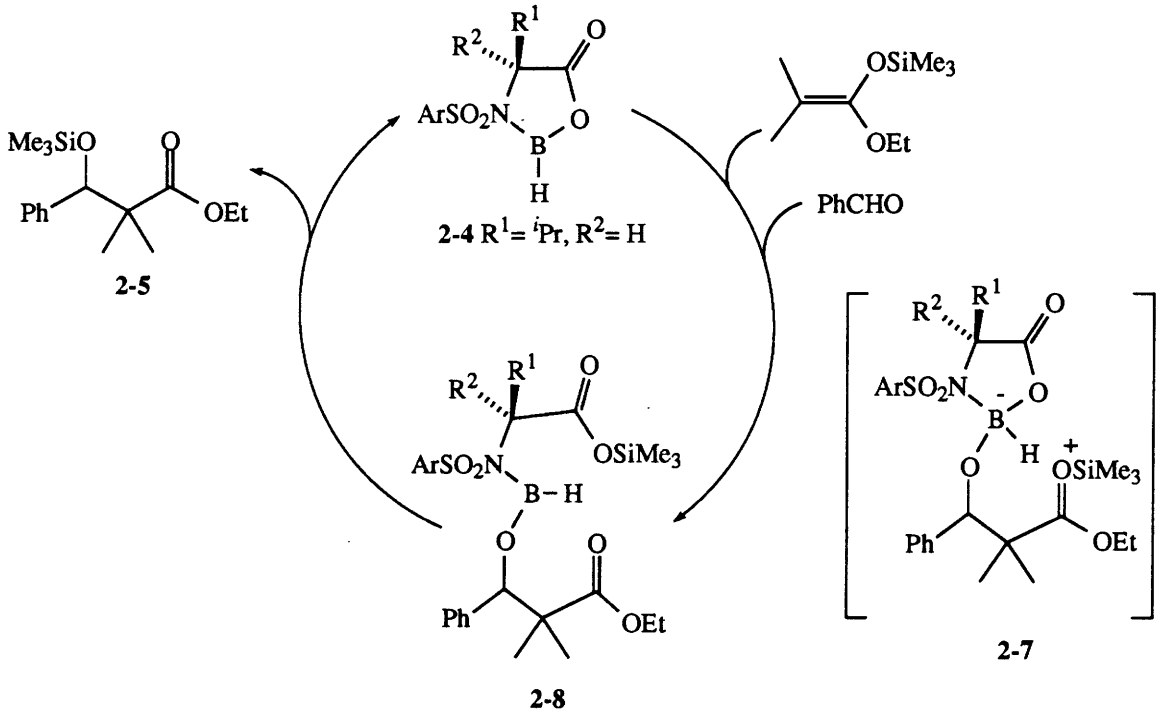

Intramolecular migration of the trimethylsilyl group to the carboxylate function of the ligand relieves the charges on boron and silicon and results in the acyclic boron aldolate **2-8**; hydrolysis at this stage affords the β-hydroxy ester directly by cleavage of the boron-oxygen bond. We hypothesized that, over longer reaction times, **2-8** experiences an intramolecular exchange of boron and silicon during which the silylated aldol product **2-5** is released with concomitant cyclization and regeneration of **2-4**. In the case of the valine-

derived Lewis acid, this step is obviously too slow to be effective, judging from the low yield in the reaction using 20 mole percent of the promoter and the small proportion of silylated product observed after workup (Table 2.3). In line with earlier observations by Mukaiyama[38] and Yamamoto[43], the polar solvent propionitrile likely facilitates the turnover step, accounting for the higher yield and larger proportion of silylated product. This cycle is analogous to that proposed for the tin(II) triflate-catalyzed aldol reaction[38] discussed in Chapter One, except that in the present case, the silyl transfer step occurs intramolecularly (for comparison, see Scheme 1.11).

The rate of this intramolecular exchange might be increased by refashioning the substitution pattern of the ligand, and one potential modification concerned the use of α,α-disubstituted amino acids instead of monosubstituted amino acids such as valine. We envisioned that, if the proposed cycle in Scheme 2.5 held true, the inclusion of a disubstituted amino acid ligand (i.e., $R^1,R^2 \neq H$ in **2-4**) in the chiral borane should facilitate ring closure of the intermediate species **2-8** as a consequence of the *gem*-dialkyl effect[59], hopefully resulting in more effective catalysis. The increase in the rate of of ring formation resulting from increased alkyl substitution is a well known phenomenon in organic chemistry, attributed to two effects: the first, called the "Thorpe–Ingold effect,"[60] was postulated almost eighty years ago and suggests that alkyl substitution on a central

Figure 2.1 Thorpe–Ingold Effect (Angle Compression)

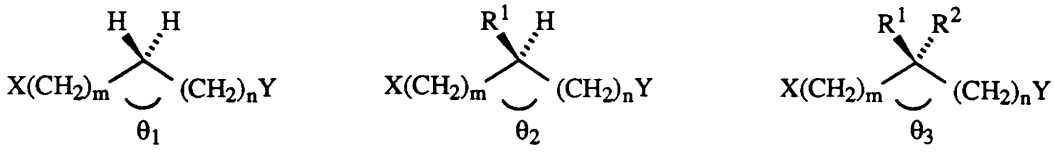

$\theta_1 > \theta_2 > \theta_3$

methylene causes compression of the internal angle owing to the larger size of the alkyl groups. This decrease in the internal angle causes the reactive groups at the ends of the chain to move closer together (Figure 2.1). An alternative explanation for the rate increase is that alkyl substitution results in a higher population of reactive rotamer conformations

that lead to productive transition states for cyclization. This so-called "reactive rotamer effect"[59a] was recently investigated by Jung and found to outweigh the Thorpe–Ingold effect in certain cases.

The first set of experiments concerned the α-substituent effect of various ligands on the turnover capability of their borane complexes, as judged by the yield of the aldol reaction using a *substoichiometric* amount (20 mole percent) of the chiral Lewis acid mediator. Thus, the *para*-toluenesulfonamides of several simple α-amino acids provided the results shown in Table 2.4 for the reaction of benzaldehyde (1 equivalent) and the

Table 2.4 Disubstitution at α-carbon of Ligand Enhances Catalytic Activity

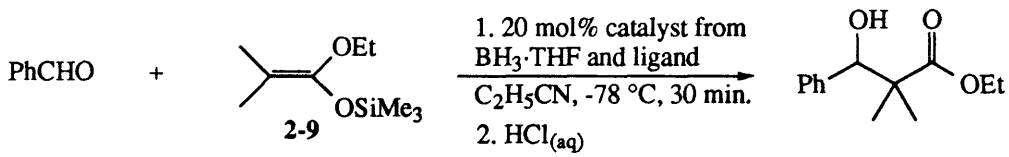

Ligand	Yield	Ligand	Yield
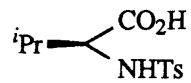 **2-10**	54%	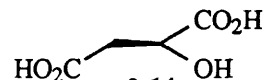 **2-14**	21%
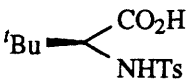 **2-11**	46%	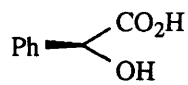 **2-15**	19%
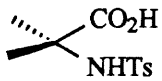 **2-12**	95%	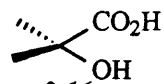 **2-16**	55%
 **2-13**	98%	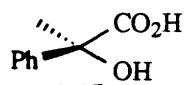 **2-17**	96%

trimethylsilyl ketene acetal **2-9** (1.2 equivalents). The chemical yield of the aldol reaction was measured in every case after a standard reaction time of 30 min. The catalysts derived from monosubstituted amino acid ligands **2-10** and **2-11** gave approximately 50% yields of the aldol products, corresponding to two reaction cycles of the catalyst as mentioned

earlier. However, with disubstituted amino acid ligands **2-12** and **2-13**, prepared from 2-amino-2-methylpropionic acid and 2-amino-2-phenylpropionic acid respectively, the aldehyde was completely consumed as evidenced by the >95% yields of aldol (mostly as the trimethylsilyl ether). α-Hydroxy carboxylic acids **2-14–2-17** chosen for comparison gave similar results: catalysts prepared from monosubstituted compounds, for example, malic acid, **2-14**, or mandelic acid, **2-15**, gave only a 20% isolated yield of β-hydroxy ester. Methyllactic acid, **2-16**, was somewhat more effective (55% yield), and with atrolactic acid, **2-17**, a ligand bearing phenyl and methyl substituents in the α-position, the aldol reaction went to completion. The trend is consistent with the argument that disubstitution at the α-carbon enhances the catalytic activity of the borane complexes in the aldol reaction. Attention was then focused on the preparation of several enantiomerically pure α,α-disubstituted sulfonamido acid ligands for use in catalytic and potentially asymmetric Mukaiyama aldol reactions.

2.3 Chiral Boranes with α,α-Disubstituted Glycine Arenesulfonamide Ligands

The major objective of the project at this point was the preparation of chiral boranes that demonstrated effective catalysis of the Mukaiyama reaction, and also provided an asymmetric environment for effective induction of chirality. There are three general approaches to the synthesis of chiral, optically active α,α-disubstituted amino acid ligands[61]: (1) the preparation (and resolution, if necessary) of amino acids from ketones, (2) the asymmetric alkylation of monosubstituted amino acids using any of a number of template-based methods, or (3) the functionalization of a naturally occurring or commercially available amino acid. The first candidate compound selected for preparation in optically pure form was the *para*-toluenesulfonamide derivative of 2-amino-2-phenylpropionic acid (2-phenylalanine); we had already demonstrated that the borane complex of this ligand in racemic form exhibited catalytic activity in the Mukaiyama aldol

reaction (Table 2.4). The amino acid **2-18** was synthesized from acetophenone by a Strecker reaction[62] (Scheme 2.6) and resolved through the quinine and cinchonine salts of the corresponding formamido acid according to literature procedures.[63] The sulfonamide

Scheme 2.6 Synthesis of the 2-Phenylalanine-derived Ligand

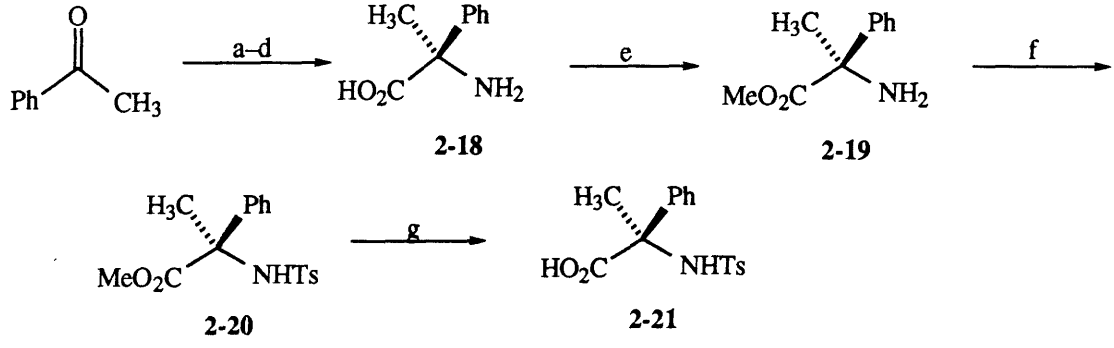

(a) NaCN, NH_4Cl, NH_4OH, H_2O, EtOH, 60 °C; (b) HCl, H_2O, 0–100 °C; (c) Py, 40% for a–c; (d) Resolution; (e) MeOH, $HC(OMe)_3$, $HCl_{(g)}$, then $NaHCO_{3(aq)}$, 79%; (f) TsCl, Et_3N, DMAP, CH_2Cl_2, 97%; (g) LiOH, THF, H_2O, then $HCl_{(aq)}$, 99%.

derivatives of amino acids are usually formed under "Schotten–Baumann conditions,"[64] that is, with a sulfonyl chloride in aqueous base (see Scheme 2.3). However, attempts to prepare the *para*-toluenesulfonamide directly from **2-18** with this protocol resulted in the recovery of starting materials or the isolation of decomposition products. The desired sulfonamido acid was successfully obtained via the methyl ester **2-19**, which was converted to sulfonamide **2-20** without difficulty. Hydrolysis of the ester using lithium hydroxide in aqueous THF afforded the ligand **2-21** in high yield.

A catalytic amount (20 mole percent) of the borane complex prepared from **2-21** and BH_3·THF was tested in the aldol reaction of benzaldehyde and ketene acetal **2-9** (Table 2.5). The chemical yields of aldol products were high as expected (85–98%), but only very low enantioselection (0–12% ee) was observed (entries 1, 2). The reaction mixtures were enriched in the trimethylsiloxy ether product, indicating that the catalytic cycle was operating efficiently despite the poor levels of asymmetric induction. The enantioselectivity was improved slightly by employing 50 or 100 mole percent of the

promoter, giving enantiomeric excesses of 33 and 45% respectively for the hydroxy ester (entries 3, 4).

Table 2.5 Aldol Reactions with Ligands Derived from 2-Amino-2-phenylpropionic Acid

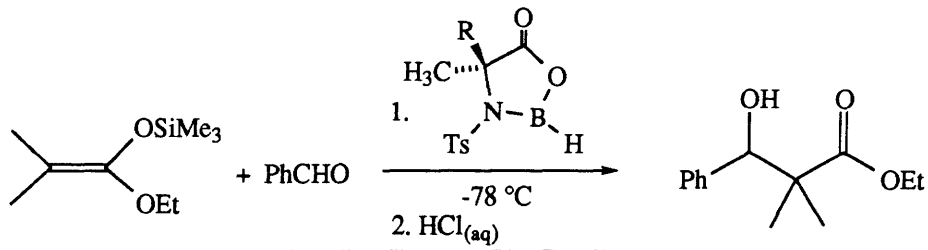

Entry	R	Promoter Amount/ mol %	Solvent	Yield/ %	ee/ %
1	Ph	20	CH_2Cl_2	89	0
2	Ph	20	EtCN	88	12
3	Ph	50	EtCN	85	33
4	Ph	100	EtCN	98	45
5	c-C_6H_{11}	100	EtCN	86	30

A second, related ligand, **2-22**, with cyclohexyl and methyl substituents in the α-position, was prepared by hydrogenation of the amino ester intermediate **2-19** over a

Scheme 2.7 Synthesis of a New Ligand From **2-19**

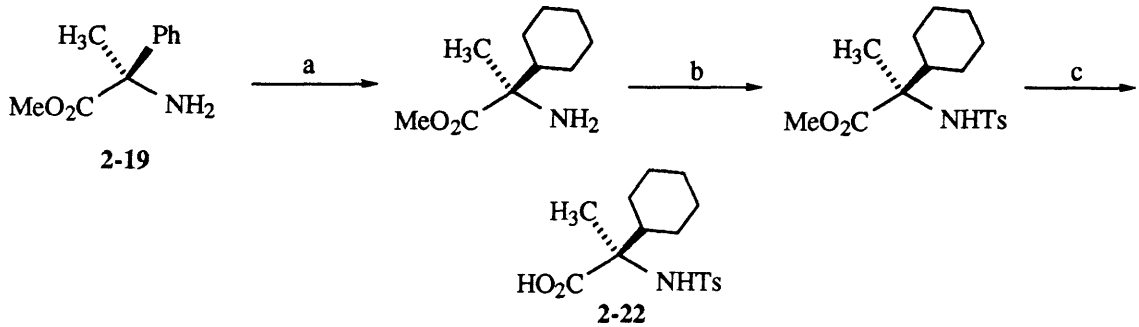

(a) Rh/Al_2O_3, MeOH, AcOH, H_2 (45 psi), 63%; (b) TsCl, Et_3N, DMAP, CH_2Cl_2, 86%; (c) LiOH, THF, H_2O, then $HCl_{(aq)}$, 88%.

rhodium catalyst, followed by sulfonamide formation and ester hydrolysis as described above (Scheme 2.7). A stoichiometric proportion of the borane complex from this ligand

in the aldol reaction did not lead to any improvement in enantioselectivity (Table 2.5, entry 5).

The next ligand examined, **2-27**, derived from the commercially available amino acid α-methyl-DOPA, displayed far more promising results. α-Methyl-DOPA, **2-23**, was

Scheme 2.8 Synthesis of a Ligand from α-Methyl-DOPA

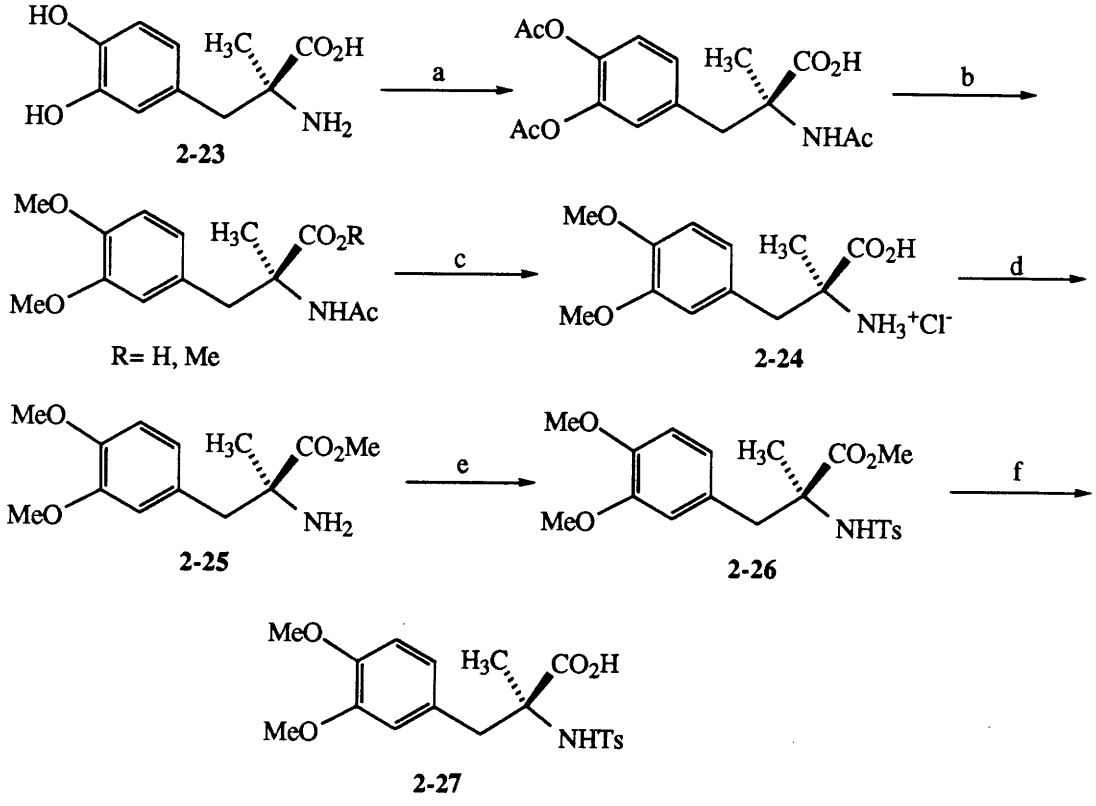

(a) Ac_2O, py, 90%; (b) KOH, $(CH_3O)_2SO_2$, 85%; (c) 6M HCl, reflux; (d) MeOH, $HCl_{(g)}$, then $NaHCO_{3(aq)}$, 71% for c–d; (e) TsCl, Et_3N, DMAP, CH_2Cl_2, 98%; (f) LiOH, THF, H_2O, then $HCl_{(aq)}$, 88%.

converted to the hydrochloride salt **2-24** containing a dimethoxyphenyl group using a 1964 literature procedure[65] from laboratories at Merck & Co. (Scheme 2.8). This amino acid was manipulated via ester **2-25** to the desired ligand in a manner identical to that described for ligand **2-21**. A stoichiometric amount of the borane complex of **2-27** capably promoted the aldol reaction, giving the β-hydroxy ester in 94% yield and with a high level of enantioselection (80% ee; Table 2.6, entry 1). Initial attempts to match this result using 20 mole percent of the promoter led to a dramatic reduction in enantiomeric excess (54%

ee), although the chemical yield remained high (entry 2). This loss of enantioselection observed upon decreasing the amount of promoter suggested that a less stereoselective Lewis acid species began to catalyze the aldol reaction after completion of the initial cycle. Possibly, the intermediate boron aldolate **2-8** (from Scheme 2.5) could act as a Lewis acid in competition with the desired cyclic catalyst and furnish aldol products with reduced enantioselectivity.

Table 2.6 Aldol Reactions with the Borane Complex of Ligand **2-27**

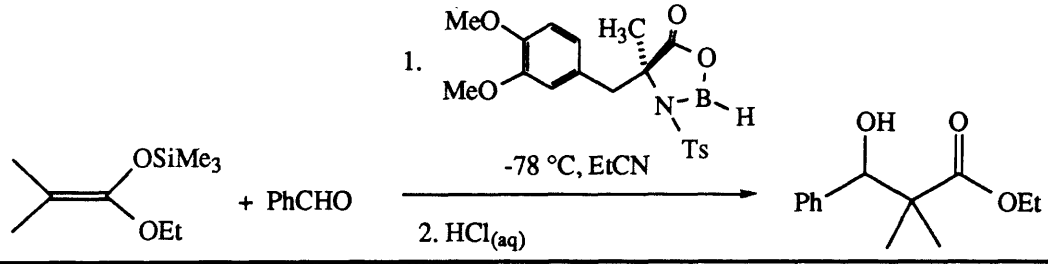

Entry	Promoter Amount/ mol%	Aldehyde Addition Time	Yield/ %	ee/ %
1	100	1 min	94	80
2	20	1 min	91	54
3	20	3.5 h	87	84
4	10	3.5 h	89	80
5	5	3.5 h	52	40

We posited that the accumulation of **2-8** could be minimized by slow addition of the aldehyde to the reaction mixture, hopefully leading to an increase in the rate of catalyst

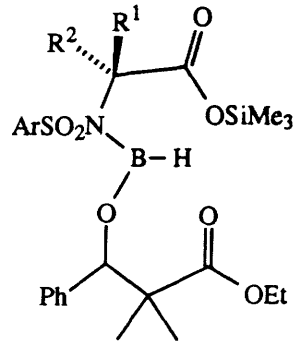

2-8

regeneration relative to that of carbon-carbon bond formation. Entry 3 in Table 2.6 shows that slow addition of benzaldehyde as a solution in propionitrile over a 3.5 h period resulted in an enhancement of product enantiopurity from 54 to 84% ee. By employing the device of slow addition, enantioselection in the catalytic reaction using ligand **2-27** was therefore brought up to same level as that observed in the stoichiometric reaction (79–84% ee). The final two entries in Table 2.6 are concerned with the turnover capability of the borane catalysts. Lowering the proportion of catalyst to 10 mole percent did not lead to a significant decrease in reactivity or enantioselectivity. However, when the aldol reaction was repeated using 5 mole percent catalyst, the chemical yield dropped to 52% and the enantioselection suffered considerably. Therefore, a standard procedure for "catalytic" aldol reactions was established, in which the chiral borane (0.2 equivalent) was generated at 40 °C in propionitrile, followed by cooling to -78 °C, addition of the ketene acetal (1.2 equivalents), and slow addition of the aldehyde (1.0 equivalent) as a solution in propionitrile over 3–3.5 h. Stirring at -78 °C was continued for a further hour or until complete consumption of the starting material was observed.

2.4 Modification of the Ligand Derived from α-Methyl-DOPA

The next set of experiments involved modification of the structure of the α-methyl-DOPA ligand to improve the enantioselectivity of the aldol reaction. Variation of the arenesulfonamide moiety of the ligand was an obvious starting point. Reaction of intermediate amino ester **2-25** (in Scheme 2.8) with a series of commercially available alkane- and arenesulfonyl chlorides led to high yields of sulfonamido esters; hydrolysis of these methyl esters afforded the sulfonamido acids, which were obtained as crystalline solids or in some cases as foams. The ligands were converted to borane complexes and surveyed as catalysts in the aldol reaction using the standard procedure. The results are listed in Table 2.7. The steric demand of the substituent in the *para* position of the aromatic ring in the arenesulfonamide is apparently not very important, as phenyl, tolyl, and 4-*t*-

Table 2.7 Effect of Varying the Arenesulfonyl Group in Ligand **2-27**

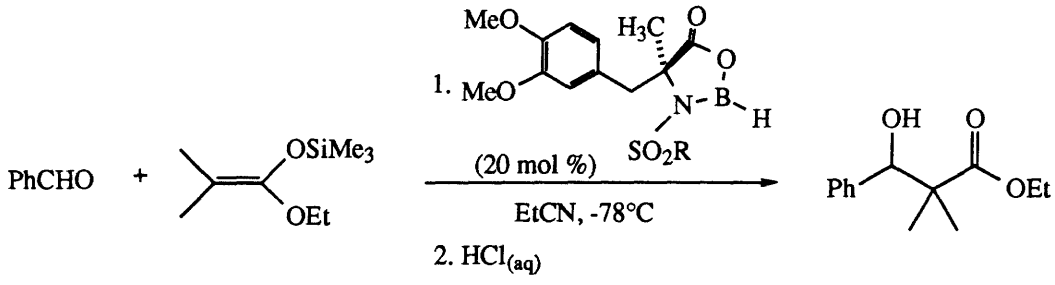

R	Yield/ %	ee/ %	R	Yield/ %	ee/ %
CF_3	87	17	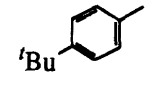	83	81
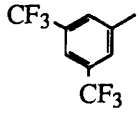	53	52		79	83
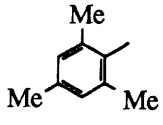	87	53	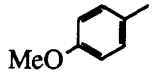	87	86
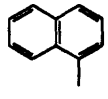	80	67	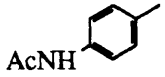	86	86
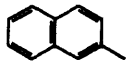	86	78	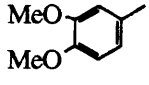	96	88

butylphenyl substituents gave similar results with respect to yield and enantioselectivity. Electron-donating substituents such as methoxy or acetamido in the *para*-position offered a small increase in enantioselectivity. Substituents in the *ortho* or *meta* positions lowered the selectivity, and larger aromatic surfaces (α- or β-naphthyl) likewise offered no improvement. Installation of a triflamide group (-$NHSO_2CF_3$) led to a significant reduction in enantioselectivity. The marginal increase in enantioselection exhibited by some of these ligands combined with the low cost and ready availability of tosyl chloride pointed to the *para*-toluenesulfonyl group as the substituent of choice.

Next, the 3,4-dimethoxyphenyl group of **2-27** was modified by the preparation of a series of related amino acid derivatives.[66] These new ligands were used in catalytic aldol reactions, and the results are shown in Table 2.8. Despite the high yields of aldol products, the enantioselectivities were in every case inferior to those obtained in experiments with the α-methyl-DOPA-derived catalyst.

Table 2.8 Variation of the Ligand Structure

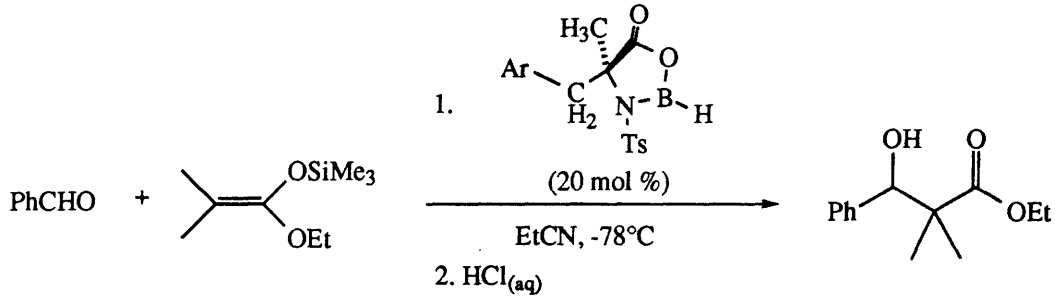

Ar	Yield/ %	ee/ %
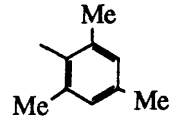	91	59
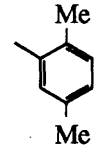	87	34
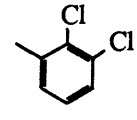	85	71
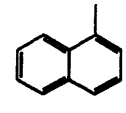	82	25
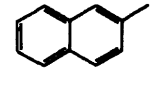	87	25

2.5 Ligands Derived from Menthone

Naturally occurring optically active ketones may be converted to amino acids by the Strecker reaction[67] or one of its variants, and are therefore another potential source of chiral ligands. Sulfonamido acid **2-35** (Scheme 2.9) was targeted as a new ligand to be

synthesized from menthone, an inexpensive starting material readily available as either enantiomer. The amino acid **2-30** was obtained diastereoselectively from (–)-menthone by a modification of the Strecker method known as the Bucherer–Bergs reaction[68], which

Scheme 2.9 Synthesis of a New Ligand from Menthone

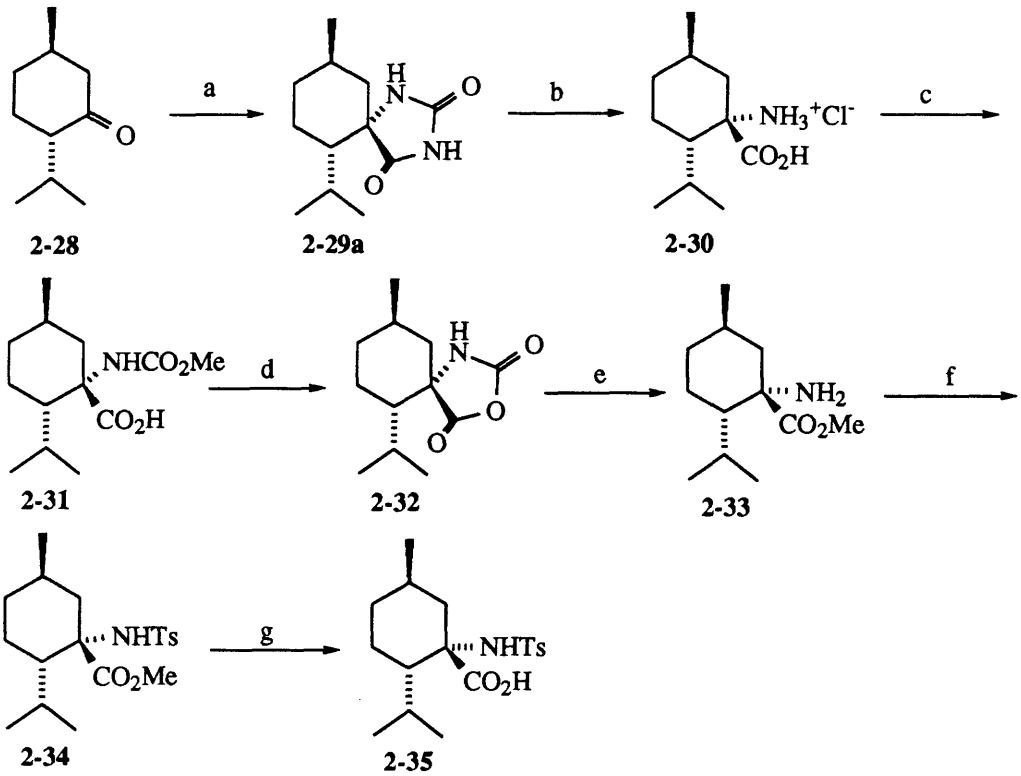

(a) NaCN, $(NH_4)_2CO_3$, EtOH, H_2O, 50–90 °C, 50%; (b) $NaOH_{(aq)}$, 150 °C then $HCl_{(aq)}$, 90%; (c) $ClCO_2Me$, py, 88%; (d) $SOCl_2$, C_6H_6, 89%; (e) $HCl_{(g)}$, MeOH then $NaHCO_{3(aq)}$, 89%; (f) TsCl, py, 80%; (g) KOH, EtOH, H_2O, 95%.

gave the hydantoin **2-29a** as the initial product, formed from the ketone, sodium cyanide, and ammonium carbonate in ethanol. The hydantoin was hydrolyzed to the amino acid by alkaline hydrolysis at high temperature. In analogy to the other disubstituted amino acids described in this chapter, direct conversion of **2-30** to the sulfonamide was not successful. Carbamate formation and thionyl chloride-promoted cyclization afforded the *spiro* compound **2-32**, which was opened to the amino ester **2-33** and converted to the *para*-toluenesulfonamide as shown in Scheme 2.9. Hydrolysis of the methyl ester **2-34** to the sulfonamido acid **2-35** was accomplished by reaction with potassium hydroxide in

refluxing aqueous ethanol, and recrystallization of the crude product afforded the desired ligand as a highly crystalline white solid.

The diastereoselectivity observed during the formation of hydantoin **2-29a** deserves some comment. In the 1960s, several conflicting reports appeared concerning the assignment of stereochemistry to the amino acids derived from (–)-menthone under both Bucherer–Bergs and conventional Strecker conditions. On the basis of hydrolysis studies as well as infrared spectra and dissociation constants, Munday[69] assigned the structure **2-29a** to the Bucherer–Bergs hydantoin, in which the nitrogen on the cyclohexane ring is in the axial position (the α-product). Cremlyn and Chisholm[70] argued for a reversal of this assignment in favor of **2-29b**, the β-product, based primarily on dissociation constants of

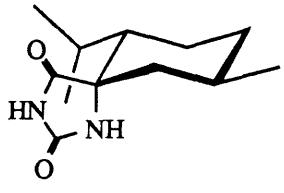

2-29a α-hydantoin

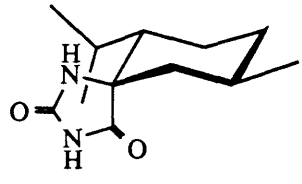

2-29b β-hydantoin

the corresponding amino acids. In 1975, Edward and Jitrangsri[71], citing evidence from ^{13}C NMR spectroscopy, showed that the Munday assignment was correct, and proposed the general rule that amino acids prepared from cyclohexanone derivatives by the Bucherer–Bergs reaction contain equatorial carboxyl groups.[72]

This selectivity is explained in Scheme 2.10.[71] Under the basic conditions of the Bucherer–Bergs reaction, the interconversion of amino nitriles **2-36a** and **2-36b** is assumed to be rapid. The rate determining step along the path to hydantoin **2-29b** is likely **2-37b→2-38b**. If this ring closure step is endothermic, the transition state will resemble **2-38b** according to the Hammond principle and experience steric hindrance between the nascent C=NH group and the 3,5-axial hydrogen atoms, thus disfavoring the path leading to the β-hydantoin. The alternate path, leading to the α-hydantoin, should be less favored in the earlier step **2-36a→2-37a** for steric reasons, but by the Curtin–Hammett principle,

Scheme 2.10 Diastereoselection in the Bucherer–Bergs Reaction of (–)-Menthone[71]

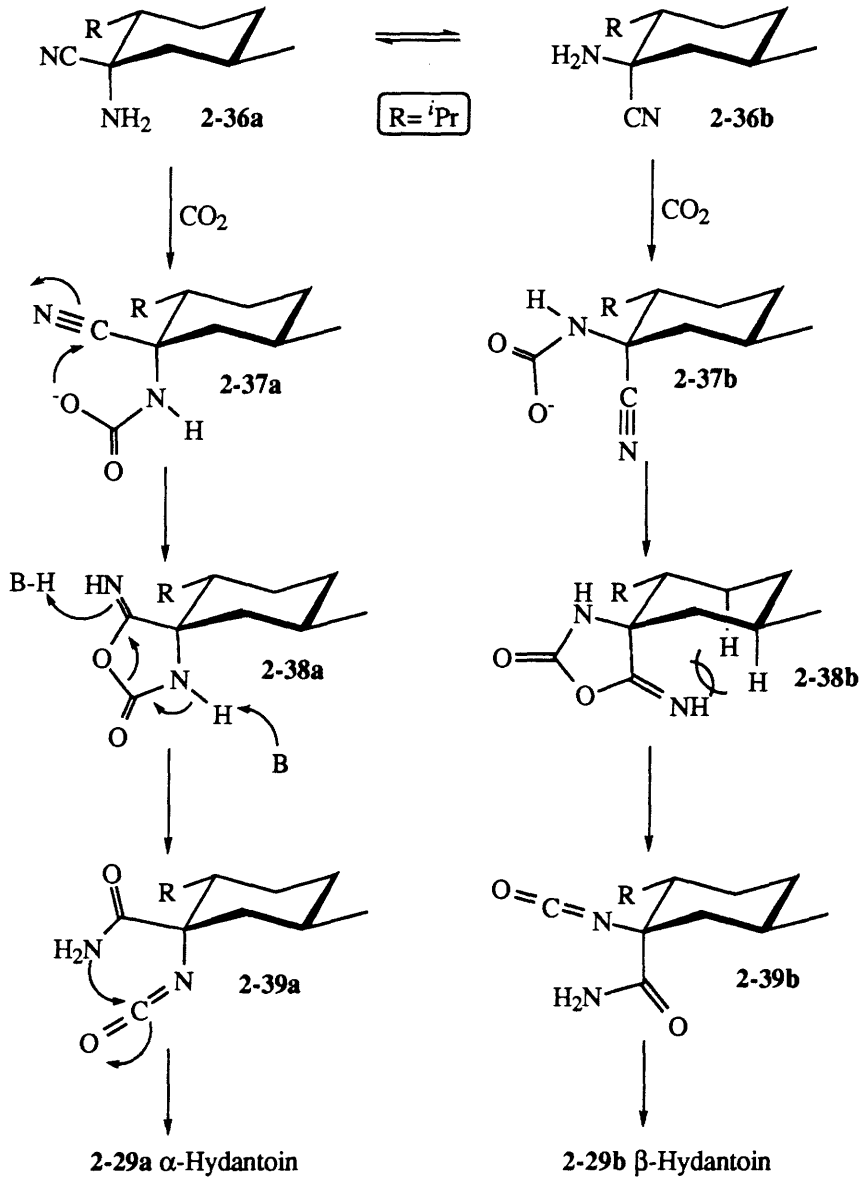

the relative rates by the α- and β-paths depend upon the *overall* barrier between **2-36b** and the intermediate after the rate-determining step, and this should be larger on the pathway to the β-product.

An X-ray crystal structure of the new ligand (Appendix Two) confirmed the *syn* relationship of the isopropyl and sulfonamido groups, the relative stereochemistry expected

from formation of the Bucherer–Bergs α-hydantoin **2-29a**. The borane complex of this ligand catalyzed the Mukaiyama aldol reaction at a comparable rate to that of the α-methyl-DOPA-derived ligand, and the β-hydroxy ester product was obtained in 83% yield and with 91% ee—the highest enantioselection observed in our experiments up to this point (Scheme 2.11).[73]

Scheme 2.11 Aldol Reaction with Ligand **2-35**

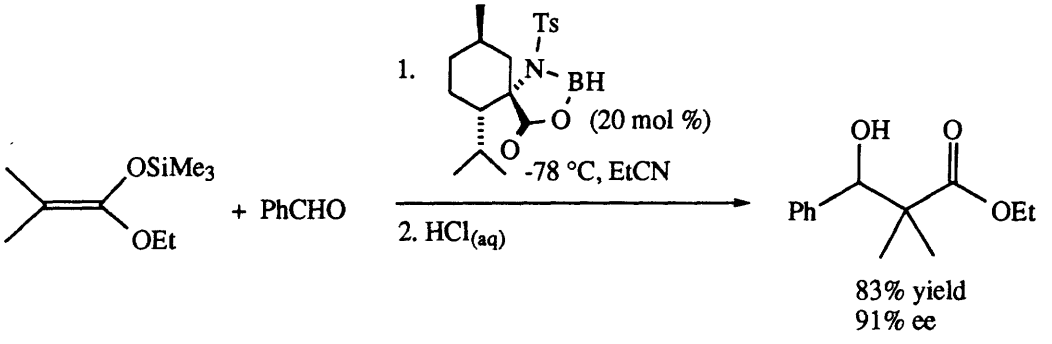

2.6 Related Results

After the completion of our early studies on aldol reaction promoters obtained from *monosubstituted* α-amino acid sulfonamides and BH_3·THF, a report on similar work

Table 2.9 Aldol Results Reported by Kiyooka[74]

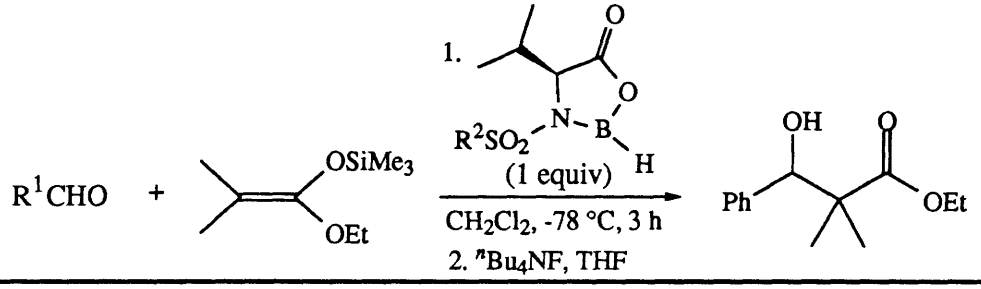

R^1	R^2	Yield/ %	ee/ %
Ph	*p*-CH_3-C_6H_4	86	83
Ph	α-Naphthyl	79	90
Ph	β-Naphthyl	85	93
(*E*)-PhCH=CH	*p*-CH_3-C_6H_4	80	85
$PhCH_2CH_2$	*p*-CH_3-C_6H_4	87	93

appeared from the research group of Kiyooka[74], including the results listed in Table 2.9. These workers observed an interesting effect upon changing the trialkylsilyl group of the ketene acetal from trimethylsilyl (TMS) to *t*-butyldimethylsilyl (TBS). Condensation of a TBS ketene acetal with benzaldehyde in the presence of the chiral borane resulted in a high yield of the β-hydroxy acetal **2-40** instead of the expected β-hydroxy ester (Scheme 2.12). The acetal apparently arose upon reduction of the intermediate ethyl ester by intramolecular hydride transfer, an alternative pathway resulting from the increased stability of the

Scheme 2.12 Unexpected Reaction Pathway: Reduction

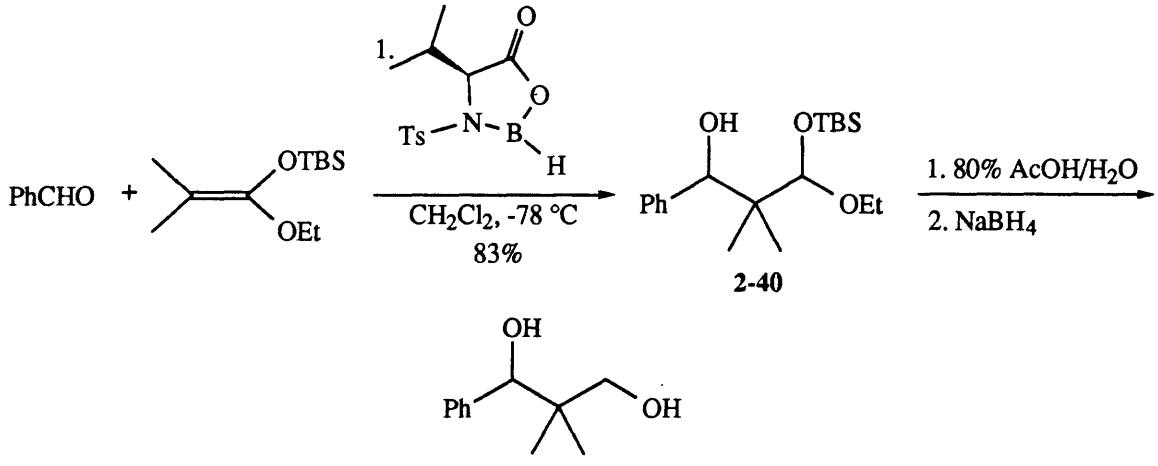

intermediate **2-42**. The optically active diol **2-41** was obtained from the TBS acetal **2-40** via hydrolysis to the corresponding aldehyde and reduction with $NaBH_4$ (Scheme 2.12).

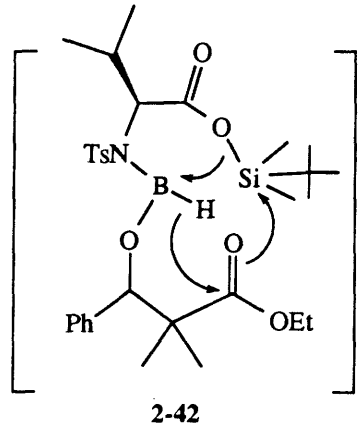

2-42

In 1992, the same group described a catalytic version of the Mukaiyama reaction using the *para*-nitrobenzenesulfonamide derivative of valine as the ligand and nitroethane as solvent; an example is shown in Scheme 2.13.[75] This combination provided enantiomeric excesses equal to those of the corresponding stoichiometric reactions in Table 2.9. However, the yields reported by these workers are puzzling to us because in our hands catalysis was never observed in the case of monosubstituted amino acid ligands under similar conditions.

Scheme 2.13 Catalytic Aldol Reaction Reported by Kiyooka[75]

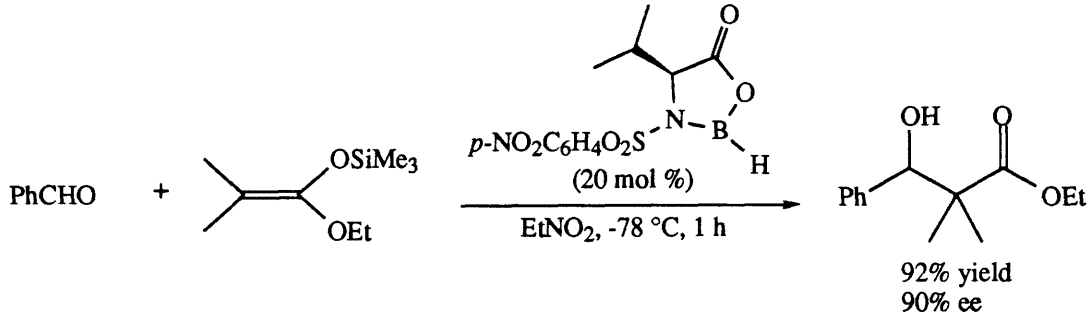

Although the hypothetical catalytic cycle depicted earlier in Scheme 2.5 has served as a guide for designing the ligands and catalysts described in this chapter, the mechanistic course of the aldol reaction is undoubtedly complicated, and even the structure of the Lewis acids are tentatively assigned. Some proof for the structural homogeneity of the borane complexes comes from their proton-decoupled ^{11}B NMR spectra, which show single broad peaks at +4–10 ppm (referenced to $BF_3{\cdot}OEt_2$; see spectra 3–5 in Appendix One). Preliminary results indicate that an intramolecular exchange reaction between boron and silicon features in the catalytic cycle, and the same is true for the CAB-catalyzed asymmetric aldol reaction reported by the Yamamoto group.[43] The CAB catalyst, described in Chapter One, consists of the borane complex of a hydroxy acid ligand derived from tartaric acid, and probably catalyzes the aldol reaction via a similar pathway.

Thus far, benzaldehyde and 1-(trimethylsiloxy)-1-ethoxy-2-methyl-1-propene have been used as model substrates to test the new catalysts for the Mukaiyama aldol reaction.

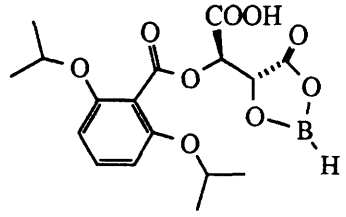

CAB

Chapter Three describes the application of these catalysts to asymmetric aldol reactions involving structurally diverse aldehydes and ketene acetals; the important question of the source of enantioselectivity is also addressed.

Chapter Three

Catalytic Asymmetric Mukaiyama Aldol Reactions

3.1 Variation of the Aldehyde

After establishing the general procedure described in Chapter Two for asymmetric Mukaiyama aldol reactions using 20 mole percent of chiral borane promoters, a series of aldehydes were examined as substrates in reactions using ligands **3-1** and **3-2** derived

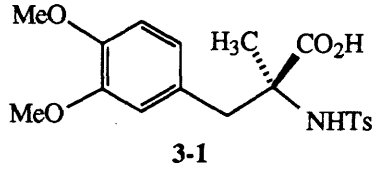

3-1

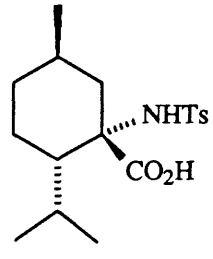

3-2

from α-methyl-DOPA and menthone. The results are shown in Table 3.1. All of the reactions were conducted in propionitrile at -78 °C and involved slow addition of the aldehyde (in propionitrile solution) over 3–4 hours. As expected, the major products in each case were the β-siloxy esters, which were desilylated in aqueous acid to provide the β-hydroxy esters. The two catalysts exhibited similar reactivity and the aldol reactions indeed proceeded smoothly, with high chemical yields, and pleasingly, with high enantioselection as well.

The data for benzaldehyde (Table 3.1, entries 1 and 2) were discussed in Chapter Two: the catalyst derived from **3-2** provided a slightly higher enantiomeric excess. The

Table 3.1 Mukaiyama Aldol Reactions

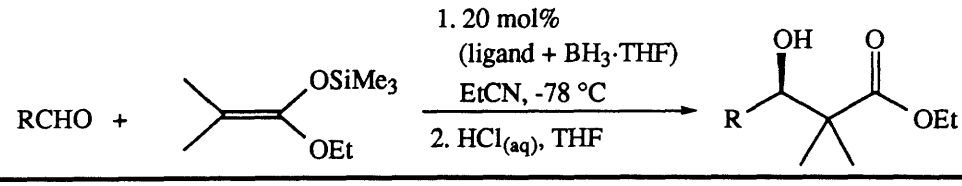

Entry	R	Ligand	Yield/ %	ee/ % (abs. config.)
1	Ph	A	80	84 (*R*)
2	Ph	B	83	91 (*R*)
3	Ph	C	84	91 (*S*)
4	c-C_6H_{11}	A	68	91 (*R*)
5	c-C_6H_{11}	B	59	96 (*R*)
6	$CH_3CH_2CH_2$	A	81	>98
7	$CH_3CH_2CH_2$	B	82	>98
8	$(CH_3)_2CHCH_2$	A	87	97
9	$(CH_3)_2CHCH_2$	B	89	>98
10	$PhCH_2CH_2$	A	83	>98
11	$PhCH_2CH_2$	B	83	>98
12	$PhCH_2OCH_2CH_2$	A	86	99
13	$^tC_4H_9$	B	0	-

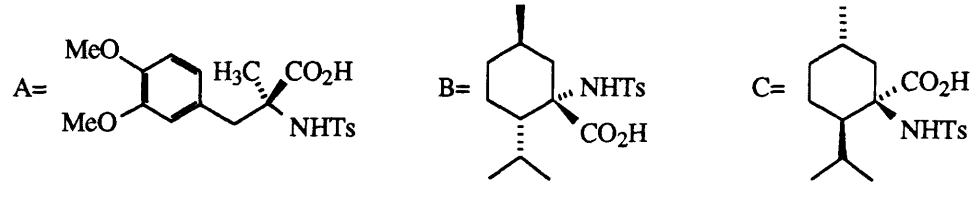

enantiomer of ligand **3-2**, prepared from (+)-menthone, afforded the antipodal aldol with comparable enantioselection. An improvement was also apparent in the reaction using cyclohexanecarboxaldehyde (compare entries 4 and 5). The yields of aldol products in the case of this secondary saturated aldehyde were lower due to incomplete consumption of the starting material.

Primary aldehydes exhibited spectacular results in the Mukaiyama reaction, giving β-hydroxy esters of >97% ee. The majority of these reactions proceeded with near-complete enantioselection and led to the exclusive formation of a single enantiomer with either ligand **3-1** or **3-2** (entries 6–12). The aldol reaction was likewise successful for an oxygenated aldehyde, 3-benzyloxypropanal (entry 12), but a very hindered aldehyde, pivalaldehyde, was almost completely unreactive with the present catalysts (the β-hydroxy ester from pivalaldehyde was obtained in 48% yield when $TiCl_4$ was used as the Lewis acid).

3.2 Determination of Enantiomeric Excess and Absolute Configuration

The determination of enantiomeric excess (ee) by high performance liquid chromatography (HPLC) using a chiral stationary phase[76] is now a routine analytical technique among the research groups involved in asymmetric synthesis. It provides highly accurate results and saves hours of time over older, more laborious methods for ee determination.[77] The enantiomeric excesses for most of the aldol products described in this thesis were obtained by HPLC using Chiralcel OJ and OD columns possessing stationary phases consisting of chiral cellulose derivatives supported on silica gel (Figure 3.1). One

Figure 3.1

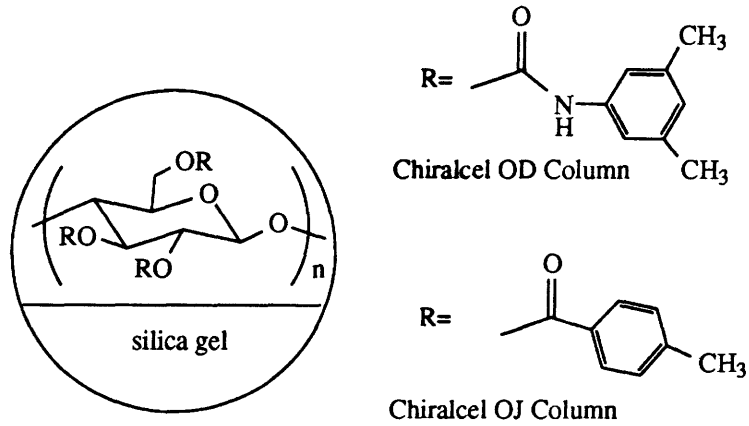

limitation of the method (with our apparatus) is that the aldol products must contain a chromophore for UV detection. For those compounds "invisible" to UV, the enantiomeric

composition was determined by ^{1}H and/or ^{19}F NMR analyses of the Mosher's esters[78] derived from the β-hydroxy esters. Regardless of the method employed, racemic samples of the aldols were analyzed side by side with the optically active samples. The racemic compounds were generally prepared in high yields by Mukaiyama reactions catalyzed by the borane complex of achiral ligand **3-3** (Section 2.2).

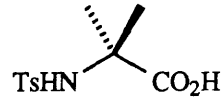

3-3

The aldol products in Table 3.1 from benzaldehyde and cyclohexanecarboxaldehyde were assigned absolute configurations. The assignment for the benzaldehyde product **3-4** was determined by hydrolysis to the corresponding carboxylic acid and comparison of

Scheme 3.1

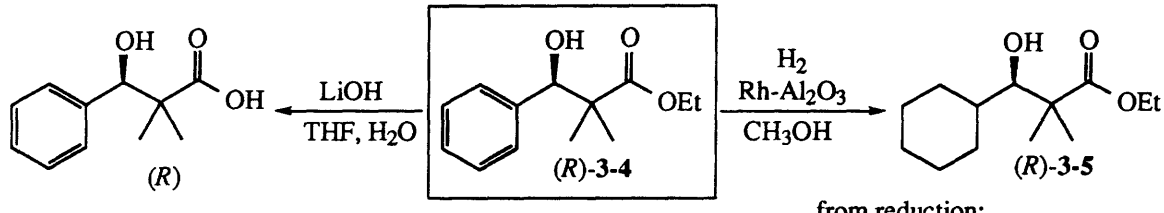

(*R*)

(*R*)-**3-4**

(*R*)-**3-5**

$[\alpha]^{24}_{D}$= -6.4 ° (c 1.0, MeOH)

Lit.[79] $[\alpha]^{24}_{D}$= -7.1 ° (c 1.0, MeOH) for (*R*)-hydroxy acid

from reduction:

$[\alpha]^{24}_{D}$= +16.6 ° (c 0.5, $CHCl_3$)

from aldol rxn.:

$[\alpha]^{24}_{D}$= +19.2 ° (c 0.4, $CHCl_3$)

optical rotations with literature values (Scheme 3.1). The absolute configuration of **3-5** was then determined by comparison with authentic material derived from reduction of the aromatic ring in (*R*)-(–)-**3-4**. The borane complexes of ligands **3-1** and **3-2** gave rise to aldol products with the same absolute configuration.

3.3 Aldol Reactions Using Acetic Acid-Derived Ketene Acetals

The next set of experiments involved Mukaiyama aldol reactions featuring unsubstituted ketene acetals prepared from alkyl and aryl acetates and *S*-alkyl ethanethioates. The enantioselective synthesis of β-hydroxy esters from ketene acetals of

acetate origin is a significant challenge, as has been mentioned earlier (Section 1.5).[37] The results in Table 3.2 demonstrate that excellent yields and stereoselection are possible using

Table 3.2 Aldol Reactions with Acetate-Derived Ketene Acetals

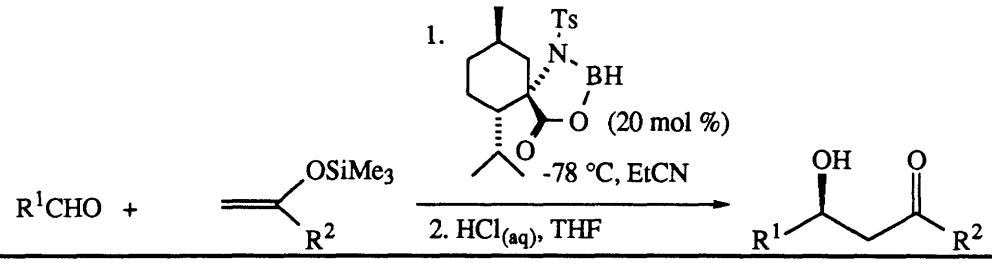

Entry	R^1	R^2	Yield/ %	ee/ % (abs. config.)
1	Ph	S^{t}Bu	86	87 (*S*)
2	Ph	SEt	89	89 (*S*)
3	Ph	OPh	77	93 (*S*)
4	Ph	OCH_2Ph	64	28
5	$PhCH_2CH_2$	S^{t}Bu	77	91 (*R*)
6	$PhCH_2CH_2$	SEt	82	89 (*R*)
7	$PhCH_2CH_2$	OPh	78	85 (*R*)
8	$CH_3CH_2CH_2$	S^{t}Bu	91	92 (*R*)
9	c-C_6H_{11}	S^{t}Bu	75	81 (*S*)
10	c-C_6H_{11}	OPh	87	84 (*S*)
11	(*E*)-^{n}PrCH=CH	S^{t}Bu	91	82
12	2-furyl	S^{t}Bu	98	85
13	2-propenyl	OPh	80	71 (*S*)

the new catalysts. The ligand **3-2** derived from (–)-menthone provided superior selectivities and was used to form the chiral catalyst in every case. The reaction proceeded in high yield and with excellent enantioselection for a variety of aldehydes.

Ketene acetals with OPh, SEt, and S^{t}Bu groups displayed comparable results. However, ketene acetals derived from *O-alkyl* acetates were considerably less reactive and

gave aldol products with low ee (e.g., Table 3.2, entry 4). This behavior of alkyl acetates is precedented but has not been satisfactorily explained: Yamamoto noted that "The reason for this observation is not clear, but certain secondary interactions between electron rich ketene acetals derived from alkyl esters and [the] Lewis acid may be responsible."[44] This, however, does not account for the excellent results with thioester-derived ketene acetals and the disubstituted ketene acetal from ethyl isobutyrate employed in Chapter Two.

3.4 Acetate Aldols: Assignment of Absolute Configuration

The absolute configurations of most of the products listed in Table 3.2 have been unambiguously assigned by the comparison of optical rotations of the corresponding 1,3-diols with those of newly or previously prepared diols of known configuration. Reduction

Scheme 3.2

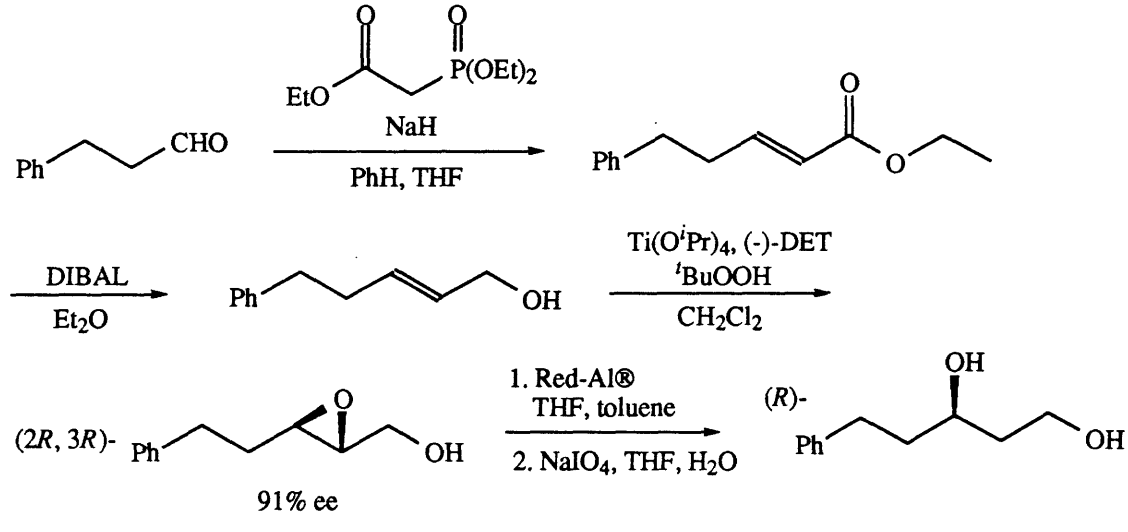

of the β-hydroxy esters to diols was accomplished by treatment with lithium aluminum hydride.[80] For example, the absolute configurations of the products in Table 3.2, entries 5–7, were determined by the preparation of an authentic sample of the diol of established absolute configuration using a sequence including asymmetric Sharpless epoxidation[81] and epoxide opening with sodium bis(2-methoxyethoxy)aluminum hydride (Red-Al®) as shown in Scheme 3.2.[82] The optical rotation values of the diols are tabulated in Table 3.3.

Table 3.3 Assignment of Absolute Configurations

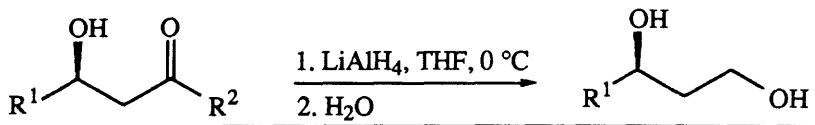

Entry	R^1	R^2	$[\alpha]_D$ for diol (c, $CHCl_3$)	Lit. $[\alpha]_D$ (c, $CHCl_3$), abs. config.	Ref.
1	Ph	S^{t}Bu	-57.4 ° (1.5)	-63.0 ° (1.0), (*S*)	80
2	Ph	SEt	-54.2 ° (1.7)	-63.0 ° (1.0), (*S*)	80
3	Ph	OPh	-34.3 ° (0.60)	-63.0 ° (1.0), (*S*)	80
4	Ph(CH_2)2	S^{t}Bu	+14.5 ° (1.2)	+16.4 ° (1.6), (*R*)	new
5	Ph(CH_2)2	SEt	+14.3 ° (0.51)	+16.4 ° (1.6), (*R*)	new
6	Ph(CH_2)2	OPh	+12.8 ° (0.90)	+16.4 ° (1.6), (*R*)	new
7	CH_3(CH_2)2	S^{t}Bu	-4.2 ° (0.50)	-6.2 ° (0.40), (*R*)	80
8	c-C_6H_{11}	S^{t}Bu	-4.8 ° (0.50)	-8.0 ° (0.59), (*S*)	80
9	c-C_6H_{11}	OPh	-6.3 ° (0.60)	-8.0 ° (0.59), (*S*)	80
10[a]	^{i}Pr	OPh	-9.4 ° (0.64)	-13.8 ° (0.45), (*S*)	80

[a]See Scheme 3.3.

Stereochemical assignment of the hydroxy ester prepared from methacrolein (entry 13 in Table 3.2) was accomplished by reduction of the double bond as well as the ester as shown in Scheme 3.3, and comparison to a diol of known configuration.

Scheme 3.3

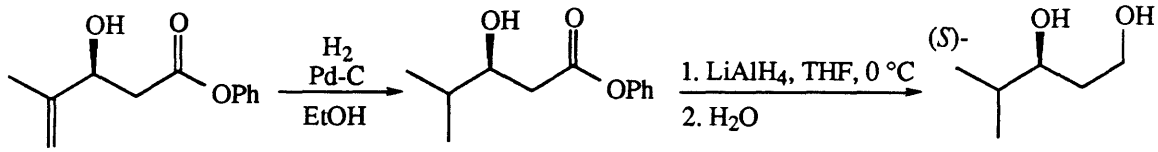

$[\alpha]^{24}_D$= -9.4 ° (c 0.64, $CHCl_3$)
Lit.[80] $[\alpha]^{24}_D$= -13.8 ° (c 0.45, $CHCl_3$)
for (*S*)-isomer

3.5 Aldol Reactions Using Propionic Acid-Derived Ketene Acetals

Next, the effect of a methyl substituent at C(2) of the ketene acetal was investigated. Ketene acetals derived from alkyl and phenyl propionates and *S*-alkyl propanethioates were prepared using LDA and TMSCl[17], with the ratio of *E(O)* and *Z(O)* isomers varying from 98/2 to 11/89 depending on the specific reaction conditions (Table 3.4). Trimethylsilyl ketene acetals prepared from *S*-ethyl propanethioate, *S*-*t*-butyl propanethioate and phenyl

Table 3.4 Preparation of Silyl Ketene Acetals: *E(O)*/*Z(O)*

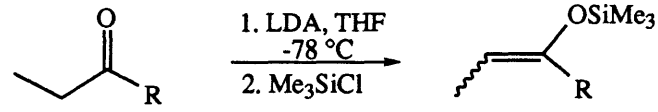

Entry	R	Conditions	Yield/ %	*E(O)* : *Z(O)*
1	OPh	a	70	87 : 13
2	SEt	a	65	94 : 6
3	SEt	a,b	73	11 : 89
4	S^{t}Bu	a	69	>98 : 2
5	O^{t}Bu	a,c	42	91 : 9

(a) Co-addition of the ester and Me3SiCl to pre-formed LDA solution; (b) Reaction mixture included HMPA; (c) Reaction mixture included additional hexane.

propionate reacted under similar conditions with a number of aldehydes to yield a mixture of *anti* and *syn* products, as summarized in Table 3.5. In the reaction between benzaldehyde and the *E(O)* ketene acetals, the *anti* products were favored with good selectivity (entries 1, 3, 4, 5). This result was somewhat unexpected, in light of the *syn* selectivity observed with some of the same substrates in the catalytic systems of Yamamoto[43] and Mukaiyama[36,38]. These new results in fact represent the first examples of this *anti* preference for the catalytic asymmetric reaction. The enantiomeric excesses of both isomers were high, the minor (*syn*) isomer especially being formed with high enantioselectivity. Other aromatic and α,β-unsaturated aldehydes behaved similarly (entries 10–14). Ligand **3-1** was chosen for the aldol reactions of propionate-derived

Table 3.5 Aldol Reactions of Propionate-Derived Ketene Acetals

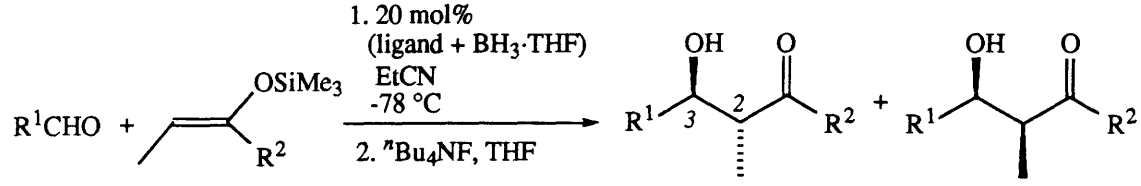

Entry	R^1	R^2 [a]	Ligand	Yield/ %	*anti* : *syn*	ee/ % *anti*/ *syn* (abs. config.)
1	Ph	SEt	**3-2**	89	87 : 13[b]	80 (2*R*, 3*S*)/ 94 (2*S*, 3*S*)
2	Ph	SEt [*Z*(*O*)]	**3-2**	84	45 : 55[b]	64 (2*R*, 3*S*)/ >98 (2*S*, 3*S*)
3	Ph	S^{t}Bu	**3-2**	78	94 : 6[b]	82 (2*R*, 3*S*)/ 66
4	Ph	OPh	**3-2**	77	77 : 23[b]	87 (2*R*, 3*S*)/ >98
5	Ph	O^{t}Bu	**3-2**	74	75 : 25[b]	50/ 37
6	$Ph(CH_2)_2$	SEt	**3-1**	85	91 : 9[e]	82/ 81
7	$Ph(CH_2)_2$	SEt	**3-2**	90	42 : 58[e]	83/ >98
8	$Ph(CH_2)_2$	OPh	**3-1**	72	90 : 10[e]	75/ >98
9	$CH_3(CH_2)_2$	SEt	**3-1**	81	88 : 12[b]	70 (2*R*, 3*R*)/ 81
10	2-furyl	SEt	**3-2**	94	67 : 33[c]	89/ 90 (2*S*, 3*S*)
11	2-furyl	S^{t}Bu	**3-2**	54	88 : 12[d]	79/ 55
12	4-anisyl	SEt	**3-2**	78	89 : 11[c]	75/ >98
13	4-anisyl	OPh	**3-2**	89	71 : 29[d]	63/ 76
14	^{n}PrCH=CH	SEt	**3-2**	80	80 : 20[c]	60/ 73 (2*S*, 3*R*)
15	c-C_6H_{11}	SEt	**3-2**	59	58 : 42[c]	86/ >98

3-1 = α-Me-DOPA-derived ligand; **3-2** = Menthone-derived ligand. [a]For *E*(*O*)/ *Z*(*O*) isomer ratio, see Table 3.4; [b]Assignment by reduction to diol and comparison with spectra in reference 80; [c]Assignment by comparison to reference 36a; [d]Assignment by reduction to diol and comparison with diols derived from compounds in entries 10 and 12; [e]Assignment by reduction to diol and comparison with spectra kindly provided by Dr. Kevin Burgess, Texas A & M University.[83]

ketene acetals with *primary* aldehydes, also giving predominantly *anti* products with high enantioselectivity (entries 6, 8, 9). The use of ligand **3-2** in these reactions led to significantly diminished diastereoselectivities (compare entries 6 and 7). Entry 5 shows again that some ketene acetals derived from alkyl esters react with low stereoselectivity under the present conditions (Section 3.3).

Reaction of the *Z(O)*-isomer of a ketene acetal with benzaldehyde (Table 3.5, entry 2) resulted in lowered reactivity and a loss of diastereoselection when ligand **3-1** or **3-2** was used to form the catalyst (although the enantioselection remained high, particularly for the *syn* isomer of the β-hydroxy ester). The breakdown in diastereoselectivity was also observed by Mukaiyama[36a] with the same ketene acetal in a tin(II)-promoted asymmetric aldol reaction. The *syn* diastereoselection independent of silyl enol ether geometry observed by Yamamoto[43] with the CAB catalyst (Section 1.6) apparently does not apply to the chiral boranes described in this chapter.[84]

3.6 Propionate Aldols: Assignment of Absolute Configuration

Absolute and relative stereochemical assignments for the β-hydroxy-α-methyl esters were determined by comparison of optical rotations with literature values for

Table 3.6 Assignment of Propionate Aldol Absolute Configurations

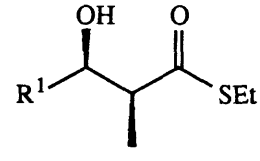

Entry	R^1	$[\alpha]_D$ for aldol	Lit. $[\alpha]_D$, abs. config. for aldol
1	Ph	+61.6 ° (1.6, PhH)	+78.5 °[a] (1.12, PhH), (2*S*, 3*S*)[38c]
2	2-furyl	+30.3 ° (0.52, PhH)	+39.3 ° (3.00, PhH), (2*S*, 3*S*)[36a]
3	(*E*)-^{n}PrCH=CH	+16.7 ° (0.12, PhH)	+39.8 ° (2.70, PhH), (2*S*, 3*R*)[36a]

[a]The sense of rotation for this compound is reported by Mukaiyama incorrectly in reference 36a and correctly in reference 38c.

hydroxy esters or the corresponding 1,3-diols (obtained by LAH reduction) of known configuration.[80] The optical rotation values are tabulated in Tables 3.6 and 3.7.

Table 3.7 Assignment of Propionate Aldol Absolute Configurations

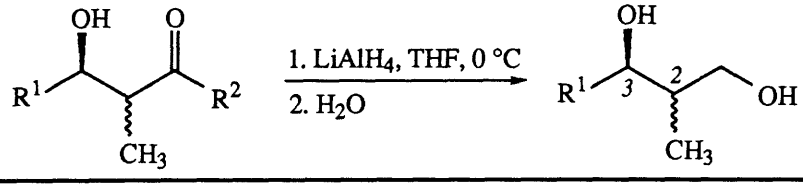

Entry	R^1	R^2	Isomer	$[\alpha]_D$ for diol	Lit. $[\alpha]_D$, abs. config. for diol
1	Ph	S^{t}Bu	*anti*	-28.9 ° (1.2, $CHCl_3$)	-46.8 ° (0.34, $CHCl_3$), (2*S*, 3*S*)[80]
2	Ph	OPh	*anti*	-26.3 ° (0.60, $CHCl_3$)	-46.8 ° (0.34, $CHCl_3$), (2*S*, 3*S*)[80]
3	Ph	SEt	*anti*	-24.2 ° (0.31, $CHCl_3$)	-46.8 ° (0.34, $CHCl_3$), (2*S*, 3*S*)[80]
4	Ph	SEt	*syn*	-30.9 ° (1.4, $CHCl_3$)	+57.8 ° (0.45, $CHCl_3$), (2*S*, 3*R*)[6,85]
5	^{n}Pr	SEt	*anti*	+17.8 ° (1.2, $CHCl_3$)	+33.6 ° (1.0, $CHCl_3$), (2*S*, 3*R*)[80]

3.7 Analysis of Transition States: Source of the Stereoselectivity

Inspection of the absolute configurations reported for the aldol products in this chapter reveals that the sense of asymmetric induction is consistent throughout and corresponds to *si*-face attack of the aldehyde. The same applies to the aldol reactions using several ligands derived from natural amino acids (Chapter Two). The transition state of the reaction is therefore similar for all cases in terms of both the conformation of the catalyst-

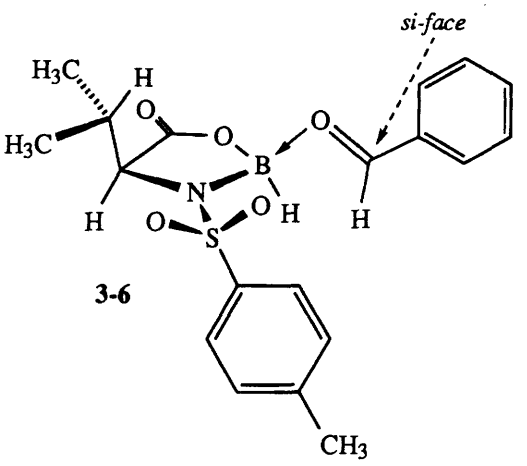

3-6

aldehyde complex, and the enantioface selection of this complex in the reaction with ketene acetals.

Although more experimental work is needed to establish the geometry of the transition state and the factors governing the degree of stereoselectivity for these reactions, an initial hypothesis was developed by examination of molecular models. Transition state **3-6** for the aldol reaction using the valine-derived ligand and benzaldehyde as a model aldehyde allows rationalization of the observed product stereochemistry. A key assumption in the formulation of this transition state is that the isopropyl group and the *para*-toluenesulfonyl group are oriented on opposite sides of the oxazaborolidine ring.[86] Molecular models indicate a severe steric interaction when the arenesulfonyl group is on the

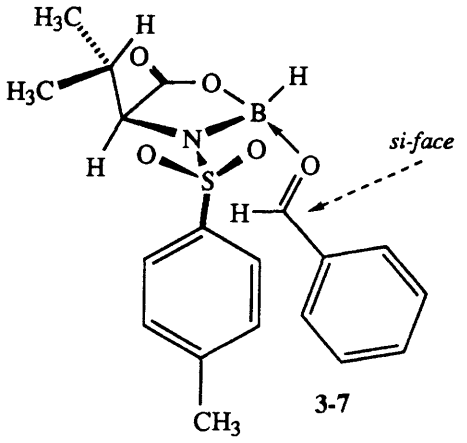

3-7

same ring face as the isopropyl group. The sulfonamide nitrogen is probably nearly planar because of electron donation into the SO_2 group; an X-ray crystal structure of a related diazaaluminolidine bearing trifluoromethylsulfonamide groups shows sp^2 geometry for the nitrogen atoms.[87,88]

The prediction that the lone pair on the aldehyde oxygen that is *anti* to the phenyl group will coordinate to boron is supported by experimental and theoretical evidence.[21a,89] The aldehyde can coordinate to either the upper or the lower face of the oxazaborolidine to be properly oriented for *si*-face attack (**3-6** or **3-7**). Upon coordination, the boron atom becomes a pyramidal stereogenic center. It seems likely that the preferred mode of coordination is to the top face as shown in **3-6**, because steric repulsion with the arenesulfonyl group in **3-7** should outweigh the interaction of the aldehyde with the isopropyl group. In fact, the aldehyde in **3-6** is pointed away from the isopropyl group. The H–B–O=C–H atoms lie in the same plane and the *re*-face of the aldehyde is well shielded by the arenesulfonyl moiety.

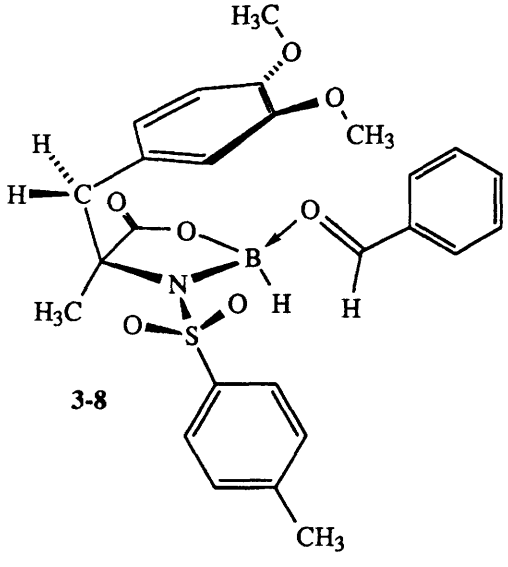

3-8

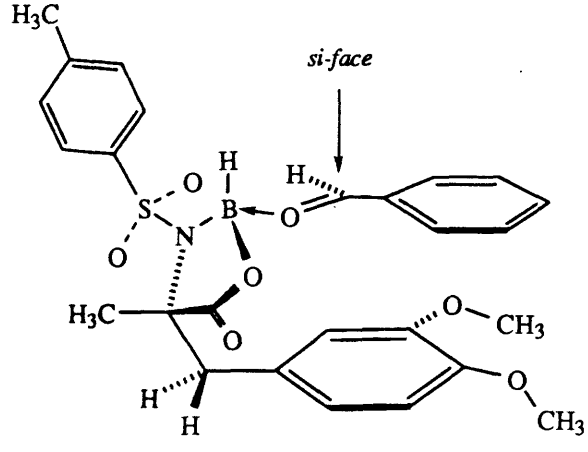

3-9

Application of these principles to the borane complexes of the other ligands provides a satisfactory explanation for the observed enantioselection. The ligand derived from α-methyl-DOPA has the same absolute stereochemistry as the valine ligand. The

analogous transition state model **3-8** allows an antiperiplanar arrangement of the 3,4-dimethoxyphenyl and α-methyl groups. The alternative transition state **3-9**, in which the *re*-face of the aldehyde is effectively shielded by the 3,4-dimethoxyphenyl group, is another possibility.

The complex of benzaldehyde and the chiral borane prepared from **3-2** (the "menthone ligand") is considerably more hindered than the systems described above. As shown in **3-10**, both sides of the oxazaborolidine ring are encumbered by the menthyl moiety: the top face is blocked largely by the isopropyl branch, and the lower face by the bulk of the six-membered ring and the methyl group. Molecular models indicate that **3-10** is the most likely ensemble for the transition state of the aldol reaction. The isopropyl group must be oriented so as to avoid any 1,3-diaxial interactions[90] in the six-membered ring. This disposes the two isopropyl methyls away from the aldehyde and the sulfonyl

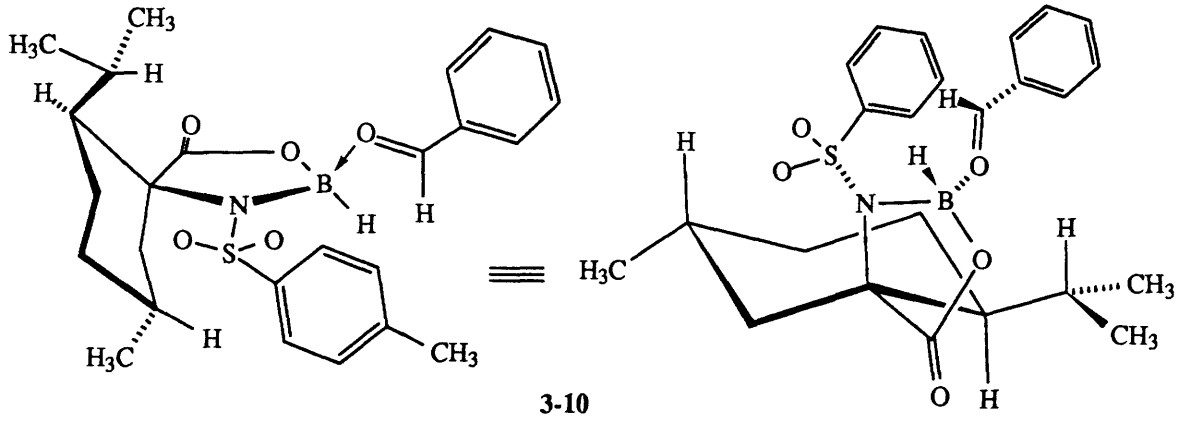

3-10

oxygens. Because both faces of the ring are hindered, the arenesulfonyl substituent likely occupies an intermediate position on the underside of the ring, directed away from the menthyl group. This orientation alleviates the steric encumbrance and also provides improved shielding of the *re*-face of the coordinated aldehyde. The size of the sulfonyl group may not be important with this bulky ligand, as an aldol reaction using the -SO_2CH_3 derivative of **3-2** was still enantioselective (Scheme 3.4).

Scheme 3.4

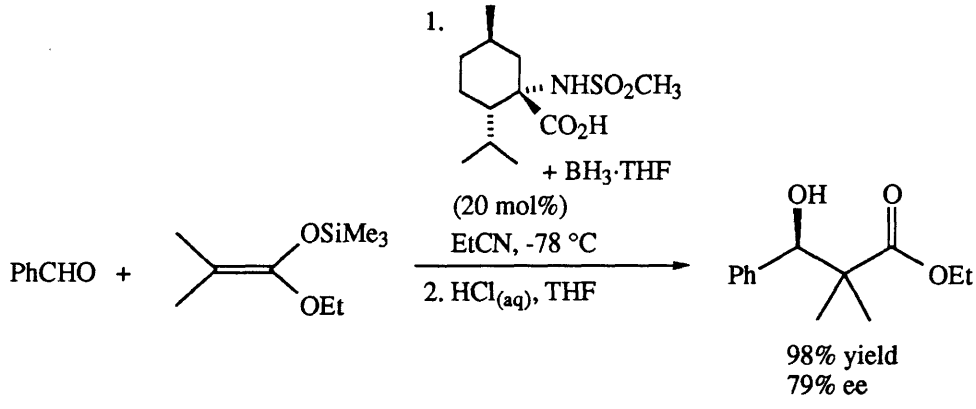

The question of *anti*-diastereoselectivity in the asymmetric aldol reactions of propionate-derived ketene acetals is a more difficult one to address. Many examples of *anti*-selective Mukaiyama-type aldol reactions are known[20] (Chapter One); in fact, $TiCl_4$- and $BF_3{\cdot}OEt_2$-promoted reactions of propionate ketene acetals with bulky groups at C(1) (e.g., ketene acetals from propanethioates such as those mentioned in Section 3.5) generally favor the *anti* aldols independent of ketene acetal double bond stereochemistry.[20] Kiyooka also recently observed *anti* selectivity in reactions using borane complexes of valine-derived ligands.[75] However, the asymmetric aldol reactions developed by Mukaiyama[36] and Yamamoto[43] are *syn*-selective. Single aldehyde and ketene acetal substrates can therefore provide aldol products enriched in *either* the *syn* or *anti* diastereomers depending on the identity of the Lewis acid catalyst.

Diastereoselection in the Mukaiyama aldol reaction is most frequently rationalized in terms of open acyclic transition states[31] (Section 1.4) such as **3-11** and **3-12**. However, these Newman projections do not take the structure of the Lewis acid into account: in the early 1980s the Lewis acids were typically simple metal halides such as $TiCl_4$.[2,20,24] In contrast, the Lewis acid catalysts in the present case incorporate chiral organic ligands, and the specific structures of these catalysts must be taken into account when examining the diastereoselectivity.

3-11 and **3-12** are transition states (for *E(O)*-ketene acetals) leading respectively to the *syn* and *anti* aldols. The *anti* transition state involves a gauche nonbonded interaction

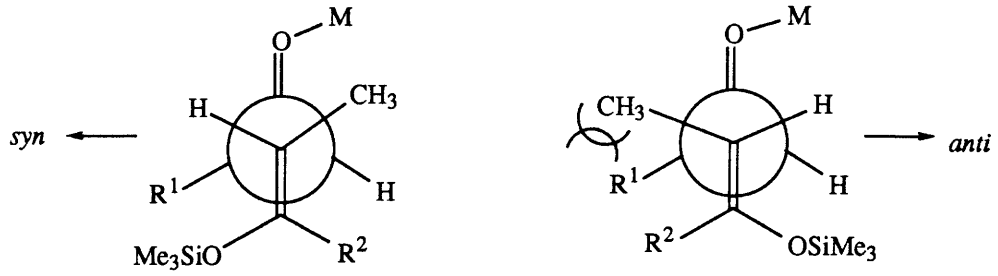

3-11 **3-12**

between the methyl group of the ketene acetal and the R group of the aldehyde, and this steric repulsion is usually invoked to explain the outcome of *syn*-selective reactions.[31] However, a closer inspection of the *syn* transition state with the menthone-derived catalyst using molecular models reveals that the same methyl group experiences steric hindrance with the oxazaborolidine ring (**3-13**). The interaction of the methyl group of the ketene acetal with the catalyst in the *syn* transition state likely overrides the gauche interaction

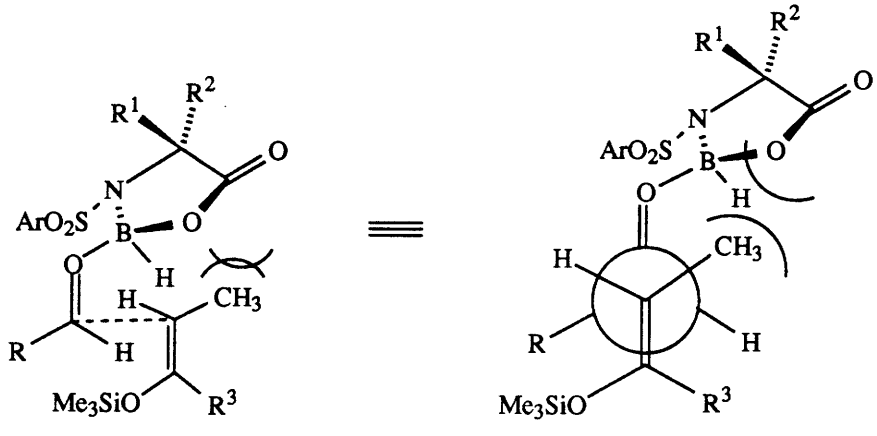

3-13

associated with the *anti* transition state **3-12**, resulting in the observed *anti* selectivity. Similar hypotheses involving contact between the ketene acetal and the catalyst have been advanced to account for *anti* selectivity in previously reported Mukaiyama reactions.[26,27]

One other possibility that has not been ruled out is that the Mukaiyama reaction with the new catalysts proceeds not by an open transition state, but by a closed Zimmerman–Traxler transition state[11] in a boron enolate such as **3-14**. However, this explanation does

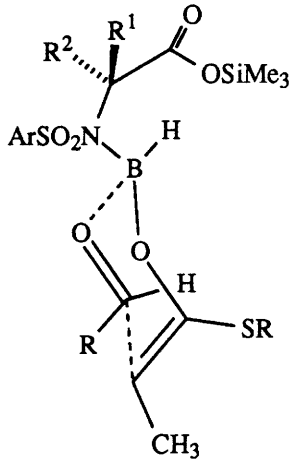

3-14

not seem likely for two reasons: (1) it is difficult to understand why reactions with the new catalysts would proceed by such a mechanism whereas reactions with similar catalysts reported by other groups would not; and (2) the rigid oxazaborolidine ring is opened in the boron enolate intermediate **3-14** and one would not predict high enantioselectivity for such an acyclic structure with a distant stereogenic center. Further conclusions concerning the source of diastereo- and enantioselectivity must await additional experimental evidence.

3.8 Comparison with Literature Results

In Table 3.8 (next page) the yields and enantiomeric excesses for aldol products in this chapter are listed alongside the results from other research groups for ready comparison; both "stoichiometric" and "catalytic" Mukaiyama reactions from the literature are included. The new results match and in many cases exceed those of previous reports, particularly for α-unsubstituted hydroxy esters. The table also shows that further efforts need to be directed toward the improvement of diastereoselectivity in aldol reactions of propionate ketene acetals.

Table 3.8 Comparison with Literature Results

Compound	New Result[a]	Kiyooka Ref. 74[b]	Kiyooka Ref. 75[a]	Yamamoto Ref. 44[a]	Mukaiyama Ref. 36[b]	Mukaiyama Ref. 38[a]
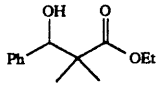	y 83 ee 91	y 77–86 ee 83–93	y 92 ee 90			
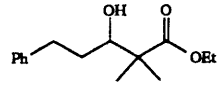	y 83 ee >98	y 87 ee 93	y 97 ee 95			
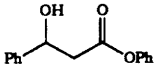	y 77 ee 93		y 66 ee 80	y 63 ee 84		
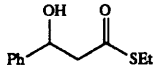	y 89 ee 89				y 52–78 ee 82–92	
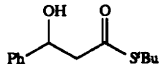	y 86 ee 87				y 73 ee 86	
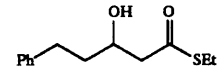	y 82 ee 89				y 50–70 ee 78–81	
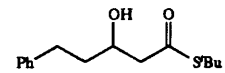	y 77 ee 91				y 71 ee 85	
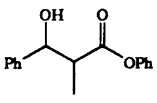	y 77 *a/s*77/23 ee 87/>98		y 91 *a/s* 76/24 ee 66/90	y 83 *a/s* 21/79 ee 6/92		
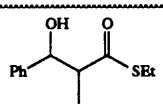	y 89 *a/s* 87/13 ee 80/94				y 86 *a/s* 0/100 ee >98	y 86 *a/s* 7/93 ee 91
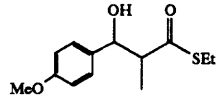	y 78 *a/s* 89/11 ee 75/>98				y 95 *a/s* 0/100 ee >98	
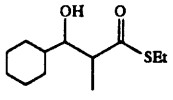	y 59 *a/s* 58/42 ee 86/>98				y 90 *a/s* 0/100 ee >98	
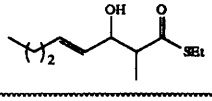	y 80 *a/s* 80/20 ee 60/73				y 91 *a/s* 0/100 ee >98	y 73 *a/s* 3/97 ee 93
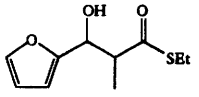	y 94 *a/s* 66/33 ee 89/90				y 93 *a/s* 0/100 ee >98	

y= yield; *a/s*= *anti/ syn* ratio. [a]"catalytic reaction"; [b]"stoichiometric reaction".

Chapter Four

Mukaiyama Reactions of Silyl Enol Ethers

4.1 Introduction

The Mukaiyama-type aldol reactions discussed up to this point have involved silyl ketene acetals as nucleophiles. Another important class of enolate equivalents are the silyl enol ethers, derived from ketones.[17] Silyl enol ethers are versatile and important intermediates, particularly for fragment coupling in the total synthesis of natural products.[16,20] For example, the $BF_3{\cdot}OEt_2$-promoted Mukaiyama reaction shown in Scheme 4.1 was featured in a recent synthesis of the marine natural product calyculin A

Scheme 4.1

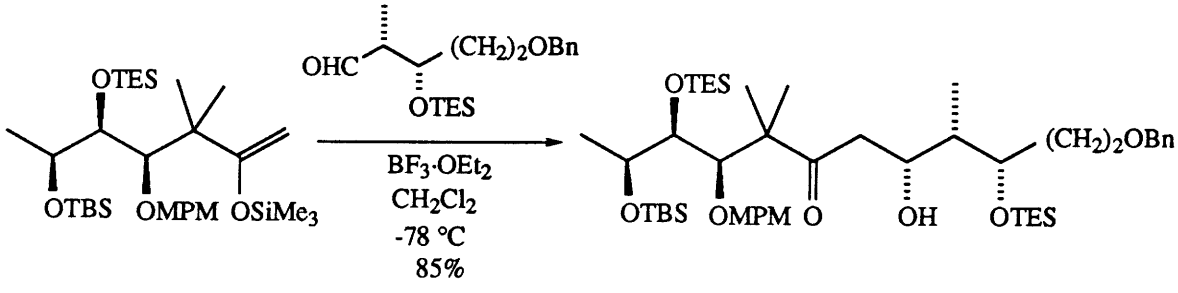

completed in the Masamune research group.[91] The stereochemistry of newly created stereogenic centers in reactions such as that shown in Scheme 4.1 depends upon the diastereofacial selectivities of the individual chiral components.[92] Unless the reaction partners fall into the "matched" case which favors the formation of the desired stereoisomer, the selectivity can be capricious.[92] Chiral Lewis acids that function as

"external" promoters or catalysts such as the chiral boranes described in Chapters Two and Three have potential application in aldol reactions based on the principle of triple asymmetric synthesis[93], wherein the coupling of two chiral fragments—a silyl enol ether and an aldehyde—is mediated by a chiral Lewis acid. One can envision the coupling of chiral substrates via a Mukaiyama reaction in which the chiral Lewis acid serves as a controlling component, enhancing or even overpowering the inherent diastereofacial selectivities of the silyl enol ether and aldehyde. The achievement of high asymmetric induction in aldol reactions of methyl ketones is a particularly challenging task[11], and the development of a catalytic asymmetric Mukaiyama reaction involving terminal silyl enol ethers derived from methyl ketones would be a significant extension of the present work. Because of its potential in the asymmetric synthesis of natural products, the catalytic asymmetric Mukaiyama reaction of silyl enol ethers, especially those of methyl ketones, was investigated.

4.2 Model Reactions

Benzaldehyde and 1-phenyl-1-trimethylsiloxyethene, a silyl enol ether prepared from acetophenone, served as model substrates for the Mukaiyama aldol reaction. The first series of experiments were conducted using a *stoichiometric* amount of the chiral promoter

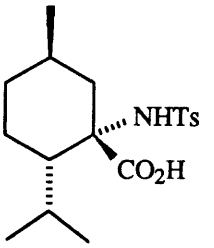

4-1

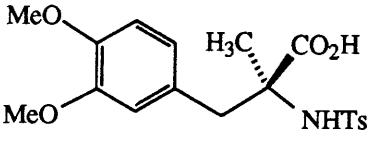

4-2

derived from **4-1**. As shown in Table 4.1, the aldol product was obtained in yields of 35–67% and with enantiomeric excesses of 71–74%, depending on the choice of solvent. However, the β-hydroxy ketone was accompanied by varying amounts of the

corresponding 1,3-diol, probably resulting from intramolecular hydride transfer from boron to the carbonyl group in an intermediate such as **4-3**. Similar reduction was observed in the work of Kiyooka when TBS ketene acetals were employed in aldol

Table 4.1 Asymmetric Aldol Reaction of a Silyl Enol Ether

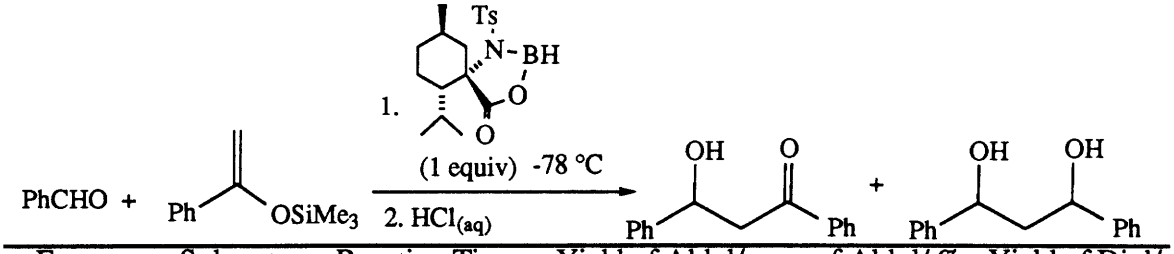

Entry	Solvent	Reaction Time	Yield of Aldol/ %	ee of Aldol/ %	Yield of Diol/ %
1	EtCN	60 min	35	74	31
2	CH_2Cl_2	15 min	59	71	22
3	$EtNO_2$	1 min	67	74	13

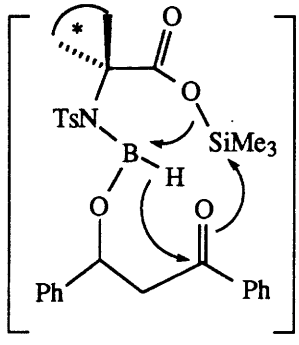

4-3

reactions (Section 2.6).[74] The extent of diol formation was lowest and the rate of the reaction was fastest in nitroethane (entry 3). Presumably, the more polar solvent increases the rate of the turnover step (Section 2.2). The problem of reduction was eliminated when a catalytic (20 mole percent) amount of chiral borane was used for the Mukaiyama reaction as shown in Table 4.2. A higher yield as well as a slightly higher enantioselectivity resulted from this decrease in the proportion of Lewis acid, and no reduced products were detected. As expected, the initial aldol products were the β-siloxy ketones, which were

converted to the corresponding β-hydroxy ketones upon treatment with dilute hydrochloric acid.

Table 4.2 Catalytic Reactions: Slow vs. Fast Addition

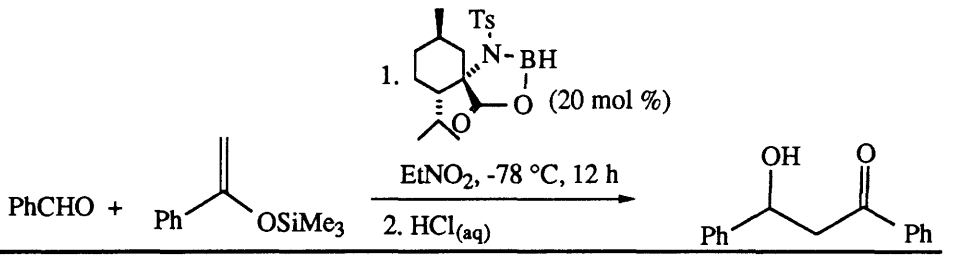

Entry	Mode of Aldehyde Addition	Yield/ %	ee/ %
1	Slow, 3.5 h	71	74
2	Fast, 1 min (neat)	80	79–84

In addition to the change of solvent to nitroethane there were two other modifications of the procedure developed for ketene acetals. Reaction times of 10–20 h were generally required for optimum conversion to β-hydroxy ketones because of the reduced nucleophilicity of silyl enol ethers. For the same reason, slow addition of the aldehyde was not necessary for achieving high enantioselectivity. The results in Table 4.2 demonstrate that comparable enantioselectivity was obtained regardless of whether the aldehyde was added in solution over 3.5 h or added neat over one minute. Apparently the rate of carbon-carbon bond formation is equal to or slower than the rate of catalyst turnover in the case of silyl enol ethers.

The model catalytic aldol reaction was carried out using 20 mole percent of the chiral boranes prepared from a series of amino acid-derived ligands. As shown in Table 4.3, sulfonamido acid ligands derived from valine offered very low yields and enantioselectivities. Ligand **4-2** from α-methyl-DOPA offered only a modest improvement; this behavior is markedly different from the reaction of ketene acetals, in which the same ligand displays much better yields and enantioselection. It is obvious from Table 4.3 that the highest yields and ee values were achieved using ligand **4-1**.[73]

Table 4.3 Asymmetric Aldol Reaction of a Silyl Enol Ether: Ligand Survey

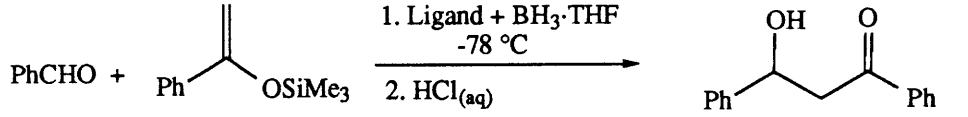

Entry	Ligand	Amt. of Promoter/ mol %	Conditions	Yield/ %	ee/ %
1	A	20	EtCN, 14 h	20	16
2	B	20	$EtNO_2$, 14 h	45	23
3	B	100	$EtNO_2$, 1 h	65	20
4	C	20	EtCN, 14 h	60	54
5	D	20	$EtNO_2$, 14 h	80	79–84

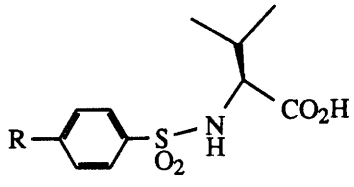

A R= CH_3
B R= NO_2

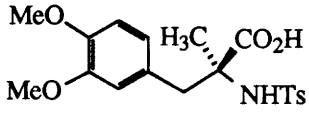

C (4-2)

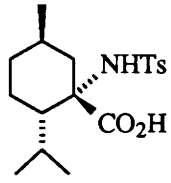

D (4-1)

4.3 Ligand Survey

In earlier chapters the *N*-tosyl derivative of **4-1** was used as a ligand in catalytic aldol reactions. A survey of sulfonyl groups for this ligand was undertaken with the hope of further improving the yield and selectivity of the aldol reaction. The derivatives were prepared by reaction of amino ester **4-4** with a number of alkane- and arenesulfonyl

Scheme 4.2

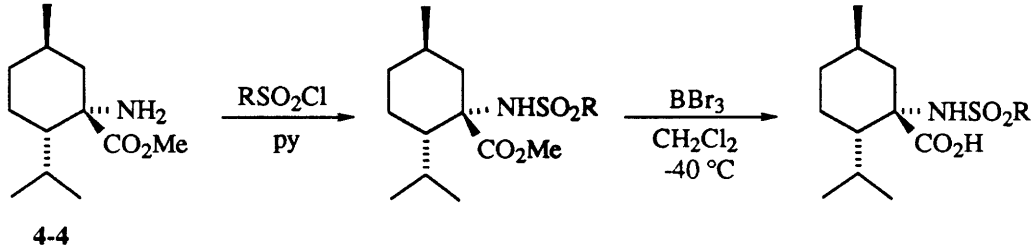

4-4

chlorides in the presence of pyridine (Scheme 4.2). In general, the formation of these sulfonamides was not as smooth as in the α-methyl-DOPA series. The longer reaction times and more intense reaction conditions required are ascribed to the steric hindrance in the amino ester. Despite the lower yields, sufficient quantities of pure sulfonamides were obtained. Hydrolysis of the methyl esters was best effected by treatment with a solution of BBr_3 at low temperature over 3–4 h. This method was an improvement over the original procedure for hydrolysis involving potassium hydroxide in refluxing ethanol and water, which required several days for completion.

Table 4.4 shows the outcome of aldol reactions catalyzed by borane complexes of the new ligands; the results parallel those obtained for the α-methyl-DOPA-derived

Table 4.4 Sulfonyl Derivatives of Ligand **4-1**

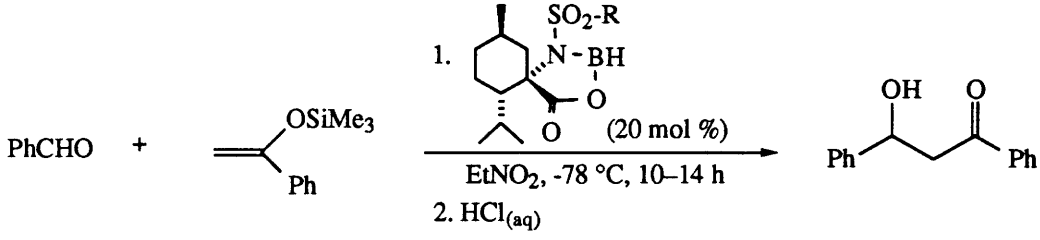

R	Yield/ %	ee/ %	R	Yield/ %	ee/ %
H_3C	80	79–84	MeO	56	40[a]
O_2N	75–80	78–83		71	68[b]
F_3C	95	84	CF_3	43	15[a]
CF_3, CF_3	72	48	CH_3	24	49

[a]Ligand purity ≥ 90%; [b]40 mol % catalyst was used.

sulfonamides in Chapter Two. The best yields and enantioselection were obtained with ligands bearing a substituent in the *para* position of the arenesulfonyl moiety: hence, tosyl, *para*-nitrobenzenesulfonyl, and *para*-(trifluoromethyl)benzenesulfonyl groups provided similar enantioselectivities, with enantiomeric excesses in the 78–84% range. The *para*-methoxy derivative offered only 40% ee but this ligand proved very difficult to purify. Incorporation of a larger aromatic surface (β-naphthyl) led to a small reduction in enantioselectivity whereas triflate and methanesulfonyl groups led to a more substantial decrease.

4.4 Aldol Reactions of Silyl Enol Ethers and Aldehydes

Ligand **4-1** as well as its *para*-nitrobenzenesulfonyl derivative were then used in a series of catalytic aldol reactions involving a variety of aldehydes and both alkyl- and phenyl-substituted terminal silyl enol ethers derived from methyl ketones. Most of the reactions were carried out in nitroethane solvent with fast addition of the neat aldehyde. As shown in Table 4.5, enantiomeric excesses in the range 75–85% were obtained for several aldehydes. The yields were highest for unsaturated aldehydes such as benzaldehyde and cinnamaldehyde. The Mukaiyama reaction of a cyclic silyl enol ether, 1-trimethylsiloxycyclohexene, is also included. Although the yield was low[43], the observed *anti* diastereoselectivity and higher enantiomeric excess of the minor diastereomer are consistent with the reactions of propionate ketene acetals described in Chapter Three.

The five absolute configurations in Table 4.5 were assigned by comparison of aldol optical rotations to literature values.[94] The sense of asymmetric induction, corresponding to *si*-face attack of the aldehyde, is the same in every case and is also consistent with the rest of the aldol reactions described in Chapter Three catalyzed by borane complexes of ligand **4-1**. For a discussion of possible transition states, see Section 3.7.

Table 4.5 Asymmetric Mukaiyama Reactions of Silyl Enol Ethers and Aldehydes

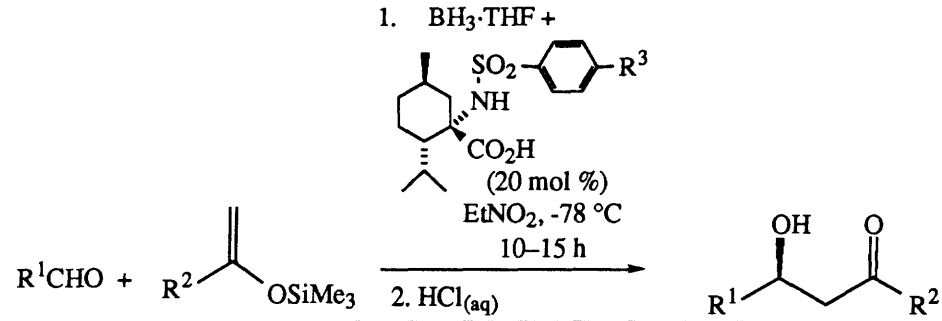

Entry	R^1	R^2	R^3	Yield/ %	ee/% (abs. config.[c])
1	Ph	Ph	CH_3	80	79–84 (*S*)
2[a]	^{n}Pr	Ph	NO_2	52	62 (*R*)
3	c-C_6H_{11}	Ph	CH_3	51	60 (*S*)
4	PhCH=CH	Ph	CH_3	75	74
5	2-furyl	Ph	CH_3	58	81
6	^{i}Pr	Ph	NO_2	45	63
7	4-anisyl	Ph	NO_2	94	69
8	2-propenyl	Ph	CH_3	10[b]	60
9	$Ph(CH_2)_2$	Ph	NO_2	76	78
10	Ph	^{n}Bu	CH_3	86	85 (*S*)
11	c-C_6H_{11}	^{n}Bu	CH_3	53	75 (*S*)
12	PhCH=CH	^{n}Bu	CH_3	77	80
13	^{n}Pr	^{n}Bu	CH_3	53	78
14	$Ph(CH_2)_2$	^{n}Bu	CH_3	63	85
15	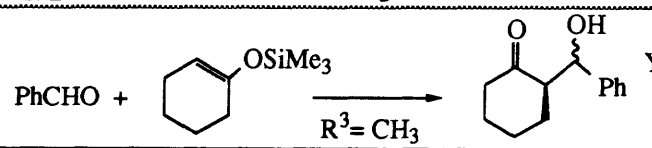				

[a]Propionitrile was used as solvent; [b]Accompanied by 40% of the isomeric 1,4-addition product 2-methyl-5-oxo-5-phenylpentenal; [c]Reference 94.

4.5 Related Literature Results

Fewer reports on the asymmetric Mukaiyama reaction of silyl enol ethers have appeared relative to those concerning ketene acetals. The successful CAB catalyst of Yamamoto has already been described in Chapter One.[43,44] CAB, a chiral borane derived from tartaric acid, efficiently catalyzes the highly stereoselective aldol reaction of silyl enol ethers and aldehydes in propionitrile at -78 °C (Section 1.6). Another important publication in this area came from the group of Corey[94] in 1992; these workers reported highly enantioselective reactions of trimethylsilyl enol ethers and aldehydes in the presence of 20 mole percent of the chiral borane derived from *N*-tosyl-(L)-tryptophane and *n*-butylboronic acid, in propionitrile at -78 °C. The reported results, some of which are shown in Table 4.6, are excellent, but the formation of the *B*-butyl catalyst in refluxing toluene and THF

Table 4.6 Mukaiyama Reactions Reported by Corey[94]

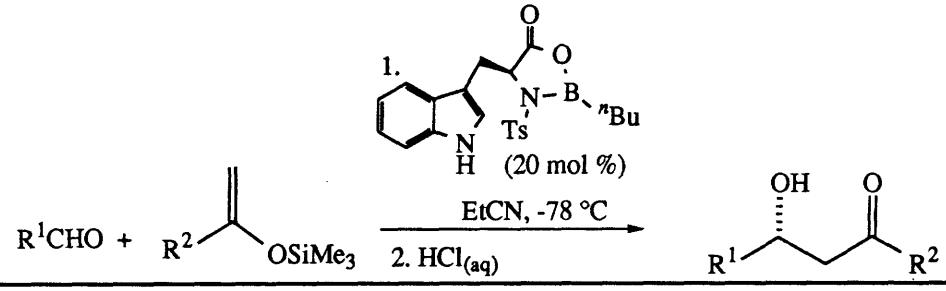

Entry	R^1	R^2	Yield/ %	ee/ % (abs. config.)
1	Ph	Ph	82	89 (*R*)
2	c-C_6H_{11}	Ph	67	93 (*R*)
3	^{n}Pr	Ph	94	89 (*S*)
4	2-furyl	Ph	100	92
5	Ph	^{n}Bu	100	90 (*R*)
6	c-C_6H_{11}	^{n}Bu	56	86 (*R*)

(Scheme 4.3) is tricky and the reaction shown in Entry 1 of Table 4.6 gave, in our hands, a somewhat lower yield (54%) and ee (78%). Corey noted that the level of enantioselection

was lower when the B-CH_3 or B-H analogs of the catalyst were used, although the extent of this difference was not stated. Secondly, silyl ketene acetals did not react with high

Scheme 4.3

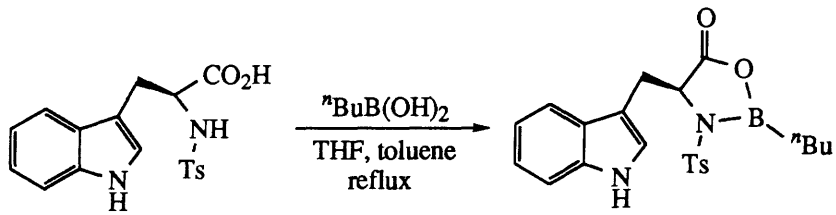

enantioselectivity under similar conditions. There is no obvious explanation for this puzzling disparity.

The absolute configurations shown in Table 4.6 correspond to *re*-face attack on the aldehyde and are opposite in every case to those obtained with the "menthone ligand" **4-1** (Table 4.5). This is somewhat surprising because the absolute configuration of the tryptophane ligand corresponds to that of the α-methyl-DOPA-derived ligand described earlier. Therefore, application of the transition states proposed in Chapter Three to the tryptophane ligand leads to prediction of the wrong β-hydroxy ketone enantiomer. To explain the *re*-face selection Corey proposed the transition state **4-5**, based on a donor-acceptor interaction between the indole ring of the catalyst and the aldehyde.[94] According

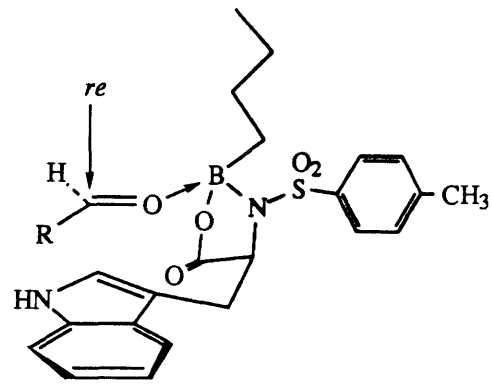

4-5

to **4-5**, the formyl carbon is positioned above the indole nitrogen π-cloud and the carbonyl bond lies above the center of the indole five-membered ring. This transition state is an

extension of a similar model, proposed on the basis of NMR studies, for a Diels–Alder reaction catalyzed by the same chiral borane[95] (see Chapter Five).

Another interesting Mukaiyama reaction, in this case catalyzed by a chiral titanium complex, was reported very recently by Mikami.[96] The reaction of silyl enol ethers with glyoxylate esters afforded aldol-type products in the presence of 5 mole percent of a chiral binaphthol-derived titanium dichloride, as shown in Table 4.7. Near-perfect enantioselection was observed, as well as very high *syn* diastereoselection regardless of the geometry of the starting silyl enol ethers. The products of the reaction are also silyl enol ethers, and this outcome is distinct from the other aldol reactions discussed in this section. The cyclic ene-type transition state **4-6** proposed by the authors has not previously been considered for the Mukaiyama reaction. The excellent results reported with the chiral titanium catalyst are apparently limited to glyoxylate esters and α-benzyloxy aldehydes.

Table 4.7 Asymmetric Ti-Catalyzed Mukaiyama Reaction Reported by Mikami[96]

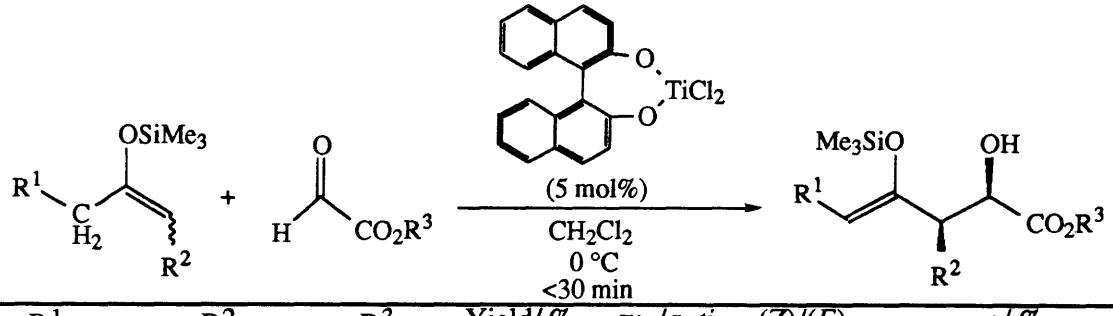

R^1	R^2	R^3	Yield/ %	*syn/anti*	(*Z*)/(*E*)	ee/ % (abs. config.)
CH_3	CH_3 [*Z*(*O*)]	Bu	63	99/1	99/1	99 (*R*)
CH_3	CH_3 [*Z*(*O*)]	Me	58	98/2	94/6	99 (*R*)
CH_3	CH_3 [*E*(*O*)]	Me	54	98/2	96/4	99 (*R*)
CH_3CH_2	H	Bu	67	-	95/5	>99 (*R*)

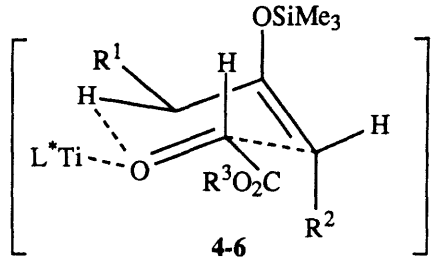

4-6

The new results described in this chapter for catalytic asymmetric aldol reactions of silyl enol ethers are promising, and further research is in progress on the development of more reactive Lewis acid catalysts as well as on the feasibility of triple asymmetric syntheses involving the catalytic Mukaiyama aldol coupling of elaborated chiral silyl enol ethers and aldehydes.

Chapter Five

Modification of the Catalyst and Application to Other Reactions

5.1 Variation of the Substituent on Boron: Alkyl and Aryl Groups

After the new catalysts were successfully applied to a variety of Mukaiyama aldol reactions, our efforts turned toward the modification of these catalysts with the prospect of further improving the reaction rate, yield, and stereoselectivity. One such change involved alteration of the third substituent on the boron atom. The promoters and catalysts described earlier were all prepared using BH_3·THF complex, leading to evolution of hydrogen and formation of a species presumably containing a B-H bond. Corey, however, reported impressive results for Diels–Alder[95] and Mukaiyama[94] reactions catalyzed by a tryptophane-derived chiral borane with an *n*-butyl group on boron. Yamamoto as well described high yields and enantioselectivities for asymmetric hetero-Diels–Alder[97] and Mukaiyama[97,98] reactions catalyzed by *B*-alkyl and *B*-aryl derivatives of the CAB species. These boranes were generally prepared by reaction of the ligand with an alkyl- or arylboronic acid. The Yamamoto catalysts were formed in propionitrile at room temperature, apparently without removal of the liberated water, whereas the Corey oxazaborolidine was prepared in refluxing THF and toluene with removal of water by calcium hydride in a Soxhlet-type apparatus. Both research groups reported sizable effects of the boron substituent on the reactivity of the catalyst and the enantioselectivity of the various reactions. Motivated by these results, we investigated the synthesis of *B*-alkyl and *B*-aryl complexes of the new α,α-disubstituted sulfonamido acid ligands.

Attempts at synthesizing a *B*-alkyl complex from **5-1** under a variety of conditions

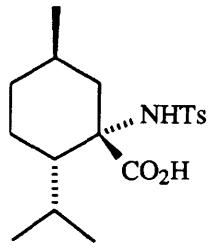

5-1

using methyl-, butyl-, or phenylboronic acids were unsuccessful; the resulting species were complex by NMR spectroscopy and did not promote the Mukaiyama reaction. In contrast, the reaction proceeded smoothly using ligand **5-2** and butylboronic acid as shown in Scheme 5.1; in the presence of 20 mole percent of the chiral borane, the β-hydroxy ketone

Scheme 5.1

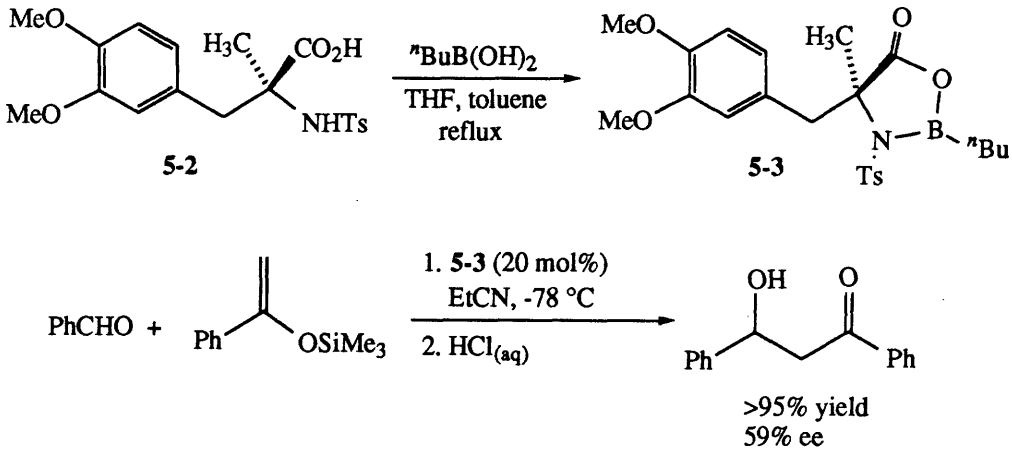

was obtained in near-quantitative yield and with 59% ee. The source of the difference in reactivity between ligands **5-1** and **5-2** is not known but may reflect the greater steric encumbrance in **5-1**.

Additional work focused on installation of the *B*-alkyl group by a different procedure. Reaction of ligand **5-1** or **5-4** with commercially available phenyldichloroborane led to liberation of hydrochloric acid and formation of the phenylboron complexes **5-5** and **5-6** (Scheme 5.2); the B-Ph complex **5-5** could in fact be

Scheme 5.2

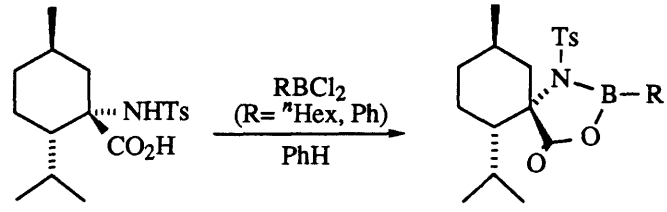

5-1

5-5 R= Ph
5-7 R= ^{n}Hex

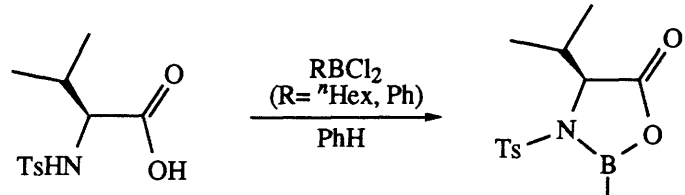

5-4

5-6 R= Ph
5-8 R= ^{n}Hex

Table 5.1 *B*-Alkyl Derivatives in Mukaiyama Aldol Reactions

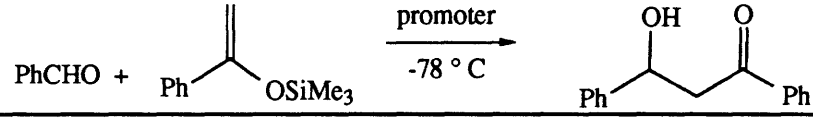

Entry	Promoter, mol %	Solvent	Yield/ %	ee/ %
1	**5-7**, 40%	EtCN	22	0
2	**5-7**, 20%	$EtNO_2$	85	0
3	**5-7**, 20%	^{n}BuCN	0	-
4	**5-5**, 28%	EtCN	94	2

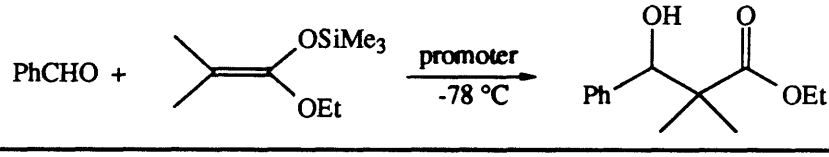

5	**5-6**, 100%	EtCN	90	20
6	**5-5**, 25%	EtCN	89	12

isolated as a white powder (see spectrum 6 in Appendix One). The preparation of *B*-*n*-hexyl complexes **5-7** and **5-8** from *n*-hexyldichloroborane[99] was also successful. Unfortunately, the performance of these new derivatives in aldol reactions was disappointing (Table 5.1). In some cases the yields were high but the enantiomeric excesses were always low (or zero). In the procedures involving *n*-hexyl- or phenyldichloroborane, the newly prepared borane complexes were flushed with solvent and evaporated several times to remove all traces of liberated hydrochloric acid. For ligand **5-1**, the reaction was attempted in several solvents (Table 5.1, entries 1–3): after addition of the aldehyde to the reaction mixture with propionitrile or nitroethane the formation of a precipitate was observed, possibly an insoluble complex of the aldehyde and the catalyst. Changing the solvent to valeronitrile solved this solubility problem, but only a trace of aldol product was detected. Because of their difficulty in preparation and poor performance in the Mukaiyama aldol reaction, the study of *B*-alkyl and *B*-aryl derivatives was shortly abandoned.

5.2 Variation of the Substituent on Boron: Electron-Withdrawing Groups

In an attempt to enhance the Lewis acidity of the promoters, the effect of electron-withdrawing groups on the boron atom was assayed. Experiments aimed at preparing B-Br and B-Cl complexes by reaction of ligands **5-1**, **-2**, and **-4** with BBr_3 and BCl_3 led to formation of complex and multiple species as indicated by ^1H NMR spectroscopy. Aldol reactions carried out in the presence of these species proceeded but without enantioselection. A higher degree of success was achieved in preparing B-OAc and B-OSO_2CH_3 derivatives. This was accomplished by formation of the B-H compound as usual using BH_3·THF, followed by addition of acetic or methanesulfonic acid (Scheme 5.3). One equivalent of methanesulfonic acid was added to a solution of borane **5-9** at -78 °C, followed by warming to 0 °C during which hydrogen was released. The ensuing aldol reaction (using one equivalent of promoter) proceeded very cleanly, giving the β-hydroxy

ester in 91% yield and with 88% ee (Table 5.2, entry 1). Trials involving triflic acid afforded complicated reaction mixtures. The aldol reaction featuring an equimolar amount of the B-OAc derivative afforded aldol product of 71% ee in 89% yield (entry 2). When the procedure was carried over to ligand **5-1**, the results shown in entries 3 and 4 were obtained. Examination of the promoter by ^{1}H and ^{11}B NMR spectroscopy again revealed

Scheme 5.3

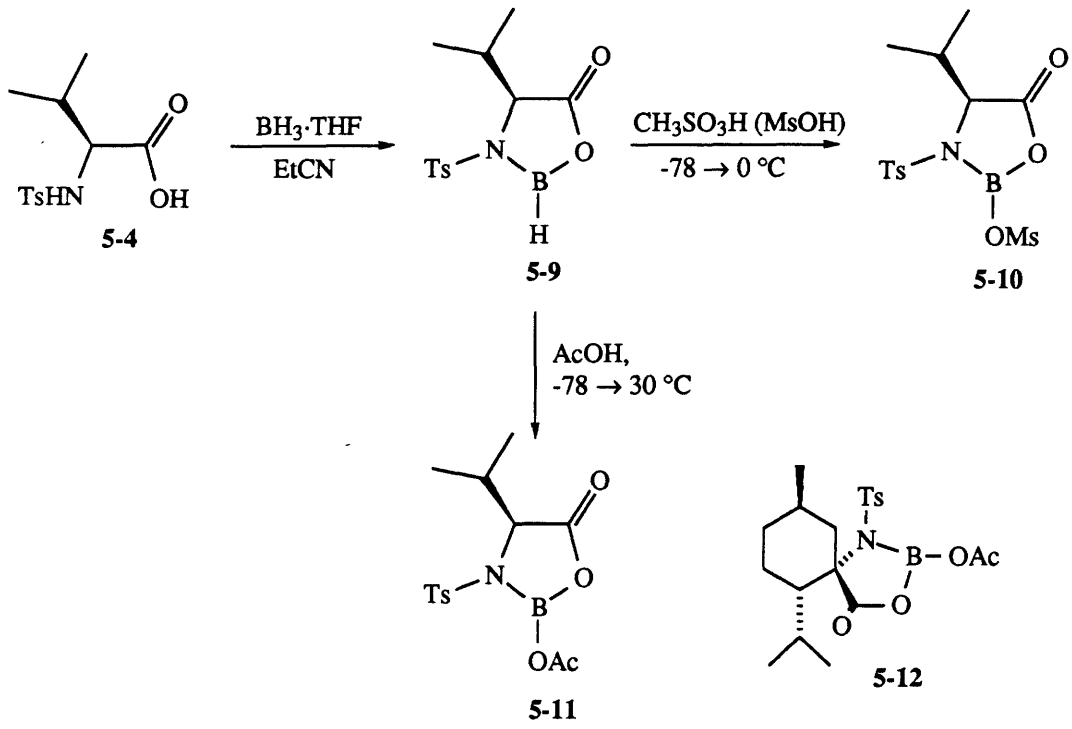

a complex mixture of components. This work was not pursued further because the yields and enantioselectivities were no better (and in some cases inferior to) those afforded by the analogous B-H complexes.

5.3 Application to Allylation, Imine Addition, and Michael Reactions

A separate set of experiments were directed toward expanding the versatility of the chiral boranes by application to different organic reactions. Allyltrimethylsilane was unreactive in a trial allylation reaction with benzaldehyde conducted in propionitrile in the presence of one equivalent of the promoter (Table 5.3). Allyltri-*n*-butylstannane was

somewhat more reactive: the extent of addition was about 50% after 10 h at -78 °C, but the enantiomeric excess of the product was low (33%). Asymmetric allylation processes

Table 5.2 Performance of B-OMs and B-OAc Derivatives in the Aldol Reaction

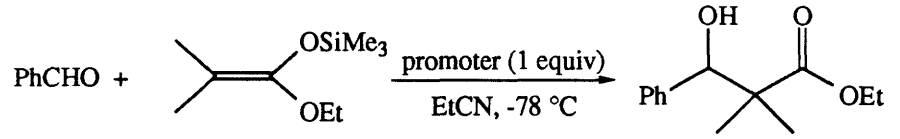

Entry	Promoter	Yield/ %	ee/ %
1	**5-10**	91	88
2	**5-11**	89	71
3	**5-12**	90	26

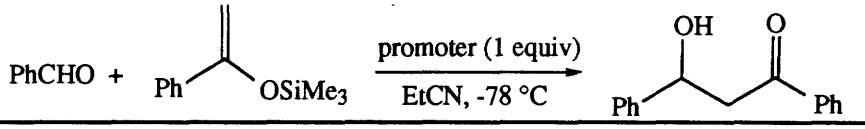

4	**5-12**	80	57

catalyzed by a chiral borane[100] (CAB) and chiral binaphthol-derived titanium complexes[101,102] have recently appeared from three other research groups.

Table 5.3 Allylation Reactions

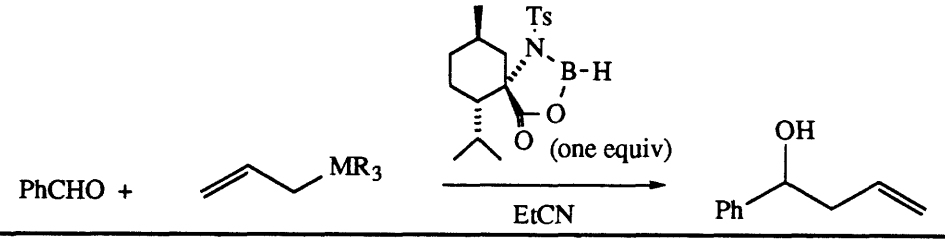

Entry	MR3	Conditions	Yield/ %	ee/ %
1	SiMe3	-78 °C → RT, 10 h	0	-
2	SnBu3	-78 °C, 10 h	~50	33

The asymmetric addition of ketene acetals to imines was also surveyed.[103] Chiral β-amino esters are precursors to β-lactams and are thus useful intermediates in organic

synthesis.[103] As shown in Table 5.4 the reaction of *N*-benzylideneaniline with a ketene acetal was efficiently promoted by chiral boranes, but disappointingly, without

Table 5.4 Imine Addition Reactions

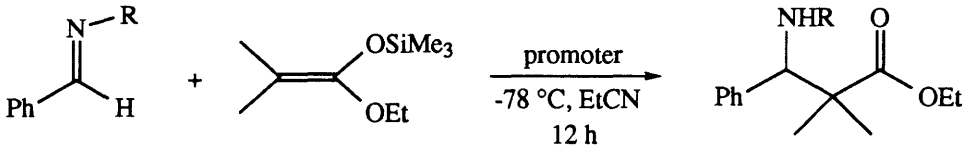

Entry	R	Promoter, mol %	Yield/ %	ee/ %
1	Ph	A, 100%	63	0
2	Ph	B, 20%	90	0
3	CH_2Ph	B, 20%	25	0

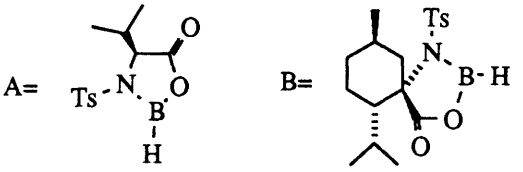

enantioselection. The reaction in entry 3 only proceeded with a 25% yield probably due to inhibition of the catalyst by irreversible coordination of the alkylamine product to boron. In contrast, the β-amino ester in entries 1 and 2 was obtained in higher yield apparently because of weaker coordination to boron due to the electron-withdrawing phenyl group on nitrogen.

Scheme 5.4

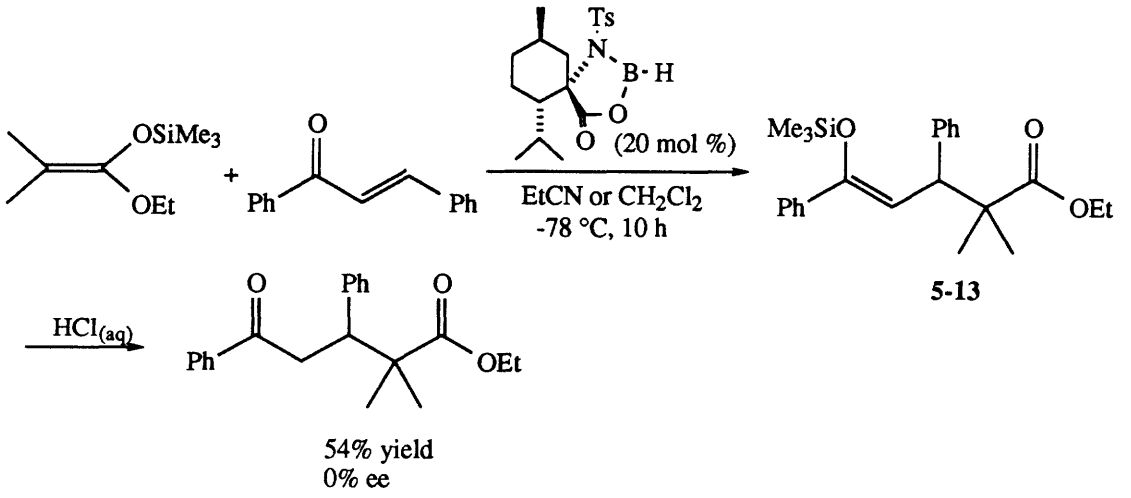

A trial Mukaiyama–Michael reaction[33b,104] of chalcone (an α,β-unsaturated ketone) and a ketene acetal led to formation of the 1,4-addition product as the silyl enol ether **5-13**, which was converted to the corresponding ketone by treatment with dilute acid (Scheme 5.4). Unfortunately, there was no enantioselectivity in this reaction either. The lack of stereoselection in this case might be due to the increased distance of the electrophilic carbon from the stereogenic center of the ligand.

5.4 Diels–Alder Reaction

More encouraging results were at hand when the chiral catalysts were applied to Diels–Alder cycloaddition reactions. This did not come as a surprise since several chiral boranes were already known to catalyze the reaction. These, as well as other Diels–Alder catalysts are shown in Figure 5.1. Cyclopentadiene and the dienophile methacrolein are

Figure 5.1 Chiral Catalysts for Diels–Alder Reactions

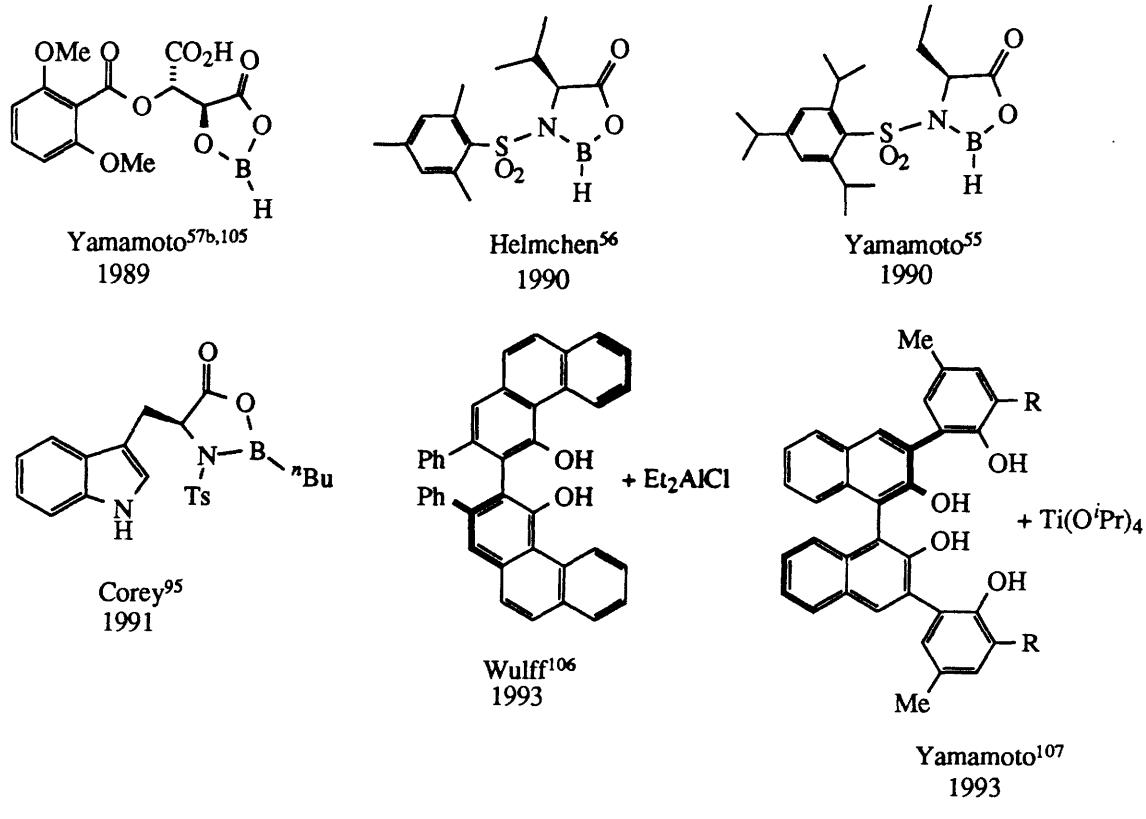

frequently chosen substrates for model studies. Diels–Alder reactions using 20 mole percent of catalyst from **5-2** under a number of conditions gave high yields of *exo* adduct with enantiomeric excesses of up to 39% (Table 5.5). The ee increased to 59% with ligand **5-1** in propionitrile. Furthermore, a dramatic improvement in enantioselectivity to 76% ee resulted upon changing the reaction solvent from propionitrile to THF. This solvent effect

Table 5.5 Catalytic Asymmetric Diels–Alder Reactions

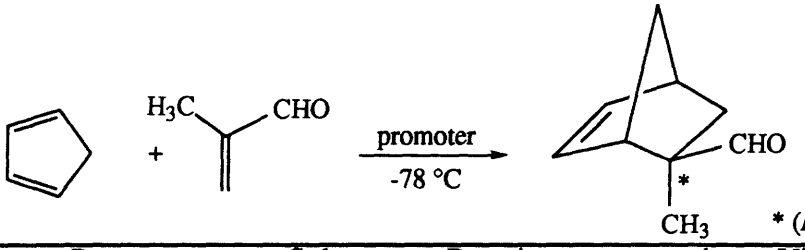

* (*R*)-(–)-isomer shown

Entry	Promoter, mol %	Solvent	Reaction Time	*exo*:*endo*	Yield/ %	ee/ % (abs config.)
1	A, 20%	EtCN	10 h	98:2	77	39 (*R*)
2	A, 20%	EtCN	3.5 h	97:3	68	38 (*R*)
3	A, 20%	CH_2Cl_2	24 h	97:3	75	28 (*R*)
4	A, 100%	EtCN	3 h	97:3	67	20 (*R*)
5	B, 20%	EtCN	12 h	98:2	87	59 (*R*)
6	B, 20%	THF	12 h	98:2	85	76 (*R*)

A= 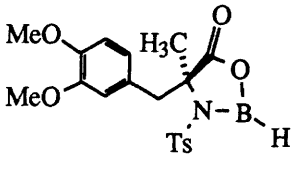

B= 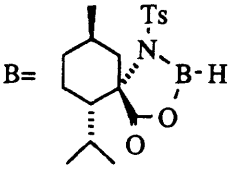

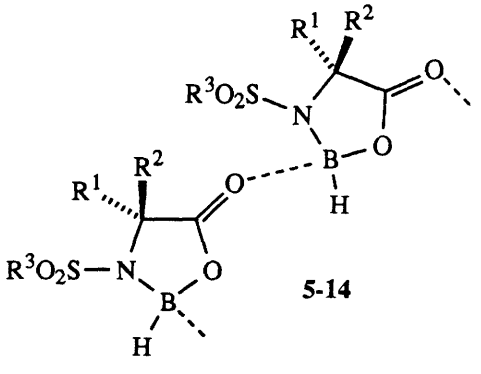

5-14

was precedented: in 1991 Helmchen reported the superiority of THF in asymmetric Diels–Alder reactions using chiral boranes derived from valine and *t*-leucine.[86] The donor solvent supposedly increases enantioselectivity by reducing species multiplicity, namely, the intermolecular association of catalyst molecules as shown in **5-14**.

Both catalysts shown in Table 5.5 provide the (*R*)-isomer of the cycloadduct; the transition states **5-15** and **5-16** give rise to the observed selectivity. These involve *si*-face attack on *s-cis* coordinated enals and are consistent with the transition state suggested by Helmchen[108] for a similar Diels–Alder reaction. **5-15** and **5-16** are also in accord with

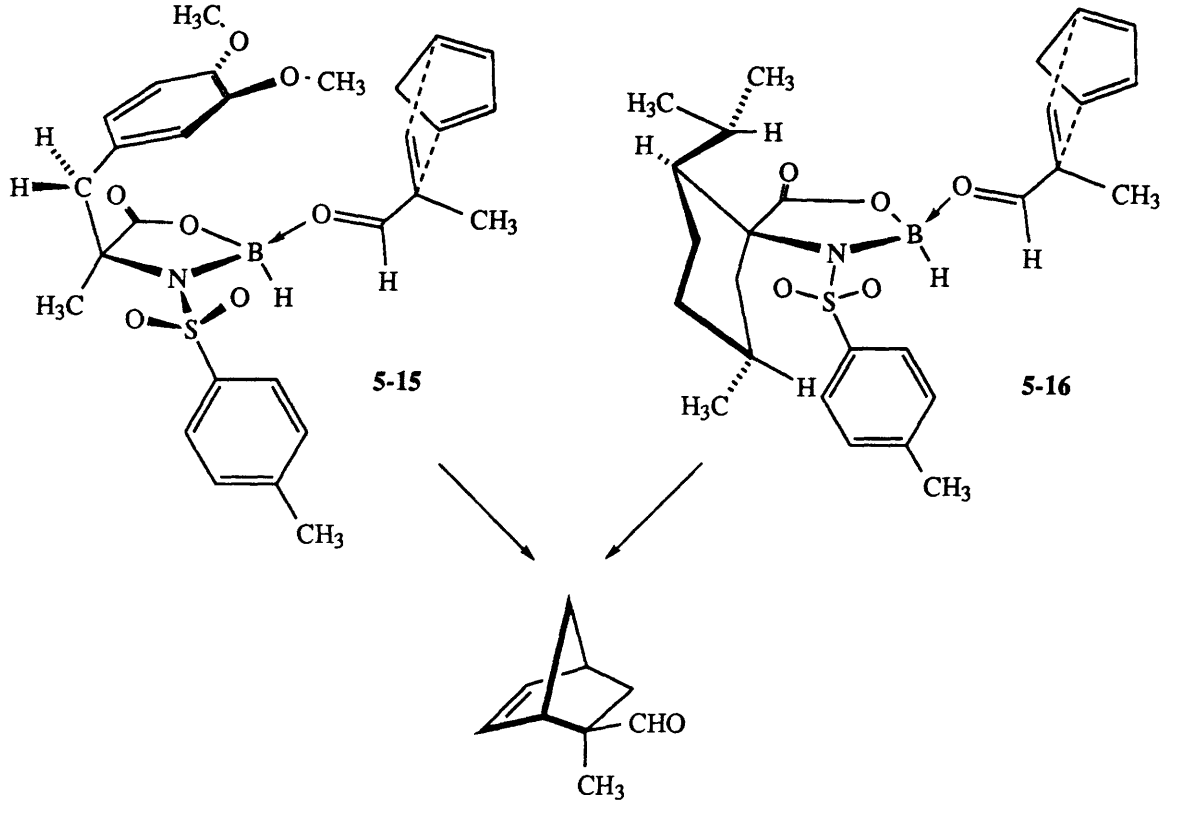

the transition states for Mukaiyama aldol reactions put forth in Chapter Three. However, the Diels–Alder transition state **5-17** proposed by Corey, featuring a donor–acceptor interaction between the enal and the aromatic indole group of the catalyst, leads to the opposite sense of asymmetric induction.[95b] Corey observed a loss of enantioselection and a reversal in selectivity when the indole in **5-17** was replaced with phenyl, cyclohexyl, or

isopropyl groups.[95b] A recent report by Scheeren and Seerden[108] also confirms that electron donor functionality at certain positions in the α-side chain substituent of the amino acid ligand brings about a change in the absolute configurations of Diels–Alder adducts.

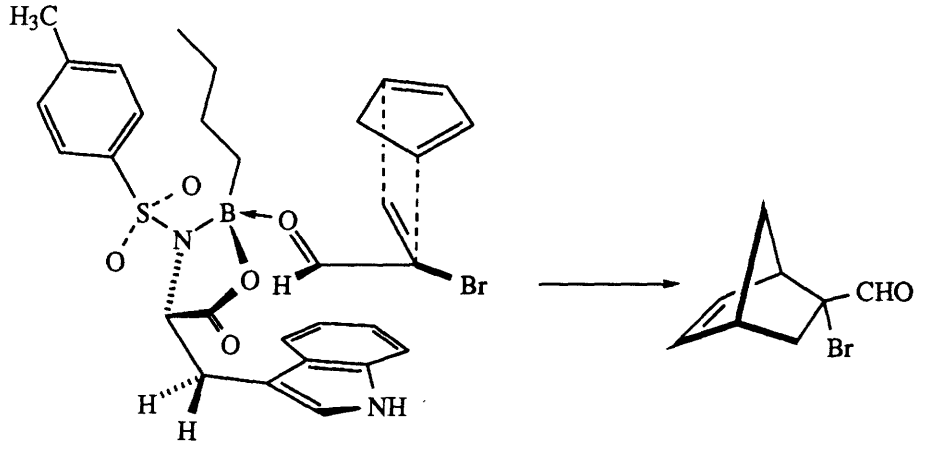

5-17

The ensembles shown above involve *s-cis* reactive conformations for the unsaturated aldehydes. *Uncomplexed* methacrolein is known to exist primarily in the *s-trans* conformation[95b,98], but the conformation of the *Lewis acid-coordinated* enal can vary. For example, in contrast to **5-15–5-17**, the transition state proposed by Yamamoto on the basis of NOE experiments for the CAB-catalyzed Diels–Alder reaction includes an *s-trans*-coordinated enal.[98] However, at equilibrium both the *s-cis* and *s-trans* coordination modes may be present and the stereoselection is ultimately determined by the relative free energies of activation for the reaction of the two complexes.[95b,98]

5.5 Conclusion

In the last four or five years, a number of remarkable reports describing catalytic asymmetric variants of key carbon-carbon bond forming reactions have appeared in the chemical literature. This new generation of transformations surpasses many of the older, more cumbersome auxiliary-based methods of stereocontrol. This thesis describes a new series of chiral, boron-based Lewis acids prepared from α,α-disubstituted amino acid

sulfonamides. The Mukaiyama aldol reaction, an important and versatile method for the synthesis of optically active β-hydroxy esters and ketones, proceeds efficiently and with a high degree of stereoselectivity in the presence of substoichiometric amounts of these Lewis acids. The chiral boranes also demonstrate some utility in asymmetric Diels–Alder cycloadditions but are less successful in allylation, conjugate addition, and imine addition reactions.

The ultimate chiral Lewis acid, one that catalyzes a broad spectrum of highly stereoselective organic reactions, has not yet been discovered. The realization of a versatile catalyst will require continued vigorous research in the field of asymmetric catalysis. As observed by Seebach[109] in a 1990 survey of the current status of organic chemistry, "Even though it has sometimes been possible to discern the mechanism of a catalytic reaction...the rational design of a structurally defined chiral catalyst is still in its infancy."

Chapter Six

Experimental

6.1 General Methods

All reactions were carried out under an argon atmosphere in flame- or oven-dried glassware. Tetrahydrofuran (THF), ether, toluene, and benzene were distilled from dark blue sodium benzophenone ketyl under argon. Dichloromethane, hexane, nitroethane, propionitrile, trimethylsilyl chloride (TMSCl), hexamethylphosphoramide (HMPA), pyridine, diisopropylamine, and triethylamine were distilled from calcium hydride under argon. Ethanol and methanol were distilled from their respective magnesium alkoxides. Aldehydes were generally washed with saturated sodium bicarbonate solution, dried with magnesium sulfate, and vacuum distilled. (*R*)- and (*S*)-Mosher's acid chloride (MTPACl) were purchased from JPS Chimie (Bevaix, Switzerland); enantiomeric purity of >98% for these compounds was confirmed by ^{1}H NMR analysis of the Mosher's esters[78] derived from racemic 2-phenyl-1-propanol. The concentration of *n*-butyllithium solutions was determined by titration using *sec*-butanol in benzene with 2,2′-bipyridine as an indicator.[110] Borane·THF solution in THF (1M, Aldrich) was taken from newly or recently opened bottles. Tosyl chloride (Fluka) of >98% purity was recrystallized from toluene/hexane. 1-(Trimethylsiloxy)cyclohexene was purchased from Fluka. Other reagents, available from Aldrich, Lancaster, Fluka, Alfa, and other companies, were used without further purification. Flash column chromatography was performed as described by Still et al.[111], using 230-400 mesh silica gel (Baker or E. Merck). Thin layer chromatography was performed on glass plates precoated with a 0.25 mm layer of 230-400

mesh silica gel (E. Merck Silica Gel 60 F-254); visualization of spots on TLC plates was facilitated by the use of 10% phosphomolybdic acid solution in ethanol as a stain.

Proton nuclear magnetic resonance (^{1}H NMR) spectra were recorded on Bruker WM250 (250 MHz), Bruker AC250 (250 MHz), Varian XL300 (300 MHz), Varian Unity 300 (300 MHz) or Varian VXR500 (500 MHz) spectrometers. Proton chemical shifts are expressed in parts per million (δ scale) downfield from tetramethylsilane and are referenced to residual proton resonances in the NMR solvent ($CDCl_3$, δ 7.24; C_6D_6, δ 7.15; CD_3OD, δ 3.30). Multiplicities of peaks in ^{1}H spectra are given the following designations: br= broad, s= singlet, d= doublet, t= triplet, q= quartet, sept= septet, dd= double doublet, m= multiplet, AB= AB multiplet, ABX= ABX multiplet. All ^{13}C (75.4 MHz), ^{11}B (96.3 MHz) and ^{19}F (282.2 MHz) spectra were recorded on a Varian XL-300 multinuclear spectrometer. Carbon nuclear magnetic resonance (^{13}C NMR) spectra are fully proton-decoupled, and chemical shifts are reported in ppm (δ scale) downfield from tetramethylsilane with solvent resonances as an internal reference ($CDCl_3$, δ 77.0; C_6D_6, δ 128.0; CD_3OD, δ 49.0). ^{11}B NMR spectra are referenced to external $BF_3{\cdot}OEt_2$ (δ 0.0). ^{19}F NMR spectra, used for Mosher's ester analysis, are unreferenced.

Infrared (IR) spectra were recorded using a Perkin-Elmer Series 1600 FT-IR spectrophotometer referenced to a polystyrene standard. Optical rotations were measured at ambient temperature in 1-dm cells on a Perkin-Elmer 241 polarimeter. Mass spectra were obtained by Mr. Edward Takach of the MIT Spectrometry Laboratory using a Finnigan Mat 8200 spectrometer. High performance liquid chromatography (HPLC) analyses were performed using a Waters Associates Model 660 solvent programmer, Model 440 absorbance detector, Models 6000A and M-45 solvent delivery systems, and Model U6K injector; a Shimadzu C-R6A Chromatopac integrator/plotter; and Chiralcel OD and OJ chiral chromatography columns (length 250 mm, i.d. 4.6 mm) manufactured by Daicel Chemical Industries, Ltd. Melting points were recorded on a Thomas-Hoover capillary melting point

apparatus and are uncorrected. Sage Instruments Model 341 or 352 syringe pumps were used in procedures requiring slow syringe pump addition.

6.2 Ligands Derived from Natural Amino Acids and 2-Amino-2-phenylpropionic acid

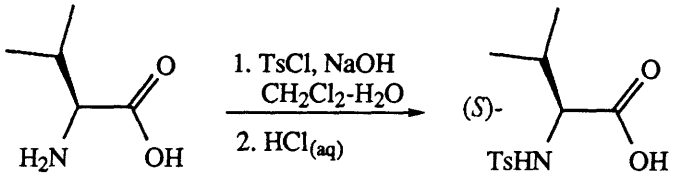

To a solution of L-valine (7.23 g, 61.7 mmol, 1 equiv) in aqueous 1.02 M NaOH solution (121 mL, 123.4 mmol, 2 equiv) at 0 °C was slowly added tosyl chloride (11.77 g, 61.74 mmol, 1 equiv) in CH_2Cl_2 (15 mL). The resulting solution was allowed to warm up to room temperature and was stirred vigorously overnight. It was then poured into a separatory funnel and after removal of the CH_2Cl_2 layer, the aqueous phase was extracted with ether (2 x 10 mL) to further remove any nonionized organic material. The aqueous layer was acidified to pH= 1 with aqueous 1 M HCl solution, resulting in a copious white precipitate which was taken up in ethyl acetate (4 x 35 mL). The ethyl acetate layers were dried ($MgSO_4$) and concentrated in vacuo, leaving behind a white solid that was further purified by recrystallization from ethyl acetate/hexane, giving the product as white crystals (10.46 g, 38.55 mmol, 63%)[74]: m.p. 152–154 °C (lit. 153–154 °C); ^{1}H NMR (300 MHz, $CDCl_3$) δ 0.81 (d, J=6.9 Hz, 3H, $CH(C\underline{H}_3)_2$), 0.90 (d, J=6.9 Hz, 3H, $CH(C\underline{H}_3)_2$), 2.05 (m, 1H, $C\underline{H}(CH_3)_2$), 2.36 (s, 3H, $ArC\underline{H}_3$), 3.74 (dd, J=4.5, 10.2 Hz, 1H, $C\underline{H}CO_2H$), 5.12 (d, J=10.2 Hz, 1H, N<u>H</u>), 7.23 (d, J=8.4 Hz, 2H, Ar<u>H</u>), 7.67 (d, J=8.4 Hz, 2H, Ar<u>H</u>); $[\alpha]_D^{20}$ +28.1° (c=1.7, EtOH) {lit.[74] $[\alpha]_D^{24}$ +27.6° (c=1.0, EtOH)}.

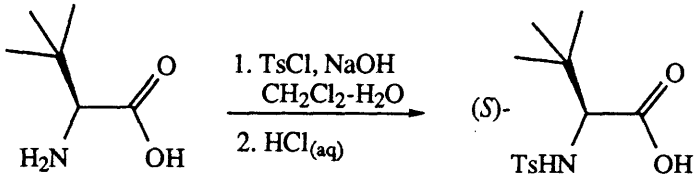

To a solution of L-*tert*-leucine (0.50 g, 3.8 mmol, 1 equiv) in aqueous 1 M NaOH solution (7.6 mL, 7.6 mmol, 2 equiv) was slowly added tosyl chloride (724.5 mg, 3.800

mmol, 1 equiv) in CH_2Cl_2 (7.5 mL) resulting in an emulsion which was stirred vigorously overnight. The CH_2Cl_2 layer was drained off and the aqueous phase was further extracted with CH_2Cl_2 (2 x 5 mL) and then acidified to pH= 1 with aqueous 1 N HCl solution. The resulting white suspension was clarified by shaking with ethyl acetate (4 x 20 mL); the combined ethyl acetate solutions were washed with brine, dried ($MgSO_4$), and concentrated in vacuo leaving white crystals (0.54 g, 1.9 mmol, 50%) which were shown to be pure by ^1H NMR spectroscopy: m.p. 250–253 °C (lit.[74] 248–253 °C); ^1H NMR (300 MHz, $CDCl_3$) δ 0.98 (s, 9H, $C(C\underline{H}_3)_3$), 2.41 (s, 3H, $ArC\underline{H}_3$), 3.62 (d, J=9.5 Hz, 1H, $C\underline{H}CO_2H$), 5.07 (d, J=9.5 Hz, 1H, N<u>H</u>), 7.27 (d, J=8.1 Hz, 2H, Ar<u>H</u>), 7.72 (d, J=8.1 Hz, 2H, Ar<u>H</u>); $[\alpha]_D^{20}$ -40.0° (c=1.0, EtOH) {lit. $[\alpha]_D^{21}$ -40.0° (c=1.0, EtOH)}.

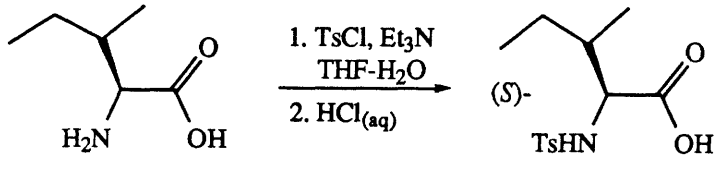

The procedure of Corey et al.[95a] was followed. To a suspension of L-isoleucine (1.00 g, 7.62 mmol, 1 equiv) in water (25 mL) and THF (3 mL) was slowly added triethylamine (2.66 mL, 19.05 mmol, 2.5 equiv). The resulting homogeneous colorless solution was cooled to 0 °C and a solution of tosyl chloride (1.45 g, 7.61 mmol, 1 equiv) in THF (5 mL) was slowly introduced. The reaction mixture was allowed to warm up to room temperature and was stirred overnight. Volatile compounds were removed in vacuo and the aqueous layer was acidified to pH= 2 with aqueous 1 M HCl solution. The resulting white suspension was clarified by shaking with ethyl acetate (4 x 20 mL) and the organic layers were dried ($MgSO_4$) and evaporated in vacuo affording a white solid. Recrystallization from ethyl acetate/hexane gave the desired product as white crystals (1.06 g, 3.71 mmol, 49%): m.p. 135–137 °C; ^1H NMR (250 MHz, $CDCl_3$) δ 0.82 (d, J=7.3 Hz, 3H, $C\underline{H}_3CH$), 0.88 (t, J=7.6 Hz, 3H, $C\underline{H}_3CH_2$), 1.15 (m, 1H, $CH_3C\underline{H}_A H_B$), 1.38 (m, 1H, $CH_3CH_A\underline{H}_B$), 1.80 (m, 1H, $CH_3C\underline{H}$), 2.39 (s, 3H, $ArC\underline{H}_3$), 3.81 (dd, J=4.9,

9.6 Hz, 1H, C<u>H</u>CO_2H), 5.08 (d, J=9.7 Hz, 1H, N<u>H</u>), 7.26 (d, J=8.2 Hz, 2H, Ar<u>H</u>), 7.70 (d, J=8.2 Hz, 2H, Ar<u>H</u>); ^{13}C NMR (75.4 MHz, $CDCl_3$) δ 11.4, 15.5, 21.6, 24.6, 38.3, 59.9, 127.2, 129.5, 136.5, 143.7, 175.9; IR (neat) 3277, 2971, 2939, 1708, 1417, 1333, 1284, 1234, 1161, 1092, 918, 807 cm^{-1}; MS (EI) *m/e* calc'd for $C_{13}H_{19}NO_4S$: 285.1035, found 285.1033; 285 (2), 240 (100), 155 (72), 91 (42), 74 (87); $[\alpha]_D^{20}$ +34.0° (c=0.80, EtOH).

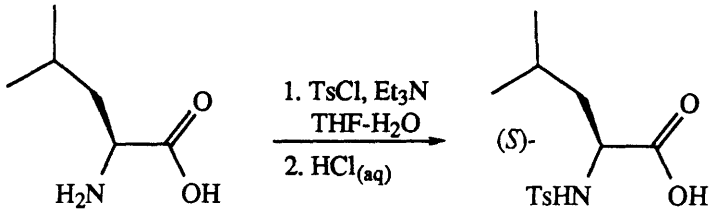

The procedure of Corey et al.[95a] was followed. To a suspension of L-leucine (1.00 g, 7.62 mmol, 1 equiv) in water (25 mL) and THF (3 mL) was slowly added triethylamine (2.66 mL, 19.05 mmol, 2.5 equiv). The resulting homogeneous colorless solution was cooled to 0 °C and a solution of tosyl chloride (1.45 g, 7.61 mmol, 1 equiv) in THF (5 mL) was slowly introduced. The reaction mixture was allowed to warm up to room temperature and was stirred overnight. Volatile compounds were removed in vacuo and the aqueous layer was acidified to pH= 2 with aqueous 1 M HCl solution. The resulting white suspension was clarified by shaking with ethyl acetate (4 x 20 mL) and the organic layers were dried ($MgSO_4$) and evaporated in vacuo affording a white solid. Recrystallization from ethyl acetate gave the desired product as white crystals (1.38 g, 4.84 mmol, 64%): m.p. 118–120 °C; ^{1}H NMR (300 MHz, $CDCl_3$) δ 0.79 (d, J=6.8 Hz, 3H, C<u>H</u>$_3$CH), 0.86 (d, J=6.8 Hz, 3H, C<u>H</u>$_3$CH), 1.47 (m, 2H, $(CH_3)_2$CHC<u>H</u>$_2$), 1.73 (m, 1H, $(CH_3)_2$C<u>H</u>), 2.38 (s, 3H, ArC<u>H</u>$_3$), 3.89 (d of t, J=10.5, 6.1 Hz, 1H, C<u>H</u>CO_2H), 4.95 (d, J=10.5 Hz, 1H, N<u>H</u>), 7.24 (d, J=9.3 Hz, 2H, Ar<u>H</u>), 7.69 (d, J=9.3 Hz, 2H, Ar<u>H</u>); ^{13}C NMR (75.4 MHz, $CDCl_3$) δ 21.3, 21.6, 22.8, 24.4, 42.2, 54.0, 127.2, 129.6, 136.5, 143.8, 177.0; IR (neat) 3272, 2959, 1718, 1458, 1420, 1334, 1164, 1092, 927 cm^{-1}; MS (EI) *m/e* calc'd

for $C_{13}H_{19}NO_4S$: 285.1035, found 285.1033; 285 (3), 240 (100), 155 (86), 91 (51), 74 (29); $[\alpha]_D^{20}$ +6.9° (c=0.75, EtOH).

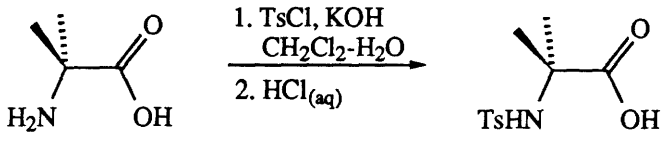

To a solution of 2-methylalanine (2-aminoisobutyric acid, 5.00 g, 48.5 mmol, 1 equiv) in aqueous 2 M KOH solution (48.5 mL, 97.0 mmol, 2 equiv) was slowly added a solution of tosyl chloride (9.25 g, 48.5 mmol, 1 equiv) in CH_2Cl_2 (50 mL). After the reaction mixture was stirred vigorously overnight at room temperature, the CH_2Cl_2 layer was discarded and the aqueous phase was acidified to pH= 2 with aqueous 1 M HCl solution. It was then extracted with CH_2Cl_2, and the organic layers were washed with brine, dried ($MgSO_4$) and evaporated in vacuo to give a white solid; recrystallization from ethyl acetate/hexane furnished the pure product as white crystals (7.49 g, 29.1 mmol, 60%): m.p. 146–149 °C; ^{1}H NMR (300 MHz, $CDCl_3$) δ 1.42 (s, 6H, 2-C<u>H</u>$_3$), 2.37 (s, 3H, ArC<u>H</u>$_3$), 5.47 (s, 1H, N<u>H</u>), 7.24 (d, J=8.4 Hz, 2H, Ar<u>H</u>), 7.73 (d, J=8.4 Hz, 2H, Ar<u>H</u>); ^{13}C NMR (75.4 MHz, $CDCl_3$) δ 21.6, 25.6, 58.8, 126.9, 129.4, 139.2, 143.3, 179.3; IR (neat) 3264, 1711, 1459, 1321, 1148, 1094, 1003, 931, 867 cm^{-1}; MS (EI) *m/e* calc'd for $C_{11}H_{15}NO_4S$: 257.0722, found 257.0719; 257 (0.3), 212 (100), 155 (100), 91 (100).

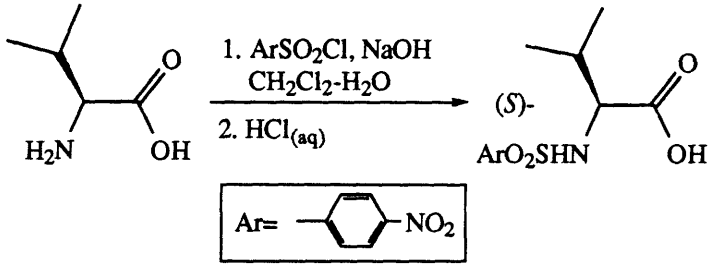

To a solution of L-valine (1.50 g, 12.8 mmol, 1 equiv) in aqueous 1.0 M NaOH solution (25.6 mL, 25.6 mmol, 2 equiv) at 0 °C was slowly added *p*-nitrobenzenesulfonyl

chloride (3.20 g, 12.8 mmol, 1 equiv) in CH_2Cl_2 (4 mL). The resulting brown solution was allowed to warm up to room temperature and was stirred vigorously overnight. It was then poured into a separatory funnel and after removal of the CH_2Cl_2 layer, the aqueous phase was extracted with ether (2 x 10 mL) to further remove any nonionized organic material. The aqueous layer was acidified to pH= 1–2 with aqueous 1 M HCl solution, resulting in a copious precipitate which was taken up in ethyl acetate (4 x 35 mL). The ethyl acetate layers were dried ($MgSO_4$) and concentrated in vacuo, leaving behind a yellow solid that was further purified by recrystallization from ethyl acetate/hexane/methanol, giving a first crop of the product as light yellow crystals (1.2898 g, 4.267 mmol, 33%): m.p. 184–186 °C (lit.[75] 192–194 °C); ^{1}H NMR (300 MHz, $CDCl_3$) δ 0.85 (d, J=6.9 Hz, 3H, $C\underline{H}_3CH$), 0.98 (d, J=6.9 Hz, 3H, $C\underline{H}_3CH$), 2.14 (m, 1H, $(CH_3)_2C\underline{H}$), 3.86 (dd, J=5.1, 11.1 Hz, 1H, $C\underline{H}CO_2H$), 5.14 (d, J=11.1 Hz, 1H, N$\underline{H}$), 8.01 (d, J=9.3 Hz, 2H, Ar$\underline{H}$), 8.32 (d, J=9.3 Hz, 2H, Ar$\underline{H}$); ^{13}C NMR (75.4 MHz, $CDCl_3$) δ 17.0, 18.8, 31.0, 61.2, 123.9, 128.3, 146.1, 149.8, 172.5; IR (neat) 3272, 1718, 1529, 1351, 1168, 1092, 854 cm^{-1}; MS (EI) *m/e* calc'd for $[M - CO_2H]^+$: 257.0596, found 257.0597; 303 (0.4), 257 (100), 186 (41), 122 (41), 74 (100), 44 (40); $[\alpha]_D^{20}$ +50.0° (c=0.78, 40% CH_3OH in $CHCl_3$) {lit. .$[\alpha]_D^{23}$ +45.0° (c=1.0, EtOH)}.

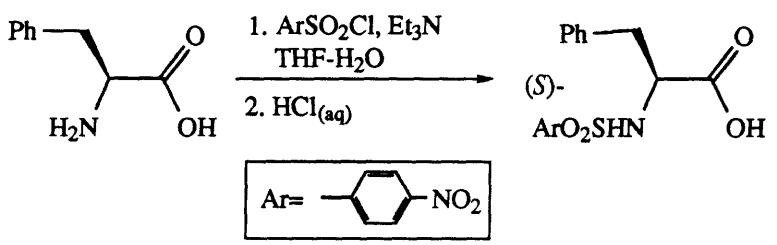

The procedure of Corey et al.[95a] was followed. To a suspension of L-phenylalanine (1.50 g, 9.08 mmol, 1 equiv) in 10:1 water/THF solution (20 mL) was slowly added triethylamine (3.20 mL, 23.0 mmol, 2.5 equiv). The resulting homogeneous colorless solution was cooled to 0 °C and a solution of *p*-nitrobenzenesulfonyl chloride (2.24 g, 9.08 mmol, 1 equiv) in THF (10 mL) was slowly introduced. The reaction

mixture was allowed to warm up to room temperature and was stirred overnight. Volatile compounds were removed in vacuo and the aqueous layer was acidified to pH= 2 with aqueous 1 M HCl solution. The resulting suspension was clarified by shaking with ethyl acetate (4 x 20 mL) and the organic layers were dried ($MgSO_4$) and evaporated in vacuo affording a yellow solid. Recrystallization from ethyl acetate/hexane gave the desired product as yellow crystals (1.56 g, 4.63 mmol, 51%): m.p. 200 °C (dec); ^{1}H NMR (300 MHz, $CDCl_3/CD_3OD$) δ 2.84 (A of ABX, 1H, J_{AB}= 14.1 Hz, J_{AX}= 7.9 Hz, $PhC\underline{H}_2$), 3.05 (B of ABX, 1H, J_{AB}= 14.1 Hz, J_{BX}= 4.7 Hz, $PhC\underline{H}_2$), 4.08 (dd, J=5.1, 7.9 Hz, 1H, $PhCH_2C\underline{H}$ (X of ABX)), 7.02 (m, 2H, phenyl-H), 7.11 (m, 3H, phenyl-H), 7.70 (d of m, J=9.3 Hz, 2H, $SO_2Ar\underline{H}$), 8.08 (d of m, J=9.3 Hz, 2H, $SO_2Ar\underline{H}$); ^{13}C NMR (75.4 MHz, $CDCl_3/CD_3OD$) δ 35.9, 53.7, 123.3, 127.0, 127.7, 128.9, 129.1, 133.6, 148.5, 150.4, 169.7; IR (neat) 3502, 2980, 1722, 1606, 1525, 1195, 1126, 854 cm^{-1}; MS (EI) *m/e* calc'd for $[M - CO_2H]^+$: 305.0596, found 305.0595; 305 (63), 259 (100), 203 (30), 120 (75), 74 (100); $[\alpha]_D^{20}$ -5.0° (c=0.66, CH_3OH).

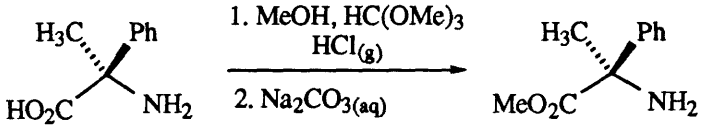

2-Amino-2-phenylpropionic acid was prepared and resolved by literature procedures[62,63]: ^{1}H NMR (250 MHz, D_2O) δ 1.80 (s, 3H, 2-$C\underline{H}_3$), 7.30–7.45 (m, 5H, Ar$\underline{H}$).

A suspension of the amino acid (2.70 g, 16.3 mmol, 1 equiv) in dry methanol (30 mL) containing trimethylorthoformate (1.98 mL, 18.1 mmol, 1.1 equiv) was heated to 60 °C before being saturated with hydrogen chloride gas. The homogeneous solution was heated under reflux for 16 h and then cooled to room temperature. The solvent was removed in vacuo and the fuming residue was carefully neutralized with 5% Na_2CO_3 solution at 0 °C. The aqueous phase was extracted with CH_2Cl_2 (5 x 30 mL), and the combined organic phases were washed with brine, dried (Na_2SO_4) and concentrated in

vacuo furnishing the amino ester as a pale yellow oil (2.34 g, 13.1 mmol, 79%). This material could be used without further purification, or purified by flash chromatography (5% CH_3OH in CH_2Cl_2): ^1H NMR (300 MHz, $CDCl_3$) δ 1.72 (s, 3H, 2-C<u>H</u>$_3$), 1.93 (br s, 2H, N<u>H</u>$_2$), 3.71 (s, 3H, CO_2C<u>H</u>$_3$), 7.26–7.51 (m, 5H, Ar<u>H</u>).

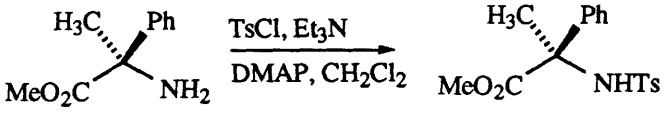

The amino ester (1.00 g, 5.58 mmol, 1 equiv) in CH_2Cl_2 (10 mL) was treated at 0 °C sequentially with triethylamine (3.7 mL, 27 mmol, 4.8 equiv), 4-DMAP (60 mg, 0.56 mmol, 0.1 equiv), and tosyl chloride (1.17 g, 6.14 mmol, 1.1 equiv). After attaining ambient temperature, the solution was stirred for 16 h, diluted with CH_2Cl_2 (15 mL) and washed with saturated $NaHCO_3$ solution (10 mL) and water (10 mL). The aqueous phases were extracted with CH_2Cl_2 (3 x 10 mL), and the combined organic layers were washed with brine, dried ($MgSO_4$) and concentrated in vacuo. The residue was purified by flash chromatography (CH_2Cl_2) to yield the desired sulfonamido ester (1.82 g, 5.47 mmol, 98%): ^1H NMR (250 MHz, $CDCl_3$) δ 1.90 (s, 3H, 2-C<u>H</u>$_3$), 2.35 (s, 3H, ArC<u>H</u>$_3$), 3.65 (s, 3H, CO_2C<u>H</u>$_3$), 5.89 (s, 1H, N<u>H</u>), 7.10–7.48 (m, 9H, Ar<u>H</u>).

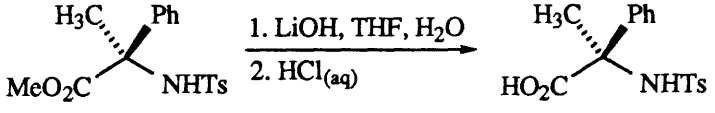

A suspension of the sulfonamido ester (1.80 g, 5.41 mmol, 1 equiv) and lithium hydroxide monohydrate (1.13 g, 26.9 mmol, 5.0 equiv) in THF (12 mL) and water (12 mL) was stirred vigorously at 50 °C until consumption of the starting material could be observed by TLC analysis (1–2 days). At this point the reaction mixture was diluted with water (10 mL) and washed with CH_2Cl_2 (2 x 10 mL). The aqueous phase was acidified to pH= 2 with aqueous 2 M HCl solution, and re-extracted with ethyl acetate (5 x 20 mL). The combined ethyl acetate extracts were washed wih brine (30 mL), dried ($MgSO_4$) and concentrated in vacuo. The residue was recrystallized from hexane/benzene to give the

pure sulfonamido acid as white crystals (1.70 g, 5.32 mmol, 99%): m.p. 134–135 °C; ^{1}H NMR (300 MHz, $CDCl_3$) δ 1.93 (s, 3H, 2-C<u>H</u>$_3$), 2.35 (s, 3H, ArC<u>H</u>$_3$), 5.94 (s, 1H, N<u>H</u>), 7.10 (d, J=8.5 Hz, 2H, SO_2Ar<u>H</u>), 7.15–7.35 (m, 5H, Ar<u>H</u>), 7.48 (d, J=8.5 Hz, 2H, SO_2Ar<u>H</u>); ^{13}C NMR (75.4 MHz, $CDCl_3$) δ 21.4, 23.4, 64.1, 126.0, 126.8, 128.3, 128.5, 129.3, 138.5, 139.0, 143.0, 177.4; IR (neat) 3271, 1717, 1385, 1322, 1158, 1092, 980, 864 cm^{-1}; MS (EI) *m/e* calc'd for $[M - CO_2H]^+$: 274.0902, found 274.0902; 274 (100), 155 (100), 91 (88); $[\alpha]_D^{20}$ +34.6° (c=0.92, $CHCl_3$) (unassigned).

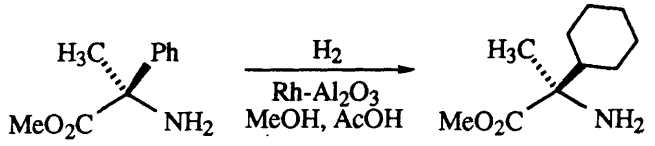

Rhodium on alumina powder (5% Rh, 129.0 mg, 0.06268 mmol, 0.02 equiv) was suspended in a solution of the aromatic amino ester (600 mg, 3.35 mmol, 1 equiv) in methanol (6 mL) and acetic acid (3 drops), and the reaction mixture was hydrogenated (45 psi) overnight in a Parr hydrogenator. The suspension was filtered through a layer of Celite, which was then washed through with ethyl acetate. The organic layers were concentrated in vacuo, and the residue was purified by flash chromatography (5% CH_3OH in CH_2Cl_2) to give the unsaturated amino ester (389.9 mg, 2.105 mmol, 63%): ^{1}H NMR (250 MHz, $CDCl_3$) δ 1.02–1.30 (m, 4H, cyclohexyl-<u>H</u>), 1.28 (s, 3H, 2-C<u>H</u>$_3$), 1.50-1.87 (m, 9H, cyclohexyl-<u>H</u> and N<u>H</u>$_2$), 3.72 (s, 3H, CO_2C<u>H</u>$_3$).

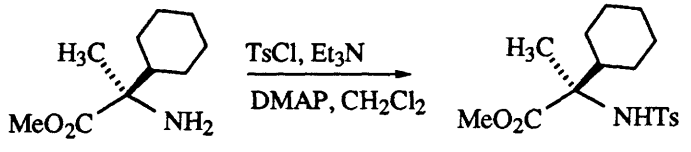

The amino ester (380.0 mg, 2.051 mmol, 1 equiv) in CH_2Cl_2 (3.5 mL) was treated at 0 °C sequentially with triethylamine (1.36 mL, 9.76 mmol, 4.8 equiv), 4-DMAP (22 mg, 0.20 mmol, 0.1 equiv), and tosyl chloride (589.0 mg, 3.089 mmol, 1.5 equiv). After attaining ambient temperature, the solution was stirred for 16 h, diluted with CH_2Cl_2 and

washed with saturated $NaHCO_3$ solution (10 mL) and water (10 mL). The aqueous phases were extracted with CH_2Cl_2 (3 x 10 mL), and the combined organic layers were washed with brine, dried ($MgSO_4$) and concentrated in vacuo. The residue was purified by flash chromatography (CH_2Cl_2) to yield the desired sulfonamido ester (620.0 mg, 1.826 mmol, 89%): ^1H NMR (250 MHz, $CDCl_3$) δ 0.90–1.29 (m, 4H, cyclohexyl-H), 1.33 (s, 3H, 2-CH_3), 1.40–1.90 (m, 7H, cyclohexyl-H), 2.39 (s, 3H, ArCH_3), 3.59 (s, 3H, CO_2CH_3), 5.20 (s, 1H, NH), 7.27 (d, J=8.5 Hz, 2H, ArH), 7.73 (d, J=8.5 Hz, 2H, ArH).

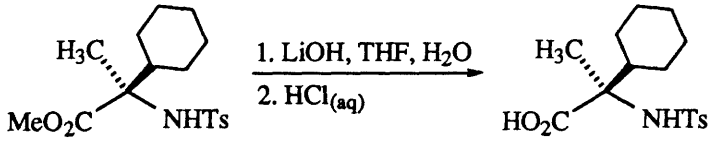

A suspension of the sulfonamido ester (500.0 mg, 1.473 mmol, 1 equiv) and sodium hydroxide (400.0 mg, 10.00 mmol, 6.8 equiv) in ethanol (7 mL) was stirred vigorously at 50–60 °C until consumption of the starting material could be observed by TLC analysis (2 days). At this point the reaction mixture was diluted with water (10 mL) and washed with ether (2 x 10 mL). The aqueous phase was acidified to pH= 2 with aqueous 2 M HCl solution, and re-extracted with ethyl acetate (5 x 20 mL). The combined ethyl acetate extracts were washed wih brine (30 mL), dried ($MgSO_4$) and concentrated in vacuo. The residue was recrystallized from hexane/CH_2Cl_2 to give the pure sulfonamido acid as white crystals (266.0 mg, 0.8174 mmol, 55%). The balance of material was unhydrolyzed ester: m.p. 159–160 °C; ^1H NMR (300 MHz, $CDCl_3$) δ 0.95–1.25 (m, 5H, cyclohexyl-H), 1.29 (s, 3H, 2-CH_3), 1.50–1.79 (m, 6H, cyclohexyl-H), 2.37 (s, 3H, ArCH_3), 5.20 (s, 1H, NH), 7.24 (d, J=8.1 Hz, 2H, ArH), 7.71 (d, J=8.1 Hz, 2H, ArH); ^{13}C NMR (75.4 MHz, $CDCl_3$) δ 17.0, 21.5, 26.0, 26.2, 26.3, 26.8, 27.0, 48.9, 65.0, 127.1, 129.5, 139.3, 143.3, 178.5; IR (neat) 3261, 2932, 2855, 1714, 1451, 1325, 1155, 1093, 977, 814 cm^{-1}; MS (EI) *m/e* calc'd for $[M - CO_2H]^+$: 280.1371, found 280.1369; 326 (1), 280 (100), 242 (100), 173 (43), 155 (97), 88 (100); $[\alpha]_D^{20}$ -26.5° (c=0.55, $CHCl_3$) (unassigned).

6.3 Derivatives of α-Methyl-DOPA and Related Compounds

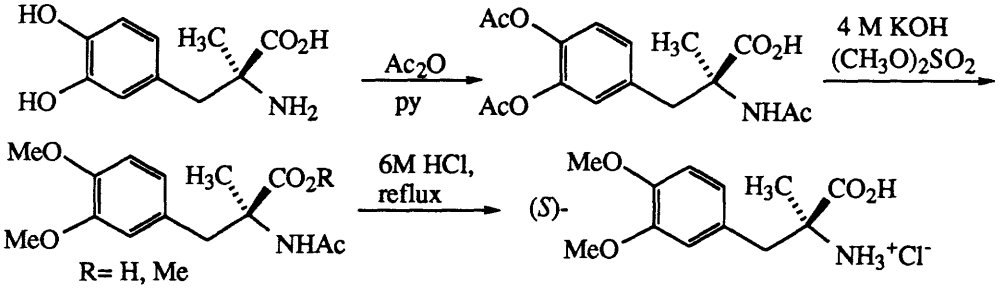

The hydrochloride salt of (L)-3-(3,4-dimethoxyphenyl)-2-methylalanine was synthesized from commercially available (L)-3-(3,4-dihydroxyphenyl)-2-methylalanine sesquihydrate (α-methyl-L-DOPA) by the literature procedure[65] in three steps and 77% overall yield: m.p. 165–7 °C (lit.[65] 235–238 °C); ^{1}H NMR (300 MHz, CD_3OD) δ 1.62 (s, 3H, 2-C<u>H</u>$_3$), 3.15 (AB q, 2H, J_{AB}=9.0 Hz, Δν= 81 Hz, C<u>H</u>$_2$), 4.81 (s, 3H, OC<u>H</u>$_3$), 4.82 (s, 3H, OC<u>H</u>$_3$), 6.80 (m, 2H, Ar-2, 6-<u>H</u>), 6.94 (d, J=12.0 Hz, 1H, Ar-5-<u>H</u>).

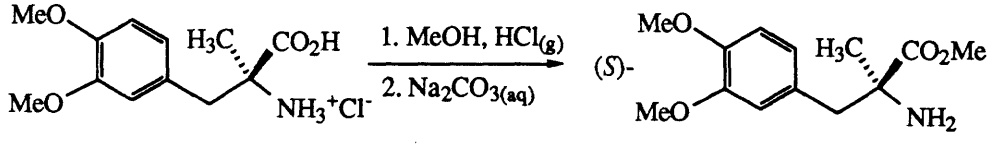

A suspension of the amino acid (2.0 g, 7.2 mmol, 1 equiv) and trimethylorthoformate (0.9 mL, 8 mmol, 1.1 equiv) in dry methanol (18 mL) was saturated with hydrogen chloride gas, and the resulting homogeneous solution was heated under reflux for 16 h. After cooling to room temperature, the reaction mixture was concentrated in vacuo and the residue was cooled to 0 °C and carefully treated with aqueous 5% Na_2CO_3 solution. The aqueous phase was shaken with CH_2Cl_2 (5 x 30 mL), and the combined organic phases were washed with brine, dried (Na_2SO_4), and concentrated to give a pale yellow oil. The crude product thus obtained was purified by flash chromatography (5% CH_3OH in CH_2Cl_2) to afford the pure amino ester (1.3 g, 5.1 mmol, 71%): ^{1}H NMR (300 MHz, $CDCl_3$) δ 1.39 (s, 3H, 2-C<u>H</u>$_3$), 1.58 (br s, 2H, N<u>H</u>$_2$), 2.90 (AB q, 2H, J_{AB}= 12.5 Hz, Δν= 108.0 Hz, C<u>H</u>$_2$), 3.71 (s, 3H, CO_2C<u>H</u>$_3$), 3.84 (s, 3H, OC<u>H</u>$_3$), 3.85 (s,

3H, $OC\underline{H}_3$), 6.67 (m, 2H, Ar$\underline{H}$), 6.78 (m, 1H, Ar$\underline{H}$); ^{13}C NMR (75.4 MHz, $CDCl_3$) δ 26.7, 46.4, 52.0, 55.8, 58.9, 111.1, 113.1, 121.9, 129.0, 148.0, 148.6, 177.5; IR (neat) 2950, 1733, 1516, 1463, 1262, 1141, 1028 cm^{-1}; MS (EI) *m/e* calc'd for $C_{13}H_{19}NO_4$: 253.1314, found 253.1313; 253 (3), 194 (15), 152 (72), 151 (68), 102 (100), 70 (14), 43 (46); $[\alpha]_D^{20}$ -15.3° (c=0.88, $CHCl_3$).

The following example serves as a general procedure for sulfonamide formation:

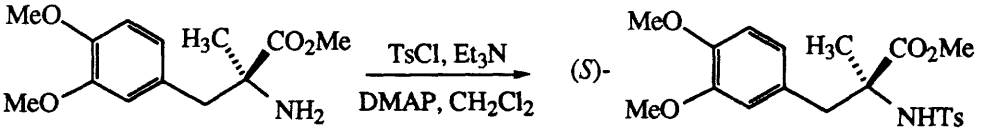

To a solution of the amino ester (863 mg, 3.41 mmol, 1 equiv) in CH_2Cl_2 (6 mL) at 0 °C was added triethylamine (2.4 mL, 17 mmol, 5 equiv), 4-DMAP (ca. 37 mg, 0.34 mmol, 0.1 equiv), and tosyl chloride (781 mg, 4.10 mmol, 1.2 equiv). The solution was allowed to warm up to room temperature and was stirred overnight, then diluted with CH_2Cl_2 (15 mL) and shaken with aqueous saturated $NaHCO_3$ (10 mL) and water (10 mL). The aqueous layers were extracted with CH_2Cl_2 (3 x 10 mL), and the combined organic phases were washed with brine, dried ($MgSO_4$), and concentrated in vacuo. The crude product was purified by flash chromatography (10–30% ethyl acetate in hexane or 1–3% CH_3OH in CH_2Cl_2), giving the pure sulfonamido ester (1.35 g, 3.31 mmol, 97%): ^1H NMR (300 MHz, $CDCl_3$) δ 1.48 (s, 3H, 2-$C\underline{H}_3$), 2.43 (s, 3H, Ar$C\underline{H}_3$), 3.10 (AB q, 2H, J_{AB}= 13.2 Hz, Δν= 69.7 Hz, $C\underline{H}_2$), 3.63 (s, 3H, $CO_2C\underline{H}_3$), 3.88 (s, 3H, $OC\underline{H}_3$), 3.89 (s, 3H, $OC\underline{H}_3$), 5.28 (s, 1H, N$\underline{H}$), 6.68 (dd, J=6.0, 2.5 Hz, 1H, Ar-6-$\underline{H}$), 6.79 (m, 2H, Ar-2, 5-$\underline{H}$), 7.27 (d, J=9.0 Hz, 2H, tosyl Ar$\underline{H}$), 7.75 (d, J=9.0 Hz, 2H, tosyl Ar$\underline{H}$); MS (EI) *m/e* calc'd for $C_{20}H_{25}NO_6S$: 407.1404, found 407.1403; 407 (8), 256 (28), 155 (34), 152 (22), 151 (100), 91 (39).

The following example serves as a general procedure for hydrolysis of the methyl ester:

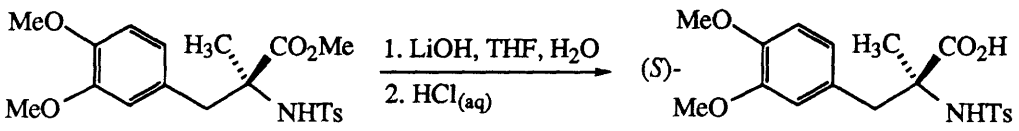

A suspension of the sulfonamido ester (1.39 g, 3.41 mmol, 1 equiv) and lithium hydroxide monohydrate (715 mg, 17.1 mmol, 5.0 equiv) in THF (10 mL) and water (10 mL) was stirred vigorously at 50–60 °C until consumption of the starting material could be observed by TLC analysis (1–2 days). At this point the reaction mixture was diluted with water (10 mL) and washed with ether (2 x 10 mL). The aqueous phase was acidified to pH= 2 with aqueous 2 M HCl solution, and the resulting white suspension was clarified by extraction with ethyl acetate (5 x 20 mL). The combined ethyl acetate extracts were washed wih brine (30 mL), dried ($MgSO_4$) and concentrated in vacuo. The residue was recrystallized from ethyl acetate/hexane to give the pure sulfonamido acid as white crystals (1.08 g, 2.74 mmol, 81%): m.p. 157.5–158.5 °C; ^{1}H NMR (300 MHz, $CDCl_3$) δ 1.46 (s, 3H, 2-C<u>H</u>$_3$), 2.40 (s, 3H, ArC<u>H</u>$_3$), 3.10 (AB q, 2H, J_{AB}= 13.7 Hz, Δν= 49.5 Hz, C<u>H</u>$_2$), 3.83 (s, 3H, OC<u>H</u>$_3$), 3.84 (s, 3H, OC<u>H</u>$_3$), 5.21 (s, 1H, N<u>H</u>), 6.70–6.80 (m, 2H, Ar-5, 6-<u>H</u>), 6.83 (d, J=1.8 Hz, 1H, Ar-2-<u>H</u>), 7.26 (d, J=8.0 Hz, 2H, SO_2Ar<u>H</u>), 7.72 (d, J=8.0 Hz, 2H, SO_2Ar<u>H</u>); ^{13}C NMR (75.4 MHz, $CDCl_3$) δ 21.0, 21.3, 45.3, 55.3, 55.4, 62.6, 110.6, 113.3, 121.8, 126.4, 129.1, 139.3, 142.9, 147.9, 148.3, 160.0, 176.8; IR ($CHCl_3$) 3400–2500, 1710, 1505, 1149, 1085, 1019 cm^{-1}; MS (EI) *m/e* calc'd for $C_{19}H_{23}NO_6S$: 393.1246, found 393.1244; 393 (3), 151 (100); $[\alpha]_D^{20}$ +18.8° (c=1.2, EtOH).

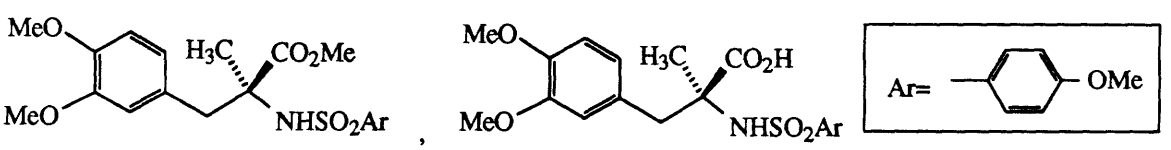

(*S*)-Methyl ester: prepared by the general procedure in 97% yield: ^{1}H NMR (250

MHz, $CDCl_3$) δ 1.48 (s, 3H, 2-C<u>H</u>$_3$), 3.11 (AB q, 2H, J_{AB}= 12.5 Hz, Δν= 57.5 Hz, C<u>H</u>$_2$), 3.65 (s, 3H, CO_2C<u>H</u>$_3$), 3.87 (s, 6H, OC<u>H</u>$_3$), 3.88 (s, 3H, SO_2-Ar-OC<u>H</u>$_3$), 5.27 (s, 1H, N<u>H</u>), 6.68 (dd, J=8.0, 2.5 Hz, 1H, Ar-6-<u>H</u>), 6.80 (m, 2H, Ar-2, 5-<u>H</u>), 6.95 (d, J=8.7 Hz, 2H, SO_2Ar<u>H</u>), 7.82 (d, J=8.7 Hz, 2H, SO_2Ar<u>H</u>).

(*S*)-Acid: prepared by the general procedure. The crude product was purified by flash chromatography (3% CH_3OH in CH_2Cl_2, 1% acetic acid) and recrystallization from ethyl acetate/hexane, providing the pure sulfonamido acid as white crystals in 73% yield: m.p. 142–4 °C; ^{1}H NMR (300 MHz, $CDCl_3$) δ 1.49 (s, 3H, 2-C<u>H</u>$_3$), 3.12 (AB q, 2H, J_{AB}= 13.8 Hz, Δν=50.7 Hz, C<u>H</u>$_2$), 3.86 (s, 9H, OC<u>H</u>$_3$), 5.20 (s, 1H, N<u>H</u>), 6.75 (dd, J=2.4, 10.5 Hz, 1H, Ar-6-<u>H</u>), 6.81 (d, J=10.5 Hz, 1H, Ar-5-<u>H</u>), 6.86 (d, J=2.1 Hz, 1H, Ar-2-<u>H</u>), 6.95 (d, J=9.3 Hz, 2H, SO_2Ar-<u>H</u>), 7.80 (d, J=9.3 Hz, 2H, SO_2Ar<u>H</u>); ^{13}C NMR (75.4 MHz, $CDCl_3$) δ 21.2, 45.3, 55.1, 55.4, 62.5, 110.7, 113.2, 113.6, 121.9, 126.4, 128.5, 133.8, 148.0, 148.3, 162.3, 177.3; IR (neat) 3000, 1710, 1593, 1258, 1145, 1089, 1020 cm^{-1}; MS (EI) *m/e* calc'd for $C_{19}H_{23}NO_7S$: 409.1195, found 409.1194; 409 (3), 171 (15), 151 (100), 107 (13); $[\alpha]_D^{20}$ +15.6° (c=0.59, $CHCl_3$).

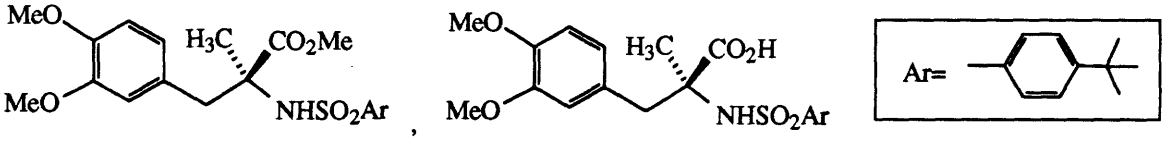

(*S*)-Methyl ester: prepared by the general procedure in quantitative yield: ^{1}H NMR (250 MHz, $CDCl_3$) δ 1.30 (s, 9H, ^{t}Bu), 1.47 (s, 3H, 2-C<u>H</u>$_3$), 3.09 (AB q, 2H, J_{AB}= 12.5 Hz, Δν= 60.0 Hz, C<u>H</u>$_2$), 3.59 (s, 3H, CO_2C<u>H</u>$_3$), 3.85 (s, 3H, OC<u>H</u>$_3$), 3.86 (s, 3H, OC<u>H</u>$_3$), 5.27 (br s, 1H, N<u>H</u>), 6.66 (dd, J=10.0, 2.5 Hz, 1H, Ar-6-<u>H</u>), 6.76 (m, 2H, Ar-2, 5-<u>H</u>), 7.47 (d, J=10.0 Hz, 2H, SO_2Ar<u>H</u>), 7.76 (d, J=10.0 Hz, 2H, SO_2Ar<u>H</u>).

(*S*)-Acid: prepared by the general procedure. The crude product was purified by recrystallization from benzene, giving the pure acid as a white foam in 85% yield: m.p. 80–90 °C (foam); ^{1}H NMR (250 MHz, $CDCl_3$) δ 1.31 (s, 9H, ^{t}Bu), 1.48 (s, 3H, 2-C<u>H</u>$_3$), 3.11 (AB q, 2H, J_{AB}= 13.6 Hz, Δν= 44.8 Hz, C<u>H</u>$_2$), 3.84 (s, 6H, OC<u>H</u>$_3$), 5.22 (br s,

1H, NH), 6.78 (m, 3H, ArH), 7.46 (d, J=8.5 Hz, 2H, SO_2ArH), 7.75 (d, J=8.5 Hz, 2H, SO_2ArH); ^{13}C NMR (75.4 MHz, $CDCl_3$) δ 21.4, 30.6, 34.6, 45.2, 55.3, 55.4, 62.7, 110.7, 113.3, 121.8, 125.4, 126.1, 126.5, 139.2, 147.9, 148.3, 155.9, 177.4; IR (neat) 3274, 2962, 1718, 1594, 1517, 1465, 1329, 1265, 1159, 1026 cm^{-1}; MS (EI) *m/e* calc'd for $C_{22}H_{29}NO_6S$: 435.1716, found 435.1714; 435 (2), 151 (100); $[\alpha]_D^{20}$ +17.2° (c=0.57, $CHCl_3$).

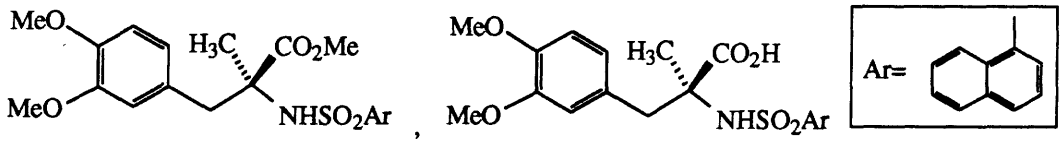

(*S*)-Methyl ester: prepared by the general procedure in quantitative yield: ^1H NMR (250 MHz, $CDCl_3$) δ 1.37 (s, 3H, 2-CH_3), 3.08 (AB q, 2H, J_{AB}= 15 Hz, Δν= 58.8 Hz, CH_2), 3.55 (s, 3H, CO_2CH_3), 3.84 (s, 3H, OCH_3), 3.85 (s, 3H, OCH_3), 5.48 (s, 1H, NH), 6.65 (dd, J=10.0, 2.5 Hz, 1H, Ar-6-H), 6.75 (m, 2H, Ar-2, 5-H), 7.48–7.68 (m, 3H, naph-3,6,7-H), 7.93 (br d, J=7.5 Hz, 1H, naph-2-H), 8.04 (br d, J=7.5 Hz, 1H, naph-4-H), 8.26 (br d, J=7.5 Hz, 1H, naph-5-H), 8.54 (br d, J=7.5 Hz, 1H, naph-8-H).

(*S*)-Acid: prepared by the general procedure. The crude product was purified by flash chromatography (8–10% CH_3OH in CH_2Cl_2, 1% acetic acid) and recrystallization (slow evaporation from ether) giving the pure acid as colorless crystals in 84% yield: m.p. 189–191 °C; ^1H NMR (250 MHz, $CDCl_3$) δ 1.37 (s, 3H, 2-CH_3), 3.11 (AB q, 2H, J_{AB}= 13.2 Hz, Δν= 46.7 Hz, CH_2), 3.84 (s, 3H, OCH_3), 3.85 (s, 3H, OCH_3), 5.42 (s, 1H, NH), 6.75 (q of d, J=1.8, 7.2 Hz, 2H, Ar-5, 6-H), 6.84 (s, 1H, Ar-2-H), 7.51 (t, J=8.4 Hz, 1H, naph-3-H), 7.61 (m, 2H, naph-6,7-H), 7.91 (br d, J=1.2, 8.0 Hz, 1H, naph-2-H), 8.04 (br d, J=1.5, 8.0 Hz, 1H, naph-4-H), 8.25 (br d, J=7.5 Hz, 1H, naph-5-H), 8.51 (br d, J=1.2, 8.6 Hz, 1H, naph-8-H); ^{13}C NMR (75.4 MHz, $CD_3OD/CDCl_3$) δ 21.3, 45.0, 55.2, 63.0, 110.5, 113.3, 121.9, 123.6, 124.0, 126.2, 127.3, 127.4, 127.6, 127.8, 128.4, 133.4, 133.7, 137.6, 147.5, 148.0, 174.4; IR (neat) 3266, 2934, 1718, 1517, 1465, 1327, 1264, 1159, 1026 cm^{-1}; MS (EI) *m/e* calc'd for $C_{22}H_{23}O_6NS$:

429.1246, found 429.1245; 429 (3), 151 (100), 127 (19); $[\alpha]_D^{20}$ +58.1° (c=0.37, $CHCl_3$).

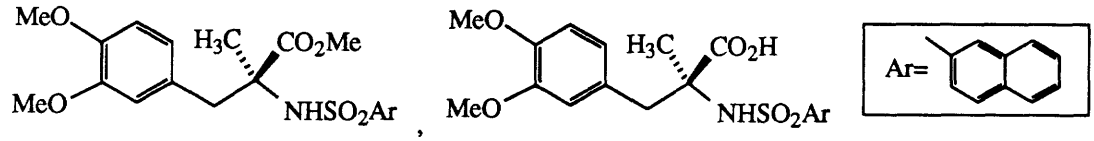

(*S*)-Methyl ester: prepared by the general procedure in quantitative yield: ^{1}H NMR (250 MHz, $CDCl_3$) δ 1.46 (s, 3H, 2-C<u>H</u>$_3$), 3.11 (AB q, 2H, J_{AB}= 12.5 Hz, Δν= 65.0 Hz, C<u>H</u>$_2$), 3.59 (s, 3H, CO_2C<u>H</u>$_3$), 3.84 (s, 3H, OC<u>H</u>$_3$), 3.85 (s, 3H, OC<u>H</u>$_3$), 5.41 (s, 1H, N<u>H</u>), 6.66 (dd, J=2.5, 7.5 Hz, 1H, Ar<u>H</u>), 6.78 (m, 2H, Ar<u>H</u>), 7.60 (m, 2H, naph-<u>H</u>), 7.88 (m, 4H, naph-<u>H</u>), 8.41 (s, 1H, naph-1-<u>H</u>).

(*S*)-Acid: prepared by the general procedure. The crude product was purified by flash chromatography (8–10% CH_3OH in CH_2Cl_2, 1% acetic acid) and recrystallization from ethyl acetate/hexane giving the pure acid as white crystals in 82% yield: m.p. 139-40 °C; ^{1}H NMR (300 MHz, $CDCl_3$) δ 1.48 (s, 3H, 2-C<u>H</u>$_3$), 3.15 (AB q, 2H, J_{AB}= 12.0 Hz, Δν= 60.0 Hz, C<u>H</u>$_2$), 3.86 (s, 3H, OC<u>H</u>$_3$), 3.87 (s, 3H, OC<u>H</u>$_3$), 5.33 (s, 1H, N<u>H</u>), 6.67 (m, 2H, Ar<u>H</u>), 6.87 (s, 1H, Ar-2-<u>H</u>), 7.60 (m, 2H, naph-<u>H</u>), 7.85 (m, 4H, naph-<u>H</u>), 8.40 (s, 1H, naph-<u>H</u>); ^{13}C NMR (75.4 MHz, $CD_3OD/CDCl_3$) δ 21.6, 45.0, 55.3, 62.9, 110.6, 113.5, 121.8, 122.1, 127.1, 128.2, 128.8, 131.7, 134.2, 139.6, 147.6, 148.1, 174.4; IR (neat) 3265, 2943, 1718, 1517, 1464, 1328, 1264, 1156 cm^{-1}; MS (EI) *m/e* calc'd for $C_{22}H_{23}O_6NS$: 429.1246, found 429.1242; 429 (2), 151 (100), 127 (23); $[\alpha]_D^{20}$ -3.2° (c=0.53, $CHCl_3$).

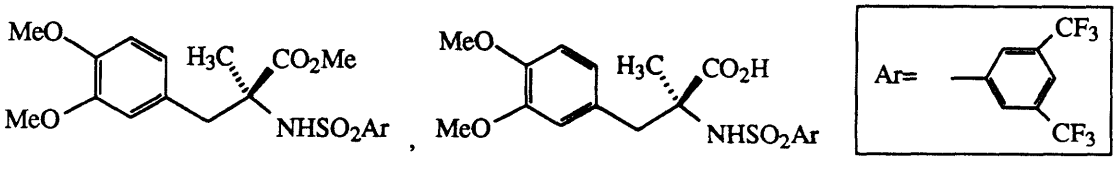

(*S*)-Methyl ester: prepared by the general procedure in quantitative yield.: ^{1}H NMR (250 MHz, $CDCl_3$) δ 1.52 (s, 3H, 2-C<u>H</u>$_3$), 3.15 (AB q, 2H, J_{AB}= 15.0 Hz, Δν= 37.5 Hz,

$C\underline{H}_2$), 3.68 (s, 3H, $CO_2C\underline{H}_3$), 3.87 (s, 3H, $OC\underline{H}_3$), 3.88 (s, 3H, $OC\underline{H}_3$), 5.41 (s, 1H, N$\underline{H}$), 6.65 (dd, J=10.0, 2.5 Hz, 1H, Ar$\underline{H}$), 6.75 (d, J=2.5 Hz, 1H, Ar$\underline{H}$), 6.79 (d, J=10.0 Hz, 1H, Ar$\underline{H}$), 8.02 (s, 1H, SO_2Ar-*para*-$\underline{H}$), 8.28 (s, 2H, SO_2Ar-*ortho*-$\underline{H}$).

(*S*)-Acid: prepared by the general procedure. The crude product was purified by flash chromatography (8–10% CH_3OH in CH_2Cl_2, 1% acetic acid) giving the pure acid as a white solid in 90% yield: m.p. 70–75 °C (foam); ^{1}H NMR (300 MHz, $CDCl_3$) δ 1.45 (s, 3H, 2-$C\underline{H}_3$), 3.08 (AB q, 2H, J_{AB}= 14.0 Hz, Δν= 22.4 Hz, $C\underline{H}_2$), 3.77 (s, 3H, $OC\underline{H}_3$), 3.78 (s, 3H, $OC\underline{H}_3$), 5.23 (s, 1H, N$\underline{H}$), 6.78 (m, 2H, Ar$\underline{H}$), 6.71 (dd, J=1.8, 8.1 Hz, 1H, Ar-6-$\underline{H}$), 7.94 (s, 1H, SO_2Ar-*para*-$\underline{H}$), 8.20 (s, 2H, SO_2Ar-*ortho*-$\underline{H}$); ^{13}C NMR (75.4 MHz, $CDCl_3$) δ 21.8, 45.1, 55.3, 55.4, 63.3, 110.8, 113.2, 121.8, 125.7, 126.6, 132.5, 132.6, 144.8, 148.2, 148.4, 160.0, 176.3; IR ($CHCl_3$) 3341, 2939, 1730, 1518, 1465, 1360, 1280, 1149 cm^{-1}; MS (EI) *m/e* calc'd for $C_{20}H_{19}F_6NO_6S$: 515.0837, found 515.0839; 515 (2), 213 (11), 151 (100); $[\alpha]_D^{20}$ +12.4° (c=0.48, $CHCl_3$).

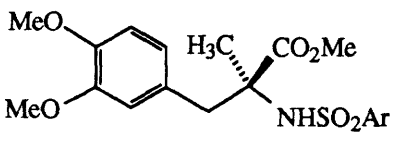

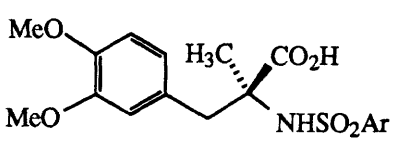

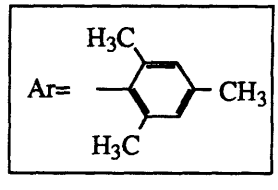

(*S*)-Methyl ester: prepared by the general procedure in quantitative yield: ^{1}H NMR (300 MHz, $CDCl_3$) δ 1.34 (s, 3H, 2-$C\underline{H}_3$), 2.27 (s, 3H, Mes-*para*-$C\underline{H}_3$), 2.62 (s, 6H, Mes-*ortho*-$C\underline{H}_3$), 3.12 (AB q, 2H, J_{AB}= 13.5 Hz, Δν= 81.0 Hz, $C\underline{H}_2$), 3.66 (s, 3H, $CO_2C\underline{H}_3$), 3.85 (s, 3H, $OC\underline{H}_3$), 3.87 (s, 3H, $OC\underline{H}_3$), 5.33 (s, 1H, N$\underline{H}$), 6.65 (d, J=8.4 Hz, 1H, Ar$\underline{H}$), 6.77 (d, J=8.4 Hz, 1H, Ar$\underline{H}$), 6.82 (d, J=1.5 Hz, 1H, Ar$\underline{H}$), 6.90 (s, 2H, Mes-$\underline{H}$).

(*S*)-Acid: prepared by the general procedure. The crude product was purified by recrystallization from benzene, providing the pure acid as white crystals in 87% yield: m.p. 159–60 °C; ^{1}H NMR (250 MHz, $CDCl_3$) δ 1.37 (s, 3H, 2-$C\underline{H}_3$), 2.27 (s, 3H, Mes-*para*-$C\underline{H}_3$), 2.62 (s, 6H, Mes-*ortho*-$C\underline{H}_3$), 3.14 (AB q, 2H, J_{AB}= 12.5 Hz, Δν= 52.5 Hz,

CH_2), 3.87 (s, 3H, OCH_3), 3.88 (s, 3H, OCH_3), 5.26 (s, 1H, NH), 6.77 (m, 2H, ArH), 6.89 (m, 1H, ArH), 6.92 (s, 2H, Mes-H); ^{13}C NMR (75.4 MHz, $CDCl_3$) δ 20.4, 20.9, 22.2, 45.3, 55.4, 62.8, 110.7, 113.3, 121.7, 126.6, 131.6, 136.6, 137.6, 141.5, 147.9, 148.3, 177.8; IR (neat) 3374, 2940, 2838, 1716, 1605, 1518, 1465, 1330, 1264, 1145, 1104, 1028 cm^{-1}; MS (EI) *m/e* calc'd for $C_{21}H_{27}NO_6S$: 421.1559, found 421.1558; 421 (3), 151 (100), 119 (25); $[\alpha]_D^{20}$ +9.8° (c=0.73, $CHCl_3$).

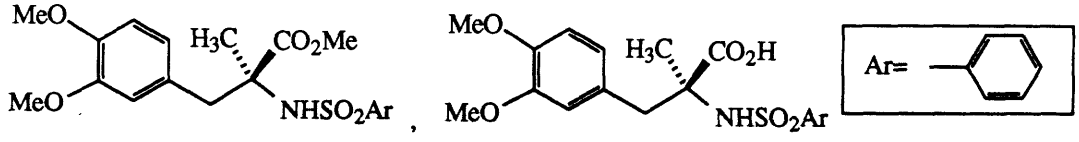

(*S*)-Methyl ester: prepared by the general procedure in quantitative yield: ^1H NMR (250 MHz, $CDCl_3$) δ 1.46 (s, 3H, 2-CH_3), 3.10 (AB q, 2H, J_{AB}= 15.0 Hz, Δν= 60.0 Hz, CH_2), 3.62 (s, 3H, CO_2CH_3), 3.85 (s, 3H, OCH_3), 3.87 (s, 3H, OCH_3), 5.33 (s, 1H, NH), 6.65 (dd, J=8.5, 2.5 Hz, 1H, Ar-6-H), 6.78 (m, 2H, Ar-2, 5-H), 7.50 (m, 3H, SO_2Ph-*meta* & *para* -H), 7.85 (d, J=7.5 Hz, 2H, SO_2Ph -*ortho* -H).

(*S*)-Acid: prepared by the general procedure. The crude product was purified by flash chromatography (5% CH_3OH in CH_2Cl_2, 1% acetic acid) giving the pure acid in 90% yield as a white foam: m.p. 89–91 °C (foam); ^1H NMR (250 MHz, $CDCl_3$) δ 1.50 (s, 3H, 2-CH_3), 3.11 (AB q, 2H, J_{AB}= 13.5 Hz, Δν= 51.3 Hz, CH_2), 3.89 (s, 6H, OCH_3), 5.32 (s, 1H, NH), 6.80 (m, 2H, Ar-5, 6-H), 6.88 (d, J=2.5 Hz, 1H, Ar-2-H), 7.53 (m, 3H, SO_2Ph-*meta* & *para*-H), 7.88 (d, J=7.5 Hz, 2H, SO_2Ph-*ortho*-H); ^{13}C NMR (75.4 MHz, $CDCl_3$) δ 21.9, 45.8, 55.9, 56.0, 63.3, 111.1, 113.7, 122.3, 126.7, 126.8, 128.9, 132.4, 142.6, 148.3, 148.6, 185.9; IR (neat) 3000, 1710, 1590, 1505, 1259, 1150, 1088, 1019 cm^{-1}; MS (EI) *m/e* calc'd for $C_{18}H_{21}NO_6S$: 379.1090, found 379.1088; 379 (3), 151 (100), 77 (14); $[\alpha]_D^{20}$ +24.9° (c=0.27, $CHCl_3$).

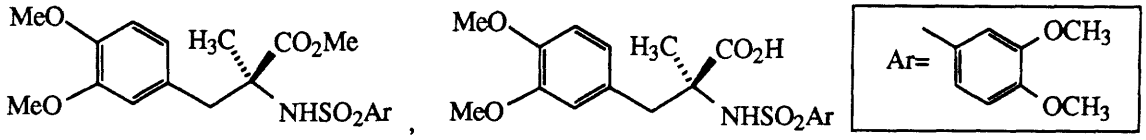

(*S*)-Methyl ester: prepared by the general procedure in 86% yield: ^{1}H NMR (300 MHz, $CDCl_3$) δ 1.47 (s, 3H, 2-C<u>H</u>$_3$), 3.08 (AB q, 2H, J_{AB}= 15.0 Hz, Δν= 69.0 Hz, C<u>H</u>$_2$), 3.64 (s, 3H, CO_2C<u>H</u>$_3$), 3.86 (s, 3H, OC<u>H</u>$_3$), 3.88 (s, 3H, OC<u>H</u>$_3$), 3.91 (s, 3H, OC<u>H</u>$_3$), 3.93 (s, 3H, OC<u>H</u>$_3$), 5.27 (s, 1H, N<u>H</u>), 6.65 (dd, J=2.5, 9.0 Hz, 1H, Ar-6-<u>H</u>), 6.78 (m, 2H, Ar-2, 5-<u>H</u>), 6.89 (d, J=9.0 Hz, 1H, SO_2Ar-5-<u>H</u>), 7.32 (d, J=2.5 Hz, 1H, SO_2Ar-2-<u>H</u>), 7.48 (dd, J=2.5, 9.0 Hz, 1H, SO_2Ar-6-<u>H</u>).

(*S*)-Acid: prepared by the general procedure. The crude product was purified by flash chromatography (5% CH_3OH in CH_2Cl_2, 1% acetic acid) and recrystallization from ethyl acetate/hexane giving the pure acid in 83% yield as a pale yellow solid: m.p. 124–7 °C; ^{1}H NMR (250 MHz, $CDCl_3$) δ 1.48 (s, 3H, 2-C<u>H</u>$_3$), 3.09 (AB q, 2H, J_{AB}= 12.5 Hz, Δν= 42.5 Hz, C<u>H</u>$_2$), 3.83 (s, 3H, OC<u>H</u>$_3$), 3.84 (s, 3H, OC<u>H</u>$_3$), 3.86 (s, 3H, OC<u>H</u>$_3$), 3.89 (s, 3H, OC<u>H</u>$_3$), 5.20 (s, 1H, N<u>H</u>), 6.78 (m, 3H, Ar-2, 5, 6-<u>H</u>), 6.86 (d, J=9.0 Hz, 1H, SO_2Ar-5-<u>H</u>), 7.29 (d, J=2.5 Hz, 1H, SO_2Ar-2-<u>H</u>), 7.46 (dd, J=2.5, 9.0 Hz, 1H, SO_2Ar-6-<u>H</u>); ^{13}C NMR (75.4 MHz, $CDCl_3$) δ 21.0, 45.2, 55.4, 55.7, 62.5, 109.0, 109.9, 110.7, 113.3, 120.3, 121.9, 126.3, 133.8, 148.0, 148.2, 148.5, 152.0, 177.6; IR (neat) 3529, 3274, 2938, 1719, 1591, 1511, 1464, 1407, 1313, 1264, 1138, 1095, 1023 cm^{-1}; MS (EI) *m/e* calc'd for $C_{20}H_{25}NO_8S$: 439.1301, found 439.1303; 439 (3), 201 (14), 151 (100), 137 (17), 107 (8); $[\alpha]_D^{20}$ +13.0° (c=0.70, $CHCl_3$).

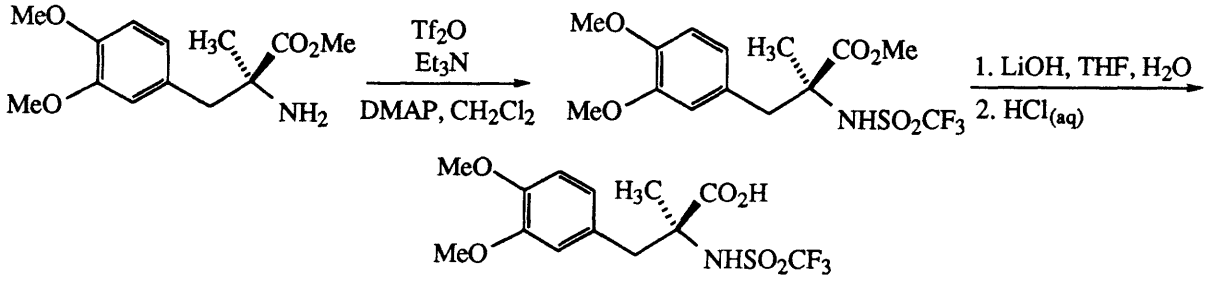

(*S*)-Methyl ester: To a solution of the amino ester (296 mg, 1.17 mmol, 1 equiv),

triethylamine (0.50 mL, 3.5 mmol, 3 equiv), and 4-DMAP (ca. 13 mg, 0.12 mmol, 0.1 equiv) in CH_2Cl_2 (2.5 mL) at -20 °C was very slowly added triflic anhydride (0.24 mL, 1.4 mmol, 1.2 equiv) via syringe. The solution was allowed to warm up to room temperature and was stirred overnight, then diluted with CH_2Cl_2 (15 mL) and shaken with aqueous saturated $NaHCO_3$ (10 mL) and water (10 mL). The aqueous layers were extracted with CH_2Cl_2 (3 x 10 mL), and the combined organic phases were washed with brine, dried ($MgSO_4$), and concentrated in vacuo. The crude product was purified by flash chromatography (10–30% ethyl acetate in hexane), giving the pure sulfonamido ester (360 mg, 0.934 mmol, 80%): ^1H NMR (250 MHz, $CDCl_3$) δ 1.78 (s, 3H, 2-$C\underline{H}_3$), 3.16 (AB q, 2H, J_{AB}= 12.5 Hz, Δν=7.5 Hz, $C\underline{H}_2$), 3.78 (s, 3H, $CO_2C\underline{H}_3$), 3.85 (s, 3H, $OC\underline{H}_3$), 3.86 (s, 3H, $OC\underline{H}_3$), 5.59 (br s, 1H, N$\underline{H}$), 6.59 (dd, J=10.0, 2.5 Hz, 1H, Ar-6-$\underline{H}$), 6.69 (d, J=2.5 Hz, 1H, Ar-2-$\underline{H}$), 6.78 (d, J=10.0 Hz, 1H, Ar-5-$\underline{H}$).

(*S*)-Acid: prepared by the general procedure. Flash chromatography (10% CH_3OH in CH_2Cl_2, 1% acetic acid) afforded the pure sulfonamido acid as a white foam in 81% yield.: ^1H NMR (250 MHz, $CDCl_3$) δ 1.82 (s, 3H, 2-$C\underline{H}_3$), 3.21 (s, 2H, $C\underline{H}_2$), 3.85 (s, 3H, $OC\underline{H}_3$), 3.86 (s, 3H, $OC\underline{H}_3$), 5.58 (br s, 1H, N$\underline{H}$), 6.70 (dd, J=7.5, 2.5 Hz, 1H, Ar-6-$\underline{H}$), 6.75 (d, J=2.5 Hz, 1H, Ar-2-$\underline{H}$), 6.80 (d, J=7.5 Hz, 1H, Ar-5-$\underline{H}$); ^{13}C NMR (75.4 MHz, CD_3OD) δ 22.0, 46.0, 56.4, 56.5, 65.9, 112.8, 115.5, 118.6, 124.3, 128.9, 150.0, 150.1, 157.4, 175.7; IR (neat) 3444, 1728, 1519, 1466, 1371, 1265, 1197, 1143, 1025 cm^{-1}; MS (EI) *m/e* calc'd for $C_{13}H_{16}NO_6SF_3$: 371.0650, found 371.0647; 371 (29), 151 (100), 107 (20), 42 (16); $[\alpha]_D^{20}$ +41.3° (c=0.52, 10% CH_3OH in $CHCl_3$).

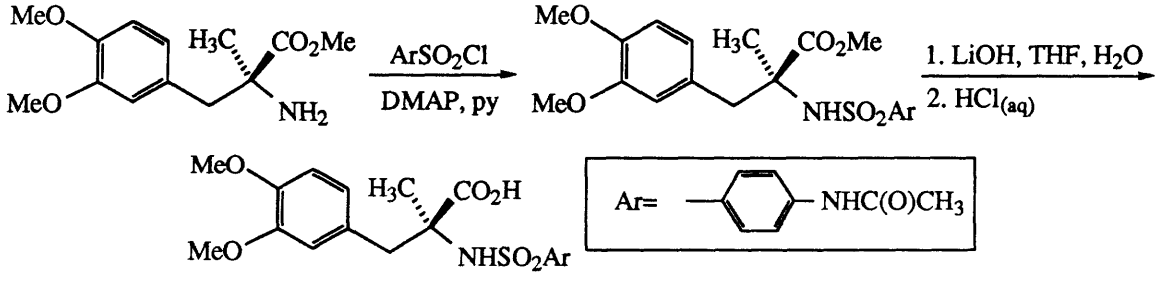

(*S*)-Methyl ester: To a solution of the amino ester (488 mg, 1.93 mmol, 1 equiv)

and 4-DMAP (ca. 20 mg, 0.19 mmol, 0.1 equiv) in pyridine (8 mL) was gradually added 4-acetamidobenzenesulfonyl chloride (630 mg, 2.69 mmol, 1.4 equiv). The resulting yellow solution was stirred overnight at 45–50 °C, then concentrated in vacuo and flushed three times with benzene on a rotary evaporator. The residue was taken up in CH_2Cl_2 (15 mL), and shaken with saturated $NaHCO_3$ (2 x 10 mL) and 1 M HCl (3 x 10 mL) aqueous solutions. The organic phases were dried ($MgSO_4$) and evaporated, providing the crude product as an orange foam. Purification was accomplished by flash chromatography (2.5% CH_3OH in CH_2Cl_2), affording the sulfonamido ester as a white solid (750 mg, 1.66 mmol, 86%): ^1H NMR (250 MHz, $CDCl_3$) δ 1.44 (s, 3H, 2-C<u>H</u>$_3$), 2.19 (s, 3H, C<u>H</u>$_3$CO-), 3.07 (AB q, 2H, J_{AB}=13.5 Hz, Δν= 55.1 Hz, C<u>H</u>$_2$), 3.62 (s, 3H, CO_2C<u>H</u>$_3$), 3.84 (s, 3H, OC<u>H</u>$_3$), 3.86 (s, 3H, OC<u>H</u>$_3$), 5.27 (br s, 1H, N<u>H</u>SO_2), 6.64 (dd, J=7.5, 2.5 Hz, 1H, Ar-6-<u>H</u>), 6.76 (m, 2H, Ar-2, 5-<u>H</u>), 7.29 (br s, 1H, $CH_3C(O)N$<u>H</u>), 7.60 (d, J=8.7 Hz, 2H, SO_2Ar<u>H</u>), 7.79 (d, J=8.7 Hz, 2H, SO_2Ar<u>H</u>).

(*S*)-Acid: prepared by the general procedure but using only 1 equiv of $LiOH{\cdot}H_2O$ to avoid hydrolysis of the amide. The reaction mixture was stirred for 2 days at room temperature and treated as previously described. The crude product was purified by flash chromatography (5% CH_3OH in CH_2Cl_2, 1% acetic acid), giving the sulfonamido acid as a white powder in 85% yield: m.p. 184–6 °C; ^1H NMR (250 MHz, $CDCl_3$) δ 1.46 (s, 3H, 2-C<u>H</u>$_3$), 2.14 (br s, 1H, COO<u>H</u>), 2.18 (s, 3H, C<u>H</u>$_3$CO), 3.07 (AB q, 2H, J_{AB}= 15.0 Hz, Δν=27.5 Hz, C<u>H</u>$_2$), 3.80 (s, 3H, OC<u>H</u>$_3$), 3.81 (s, 3H, OC<u>H</u>$_3$), 5.30 (s, 1H, N<u>H</u>SO_2), 6.78 (m, 3H, Ar-2, 5, 6-<u>H</u>), 7.54 (br s, 1H, N<u>H</u>CO), 7.58 (d, J=7.5 Hz, 2H, SO_2Ar<u>H</u>), 7.78 (d, J=7.5 Hz, 2H, SO_2Ar<u>H</u>); ^{13}C NMR (75.4 MHz, CD_3OD) δ 21.8, 23.5, 45.6, 55.9, 56.0, 63.4, 112.2, 115.3, 119.8, 123.8, 128.5, 129.2, 138.7, 143.3, 149.2, 149.5, 171.5, 175.8; IR (neat) 3337, 1721, 1681, 1592, 1518, 1317, 1263, 1155, 1094, 1024 cm^{-1}; MS (EI) *m/e* calc'd for $C_{20}H_{24}N_2O_7S$: 436.1304, found 436.1303; 436 (2), 151 (100), 198 (8), 107 (6); $[\alpha]_D^{20}$ +22.4° (c=0.46, 20% CH_3OH in $CHCl_3$).

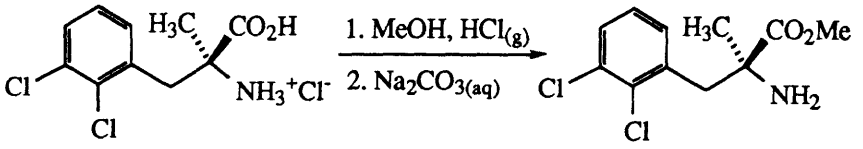

The resolved (*S*)-amino acid was kindly provided by Dr. Dominique Depernet of SIPSY (Avrillé Cedex, France): m.p. >250° (dec); ^{1}H NMR (300 MHz, $CDCl_3$) δ 1.43 (s, 3H, C<u>H</u>$_3$), 3.00 (AB q, 2H, J_{AB}=14.0 Hz, Δν= 103.6 Hz, C<u>H</u>$_2$), 7.10 (dd, J=1.8, 8.1 Hz, 1H, Ar<u>H</u>), 7.34–7.42 (m, 2H, Ar<u>H</u>), 11.04 (br s, 1H, COO<u>H</u>); ^{13}C NMR (75.4 MHz, CD_3OD/1 N HCl) δ 22.6, 42.4, 61.5, 131.0, 131.8, 132.8, 132.9, 133.2, 135.0, 173.5; IR (Nujol) 2923, 1619, 1516, 1399, 1305 cm^{-1}; MS (EI) *m/e* calc'd for [M - CO_2H]$^+$: 202.0190, found 202.0190; 202 (20), 88 (100), 43 (53); $[\alpha]_D^{20}$ +16.6° (c=0.92, CH_3OH/1N HCl).

(*S*)-Amino ester: A suspension of the amino acid (2.5 g, 10.1 mmol, 1 equiv) and trimethylorthoformate (1.3 mL, 12 mmol, 1.2 equiv) in dry methanol (40 mL) was saturated with hydrogen chloride gas, and the resulting homogeneous solution was heated under reflux overnight. After cooling to room temperature, the reaction mixture was concentrated in vacuo and the residue was cooled to 0 °C and carefully treated with aqueous 5% Na_2CO_3 solution. The aqueous phase was shaken with CH_2Cl_2 (5 x 30 mL), and the combined organic phases were washed with brine, dried ($MgSO_4$), and concentrated to give the amino ester, which was used in the next step without further purification (1.93 g, 7.36 mmol, 73%): ^{1}H NMR (300 MHz, $CDCl_3$) δ 1.36 (s, 3H, 2-C<u>H</u>$_3$), 1.58 (br s, 2H, N<u>H</u>$_2$), 2.88 (AB q, 2H, J_{AB}= 13.2 Hz, Δν= 91.2 Hz, C<u>H</u>$_2$), 3.69 (s, 3H, CO_2C<u>H</u>$_3$), 6.98 (dd, J=2.1, 8.1 Hz, 1H, Ar<u>H</u>), 7.25 (m, 1H, Ar<u>H</u>), 7.32 (d, J=8.1 Hz, 1H, Ar<u>H</u>); ^{13}C NMR (75.4 MHz, $CDCl_3$) δ 26.5, 45.9, 52.2, 58.7, 129.2, 130.0, 131.0, 131.7, 132.1, 136.7, 176.8; IR (neat) 3378, 2951, 1732, 1594, 1560, 1472, 1396, 1264, 1201, 1105, 1032, 895, 828 cm^{-1}; MS (EI) *m/e* calc'd for [M - CH_3]$^+$: 246.0089, found 246.0089; 262 (1), 202 (33), 102 (100), 43 (39); $[\alpha]_D^{20}$ -11.2° (c=0.71, $CHCl_3$).

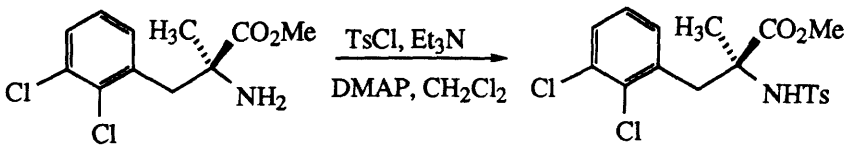

(*S*)-Methyl ester: To a solution of the amino ester (1.93 g, 7.36 mmol, 1 equiv) in CH_2Cl_2 (20 mL) at 0 °C was added triethylamine (5.1 mL, 37 mmol, 5 equiv), 4-DMAP (ca. 20 mg, 0.18 mmol, 0.02 equiv), and tosyl chloride (1.54 g, 8.10 mmol, 1.1 equiv) . The solution was allowed to warm up to room temperature and was stirred overnight, then diluted with CH_2Cl_2 (15 mL) and shaken with aqueous saturated $NaHCO_3$ (10 mL) and water (10 mL). The aqueous layers were extracted with CH_2Cl_2 (3 x 10 mL), and the combined organic phases were washed with brine, dried ($MgSO_4$), and concentrated in vacuo. The crude product, a brown oil, was purified by flash chromatography (10–45% ethyl acetate in hexane), giving the pure sulfonamido ester as a pale yellow foam (2.86 g, 6.87 mmol, 93%): ^{1}H NMR (250 MHz, $CDCl_3$) δ 1.42 (s, 3H, 2-C<u>H</u>$_3$), 2.39 (s, 3H, ArC<u>H</u>$_3$), 3.12 (AB q, 2H, J_{AB}= 13.6 Hz, Δν= 78.1 Hz, C<u>H</u>$_2$), 3.64 (s, 3H, CO_2C<u>H</u>$_3$), 5.36 (br s, 1H, N<u>H</u>), 7.06 (dd, J=2.1, 8.2 Hz, 1H, Ar<u>H</u>), 7.19–7.27 (m, 3H, Ar<u>H</u>), 7.34 (d, J=8.2 Hz, 1H, Ar<u>H</u>), 7.72 (d, J=7.5 Hz, 2H, Ar<u>H</u>).

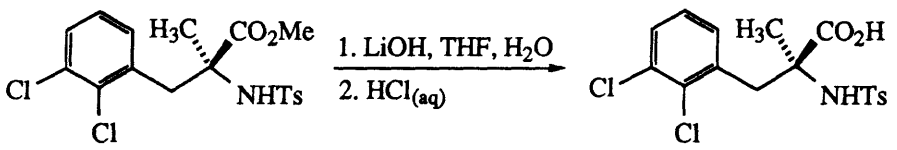

(*S*)-Acid: prepared by the general procedure. The crude product was purified by recrystallization from ethyl acetate/hexane giving the pure acid in 82% yield as white crystals: m.p. 181–3 °C; ^{1}H NMR (300 MHz, $CDCl_3/CD_3OD$) δ 1.30 (s, 3H, 2-C<u>H</u>$_3$), 2.29 (s, 3H, ArC<u>H</u>$_3$), 3.03 (AB q, 2H, J_{AB}= 13.2 Hz, Δν= 82.4 Hz, C<u>H</u>$_2$), 7.06 (d, J=8.1 Hz, 1H, Ar<u>H</u>), 7.15 (d, J=7.8 Hz, 2H, Ar<u>H</u>), 7.21–7.25 (m, 2H, Ar<u>H</u>), 7.60 (d, J=8.1 Hz, 2H, Ar<u>H</u>); ^{13}C NMR (75.4 MHz, $CDCl_3/CD_3OD$) δ 21.3, 22.2, 44.2, 62.7, 126.5, 129.4, 129.9, 130.0, 131.0, 131.8, 132.0, 135.8, 139.9, 143.2, 174.4; IR (neat) 3261, 1712, 1470, 1304, 1153, 1091 cm^{-1}; MS (EI) *m/e* calc'd for [M - CO_2H]$^+$:

356.0279, found 356.0276; 356 (10), 242 (100), 173 (87), 155 (100), 91 (69); $[\alpha]_D^{20}$ +19.2° (c=0.77, CH_3OH).

6.4 Compounds Derived from Menthone

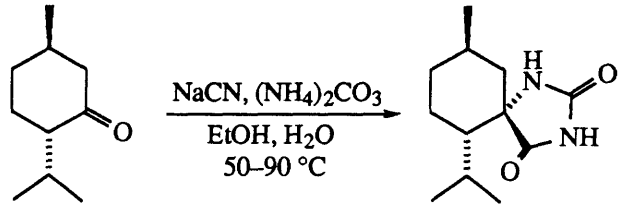

The hydantoin was prepared from (–)-menthone by a modification of the literature procedures[69] for the Bucherer–Bergs reaction. A solution of (–)-menthone (25.0 g, 162 mmol, 1 equiv), potassium cyanide (12.0 g, 184 mmol, 1.1 equiv), and ammonium carbonate (32.0 g, 333 mmol, 2.1 equiv) in ethanol (150 mL)-water (150 mL) was heated at 50–55 °C for 8 h, then at 90–95 °C for 1 h. The reaction mixture was cooled to 0 °C, and the crude product was removed by filtration, washed with water, and recrystallized from ethanol to give the pure (1*S*,2*S*,5*R*)-*spiro*-hydantoin as white crystals (16.3 g, 72.6 mmol, 45%): m.p. 223–6 °C (lit.[69] 228–231.5 °C); ^{1}H NMR (300 MHz, $CDCl_3/CD_3OD$) δ 0.68 (d, J=7.2 Hz, 3H, 5-C<u>H</u>$_3$), 0.74 (d, J=6.6 Hz, 3H, ^{i}Pr-C<u>H</u>$_3$), 0.76 (d, J=5.4 Hz, 3H, ^{i}Pr-C<u>H</u>$_3$), 0.86 (br q, J=11.7 Hz, 1H, cyclohexyl-<u>H</u>), 1.10 (br q of d, J=12.9, 3.3 Hz, 1H, cyclohexyl-<u>H</u>), 1.26–1.70 (m, 7H, cyclohexyl-<u>H</u> and ^{i}Pr-C<u>H</u>), 7.57 (br s, 1H, N<u>H</u>), 9.92 (br s, 1H, N<u>H</u>); ^{13}C NMR (75.4 MHz, $CDCl_3/CD_3OD$) δ 17.9, 21.6, 21.9, 22.9, 28.1, 33.9, 44.1, 45.8, 68.2, 157.5, 179.1; IR (neat) 3238, 2954, 1716, 1410, 1021 cm^{-1}; MS (EI) *m/e* calc'd for $C_{12}H_{20}N_2O_2$: 224.1525, found 224.1523; 224 (51), 139 (13), 113 (100), 69 (31), 56 (27), 41 (23); $[\alpha]_D^{20}$ +12.8° (c=1.0, CH_3OH).

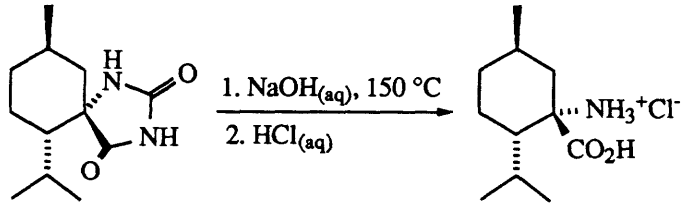

A solution of the *spiro*-hydantoin (10.6 g, 47.3 mmol, 1 equiv) in aqueous 5 M NaOH solution (150 mL, 750 mmol, 16 equiv) was heated to 150 °C for 5 days in an

autoclave or Parr bomb. The reaction mixture was cooled to room temperature, carefully acidified with concentrated HCl solution to pH= 1–2, and evaporated to dryness in vacuo. The remaining white solid was washed with water and taken up in ethanol, and residual solid impurities were removed by filtration. The ethanolic solution was evaporated in vacuo, and the pure hydrochloride salt of the (1*S*,2*S*,5*R*)-amino acid was obtained by recrystallization of the crude product from ethanol (5.73 g, 24.3 mmol, 51%): m.p. 240–245 °C (lit.[69] 330 °C); ^{1}H NMR (300 MHz, $CDCl_3/CD_3OD$) δ 0.85 (d, J=6.6 Hz, 3H, 5-C<u>H</u>$_3$), 0.89 (d, J=6.3 Hz, 3H, ^{i}Pr-C<u>H</u>$_3$), 0.94 (d, J=6.9 Hz, 3H, ^{i}Pr-C<u>H</u>$_3$), 1.03 (br dd, J=12.0, 12.0 Hz, 1H, 6-ax-<u>H</u>), 1.28 (br dd, J=12.0, 15.0 Hz, 1H, 2-ax-<u>H</u>), 1.40–1.98 (m, 7H, cyclohexyl-<u>H</u> and ^{i}Pr-C<u>H</u>), 2.85 (br s, 3H, N<u>H</u>$_3^+$); IR (neat) 3150, 2954, 1693, 1381 cm^{-1}; $[\alpha]_D^{20}$ +16.1° (c=0.31, CH_3OH).

To a stirred suspension of the hydrochloride salt of the (1*S*,2*S*,5*R*)-amino acid (5.58 g, 23.7 mmol, 1 equiv) in pyridine (100 mL) at 0 °C was added dropwise methyl chloroformate (3.7 mL, 47 mmol, 2 equiv). The reaction mixture was allowed to warm up and was stirred at room temperature for 1 h, then poured into an ice-sulfuric acid mixture (pH= 2) and extracted with CH_2Cl_2. The organic layers were dried ($MgSO_4$) and concentrated in vacuo giving the crude product. Purification was accomplished by recrystallization from ethyl acetate/hexane and the pure (1*S*,2*S*,5*R*)-carbamate was obtained as a white solid (3.76 g, 14.6 mmol, 62%): m.p. 142–144 °C; ^{1}H NMR (300 MHz, $CDCl_3$) δ 0.88 (d, J=6.0 Hz, 3H, 5-C<u>H</u>$_3$), 0.91 (d, J=6.0 Hz, 3H, ^{i}Pr-C<u>H</u>$_3$), 0.93 (d, J=6.0 Hz, 3H, ^{i}Pr-C<u>H</u>$_3$), 1.00 (m, 1H, 6-ax-<u>H</u>), 1.21–1.85 (m, 7H, cyclohexyl-<u>H</u> and ^{i}Pr-C<u>H</u>), 2.71 (br d, J=12.5 Hz, 1H, 6-eq-<u>H</u>), 3.70 (s, 3H, CO_2C<u>H</u>$_3$), 4.92 (br s, 1H,

NH), 10.30 (br s, 1H, COOH); ^{13}C NMR (75.4 MHz, $CDCl_3$) δ 18.8, 21.8, 23.9, 27.1, 28.0, 34.4, 40.3, 48.2, 52.2, 64.5, 156.0, 178.5; IR (neat) 2955, 1716, 1511, 1456, 1382, 1252, 779, 738 cm^{-1}; MS (EI) *m/e* calc'd for $C_{13}H_{23}NO_4$: 257.1627, found 257.1624; 257 (1), 213 (20), 212 (100), 137 (100), 95 (55), 81 (57), 76 (57), 42 (42); $[\alpha]_D^{20}$ -16.2° (c=1.0, $CHCl_3$); Analysis calc'd for $C_{13}H_{23}NO_4$: C, 60.68; H, 9.01; N, 5.44; found: C, 60.87; H, 9.07; N, 5.44.

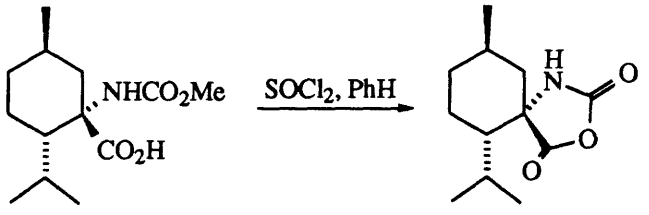

To a solution of the carbamate (3.76 g, 14.6 mmol, 1 equiv) in benzene (38 mL) was added thionyl chloride (1.59 mL, 21.9 mmol, 1.5 equiv) at 0 °C. The mixture was heated under reflux for 2 h, when gas evolution ceased. Evaporation of the reaction mixture three times from benzene on a rotary evaporator afforded the anhydride as a brown solid, which was either used directly in the next reaction or purified by flash chromatography (10–20% ethyl acetate in hexane) to give the (1*S*,2*S*,5*R*)-*spiro*-compound as a white solid (2.47 g, 11.0 mmol, 75%): m.p. 112–114 °C; ^{1}H NMR (250 MHz, $CDCl_3$) δ 0.85 (d, J=6.8 Hz, 3H, 5-CH$_3$), 0.93 (d, J=6.7 Hz, 3H, ^{i}Pr-CH$_3$), 0.95 (d, J=6.7 Hz, 3H, ^{i}Pr-CH$_3$), 1.00–1.34 (m, 2H, 6-ax-H, 2-ax-H), 1.54–1.89 (m, 7H, cyclohexyl-H and ^{i}Pr-CH), 7.65 (br s, 1H, NH); ^{13}C NMR (75.4 MHz, $CDCl_3$) δ 18.4, 21.7, 22.8, 23.0, 28.5, 29.0, 33.7, 44.3, 46.6, 68.5, 153.0, 172.7; IR (neat) 3230, 2959, 1762, 1345, 1191, 934 cm^{-1}; MS (EI) *m/e* calc'd for $C_{12}H_{19}NO_3$: 225.1365, found 225.1366; 225 (2), 180 (100), 114 (24), 83 (37), 70 (46), 69 (69), 57 (53), 56 (71), 55 (57), 44 (39), 42 (64); $[\alpha]_D^{20}$ +16.4° (c=1.0, $CHCl_3$); Analysis calc'd for $C_{12}H_{19}NO_3$: C, 63.98; H, 8.5; N, 6.21; found: C, 63.71; H, 8.34; N, 6.19.

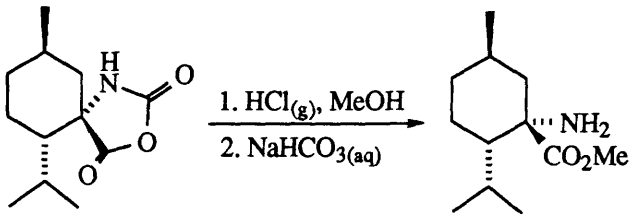

A solution of the anhydride (2.40 g, 10.7 mmol, 1 equiv) in methanol (50 mL) was saturated with hydrochloric acid gas at room temperature, then heated under reflux for 2 h, at which point TLC analysis indicated the complete consumption of starting material. The solvent was removed in vacuo, and the residue was cooled to 0 °C and cautiously neutralized with saturated aqueous $NaHCO_3$ solution. The aqueous solution was extracted with ether, and the organic layers were dried ($MgSO_4$) and concentrated in vacuo, giving the (1*S*,2*S*,5*R*)-amino ester as a pale yellow oil (2.21g, 10.4 mmol, 97%). This was used in the next step without additional purification: b.p. 50–53 °C/0.025 mm Hg; ^1H NMR (300 MHz, $CDCl_3$) δ 0.82 (d, J=6.0 Hz, 3H, 5-C<u>H</u>$_3$), 0.84 (d, J=6.6 Hz, 3H, ^{i}Pr-C<u>H</u>$_3$), 0.87 (d, J=6.6 Hz, 3H, ^{i}Pr-C<u>H</u>$_3$), 0.96 (m, 1H, 6-ax-<u>H</u>), 1.30–1.80 (m, 10H, cyclohexyl-<u>H</u>, ^{i}Pr-C<u>H</u>, N<u>H</u>$_2$), 3.70 (s, 3H, $CO_2C\underline{H}_3$); ^{13}C NMR (75.4 MHz, $CDCl_3$) δ 19.9, 22.1, 22.9, 23.1, 27.0, 29.3, 35.0, 47.0, 47.2, 52.0, 62.5, 179.5; IR (neat) 2950, 1729, 1597, 1456, 1367, 1259, 1220, 1160, 1096, 1014, 850 cm^{-1}; MS (EI) *m/e* calc'd for $C_{12}H_{23}NO_2$: 213.1729, found 213.1718; 213 (0.3), 154 (100), 128 (33), 112 (27), 95 (23), 81 (23), 69 (18), 55 (13), 42 (14); $[\alpha]_D^{20}$ +10.5° (c=1.1, $CHCl_3$); Analysis calc'd for $C_{12}H_{23}NO_2$: C, 67.57; H, 10.87; N, 6.56; found: C, 67.39; H, 10.91; N, 6.46.

<u>The following serves as a general procedure for sulfonamide formation</u>:

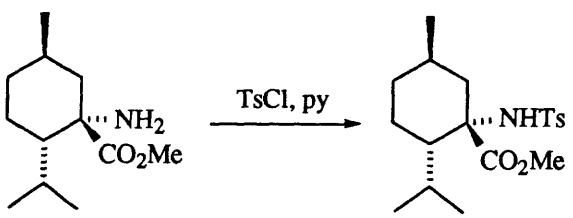

A mixture of the amino ester (3.4 g, 16 mmol, 1 equiv) and tosyl chloride (6.0 g, 32 mmol, 2 equiv) in pyridine (50 mL) was stirred at room temperature overnight, then poured into an ice-aqueous 1 M HCl solution (pH= 1) and extracted with CH_2Cl_2. The combined organic extracts were washed with saturated aqueous $NaHCO_3$ and brine, then dried ($MgSO_4$) and evaporated to provide an orange oil. The crude product was purified by flash chromatography (5–10% ethyl acetate in hexane to elute the excess tosyl chloride, followed by 25–35%), affording the pure (1*S*,2*S*,5*R*)-sulfonamido ester as a white solid (4.39 g, 11.9 mmol, 75%): m.p. 110–111 °C; ^{1}H NMR (250 MHz, $CDCl_3$) δ 0.64 (d, J=6.4 Hz, 3H, 5-C<u>H</u>$_3$), 0.82 (d, J=6.9 Hz, 3H, ^{i}Pr-C<u>H</u>$_3$), 0.86 (d, J=6.7 Hz, 3H, ^{i}Pr-C<u>H</u>$_3$), 0.98–1.40 (m, 2H, 2-ax-<u>H</u>, 6-ax-<u>H</u>), 1.45–1.80 (m, 6H, cyclohexyl-<u>H</u> and ^{i}Pr-C<u>H</u>), 2.37 (br d, J=10.0 Hz, 1H, 6-eq-<u>H</u>), 2.40 (s, 3H, ArC<u>H</u>$_3$), 3.62 (s, 3H, CO_2C<u>H</u>$_3$), 4.71 (s, 1H, N<u>H</u>), 7.25 (d, J=8.3 Hz, 2H, SO_2Ar-<u>H</u>), 7.74 (d, J=8.3 Hz, 2H, SO_2Ar-<u>H</u>); ^{13}C NMR (75.4 MHz, $CDCl_3$) δ 18.6, 21.3, 21.4, 23.7, 26.8, 27.0, 34.3, 40.3, 49.8, 52.0, 67.8, 126.8, 129.1, 139.8, 142.7, 174.1; IR (neat) 3316, 2953, 1735, 1457, 1325, 1151, 1094 cm^{-1}; MS (EI) *m/e* calc'd for [M - CO_2CH_3]$^+$: 308.1684, found 308.1686; 368 (0.3), 309 (100), 155 (37), 137 (55), 91 (45), 81 (40), 69 (32), 55 (26), 42 (37); $[\alpha]_D^{20}$ -27.1° (c=1.0, $CHCl_3$); Analysis calc'd for $C_{19}H_{29}NO_4S$: C, 62.10; H, 7.95; N, 3.81; S, 8.73; found: C, 62.02; H, 7.89; N, 3.75; S, 8.80.

<u>The following serve as general procedures for the hydrolysis of the methyl ester:</u>

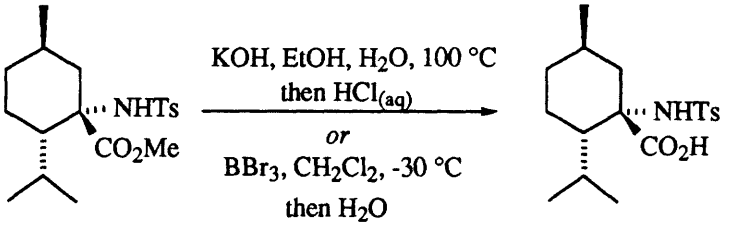

<u>KOH Method</u>: A solution of the ester (5.0 g, 14 mmol, 1 equiv) and potassium hydroxide (3.6 g, 56 mmol, 4 equiv) in 9:1 ethanol-water (120 mL) was heated at reflux

for 5 days, when starting material was no longer visible by TLC analysis. The reaction mixture was cooled to 0 °C, acidified with 1 M H_2SO_4 solution, and extracted with CH_2Cl_2. The organic phases were dried ($MgSO_4$) and evaporated, and the crude product thus obtained was recrystallized from ethyl acetate/hexane, affording the pure (1*S*,2*S*,5*R*)-sulfonamide-acid as white crystals (4.4 g, 12 mmol, 86%).

BBr3 Method: To a solution of the ester (2.19 g, 5.96 mmol, 1 equiv) in CH_2Cl_2 (50 mL) at -30 °C was slowly added boron tribromide (12 mL of a 1 M solution in CH_2Cl_2, 12 mmol, 2 equiv). The reaction mixture was allowed to warm up and was stirred an additional hour at room temperature. After re-cooling the solution to 0 °C, the reaction was quenched by dropwise addition of water (10 mL). The layers were separated, the aqueous layers were extracted with CH_2Cl_2, and the combined organic phases were washed with water and brine, dried ($MgSO_4$), and evaporated. The residue was purified by flash chromatography (1–5% CH_3OH in CH_2Cl_2) affording the pure sulfonamido acid as a white solid (1.79 g, 5.06 mmol, 85%): m.p. 187–189 °C; ^1H NMR (300 MHz, $CDCl_3$) δ 0.63 (d, J=6.4 Hz, 3H, 5-C<u>H</u>$_3$), 0.83 (d, J=7.2 Hz, 3H, ^{i}Pr-C<u>H</u>$_3$), 0.85 (d, J=7.1 Hz, 3H, ^{i}Pr-C<u>H</u>$_3$), 0.86 (buried m, 1H, 5-ax-<u>H</u>), 1.07 (m, 1H, 4-ax-<u>H</u>), 1.27 (ddd, J=21.0, 15.0, 6.0 Hz, 1H, 3-ax-<u>H</u>), 1.46-1.63 (m, 4H, cyclohexyl-<u>H</u>), 1.81 (sep of d, J=7.1, 3.0 Hz, 1H, ^{i}Pr-C<u>H</u>), 2.37 (s, 3H, ArC<u>H</u>$_3$), 2.43 (br d, J=14.7 Hz, 1H, 6-eq-<u>H</u>), 4.77 (s, 1H, N<u>H</u>), 7.24 (d, J=8.6 Hz, 2H, SO_2Ar<u>H</u>), 7.73 (d, J=8.5 Hz, 2H, SO_2Ar<u>H</u>), 10.95 (br s, 1H, COO<u>H</u>); ^{13}C NMR (75.4 MHz, $CDCl_3$) δ 18.7, 21.5, 24.0, 27.1, 27.2, 34.4, 40.0, 49.7, 67.9, 127.1, 129.3, 139.6, 143.2, 177.9; IR (neat) 2950, 1740, 1705, 1375, 1320, 1144, 1085 cm^{-1}; MS (EI) *m/e* calc'd for $[M - CO_2H]^+$: 308.1684, found 308.1683; 308 (100), 137 (51), 91 (76); $[\alpha]_D^{20}$ -9.6° (c=1.0, EtOH).

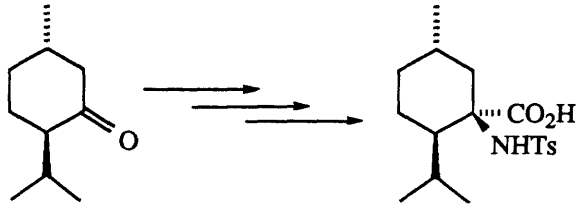

The enantiomeric ligand, the (1*R*,2*R*,5*S*)-sulfonamide-acid {$[\alpha]_D^{20}$ +12.2° (c=1.0, EtOH)}, was prepared in an identical sequence starting with (+)-menthone (obtained by PDC oxidation of (1*S*,2*R*,5*S*)-(+)-menthol in CH_2Cl_2-DMF, 97% yield).

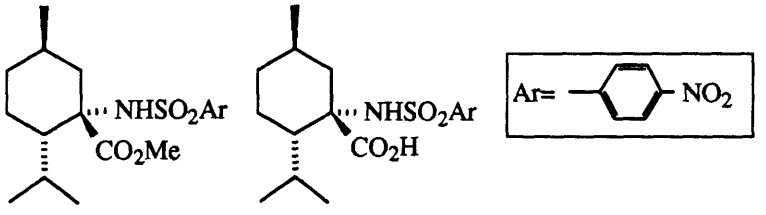

(1*S*,2*S*,5*R*)-Methyl ester: prepared by the general procedure in 69% yield; purified by recrystallization from ethyl acetate/hexane: ^{1}H NMR (300 MHz, $CDCl_3$) δ 0.83 (d, J=6.3 Hz, 3H, 5-C<u>H</u>$_3$), 0.86 (d, J=6.6 Hz, 3H, ^{i}Pr-C<u>H</u>$_3$), 0.93 (d, J=6.6 Hz, 3H, ^{i}Pr-C<u>H</u>$_3$), 1.02 (m, 1H, cyclohexyl-<u>H</u>), 1.35 (m, 2H, cyclohexyl-<u>H</u>), 1.68 (m, 5H, cyclohexyl-<u>H</u>, ^{i}Pr-C<u>H</u>), 2.48 (br d, J=13.8 Hz, 1H, 6-eq-<u>H</u>), 3.68 (s, 3H, CO_2C<u>H</u>$_3$), 4.78 (s, 1H, N<u>H</u>), 8.08 (d, J=8.7 Hz, 2H, SO_2Ar<u>H</u>), 8.38 (d, J=8.7 Hz, 2H, SO_2Ar<u>H</u>).

(1*S*,2*S*,5*R*)-Acid: prepared by the general procedure (BBr_3 method) in 79% yield; purified by recrystallization from ethyl acetate/hexane: m.p. 150–160 °C; ^{1}H NMR (300 MHz, $CDCl_3$) δ 0.82 (d, J=6.3 Hz, 3H, 5-C<u>H</u>$_3$), 0.89 (d, J=7.2 Hz, 3H, ^{i}Pr-C<u>H</u>$_3$), 0.92 (d, J=7.2 Hz, 3H, ^{i}Pr-C<u>H</u>$_3$), 1.01 (m, 1H, cyclohexyl-<u>H</u>), 1.30 (m, 2H, cyclohexyl-<u>H</u>), 1.55–1.80 (m, 5H, cyclohexyl-<u>H</u> and ^{i}Pr-C<u>H</u>), 2.51 (br d, J=13.8 Hz, 1H, 6-eq-<u>H</u>), 4.85 (br s, 1H, N<u>H</u>), 8.06 (d, J=8.9 Hz, 2H, SO_2Ar<u>H</u>), 8.36 (d, J=8.9 Hz, 2H, SO_2Ar<u>H</u>); ^{13}C NMR (75.4 MHz, $CDCl_3$) δ 18.7, 21.4, 21.7, 23.7, 27.1, 27.5, 34.1, 41.0, 49.3, 68.8, 123.9, 128.2, 148.2, 149.7, 178.7; IR (neat) 3321, 2958, 1713, 1532, 1350, 1153, 1093, 853 cm^{-1}; MS (Ei) *m/e* calc'd for $[M - CO_2H]^+$: 339.1379, found 339.1372; 339

(100), 198 (31), 137 (100), 95 (68), 81 (93), 69 (90), 55 (56), 42 (70); $[\alpha]_D^{20}$ +1.9° (c=1.0, $CHCl_3$).

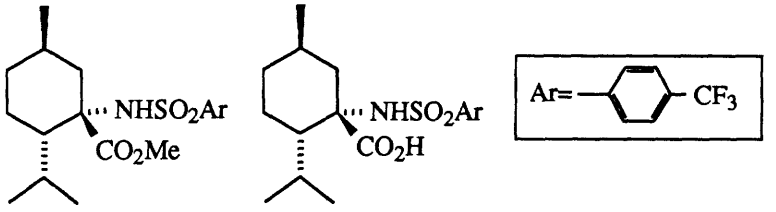

(1*S*,2*S*,5*R*)-Methyl ester: prepared by the general procedure in 49% yield: ^1H NMR (300 MHz, $CDCl_3$) δ 0.69 (d, J=6.3 Hz, 3H, 5-C<u>H</u>$_3$), 0.79 (d, J=7.1 Hz, 3H, ^{i}Pr-C<u>H</u>$_3$), 0.84 (d, J=6.3 Hz, 3H, ^{i}Pr-C<u>H</u>$_3$), 0.95 (m, 1H, 6-ax-<u>H</u>), 1.25 (m, 2H, 4-ax-<u>H</u> and 2-ax-<u>H</u>), 1.58 (m, 4H, cyclohexyl-<u>H</u>), 1.77 (sep of d, J=9.0, 3.0 Hz, 1H, ^{i}Pr-C<u>H</u>), 2.38 (br d, J=15.0 Hz, 1H, 6-eq-<u>H</u>), 3.59 (s, 3H, CO_2C<u>H</u>$_3$), 4.72 (s, 1H, N<u>H</u>), 7.70 (d, J=8.4 Hz, 2H, SO_2Ar<u>H</u>), 7.95 (d, J=8.4 Hz, 2H, SO_2Ar<u>H</u>).

(1*S*,2*S*,5*R*)-Acid: prepared by the general procedure (BBr_3 method) in 92% yield; purified by recrystallization from ethyl acetate/hexane: m.p. 156–158 °C; ^1H NMR (300 MHz, $CDCl_3$) δ 0.69 (d, J=6.3 Hz, 3H, 5-C<u>H</u>$_3$), 0.84 (d, J=6.9 Hz, 3H, ^{i}Pr-C<u>H</u>$_3$), 0.88 (d, J=6.9 Hz, 3H, ^{i}Pr-C<u>H</u>$_3$), 0.93 (m, 1H, 6-ax-<u>H</u>), 1.20 (m, 2H, cyclohexyl-<u>H</u>), 1.49–1.82 (m, 5H, cyclohexyl-<u>H</u> and ^{i}PrC<u>H</u>), 2.45 (br d, J=15.0 Hz, 1H, 6-eq-<u>H</u>), 4.73 (s, 1H, N<u>H</u>), 7.72 (d, J=8.4 Hz, 2H, SO_2Ar<u>H</u>), 7.98 (d, J=8.4 Hz, 2H, SO_2Ar<u>H</u>); ^{13}C NMR (75.4 MHz, $CDCl_3$) δ 18.7, 21.4, 21.6, 23.8, 27.1, 27.4, 34.2, 40.6, 49.5, 68.5, 105.3, 125.8, 126.0, 127.5, 146.1, 178.4; IR (neat) 3312, 2958, 1715, 1405, 1323, 1170 cm^{-1}; MS (EI) *m/e* calc'd for $[M - F]^+$: 388.1394, found 388.1396; 362 (100), 145 (31), 137 (94), 95 (42), 81 (53), 69 (43), 55 (31), 42 (40); $[\alpha]_D^{20}$ -7.8° (c=0.27, $CHCl_3$).

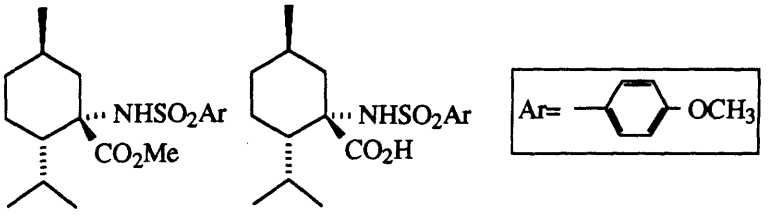

(1*S*,2*S*,5*R*)-Methyl ester: prepared by the general procedure in 29% yield: ^{1}H NMR (300 MHz, $CDCl_3$) δ 0.63 (d, J=6.6 Hz, 3H, 5-C<u>H</u>$_3$), 0.79 (d, J=6.9 Hz, 3H, ^{i}Pr-C<u>H</u>$_3$), 0.84 (d, J=6.9 Hz, 3H, ^{i}Pr-C<u>H</u>$_3$), 0.90 (m, 1H, cyclohexyl-<u>H</u>), 1.05–1.35 (m, 2H, cyclohexyl-<u>H</u>), 1.50–1.76 (m, 5H, cyclohexyl-<u>H</u> and ^{i}Pr-C<u>H</u>), 2.35 (br d, J=12.0 Hz, 1H, 6-eq-<u>H</u>), 3.64 (s, 3H, CO_2C<u>H</u>$_3$), 3.82 (s, 3H, Ar-OC<u>H</u>$_3$), 4.67 (s, 1H, N<u>H</u>), 6.91 (d, J=9.0 Hz, 2H, SO_2Ar<u>H</u>), 7.78 (d, J=9.0 Hz, 2H, SO_2Ar<u>H</u>).

(1*S*,2*S*,5*R*)-Acid: prepared by the general procedure (BBr_3 method) in 60% yield: ^{1}H NMR (300 MHz, $CDCl_3$) δ 0.64 (d, J=6.6 Hz, 3H, 5-C<u>H</u>$_3$), 0.87 (d, J=6.9 Hz, 3H, ^{i}Pr-C<u>H</u>$_3$), 0.88 (d, J=6.9 Hz, 3H, ^{i}Pr-C<u>H</u>$_3$), 0.92 (m, 1H, cyclohexyl-<u>H</u>), 1.22 (m, 2H, cyclohexyl-<u>H</u>), 1.42-1.65 (m, 5H, cyclohexyl-<u>H</u> and ^{i}Pr-C<u>H</u>), 2.41 (br d, J=12.0 Hz, 1H, 6-eq-<u>H</u>), 3.83 (s, 3H, Ar-OC<u>H</u>$_3$), 4.68 (s, 1H, N<u>H</u>), 6.92 (d, J=9.0 Hz, 2H, SO_2Ar<u>H</u>), 7.78 (d, J=9.0 Hz, 2H, SO_2Ar<u>H</u>); ^{13}C NMR (75.4 MHz, $CDCl_3$) δ 18.2, 21.0, 21.1, 23.5, 26.6, 33.9, 39.4, 49.2, 55.1, 67.4, 113.4, 128.7, 133.7, 162.3, 178.2; IR (neat) 3298, 2957, 1712, 1597, 1499, 1260 cm^{-1}; MS (EI) *m/e* calc'd for $C_{18}H_{27}NO_5S$: 369.1610, found 369.1608; 369 (0.3), 324 (100), 171 (80), 137 (50), 107 (42), 69 (42); $[\alpha]_D^{20}$ -14.9° (c=0.61, $CHCl_3$).

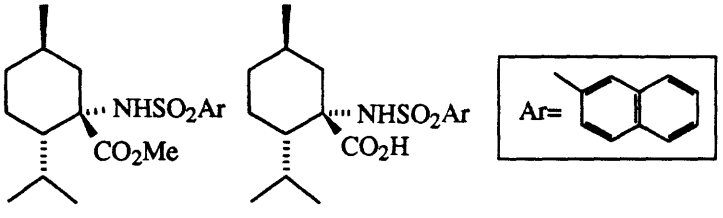

(1*S*,2*S*,5*R*)-Methyl ester: prepared by the general procedure in 40% yield: ^{1}H NMR (250 MHz, $CDCl_3$) δ 0.51 (d, J=6.4 Hz, 3H, 5-C<u>H</u>$_3$), 0.82 (d, J=6.9 Hz, 3H, ^{i}Pr-C<u>H</u>$_3$), 0.89 (d, J=6.7 Hz, 3H, ^{i}Pr-C<u>H</u>$_3$), 1.00 (m, 1H, cyclohexyl-<u>H</u>), 1.25 (m, 2H,

cyclohexyl-H), 1.55-1.85 (m, 5H, cyclohexyl-H and ^{i}Pr-CH$_3$), 2.48 (br d, J=13.1 Hz, 1H, 6-eq-H), 3.60 (s, 3H, CO_2CH_3), 4.80 (s, 1H, NH), 7.60 (m, 2H, naph-6, 7-H), 7.90 (m, 4H, naph-3, 4, 5, 8-H), 8.39 (s, 1H, naph-1-H).

(1*S*,2*S*,5*R*)-Acid: prepared by the general procedure (BBr_3 method) in 46% yield: m.p. 178–181 °C; ^{1}H NMR (300 MHz, $CDCl_3$) δ 0.46 (d, J=6.4 Hz, 2H, 5-CH$_3$), 0.86 (d, J=6.9 Hz, 3H, ^{i}Pr-CH$_3$), 0.89 (d, J=6.9 Hz, 3H, ^{i}Pr-CH$_3$), 1.25 (m, 1H, 6-ax-H), 1.55 (m, 6H, cyclohexyl-H), 1.85 (m, 1H, ^{i}Pr-CH), 2.50 (br d, J=13.1 Hz, 1H, 6-eq-H), 4.79 (s, 1H, NH), 7.58 (m, 2H, naph-6, 7-H), 7.88 (m, 4H, naph-3, 4, 5, 8-H), 8.40 (s, 1H, naph-1-H); ^{13}C NMR (75.4 MHz, $CDCl_3$) δ 18.7, 21.3, 21.6, 24.0, 27.1, 27.2, 34.3, 40.0, 49.7, 68.1, 122.5, 127.4, 127.8, 128.1, 128.7, 129.1, 129.2, 132.0, 134.6, 139.2, 178.6; IR (neat) 3285, 2956, 2360, 1709, 1323, 1151, 1075 cm^{-1}; MS (EI) *m/e* calc'd for $C_{21}H_{27}NO_4S$: 389.1661, found 389.1659; 389 (1), 344 (100), 191 (50), 154 (54), 137 (100), 127 (100), 81 (60), 69 (59), 55 (40), 42 (47); $[\alpha]_D^{20}$ +1.2° (c=0.22, $CHCl_3$).

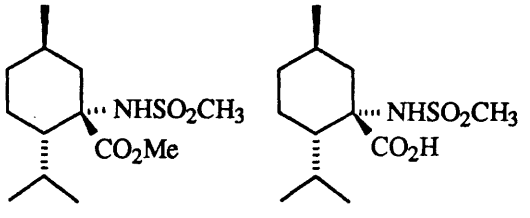

(1*S*,2*S*,5*R*)-Methyl ester: prepared by the general procedure in 43% yield: ^{1}H NMR (250 MHz, $CDCl_3$) δ 0.85–0.93 (3 overlapping d, J=6.6 Hz, 9H, ^{i}Pr-CH$_3$ and 5-CH$_3$), 1.01 (m, 1H, 6-ax-H), 1.30 (m, 1H, 4-ax-H), 1.70 (m, 4H, cyclohexyl-H and ^{i}Pr-CH), 1.84 (m, 2H, cyclohexyl-H), 2.47 (br d, J=13.7 Hz, 1H, 6-eq-H), 3.20 (s, 3H, SO_2CH_3), 3.77 (s, 3H, CO_2CH_3), 4.31 (s, 1H, NH).

(1*S*,2*S*,5*R*)-Acid: prepared by the general procedure (BBr_3 method) in 90% yield: m.p. 129–133 °C; ^{1}H NMR (250 MHz, $CDCl_3$) δ 0.89–0.95 (3 overlapping d, J=6.6 Hz, 9H, ^{i}Pr-CH$_3$ and 5-CH$_3$), 1.04 (m, 1H, 6-ax-H), 1.30 (m, 1H, 4-ax-H), 1.72 (m, 6H, cyclohexyl-H and ^{i}PrCH), 2.54 (br d, J=12.5 Hz, 1H, 6-eq-H), 3.19 (s, 3H, SO_2CH_3),

4.37 (s, 1H, NH); ^{13}C NMR (75.4 MHz, $CDCl_3$) δ 18.7, 21.6, 21.8, 23.6, 27.1, 27.9, 34.3, 42.2, 44.2, 49.6, 68.6, 178.4; IR (neat) 3310, 2956, 1716, 1313, 1142, 977 cm^{-1}; MS (EI) *m/e* calc'd for [M - CO_2H]$^+$: 232.1371, found 232.1373; 277 (2), 232 (100), 198 (20), 137 (100), 95 (45), 81 (49), 69 (53), 55 (32), 42 (39); $[\alpha]_D^{20}$ -9.7° (c=0.62, $CHCl_3$).

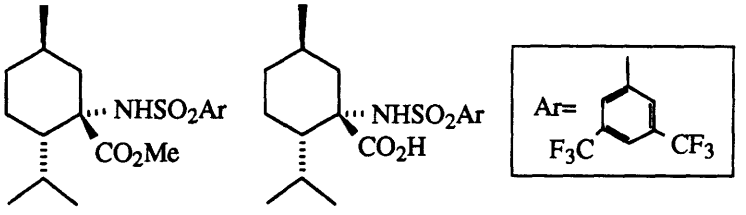

(1*S*,2*S*,5*R*)-Methyl ester: prepared by the general procedure in 58% yield: ^{1}H NMR (250 MHz, $CDCl_3$) δ 0.82 (d, J=7.5 Hz, 3H, 5-C<u>H</u>$_3$), 0.83 (d, J=7.5 Hz, 3H, ^{i}Pr-C<u>H</u>$_3$), 0.88 (d, J=7.5 Hz, 3H, ^{i}Pr-C<u>H</u>$_3$), 0.95 (m, 1H, 6-ax-<u>H</u>), 1.25 (m, 2H, 4-ax-<u>H</u> and 2-ax-<u>H</u>), 1.65 (m, 5H, cyclohexyl-<u>H</u> and ^{i}Pr-C<u>H</u>), 2.43 (br d, J=12.5 Hz, 1H, 6-eq-<u>H</u>), 3.62 (s, 3H, CO_2C<u>H</u>$_3$), 4.76 (s, 1H, N<u>H</u>), 8.03 (s, 1H, SO_2Ar-*para*-<u>H</u>), 8.31 (s, 2H, SO_2Ar-*ortho*-<u>H</u>).

(1*S*,2*S*,5*R*)-Acid: prepared by the general procedure (BBr_3 method) in 80% yield: m.p. 180–185 °C; ^{1}H NMR (250 MHz, $CDCl_3$) δ 0.83–0.90 (3 overlapping d, J=6.6 Hz, 9H, ^{i}Pr-C<u>H</u>$_3$ and 5-C<u>H</u>$_3$), 0.98 (m, 1H, 6-ax-<u>H</u>), 1.25 (m, 2H, cyclohexyl-<u>H</u>), 1.66 (m, 5H, cyclohexyl-<u>H</u>), 1.80 (br s, 1H, COO<u>H</u>), 2.51 (br d, J=12.5 Hz, 1H, 6-eq-<u>H</u>), 4.75 (s, 1H, N<u>H</u>), 8.02 (s, 1H, SO_2Ar-*para*-<u>H</u>), 8.30 (s, 2H, SO_2Ar-*ortho*-<u>H</u>); ^{13}C NMR (75.4 MHz, $CDCl_3$) δ 18.6, 21.4, 21.6, 23.4, 27.1, 27.8, 34.1, 41.6, 49.2, 69.1, 120.7, 124.3, 125.6, 127.2, 131.6, 132.1, 132.6, 145.4, 178.0; IR (neat) 3331, 2960, 1716, 1279, 1145 cm^{-1}; MS (EI) *m/e* calc'd for $C_{19}H_{23}NO_4SF_6$: 475.1252, found 475.1253; 475 (0.1), 430 (100), 213 (39), 198 (57), 137 (100), 95 (91), 81 (100), 69 (100), 55 (77), 42 (90); $[\alpha]_D^{20}$ +1.0° (c=0.42, $CHCl_3$).

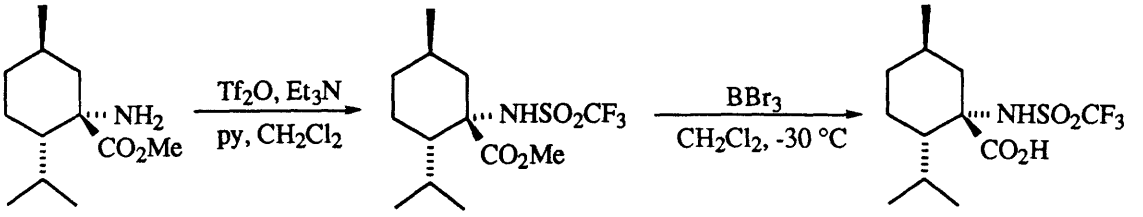

(1*S*,2*S*,5*R*)-Methyl ester: To a solution of the amino ester (280 mg, 1.31 mmol, 1 equiv), triethylamine (0.25 mL, 1.8 mmol, 1.4 equiv), and pyridine (3 drops) in CH_2Cl_2 (2.0 mL) at -20 °C was very slowly added triflic anhydride (0.25 mL, 1.5 mmol, 1.1 equiv) via syringe. The solution was allowed to warm up to room temperature and was stirred overnight, then diluted with CH_2Cl_2 (15 mL) and shaken with aqueous 1 M HCl (10 mL), saturated $NaHCO_3$ (10 mL), and water (10 mL). The aqueous layers were extracted with CH_2Cl_2 (3 x 10 mL), and the combined organic phases were washed with brine, dried ($MgSO_4$), and concentrated in vacuo. The crude product was purified by flash chromatography (10–15% ethyl acetate in hexane), giving the pure sulfonamide-ester (373 mg, 1.08 mmol, 82%): ^{1}H NMR (250 MHz, $CDCl_3$) δ 0.87–0.92 (m, 9H, 5-C$\underline{H}_3$ and ^{i}Pr-C$\underline{H}_3$), 1.00 (m, 1H, 6-ax-$\underline{H}$), 1.27 (dd, J=10.0, 2.5 Hz, 1H, 2-ax-$\underline{H}$), 1.36 (t, J=5.0 Hz, 1H, 4-ax-$\underline{H}$), 1.50–1.83 (m, 5H, cyclohexyl-$\underline{H}$ and ^{i}Pr-C$\underline{H}$), 2.33 (br d, J=12.5 Hz, 1H, 6-eq-$\underline{H}$), 3.78 (s, 3H, $CO_2C\underline{H}_3$), 4.69 (s, 1H, N$\underline{H}$).

(1*S*,2*S*,5*R*)-Acid: prepared by the general procedure (BBr_3 method) in 83% yield: ^{1}H NMR (250 MHz, $CDCl_3$) δ 0.90–0.96 (m, 9H, 5-C$\underline{H}_3$ and ^{i}Pr-C$\underline{H}_3$), 1.03 (m, 1H, cyclohexyl-$\underline{H}$), 1.30 (m, 2H, cyclohexyl-$\underline{H}$), 1.58–1.90 (m, 5H, cyclohexyl-$\underline{H}$ and ^{i}Pr-C$\underline{H}$), 2.40 (br d, J=12.5 Hz, 1H, 6-eq-$\underline{H}$), 4.73 (s, 1H, N$\underline{H}$); ^{13}C NMR (75.4 MHz, $CDCl_3$) δ 18.7, 21.4, 21.8, 23.7, 27.0, 27.4, 34.2, 40.3, 49.3, 70.4, 119.2, 178.0; IR (neat) 3320, 2960, 1721, 1423, 1361, 1197, 1140 cm^{-1}; MS (EI) *m/e* calc'd for $C_{12}H_{20}NO_4SF_3$: 331.1065, found 331.1067; 331 (0.2), 286 (100), 137 (100), 95 (81), 81 (100), 69 (100), 55 (54), 44 (69); $[\alpha]_D^{20}$ -22.8° (c=1.7, $CHCl_3$).

6.5 Aldol Products from 1-(Trimethylsiloxy)-1-ethoxy-2-methyl-1-propene

Yields and enantiomeric excesses for aldol reactions are given in the text. Racemic samples were used as standards for all ee determinations on optically active material.

General Procedures

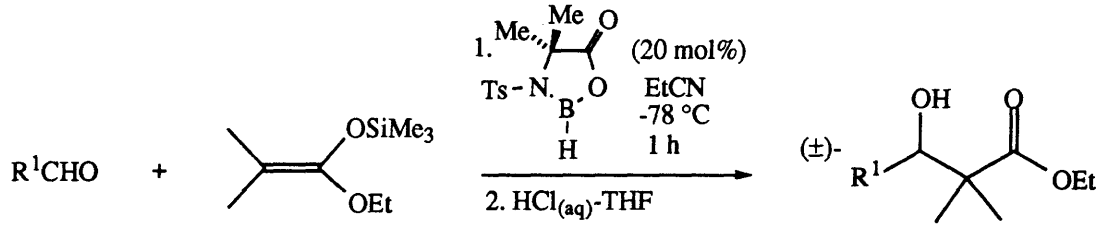

A general procedure for the preparation of *racemic* β-hydroxy esters (Procedure A): The achiral ligand *N*-tosyl-2-methylalanine (25.7 mg, 0.100 mmol, 0.2 equiv) in propionitrile (2.5 mL) was treated with BH_3·THF complex (100 μL of a 1 M solution in THF, 0.1 mmol, 0.2 equiv). The solution was warmed to 45 °C for 1 h and cooled to -78 °C before the addition of 1-(trimethylsiloxy)-1-ethoxy-2-methyl-1-propene (130 μL, 0.60 mmol, 1.2 equiv) and the aldehyde (0.50 mmol, 1 equiv). The reaction mixture was stirred for 1 h at -78 °C, then treated with 1:1 aqueous 1 M HCl/THF (1 mL), and allowed to stir for 1 h at room temperature. Following extraction with ether, the organic layers were dried ($MgSO_4$) and concentrated in vacuo, and the crude product was purified by flash chromatography (10–20% ethyl acetate in hexane) giving the racemic β-hydroxy ester.

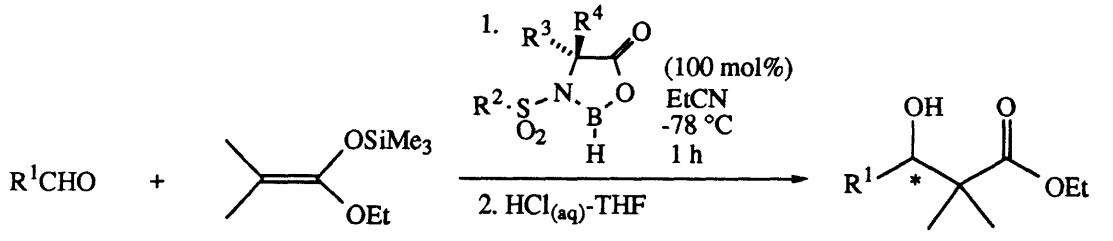

A general procedure for asymmetric aldol reactions using a stoichiometric amount of promoter(Procedure B): The ligand (0.50 mmol, 1 equiv) in propionitrile (2.5 mL) was treated with BH_3·THF complex (500 μL of a 1 M solution in THF, 0.5 mmol, 1 equiv).

The solution was warmed to 45 °C for 1 h and cooled to -78 °C before the addition of 1-(trimethylsiloxy)-1-ethoxy-2-methyl-1-propene (130 μL, 0.60 mmol, 1.2 equiv) and the aldehyde (0.50 mmol, 1 equiv). The reaction mixture was stirred 1 h at -78 °C before it was treated with pH= 7 buffer (or 1:1 aqueous 1 M HCl/THF if complete desilylation of the aldol products is desired) (1 mL) and allowed to stir for 1 h at room temperature. Following extraction with ether, the organic layers were dried ($MgSO_4$) and concentrated in vacuo, and the crude product was purified by flash chromatography (10–20% ethyl acetate in hexane) giving the β-hydroxy ester.

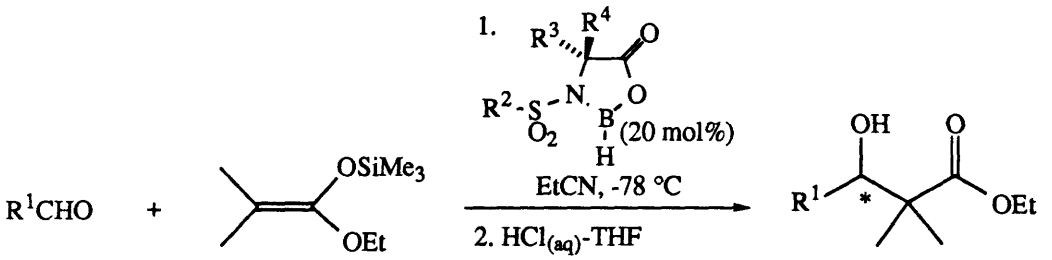

A general procedure for aldol reactions using a catalytic amount of promoter (Procedure C): The ligand (0.10 mmol, 0.2 equiv) in propionitrile (1.5 mL) was treated with BH_3·THF complex (100 μL of a 1 M solution in THF, 0.1 mmol, 0.2 equiv). The solution was warmed to 45 °C for 1 h and cooled to -78 °C before the addition of 1-(trimethylsiloxy)-1-ethoxy-2-methyl-1-propene (130 μL, 0.60 mmol, 1.2 equiv). The aldehyde (0.50 mmol, 1 equiv) was then added as a solution in propionitrile (1 mL) over 3.5 h (syringe pump) and the reaction mixture was stirred a further 1 h at the same temperature before being poured into pH 7 buffer at 0 °C. The aqueous layer was extracted with ether, and the combined organic layers were dried ($MgSO_4$) and concentrated in vacuo, affording the silyl ether accompanied by a small amount of β-hydroxy ester . Desilylation was effected by stirring with 1:1 aqueous 1 M HCl/THF (1 mL) for 1 h at room temperature (direct treatment of the original reaction mixture with 1 M HCl/THF provides the β-hydroxy ester without isolation of the silyl ether). Following extraction with ether, the organic layers were dried ($MgSO_4$) and concentrated in vacuo, and the residue

was purified by flash chromatography (10–20% ethyl acetate in hexane) giving the pure β-hydroxy ester.

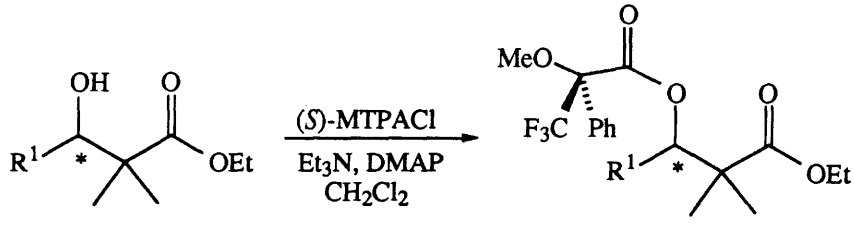

A general procedure for the preparation of Mosher's ester derivatives[78] of hydroxy esters (Procedure D): A solution of the β-hydroxy ester (10–20 mg, 1 equiv) in CH_2Cl_2 (1 mL) at room temperature was treated sequentially with triethylamine (5 equiv), 4-DMAP (2–5 mg), and Mosher's acid chloride ((*S*)-MTPACl) (d= 1.34, 2 equiv). The reaction mixture was stirred overnight, at which point conversion to the ester appeared complete by TLC analysis (10% ethyl acetate in hexane). The yellow solution was concentrated in vacuo, diluted with ether (15 mL), and shaken with saturated $NaHCO_3$ solution (2 x 10 mL) and water (1 x 10 mL). The aqueous layers were back-extracted with ether (1 x 10 mL), and the combined ethereal solutions were washed with brine, dried ($MgSO_4$), and evaporated to give the crude Mosher's ester, which was analyzed without further purification.

Aldols and Related Compounds

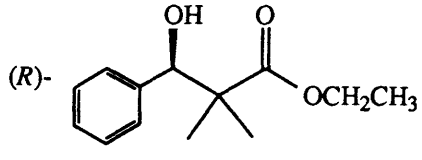

^{1}H NMR (300 MHz, $CDCl_3$) δ 1.15 (s, 3H, 2-C$\underline{H}_3$), 1.17 (s, 3H, 2-C$\underline{H}_3$), 1.30 (t, J=7.2 Hz, 3H, $OCH_2C\underline{H}_3$), 3.20 (d, J=4.3 Hz, 1H, O$\underline{H}$), 4.21 (q, J=7.2 Hz, 2H, $OC\underline{H}_2CH_3$), 4.92 (d, J=4.0 Hz, 1H, C$\underline{H}$OH), 7.24–7.38 (m, 5H, Ar$\underline{H}$); IR (neat) 3501, 2981, 1717, 1453, 1386, 1255, 1132, 1050, 1028, 898 cm^{-1}; $[\alpha]_D^{20}$ -22.6° (c=0.39, $CHCl_3$) for (*R*)-aldol[74] of 91% ee; HPLC analysis using a Chiralcel OD column (10%

^{i}PrOH/Hexane, 0.5 mL/min): retention times 14.3 (*R*), 16.1 (*S*) min.

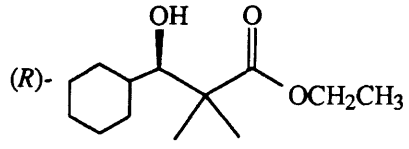

^{1}H NMR (300 MHz, $CDCl_3$) δ 1.15 (s, 3H, 2-C<u>H</u>$_3$), 1.25 (s, 3H, 2-C<u>H</u>$_3$), 1.25 (t, J=7.5 Hz, 3H, OCH$_2$C<u>H</u>$_3$), 1.00–1.40 (m, 3H, cyclohexyl-<u>H</u>), 1.45 (m, 4H, cyclohexyl-<u>H</u>), 1.58 (m, 2H, cyclohexyl-<u>H</u>), 1.70 (m, 2H, cyclohexyl-<u>H</u>), 2.92 (d, J=6.0 Hz, 1H, O<u>H</u>), 3.32 (dd, J=9.0, 3.0 Hz, 1H, C<u>H</u>OH), 4.13 (q, J=7.5 Hz, 2H, OC<u>H</u>$_2$CH$_3$); ^{13}C NMR (75.4 MHz, $CDCl_3$) δ 14.0, 22.5, 23.9, 26.2, 26.3, 26.7, 26.8, 31.7, 40.3, 45.6, 60.7, 81.7, 178.3; IR (neat) 3481, 2926, 1728, 1447, 1386, 1258, 1138, 1026 cm^{-1}; MS (EI) *m/e* calc'd for [M - H_2O]$^+$: 210.1620, found 210.1618; 210 (0.5), 145 (36), 116 (100), 99 (23), 88 (69), 71 (32), 70 (43), 55 (54), 43 (26), 41 (53), 39 (18); $[\alpha]_D^{20}$ +19.2° (c=0.40, $CHCl_3$) for (*R*)-aldol of 97% ee; diagnostic peaks in the ^{1}H NMR spectrum of the corresponding (*S*)-MTPA ester: (300 MHz, C_6D_6) δ 3.41 (br s, OC<u>H</u>$_3$, (*R*)-aldol), 3.45 (br s, OC<u>H</u>$_3$, (*S*)-aldol).

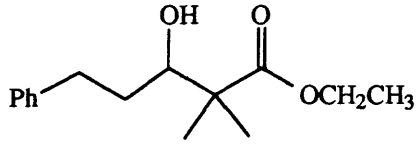

^{1}H NMR (250 MHz, $CDCl_3$) δ 1.12 (s, 3H, 2-C<u>H</u>$_3$), 1.15 (s, 3H, 2-C<u>H</u>$_3$), 1.24 (t, J=7.5 Hz, 3H, OCH$_2$C<u>H</u>$_3$), 1.51–1.82 (m, 2H, PhCH$_2$C<u>H</u>$_2$), 2.63 (m, 1H, PhC<u>H</u>$_A$H$_B$), 2.95 (ddd, J=5.5, 11.3, 14.0 Hz, 1H, PhCH$_A$<u>H</u>$_B$), 3.61 (m, 1H, C<u>H</u>OH), 4.12 (q, J=7.5 Hz, 2H, OC<u>H</u>$_2$CH$_3$), 7.15–7.31 (m, 5H, ArH); IR (neat) 3501, 2980, 1716, 1455, 1386, 1270, 1133, 1075, 1030 cm^{-1}; $[\alpha]_D^{20}$ +33.5° (c=0.36, $CHCl_3$) for aldol[74] of 95% ee (unassigned); diagnostic peaks in the ^{1}H NMR spectrum of the corresponding (*S*)-MTPA ester: (300 MHz, C_6D_6) δ 3.45 (br s, OC<u>H</u>$_3$, major), 3.51 (br s, OC<u>H</u>$_3$, minor).

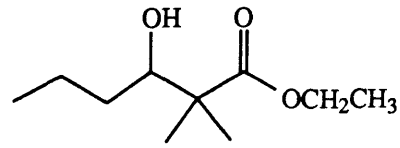

^{1}H NMR (300 MHz, $CDCl_3$) δ 0.91 (t, J=7.2 Hz, 3H, $C\underline{H}_3CH_2CH_2$), 1.14 (s, 3H, 2-$C\underline{H}_3$), 1.16 (s, 3H, 2-$C\underline{H}_3$), 1.24 (t, J=7.5 Hz, 3H, $OCH_2C\underline{H}_3$), 1.25 (buried m, 1H, $CH_3CH_2C\underline{H}_2$), 1.35 (m, 2H, $CH_3C\underline{H}_2CH_2$), 1.60 (m, 1H, $CH_3CH_2C\underline{H}_2$), 2.41 (d, J=6.9 Hz, 1H, O$\underline{H}$), 3.58 (t of d, J=6.9, 3.3 Hz, 1H, C$\underline{H}$OH), 4.13 (q, J=7.5 Hz, 2H, $OC\underline{H}_2CH_3$); ^{13}C NMR (75.4 MHz, $CDCl_3$) δ 14.0, 14.1, 19.8, 20.4, 22.3, 33.9, 47.0, 60.6, 177.8; IR (neat) 3505, 2959, 1719, 1466, 1388, 1261, 1142, 1026, 983, 863 cm^{-1}; MS (EI) *m/e* calc'd for $[M - OCH_2CH_3]^+$: 143.1072, found 143.1071; 145 (15), 116 (99), 99 (20), 88 (100), 73 (49), 70 (63), 55 (22), 43 (43), 41 (47), 39 (19); $[\alpha]_D^{20}$ +22.8° (c=0.40, $CHCl_3$) for aldol of >98% ee (unassigned); diagnostic peaks in the ^{1}H NMR spectrum of the corresponding (*S*)-MTPA ester: (300 MHz, C_6D_6) δ 3.44 (br s, $OC\underline{H}_3$, major), 3.47 (br s, $OC\underline{H}_3$, minor).

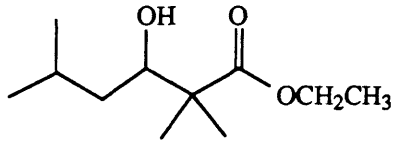

^{1}H NMR (300 MHz, $CDCl_3$) δ 0.93 (d, J=6.6 Hz, 3H, $CH(C\underline{H}_3)_2$), 0.96 (d, J=6.6 Hz, 3H, $CH(C\underline{H}_3)_2$), 1.18 (s, 3H, 2-$C\underline{H}_3$), 1.19 (s, 3H, 2-$C\underline{H}_3$), 1.29 (t, J=6.9 Hz, 3H, $OCH_2C\underline{H}_3$), 1.11–1.37 (m, 2H, $(CH_3)_2CHC\underline{H}_2$), 1.88 (m, 1H, C$\underline{H}(CH_3)_2$), 2.38 (d, J=7.2 Hz, 1H, O$\underline{H}$), 3.71 (ddd, J=1.8, 6.9, 10.2 Hz, 1H, C$\underline{H}$OH), 4.18 (q, J=6.9 Hz, 2H, $OC\underline{H}_2CH_3$); IR (neat) 3510, 2955, 1717, 1468, 1367, 1263, 1140, 1073 cm^{-1}; $[\alpha]_D^{20}$ +31.8° (c=0.38, $CHCl_3$) for aldol[112] of >98% ee (unassigned); diagnostic peaks in the ^{1}H NMR spectrum of the corresponding (*S*)-MTPA ester: (300 MHz, C_6D_6) δ 0.69 (br s, J= 6.6 Hz, $CH(C\underline{H}_3)_2$, minor), 0.77 (br s, J= 6.6 Hz, $CH(C\underline{H}_3)_2$, major).

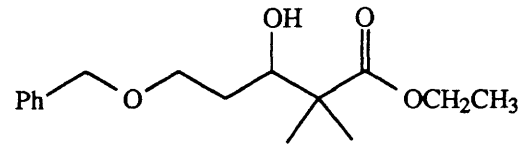

^{1}H NMR (300 MHz, $CDCl_3$) δ 1.09 (s, 3H, 2-C<u>H</u>$_3$), 1.10 (s, 3H, 2-C<u>H</u>$_3$), 1.17 (t, J=7.2 Hz, 3H, OCH$_2$C<u>H</u>$_3$), 1.63 (m, 2H, BnOCH$_2$C<u>H</u>$_2$), 3.06 (br s, 1H, O<u>H</u>), 3.62 (m, 2H, BnOC<u>H</u>$_2$), 3.82 (dd, J=3.0, 9.0 Hz, 1H, C<u>H</u>OH), 4.05 (q, J=7.2 Hz, 2H, OC<u>H</u>$_2$CH$_3$), 4.44 (AB q, 2H, J_{AB}= 12.3 Hz, Δν= 6.1 Hz, OC<u>H</u>$_2$Ph), 7.20 (m, 5H, Ar<u>H</u>); ^{13}C NMR (75.4 MHz, $CDCl_3$) δ 20.4, 21.6, 31.6, 46.9, 47.0, 60.5, 69.2, 73.3, 75.4, 127.7, 128.4, 138.0, 177.4; IR (neat) 3508, 2931, 1723, 1454, 1366, 1266, 1097, 1028 cm^{-1}; MS (EI) *m/e* calc'd for $C_{16}H_{24}O_4$: 280.1675, found 280.1673; 280 (0.8), 156 (46), 116 (66), 107 (37), 91 (100), 88 (45), 83 (28), 82 (33), 73 (23), 70 (28), 65 (25), 41 (22); $[\alpha]_D^{20}$ +4.0° (c=0.40, $CHCl_3$) for aldol of 99% ee (unassigned); HPLC analysis using a Chiralcel OD column (8% ^{i}PrOH/Hexane, 0.5 mL/min): retention times 13.6 (minor), 14.4 (major) min.

<u>Determination of Absolute Configuration</u>

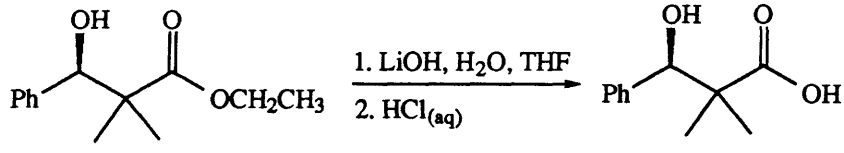

A solution of the β-hydroxy ester (30.8 mg, 0.139 mmol, 1 equiv, 91% ee) and lithium hydroxide monohydrate (35.0 mg, 0.834 mmol, 6 equiv) in THF (0.5 mL) and water (0.5 mL) at 60 °C was stirred vigorously for 2 days. The reaction mixture was diluted with water (5 mL), washed with ether (1 x 5 mL), acidified with aqueous 1 M HCl, and extracted with ethyl acetate (4 x 10 mL). The ethyl acetate layers were washed with brine, dried ($MgSO_4$), and concentrated to give the crude β-hydroxy acid (24.2 mg, 0.125 mmol, 90%): m.p. 154–156 °C; ^{1}H NMR (300 MHz, $CDCl_3$/CD_3OD) δ 1.09 (s, 3H, 2-C<u>H</u>$_3$), 1.10 (s, 3H, 2-C<u>H</u>$_3$), 4.83 (s, 1H, PhC<u>H</u>OH), 7.27 (m, 5H, Ar<u>H</u>); $[\alpha]_D^{20}$ -6.4°

(c=1.0, CH_3OH): assigned the (*R*)-configuration by comparison to the literature value.[79]

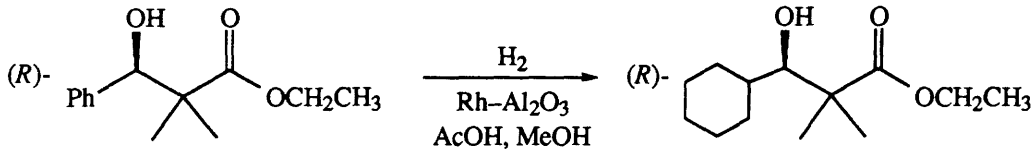

Rhodium on alumina powder (5% Rh, spatula tip, ca. 5 mg) was added to a solution of the (*R*)-hydroxy ester with 91% ee (23 mg, 0.10 mmol, 1 equiv) in methanol (3 mL) and acetic acid (1 drop), and the reaction mixture was hydrogenated (45 psi) overnight in a Parr hydrogenator. The suspension was filtered through a layer of Celite, which was then washed through with ethyl acetate. The organic layers were concentrated in vacuo to give the crude product (23 mg, 0.10 mmol, 100%) with the (*R*) configuration, $[\alpha]_D^{20}$ +16.6° (c=0.47, CHCl3). The sense of rotation is the same for material prepared by the aldol reaction (shown earlier in this section).

6.6 Aldol Products from Acetate-Derived Ketene Acetals

Yields and enantiomeric excesses for aldol reactions are given in the text. Racemic samples were used as standards for all ee determinations on optically active material.

General Procedures

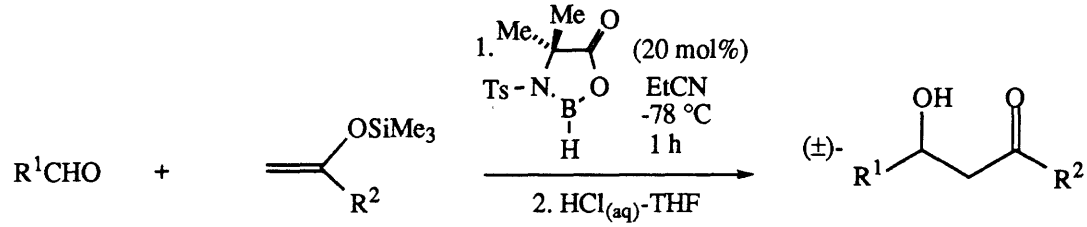

A general procedure for the preparation of *racemic* β-hydroxy esters (Procedure E): The achiral ligand *N*-tosyl-2-methylalanine (25.7 mg, 0.100 mmol, 0.2 equiv) in propionitrile (2.5 mL) was treated with BH_3·THF complex (100 μL of a 1 M solution in THF, 0.1 mmol, 0.2 equiv). The solution was warmed to 45 °C for 1 h and cooled to -78 °C before the addition of the ketene acetal (0.60 mmol, 1.2 equiv) and the aldehyde (0.50 mmol, 1 equiv). The reaction mixture was stirred for 1 h at -78 °C, treated with 1:1 aqueous 1 M HCl/THF (1 mL), and allowed to stir for 1 h at room temperature. Following extraction with ether, the organic layers were dried ($MgSO_4$) and concentrated in vacuo, and the crude product was purified by flash chromatography (10–20% ethyl acetate in hexane) giving the racemic β-hydroxy ester.

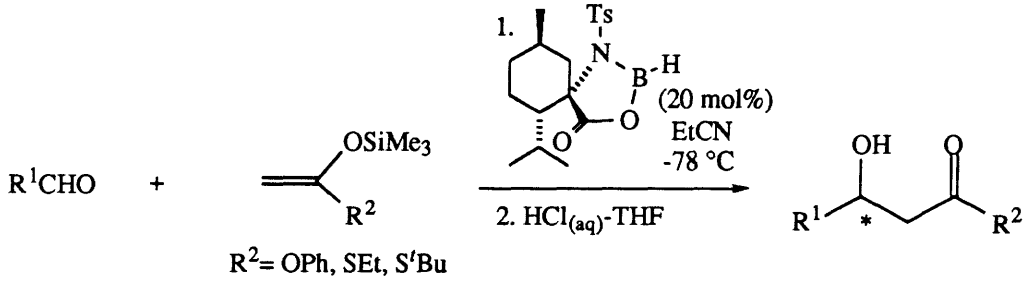

A general procedure for catalytic aldol reactions using acetate-derived ketene acetals

(Procedure F): The menthone-derived ligand (35.3 mg, 0.100 mmol, 0.2 equiv) in propionitrile (1.5 mL) was treated with BH_3·THF complex (100 μL of a 1 M solution in THF, 0.1 mmol, 0.2 equiv). The solution was warmed to 45 °C for 1 h and cooled to -78 °C before the addition of the ketene acetal (0.60 mmol, 1.2 equiv). The aldehyde (0.50 mmol, 1 equiv) was then added as a solution in propionitrile (1 mL) over 3.5 h (syringe pump) and the reaction mixture was stirred a further 1 h at the same temperature before being poured into pH 7 buffer at 0 °C. The aqueous layer was extracted with ether, and the combined organic layers were dried ($MgSO_4$) and concentrated in vacuo, affording the silyl ether accompanied by a small amount of β-hydroxy ester . Desilylation was effected by stirring with 1:1 aqueous 1 M HCl/THF (1 mL) for 1 h at room temperature. Following extraction with ether, the organic layers were dried ($MgSO_4$) and concentrated in vacuo, and the residue was purified by flash chromatography (10–20% ethyl acetate in hexane) giving the pure β-hydroxy ester.

Aldol Products

(*S*)-

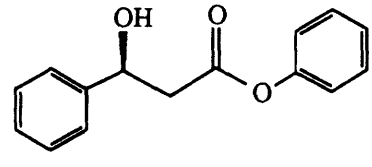

m.p. 65–66 °C; ^{1}H NMR (300 MHz, $CDCl_3$) δ 2.94 (A of ABX, 1H, J_{AB}= 16.2 Hz, J_{AX}= 4.8 Hz, C$\underline{H}_2$), 3.02 (B of ABX, 1H, J_{AB}= 16.2 Hz, J_{BX}= 8.1 Hz, C$\underline{H}_2$), 5.23 (dd, J=3.9, 8.4 Hz, 1H, C$\underline{H}$OH), 7.01 (d, J=8.1 Hz, 2H, Ar$\underline{H}$), 7.22–7.40 (m, 8H, ArH); IR (neat) 3472, 1734, 1448, 1276, 1200, 1146, 1068, 1019 cm^{-1}; $[\alpha]_D^{20}$ -33.7° (c=0.40, $CHCl_3$) for (*S*)-aldol[44,75] of 93% ee; HPLC analysis using a Chiralcel OD column (10% ^{i}PrOH/Hexane, 0.7 mL/min): retention times 22.8 (*S*), 25.9 (*R*) min.

(*R*)- 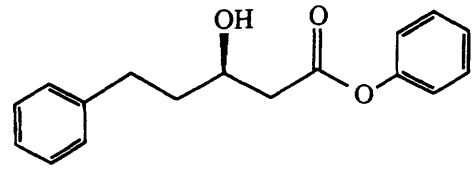

m.p. 59–60 °C; ^{1}H NMR (250 MHz, $CDCl_3$) δ 1.78–2.08 (m, 2H, $PhCH_2C\underline{H}_2$), 2.68–2.97 (m, 4H, $PhC\underline{H}_2$, $C\underline{H}_2CO$), 4.18 (m, 1H, C<u>H</u>OH), 7.11 (d, J=6.4 Hz, 2H, Ar<u>H</u>), 7.23–7.48 (m, 8H, Ar<u>H</u>); ^{13}C NMR (75.4 MHz, $CDCl_3$) δ 31.8, 38.2, 41.6, 67.3, 121.5, 126.0, 126.1, 128.5, 129.5, 141.6, 150.3, 171.5; IR (neat) 3510, 1730, 1591, 1223, 1195, 1138 cm^{-1}; MS (EI) *m/e* calc'd for $C_{17}H_{18}O_3$: 270.1256, found 270.1253; 270 (3), 94 (100), 91 (49), 65 (13); $[\alpha]_D^{20}$ +5.2° (c=0.23, $CHCl_3$) for (*R*)-aldol of 85% ee; HPLC analysis using Chiralcel OD column (15% ^{i}PrOH/Hexane, 0.8 mL/min): retention times 17.3 (*S*), 26.5 (*R*) min.

(*S*)- 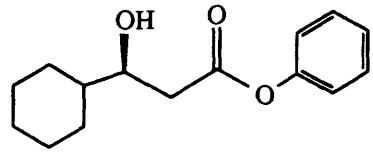

m.p. 64–66 °C; ^{1}H NMR (300 MHz, $CDCl_3$) δ 1.00–1.30 (m, 5H, cyclohexane-<u>H</u>), 1.45 (m, 1H, cyclohexane-<u>H</u>), 1.60–1.95 (m, 5H, cyclohexane-<u>H</u>), 2.61 (m, 1H, O<u>H</u>), 2.67 (A of ABX, 1H, J_{AB}= 16.1 Hz, J_{AX}= 9.7 Hz, $C\underline{H}_2CO$), 2.77 (B of ABX, 1H, J_{AB}= 16.1 Hz, J_{BX}= 3.0 Hz, $C\underline{H}_2CO$), 3.90 (m, 1H, C<u>H</u>OH), 7.07 (dd, J=1.8, 7.5 Hz, 2H, Ph-*ortho*-<u>H</u>), 7.25 (m, 1H, Ph-*para*-<u>H</u>), 7.38 (d of t, J=2.7, 7.8 Hz, 2H, Ph-*meta*-<u>H</u>); ^{13}C NMR (75.4 MHz, $CDCl_3$) δ 26.1, 26.2, 26.5, 28.3, 28.9, 38.9, 43.2, 72.3, 121.4, 125.9, 129.4, 150.3, 171.8; IR (neat) 3358, 2920, 1752, 1593, 1450, 1369, 1198, 934 cm^{-1}; MS (EI) *m/e* calc'd for $C_{15}H_{20}O_3$: 248.1412, found 248.1412; 248 (3), 165 (15), 94 (100), 55 (36), 41 (31), 39 (20); $[\alpha]_D^{20}$ -18.9° (c=0.37, $CHCl_3$) for (*S*)-aldol of 84% ee; HPLC analysis using Chiralcel OD column (10% ^{i}PrOH/Hexane, 0.5 mL/min): retention times 24.0 (*R*), 26.5 (*S*) min.

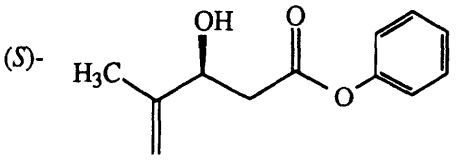

^{1}H NMR (250 MHz, $CDCl_3$) δ 1.81 (s, 3H, C<u>H</u>$_3$), 2.81 (m, 2H, A and B of ABX, C<u>H</u>$_2$CO), 4.60 (apparent t, J=6.2 Hz, 1H, X of ABX, C<u>H</u>OH), 4.94 (br d, 1H, C<u>H</u>$_2$=C), 5.09 (br d, 1H, C<u>H</u>$_2$=C), 7.08 (dd, J=1.4, 7.5 Hz, 2H, Ph-*ortho*-<u>H</u>), 7.24 (m, 1H, Ar<u>H</u>), 7.37 (m, 2H, Ar<u>H</u>); ^{13}C NMR (75.4 MHz, $CDCl_3$) δ 17.7, 39.8, 71.2, 111.3, 121.0, 125.5, 129.0, 144.9, 149.9, 170.4; IR (neat) 3448, 2920, 1752, 1593, 1491, 1194, 1139, 1070, 1023, 902, 817 cm^{-1}; MS (EI) *m/e* calc'd for $C_{12}H_{14}O_3$: 206.0943, found 206.0943; 206 (2), 94 (100), 71 (49), 43 (24), 41 (25), 39 (23); $[\alpha]_D^{20}$ -19.6° (c=0.83, $CHCl_3$) for (*S*)-aldol of 71% ee; HPLC analysis using Chiralcel OD column (10% ^{i}PrOH/Hexane, 1.0 mL/min): retention times 9.7 (*S*), 12.5 (*R*) min.

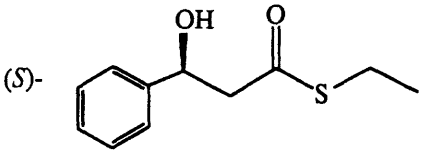

^{1}H NMR (300 MHz, $CDCl_3$) δ 1.22 (t, J=7.5 Hz, 3H, SCH$_2$C<u>H</u>$_3$), 2.87 (A of ABX, 1H, J_{AB}= 15.9 Hz, J_{AX}= 2.1 Hz, C<u>H</u>$_2$CO), 2.90 (q, J=7.5 Hz, 2H, SC<u>H</u>$_2$CH$_3$), 2.96 (B of ABX, 1H, J_{AB}= 15.9 Hz, J_{BX}= 8.7 Hz, C<u>H</u>$_2$CO), 3.01 (d, J=3.0 Hz, 1H, O<u>H</u>), 5.13 (ddd, J=2.1, 3.0, 8.7 Hz, 1H, C<u>H</u>OH), 7.21–7.35 (m, 5H, Ar<u>H</u>); IR (neat) 3445, 2931, 1683, 1456, 1056, 973 cm^{-1}; $[\alpha]_D^{20}$ -54.3° (c=2.2, benzene) for (*S*)-aldol[36a] of 89% ee; HPLC analysis using Chiralcel OD column (10% ^{i}PrOH/Hexane, 0.5 mL/min): retention times 17.7 (*S*), 19.6 (*R*) min.

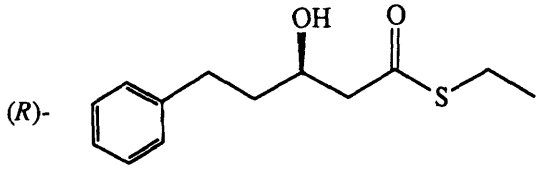

^{1}H NMR (250 MHz, $CDCl_3$) δ 1.28 (t, J=7.5 Hz, 3H, $SCH_2C\underline{H}_3$), 1.67–1.93 (m, 2H, $PhCH_2C\underline{H}_2$), 2.64–2.88 (m, 4H, $PhC\underline{H}_2$ and $C\underline{H}_2CO$), 2.92 (q, J=7.5 Hz, 2H, $SC\underline{H}_2CH_3$), 4.08 (m, 1H, C<u>H</u>OH), 7.20–7.34 (m, 5H, Ar<u>H</u>); IR (neat) 3445, 2930, 1683, 1455, 1415, 1266, 1055, 747 cm^{-1}; $[\alpha]_D^{20}$ -11.2° (c=2.2, benzene) for (*R*)-aldol[36a] of 89% ee; HPLC analysis using Chiralcel OD column (10% ^{i}PrOH/Hexane, 0.5 mL/min): retention times 19.2 (*S*), 23.5 (*R*) min.

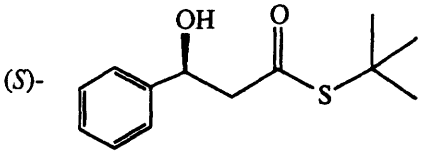

^{1}H NMR (300 MHz, $CDCl_3$) δ 1.43 (s, 9H, $SC(C\underline{H}_3)_3$, 2.78 (A of ABX, 1H, J_{AB}= 15.0 Hz, J_{AX}= 3.3 Hz, $C\underline{H}_2CO$), 2.86 (B of ABX, 1H, J_{AB}= 15.0 Hz, J_{BX}= 8.7 Hz, $C\underline{H}_2CO$), 5.11 (dd, J=8.4, 3.3 Hz, 1H, C<u>H</u>OH), 7.22–7.32 (m, 5H, Ar<u>H</u>); IR (neat) 3448, 2963, 1676, 1454, 1364, 1163, 1057, 972 cm^{-1}; $[\alpha]_D^{20}$ -47.9° (c=2.3, benzene) for (*S*)-aldol[36a] of 87% ee; HPLC analysis using Chiralcel OJ column (8% ^{i}PrOH/Hexane, 0.5 mL/min): retention times 20.9 (*S*), 25.3 (*R*) min.

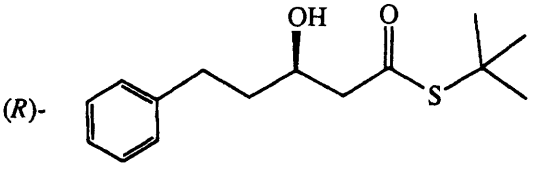

^{1}H NMR (300 MHz, $CDCl_3$) δ 1.42 (s, 9H, $SC(C\underline{H}_3)_3$), 1.60–1.85 (m, 2H, $PhCH_2C\underline{H}_2$), 2.50–2.95 (m, 4H, $PhC\underline{H}_2$ and $C\underline{H}_2CO$), 3.98 (m, 1H, C<u>H</u>OH), 7.12–7.27 (m, 5H, Ar<u>H</u>); IR (neat) 3448, 2924, 1677, 1455, 1364, 1161, 1055, 994 cm^{-1}; $[\alpha]_D^{20}$ -23.4° (c=2.3, benzene) for (*R*)-aldol[36a] of 91% ee; HPLC analysis using Chiralcel OD

column (10% ^{i}PrOH/Hexane, 0.5 mL/min): retention times 14.8 (*S*), 18.2 (*R*) min.

(*R*)-

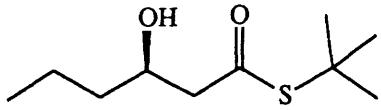

^{1}H NMR (300 MHz, $CDCl_3$) δ 0.90 (t, J=6.6 Hz, 3H, $C\underline{H}_3CH_2$), 1.23–1.52 (m, 4H, $CH_3C\underline{H}_2C\underline{H}_2$), 1.44 (s, 9H, $SC(C\underline{H}_3)_3$), 2.53 (A of ABX, 1H, J_{AB}= 15.6 Hz, J_{AX}= 8.1 Hz, $C\underline{H}_2CO$), 2.63 (B of ABX, 1H, J_{AB}= 15.6 Hz, J_{BX}= 3.5 Hz, $C\underline{H}_2CO$), 2.73 (br d, J=3.0 Hz, 1H, O<u>H</u>), 4.01 (m, 1H, C<u>H</u>OH); ^{13}C NMR (75.4 MHz, $CDCl_3$) δ 13.9, 18.6, 29.8, 38.7, 48.5, 50.9, 68.5, 200.7; IR (neat) 3445, 2961, 1674, 1456, 1365, 1163, 1126, 1076, 1028 cm^{-1}; MS (EI) *m/e* calc'd for $C_{10}H_{20}O_2S$: 204.1184, found 204.1184; 204 (3), 97 (23), 73 (17), 57 (100), 55 (23), 43 (23), 41 (80), 39 (26); $[\alpha]_D^{20}$ -23.8° (c=0.50, $CHCl_3$) for (*R*)-aldol of 91% ee; HPLC analysis using Chiralcel OD column (5% ^{i}PrOH/Hexane, 0.5 mL/min): retention times 20.8 (*R*), 22.7 (*S*) min.

(*S*)-

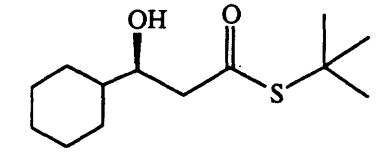

^{1}H NMR (300 MHz, $CDCl_3$) δ 1.44 (s, 9H, $SC(C\underline{H}_3)_3$), 0.88–1.85 (m, 11H, cyclohexane-<u>H</u>), 2.52 (A of ABX, 1H, J_{AB}= 15.1 Hz, J_{AX}= 7.5 Hz, $C\underline{H}_2CO$), 2.62 (B of ABX, 1H, J_{AB}= 15.1 Hz, J_{BX}= 3.5 Hz, $C\underline{H}_2CO$), 2.66 (d, J=3.0 Hz, 1H, O<u>H</u>), 3.75 (m, 1H, C<u>H</u>OH); ^{13}C NMR (75.4 MHz, $CDCl_3$) δ 26.1, 26.2, 26.5, 28.2, 28.9, 29.8, 43.2, 48.3, 48.4, 72.8, 200.9; IR (neat) 3449, 2925, 2853, 1684, 1450, 1364, 1163, 1040 cm^{-1}; MS (EI) *m/e* calc'd for $[M - H_2O]^+$: 226.1391, found 226.1390; 226 (2), 137 (53), 126 (57), 95 (100), 83 (26), 57 (100), 55 (38), 43 (36), 41 (56); $[\alpha]_D^{20}$ -19.1° (c=0.47, $CHCl_3$) for (*S*)-aldol of 81% ee; HPLC analysis using Chiralcel OJ column (2% ^{i}PrOH/Hexane, 0.5 mL/min): retention times 12.3 (*R*), 13.7 (*S*) min.

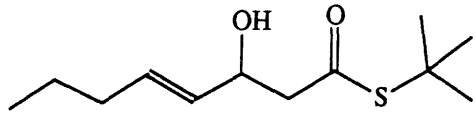

^{1}H NMR (250 MHz, $CDCl_3$) δ 0.92 (t, J=7.5 Hz, 3H, $C\underline{H}_3CH_2$), 1.33–1.50 (m, 2H, $CH_3C\underline{H}_2$), 1.49 (s, 9H, $SC(C\underline{H}_3)_3$), 2.01 (q, J=7.1 Hz, 2H, $CH_3CH_2C\underline{H}_2$), 2.69 (m, 3H, $C\underline{H}_2CO$ and O<u>H</u>), 4.53 (m, 1H, C<u>H</u>OH), 5.47 (dd, J=7.1, 14.1 Hz, 1H, $CH_2CH{=}C\underline{H}$), 5.73 (d of t, J=7.1, 14.1 Hz, 1H, $CH_2C\underline{H}{=}CH$); ^{13}C NMR (75.4 MHz, $CDCl_3$) δ 13.8, 22.3, 29.8, 34.3, 48.6, 51.1, 69.7, 130.4, 132.5, 199.6; IR (neat) 3425, 2926, 1682, 1456, 1364, 1163, 1043, 969 cm^{-1}; MS (EI) *m/e* calc'd for $C_{12}H_{22}O_2S$: 230.1341, found 230.1339; 230 (2), 174 (67), 141 (26), 123 (23), 112 (63), 99 (100), 96 (90), 81 (56), 57 (100), 55 (27), 43 (43), 41 (90), 39 (21); $[\alpha]_D^{20}$ -6.8° (c=0.52, $CHCl_3$) for aldol of 82% ee (unassigned); HPLC analysis using Chiralcel OD column (5% ^{i}PrOH/Hexane, 0.5 mL/min): retention times 20.0 (major), 22.3 (minor) min.

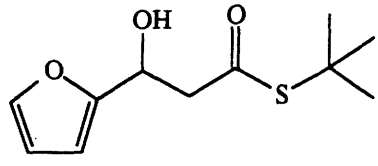

^{1}H NMR (300 MHz, $CDCl_3$) δ 1.45 (s, 9H, $SC(C\underline{H}_3)_3$), 2.93 (A of ABX, 1H, J_{AB}= 15.3 Hz, J_{AX}= 3.9 Hz, $C\underline{H}_2CO$), 3.02 (B of ABX, 1H, J_{AB}= 15.3 Hz, J_{BX}=8.6 Hz, $C\underline{H}_2CO$), 3.10 (br d, J=4.5 Hz, 1H, O<u>H</u>), 5.13 (ddd, J=3.9, 4.5, 8.6 Hz, 1H, C<u>H</u>OH), 6.24 (br d, J=2.7 Hz, 1H, furan-3-<u>H</u>), 6.30 (dd, J=3.0, 3.0 Hz, 1H, furan-4-<u>H</u>), 7.34 (br d, J=3.0 Hz, 1H, furan-5-<u>H</u>); ^{13}C NMR (75.4 MHz, $CDCl_3$) δ 29.7, 48.7, 49.1, 64.7, 106.3, 110.2, 142.2, 154.6, 199.3; IR (neat) 3446, 2964, 1682, 1456, 1365, 1163, 1062, 1011 cm^{-1}; MS (EI) *m/e* calc'd for $C_{11}H_{16}O_3S$: 228.0820, found 228.0821; 228 (11), 171 (65), 137 (36), 110 (61), 97 (100), 94 (60), 57 (94), 41 (48); $[\alpha]_D^{20}$ -27.4° (c=1.1, $CHCl_3$) for aldol of 85% ee (unassigned); HPLC analysis using Chiralcel OD column (10% ^{i}PrOH/Hexane, 0.5 mL/min): retention times 19.9 (major), 21.5 (minor) min.

6.7 Aldol Products from Propionate-Derived Ketene Acetals

Yields and enantiomeric excesses for aldol reactions are given in the text. Racemic samples were used as standards for all ee determinations on optically active material. Optical rotations are not given in cases where the diastereomers are inseparable. For the preparation of Mosher's ester derivatives, see Procedure D in Section 6.5.

General Procedures

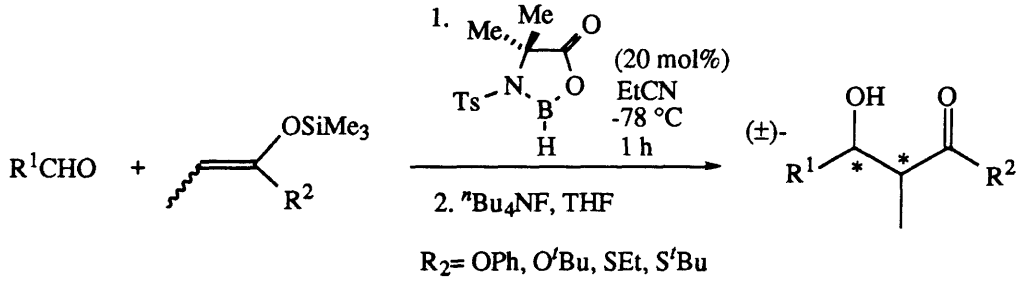

A general procedure for the preparation of racemic β-hydroxy esters using propionate-derived ketene acetals (Procedure G): The achiral ligand *N*-tosyl-2-methylalanine (25.7 mg, 0.100 mmol, 0.2 equiv) in propionitrile (2.5 mL) was treated with BH_3·THF complex (100 μL of a 1 M solution in THF, 0.1 mmol, 0.2 equiv). The solution was warmed to 45 °C for 1 h and cooled to -78 °C before the addition of the ketene acetal (0.60 mmol, 1.2 equiv) and the aldehyde (0.50 mmol, 1 equiv). The reaction was stirred for 1 h at -78 °C and quenched by pouring into pH 7 buffer at 0 °C. The aqueous layer was extracted with ether, and the combined organic layers were dried ($MgSO_4$) and concentrated in vacuo, affording the silylated product accompanied by a small amount of β-hydroxy ester. Desilylation was effected by stirring with tetrabutylammonium fluoride (TBAF, 0.5 mL of a 1 M solution in THF, 0.5 mmol, 1 equiv) in THF (1.5 mL) for 10–30 min at 0 °C. The reaction mixture was extracted with ether, and the organic layers were dried ($MgSO_4$) and concentrated in vacuo. The crude product was purified by flash chromatography (10–20% ethyl acetate in hexane) giving the racemic *syn* and *anti* isomers of the β-hydroxy ester.

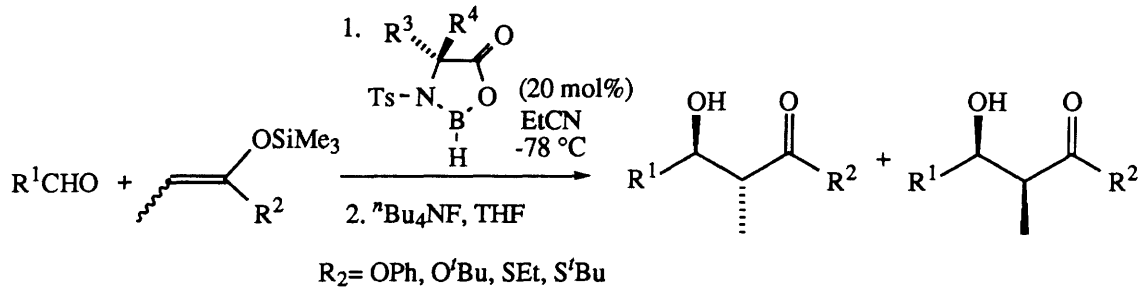

A representative procedure for catalytic aldol reactions with propionate-derived ketene acetals (Procedure H): The ligand (0.10 mmol, 0.2 equiv) in propionitrile (1.5 mL) was treated with BH_3·THF complex (100 μL of a 1 M solution in THF, 0.1 mmol, 0.2 equiv). The solution was warmed to 45 °C for 1 h and cooled to -78 °C before the addition of the ketene acetal (0.60 mmol, 1.2 equiv). The aldehyde (0.50 mmol, 1 equiv) was then added as a solution in propionitrile (1 mL) over 3.5 h (syringe pump) and the reaction mixture was stirred a further 1 h at the same temperature before being poured into pH 7 buffer at 0 °C. The aqueous layer was extracted with ether, and the combined organic layers were dried ($MgSO_4$) and concentrated in vacuo, affording the silylated product accompanied by a small amount of β-hydroxy ester. Desilylation was effected by stirring with tetrabutylammonium fluoride (TBAF, 0.5 mL of a 1 M solution in THF, 0.5 mmol, 1 equiv) in THF (1.5 mL) for 10–30 min at 0 °C. The reaction mixture was extracted with ether, and the organic layers were dried ($MgSO_4$) and concentrated in vacuo. The crude product was purified by flash chromatography (10–20% ethyl acetate in hexane) giving the *syn* and *anti* isomers of the β-hydroxy ester.

Aldol Products

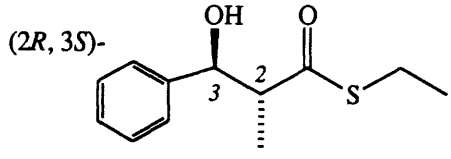

^1H NMR (300 MHz, $CDCl_3$) δ 1.05 (d, J=6.9 Hz, 3H, CH_3CH), 1.28 (t, J=7.5

Hz, 3H, $SCH_2C\underline{H}_3$), 2.68 (d, J=3.9 Hz, 1H, O<u>H</u>), 2.94 (q, J=7.6 Hz, 2H, $SC\underline{H}_2CH_3$), 3.00 (q of d, J=7.2, 3.3 Hz, 1H, $C\underline{H}CH_3$), 4.84 (dd, J=3.3, 8.1 Hz, 1H, C<u>H</u>OH), 7.28–7.45 (m, 5H, Ar<u>H</u>); ^{13}C NMR (75.4 MHz, $CDCl_3$) δ 14.7, 15.6, 23.4, 55.5, 76.6, 126.5, 128.0, 128.4, 141.5, 203.4; IR (neat) 3474, 2970, 2931, 2875, 1682, 1454, 1373, 1265, 1072, 1040, 962, 768 cm^{-1}; $[\alpha]_D^{20}$ -44.6° (c=1.0, benzene) for *anti* (2*R*, 3*S*)-aldol[36a,38c] of 64% ee; HPLC analysis using Chiralcel OD column (10% ^iPrOH/Hexane, 0.5 mL/min): retention times 18.0 (2*R*, 3*S*), 23.4 (2*S*, 3*R*) min.

(2*S*, 3*S*)-

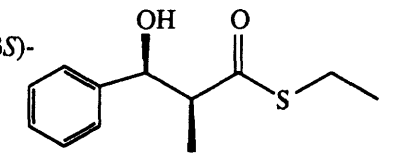

^1H NMR (300 MHz, $CDCl_3$) δ 1.19 (d, J=6.9 Hz, 3H, $C\underline{H}_3CH$), 1.24 (t, J=7.5 Hz, 3H, $SCH_2C\underline{H}_3$), 2.89 (q, J=7.4 Hz, 2H, $SC\underline{H}_2CH_3$), 2.95 (q of d, J=7.5, 3.9 Hz, 1H, $C\underline{H}CH_3$), 5.14 (d, J=3.6 Hz, 1H, C<u>H</u>OH), 7.25–7.45 (m, 5H, Ar<u>H</u>); $[\alpha]_D^{20}$ +61.6° (c=1.6, benzene) for *syn* (2*S*, 3*S*)-aldol[36a,38c] of >98% ee; HPLC analysis using Chiralcel OJ column (7% ^iPrOH/Hexane, 0.5 mL/min): retention times 34.2 (2*R*, 3*R*), 38.6 (2*S*, 3*S*) min.

(2*R*, 3*R*)-

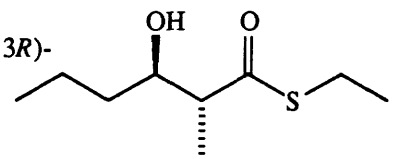

^1H NMR (250 MHz, $CDCl_3$) δ 0.91 (br t, J=6.9 Hz, 3H, $C\underline{H}_3CH_2CH_2$), 1.22 (d, J=7.5 Hz, 3H, $C\underline{H}_3CH$), 1.23 (t, J=7.2 Hz, 3H, $SCH_2C\underline{H}_3$), 1.30–1.60 (m, 4H, $C\underline{H}_2C\underline{H}_2$), 2.32 (d, J=5.0 Hz, 1H, O<u>H</u>), 2.70 (q of d, J=7.5, 3.0 Hz, 1H, $CH_3C\underline{H}$), 2.87 (q, J=7.5 Hz, 2H, $SC\underline{H}_2CH_3$), 3.67 (br m, 1H, C<u>H</u>OH); ^{13}C NMR (75.4 MHz, $CDCl_3$) δ 14.1, 14.7, 15.4, 18.9, 23.3, 37.2, 53.7, 73.7, 204.0; additional peaks for the *syn* isomer: 19.4, 36.2, 53.0, 71.5; IR (neat) 3448, 2960, 2932, 2873, 1685, 1458, 1375, 1265, 1122, 1060, 962, 752 cm^{-1}; MS (EI) *m/e* calc'd for $[M - H_2O]^+$: 172.0922, found

172.0922; 172 (0.1), 129 (56), 111 (46), 83 (85), 73 (38), 57 (100), 44 (27); ee determination by ^{19}F NMR (282.2 MHz, C_6D_6) analysis of the corresponding (*R*)-MTPA esters.

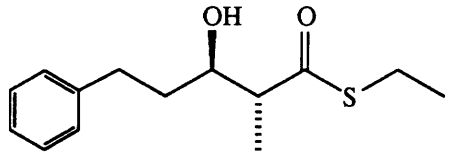

^1H NMR (250 MHz, $CDCl_3$) δ 1.20 (m, 8H, $PhCH_2C\underline{H}_2$, $C\underline{H}_3CH$, $SCH_2C\underline{H}_3$), 1.75 (m, 2H, $PhC\underline{H}_2$), 2.43 (d, J=7.4 Hz, 1H, O<u>H</u>), 2.55–2.89 (m, 1H, $CH_3C\underline{H}$), 2.83 (q, J=7.5 Hz, 2H, $SC\underline{H}_2CH_3$), 3.64 (m, 1H, C<u>H</u>OH), 7.08–7.27 (m, 5H, Ar<u>H</u>); ^{13}C NMR (75.4 MHz, $CDCl_3$) δ 11.7, 14.7, 23.3, 32.3, 35.9, 53.1, 71.3, 125.8, 128.3, 141.6, 141.7, 204.0; additional peaks for the *syn* isomer: 15.4, 23.4, 32.1, 36.9, 53.6, 73.2; IR (neat) 3452, 3026, 2970, 2931, 2874, 1681, 1496, 1454, 1375, 1265, 1057, 962 cm^{-1}; MS (EI) *m/e* calc'd for $C_{14}H_{20}O_2S$: 252.1184, found 252.1183; 252 (1), 190 (57), 173 (29), 145 (45), 117 (64), 91 (100), 57 (31); ee determination by ^{19}F NMR (282.2 MHz, C_6D_6) analysis of the corresponding (*R*)-MTPA esters.

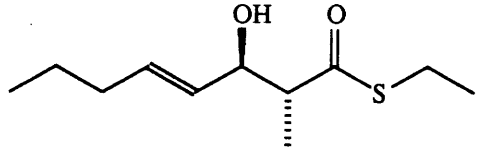

^1H NMR (300 MHz, $CDCl_3$) δ 0.87 (t, J=7.3 Hz, 3H, $C\underline{H}_3CH_2CH_2$), 1.13 (d, J=6.9 Hz, 3H, $C\underline{H}_3CH$), 1.23 (t, J=7.5 Hz, 3H, $SCH_2C\underline{H}_3$), 1.37 (m, 2H, $CH_3C\underline{H}_2CH_2$), 2.00 (q of d, J=7.2, 1.2 Hz, 2H, $CH_3CH_2C\underline{H}_2$), 2.26 (d, J=4.9 Hz, 1H, O<u>H</u>), 2.70 (q of d, J=7.4, 7.4 Hz, 1H, $CH_3C\underline{H}$), 2.86 (q of d, J=7.8, 1.7 Hz, 2H, $SC\underline{H}_2CH_3$), 4.18 (br q, J=7.5 Hz, 1H, C<u>H</u>OH), 5.39 (ddt, J=15.1, 7.3, 1.7 Hz, 1H, $CH_2CH{=}C\underline{H}$), 5.68 (br d of t, J=15.5, 6.6 Hz, 1H, $CH_2C\underline{H}{=}CH$); ^{13}C NMR (75.4 MHz, $CDCl_3$) δ 13.7, 14.7, 15.1, 22.3, 23.3, 34.3, 54.0, 75.1, 129.8, 134.1, 203.2; IR (neat) 3466, 2931, 1685, 1455, 1375, 1265 cm^{-1}; $[\alpha]_D^{20}$ -23.7° (c=0.27, benzene) for >95%

anti aldol[36a] of 60% ee (absolute configuration unassigned); HPLC analysis using Chiralcel OD column (7% ^{i}PrOH/Hexane, 0.5 mL/min): retention times 14.3 (major), 18.1 (minor) min.

(2*S*, 3*R*)-

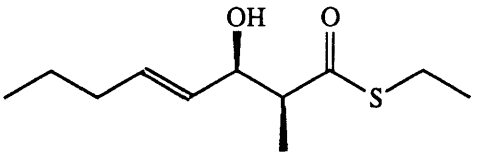

^{1}H NMR (300 MHz, $CDCl_3$) δ 0.87 (t, J=7.5 Hz, 3H, $C\underline{H}_3CH_2CH_2$), 1.21 (t, J=7.5 Hz, 3H, $SCH_2C\underline{H}_3$), 1.24 (d, J=6.9 Hz, 3H, $C\underline{H}_3CH$), 1.37 (m, 2H, $CH_3C\underline{H}_2CH_2$), 2.00 (br q of d, J=6.6, 6.6 Hz, 2H, $CH_3CH_2C\underline{H}_2$), 2.33 (br d, J=3.6 Hz, 1H, O<u>H</u>), 2.73 (q of d, J=6.9, 4.2 Hz, 1H, $CH_3C\underline{H}$), 2.85 (q, J=7.5, 1.7 Hz, 2H, $SC\underline{H}_2CH_3$), 4.33 (m, 1H, C<u>H</u>OH), 5.42 (br dd, J=15.6, 6.8 Hz, 1H, $CH_2CH{=}C\underline{H}$), 5.68 (br d of t, J=15.6, 8.4 Hz, 1H, $CH_2C\underline{H}{=}CH$); $[\alpha]_D^{20}$ +16.7° (c=0.12, benzene) for *syn* (2*S*, 3*R*)-aldol[36a] of 73% ee; HPLC analysis using Chiralcel OD column (7% ^{i}PrOH/Hexane, 0.5 mL/min): retention times 12.8 (2*R*, 3*S*), 14.2 (2*S*, 3*R*) min.

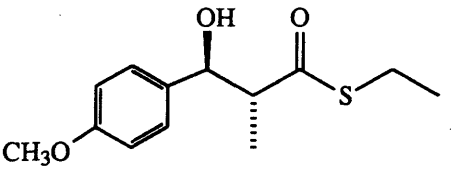

^{1}H NMR (300 MHz, $CDCl_3$) δ 0.94 (d, J=7.1 Hz, 3H, $C\underline{H}_3CH$), 1.22 (t, J=7.4 Hz, 3H, $SCH_2C\underline{H}_3$), 2.55 (d, J=4.0 Hz, 1H, O<u>H</u>), 2.89 (overlapping m, 3H, $CH_3C\underline{H}$ and $SC\underline{H}_2CH_3$), 3.76 (s, 3H, $OC\underline{H}_3$), 4.72 (dd, J=3.6, 8.4 Hz, 1H, C<u>H</u>OH), 6.83 (dd, J=2.1, 6.6 Hz, 2H, Ar<u>H</u>), 7.20 (dd, J=2.0, 6.6 Hz, 2H, Ar<u>H</u>); additional peak for *syn* isomer[36a]: 4.98 (br dd, 1H, C<u>H</u>OH); ^{13}C NMR (75.4 MHz, $CDCl_3$) δ 14.7, 15.6, 23.4, 55.3, 55.6, 76.2, 113.8, 127.7, 133.7, 159.3, 203.4; IR (neat) 3492, 2969, 2932, 2836, 1682, 1611, 1514, 1455, 1372, 1250, 1176, 1035 cm^{-1}; HPLC analysis using Chiralcel OD column (7% ^{i}PrOH/Hexane, 0.5 mL/min): retention times 36.3 (major, *syn*), 37.2 (minor, *syn*), 46.9 (major, *anti*), 49.7 (minor, *anti*) min.

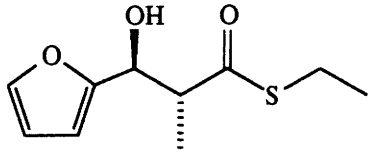

^{1}H NMR (300 MHz, $CDCl_3$) δ 1.08 (d, J=7.2 Hz, 3H, $C\underline{H}_3CH$), 1.23 (t, J=7.4 Hz, 3H, $SCH_2C\underline{H}_3$), 2.79 (d, J=6.3 Hz, 1H, O<u>H</u>), 2.89 (q of d, J=7.5, 1.2 Hz, 2H, $SC\underline{H}_2CH_3$), 3.18 (q of d, J=7.2, 7.2 Hz, 1H, $CH_3C\underline{H}$), 4.83 (dd, J=7.8, 6.0 Hz, 1H, C<u>H</u>OH), 6.27 (dd, J=0.7, 3.3 Hz, 1H, furan-3-<u>H</u>), 6.32 (dd, J=1.5, 3.3 Hz, 1H, furan-4-<u>H</u>), 7.36 (dd, J=0.9, 1.8 Hz, 1H, furan-5-<u>H</u>); ^{13}C NMR (75.4 MHz, $CDCl_3$) δ 14.7, 15.3, 23.4, 52.8, 70.1, 107.6, 110.1, 142.2, 153.9, 203.1; IR (neat) 3476, 2973, 2932, 2876, 1678, 1504, 1455, 1374, 1266, 1150, 1010 cm^{-1}; $[\alpha]_D^{20}$ -76.3° (c=0.63, $CHCl_3$) for 92% *anti* aldol[36a] of 89% ee (unassigned); HPLC analysis using Chiralcel OD column (7% ^{i}PrOH/Hexane, 0.5 mL/min): retention times 28.2 (major), 45.7 (minor) min.

(2*S*, 3*S*)-

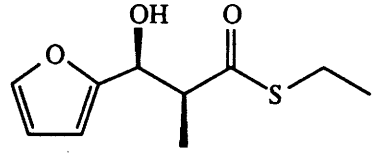

^{1}H NMR (300 MHz, $CDCl_3$) δ 1.21 (t, J=7.4 Hz, 3H, $SCH_2C\underline{H}_3$), 1.25 (d, J=7.1 Hz, 3H, $C\underline{H}_3CH$), 2.74 (d, J=4.6 Hz, 1H, O<u>H</u>), 2.84 (q, J=7.2 Hz, 2H, $SC\underline{H}_2CH_3$), 3.10 (q of d, J=7.2, 4.8 Hz, 1H, $CH_3C\underline{H}$), 5.03 (dd, J=4.3, 4.3 Hz, 1H, C<u>H</u>OH), 6.27 (dd, J=0.9, 3.3 Hz, 1H, furan-3-<u>H</u>), 6.31 (dd, J=1.8, 3.3 Hz, 1H, furan-4-<u>H</u>), 7.34 (dd, J=0.9, 1.8 Hz, 1H, furan-5-<u>H</u>); $[\alpha]_D^{20}$ +30.3° (c=0.52, benzene) for *syn* (2*S*, 3*S*)-aldol[36a] of 90% ee; HPLC analysis using Chiralcel OD column (7% ^{i}PrOH/Hexane, 0.5 mL/min): retention times 24.0 (2*R*, 3*R*), 26.7 (2*S*, 3*S*).

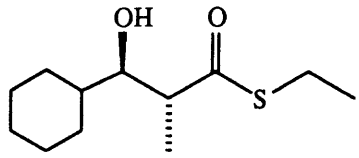

^{1}H NMR (300 MHz, $CDCl_3$) δ 1.25 (d, J=7.2 Hz, 3H, $C\underline{H}_3CH$), 1.30 (t, J=7.4 Hz, 3H, $SCH_2C\underline{H}_3$), 1.00–1.96 (m, 11H, cyclohexane-H), 2.93 (m, 2H, O<u>H</u> and $CH_3C\underline{H}$), 3.34 (m, 1H, C<u>H</u>OH), 3.52 (q, J=7.4 Hz, 2H, $SC\underline{H}_2CH_3$); additional peaks for *syn* isomer[36a]: 3.68 (dd, J=3.5, 7.5 Hz, 2H, C<u>H</u>OH), 3.77 (q, J=7.4 Hz, 1H, $SC\underline{H}_2CH_3$); ^{13}C NMR (75.4 MHz, $CDCl_3$) δ 14.7, 16.0, 23.3, 26.1, 26.3, 26.4, 27.3, 30.1, 41.3, 50.3, 78.4, 204.5; IR (neat) 3446, 2926, 1684, 1456 cm^{-1}; ee determination by ^{19}F NMR (282.2 MHz, C_6D_6) analysis of the corresponding (*R*)-MTPA esters.

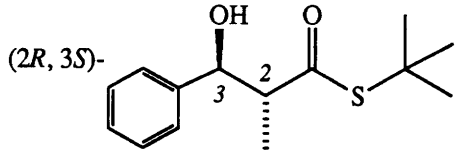

^{1}H NMR (300 MHz, $CDCl_3$) δ 1.00 (d, J=7.2 Hz, 3H, $C\underline{H}_3CH$), 1.45 (s, 9H, $SC(C\underline{H}_3)_3$), 2.73 (d, J=4.8 Hz, 1H, O<u>H</u>), 2.86 (q of d, J=7.8, 7.8 Hz, 1H, $CH_3C\underline{H}$), 4.75 (dd, J=4.5, 7.8 Hz, 1H, C<u>H</u>OH), 7.24–7.36 (m, 5H, ArH); additional peaks for the *syn* isomer: 1.18 (d, J=7.2 Hz, 3H, $C\underline{H}_3CH$), 5.12 (d, J=3.9 Hz, 1H, C<u>H</u>OH); ^{13}C NMR (75.4 MHz, $CDCl_3$) δ 16.1, 30.3, 48.9, 56.1, 77.0, 127.0, 128.4, 128.8, 142.1, 204.7; IR (neat) 3448, 2965, 2922, 1678, 1455, 1364, 1163, 1082, 1046, 1020, 959, 766, 739 cm^{-1}; MS (EI) *m/e* calc'd for $C_{14}H_{20}O_2S$: 252.1184, found 252.1185; 252 (7), 195 (22), 163 (41), 146 (72), 134 (50), 107 (100), 90 (63), 57 (96); $[\alpha]_D^{20}$ -120.0° (c=0.40, $CHCl_3$) for *anti* (2*R*, 3*S*)-aldol of 82% ee; HPLC analysis using Chiralcel OD column (10% ^{i}PrOH/Hexane, 0.5 mL/min): retention times 12.2 (minor, *syn*), 17.7 (major *syn*), 14.2 (2*R*, 3*S*, *anti*), 15.3 (2*S*, 3*R*, *anti*) min.

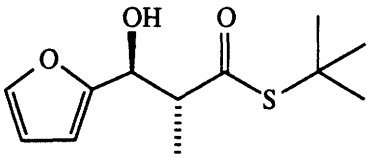

^{1}H NMR (300 MHz, $CDCl_3$) δ 1.06 (d, J=7.2 Hz, 3H, C<u>H</u>$_3$CH), 1.42 (s, 9H, SC(C<u>H</u>$_3$)$_3$), 2.82 (br d, 1H, O<u>H</u>), 3.05 (m, 1H, CH$_3$C<u>H</u>), 4.75 (m, 1H, C<u>H</u>OH), 6.23 (dd, J=0.6, 3.3 Hz, 1H, furan-3-<u>H</u>), 6.28 (dd, J=1.8, 3.0 Hz, 1H, furan-4-<u>H</u>), 7.33 (d, J=1.8 Hz, 1H, furan-5-<u>H</u>); additional peaks for the *syn* isomer: 1.20 (d, J=7.2 Hz, 3H, C<u>H</u>$_3$CH), 1.39 (s, 9H, SC(C<u>H</u>$_3$)$_3$), 4.70 (m, 1H, C<u>H</u>OH); ^{13}C NMR (75.4 MHz, $CDCl_3$) δ 15.4, 29.8, 48.5, 52.9, 70.2, 107.4, 110.1, 142.2, 154.2, 204.0; IR (neat) 3454, 2965, 2926, 1674, 1456, 1365, 1151, 1072 cm^{-1}; MS (EI) *m/e* calc'd for $C_{12}H_{18}O_3S$: 242.0977, found 242.0978; 242 (5), 185 (18), 151 (12), 124 (31), 108 (18), 97 (100), 57 (47), 41 (26); HPLC analysis using Chiralcel OD column (6% ^{i}PrOH/Hexane, 0.4 mL/min): retention times 27.2 (minor, *syn*), 28.8 (major *syn*), 32.1 (major, *anti*), 35.8 (minor, *anti*) min.

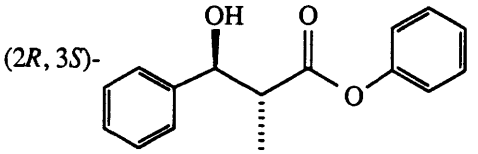

^{1}H NMR (300 MHz, C_6D_6) δ 0.97 (d, J=7.2 Hz, 3H, C<u>H</u>$_3$CH), 2.15 (br s, 1H, O<u>H</u>), 2.95 (q of d, J=7.5, 7.5 Hz, 1H, CH$_3$C<u>H</u>), 4.68 (d, J=7.5 Hz, 1H, C<u>H</u>OH), 6.86–7.28 (m, 10H, Ar<u>H</u>); IR (neat) 3453, 3063, 3031, 2978, 2938, 2881, 1752, 1593, 1493, 1456, 1376, 1194, 1163 cm^{-1}; diagnostic peaks in the ^{1}H NMR spectrum of the corresponding (*S*)-MTPA esters: (300 MHz, C_6D_6) δ 6.58 (d, J= 6.7 Hz, PhC<u>H</u>, major, *syn*), 6.62 (d, J= 6.7 Hz, PhC<u>H</u>, minor, *syn*), 6.30 (d, J= 9.5 Hz, PhC<u>H</u>, (2*S*, 3*R*), *anti*), 6.43 (d, J= 9.5 Hz, PhC<u>H</u>, (2*R*, 3*S*), *anti*).[44,75]

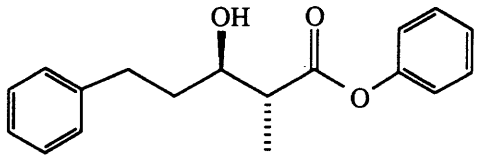

^{1}H NMR (300 MHz, $CDCl_3$) δ 1.34 (d, J=7.2 Hz, 3H, $C\underline{H}_3CH$), 1.85 (m, 2H, $PhCH_2C\underline{H}_2$), 2.58 (br s, 1H, O<u>H</u>), 2.75 (m, 2H, $PhC\underline{H}_2CH_2$), 2.88 (m, 1H, $CH_3C\underline{H}$), 3.79 (br m, 1H, C<u>H</u>OH), 7.03 (dd, J=7.6, 1.2 Hz, 2H, Ar<u>H</u>), 7.15–7.38 (m, 8H, Ar<u>H</u>); additional peaks for the *syn* isomer: 1.33 (d, J=7.2 Hz, 3H, $C\underline{H}_3CH$), 4.05 (br m, 1H, C<u>H</u>OH); ^{13}C NMR (75.4 MHz, $CDCl_3$) δ 14.3, 32.0, 36.5, 45.7, 72.7, 121.3, 125.8, 125.9, 128.2, 128.3, 129.3, 141.6, 150.3, 174.2; additional peaks for the *syn* isomer: 35.8, 44.7, 71.0; IR (neat) 3478, 3026, 2941, 1754, 1593, 1493, 1455, 1357, 1194, 1163 cm^{-1}; MS (EI) *m/e* calc'd for $C_{18}H_{20}O_3$: 284.1412, found 284.1410; 284 (4), 117 (12), 94 (100); HPLC analysis using Chiralcel OD column (8% ^{i}PrOH/Hexane, 0.5 mL/min): retention times 48.0 (minor, *syn*), 65.1 (major, *syn*), 40.7 (minor, *anti*), 50.3 (major, *anti*) min.

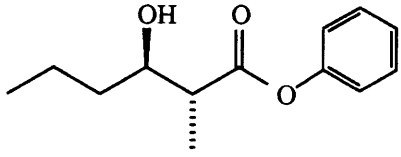

^{1}H NMR (250 MHz, C_6D_6) δ 0.93 (t, J=7.3 Hz, 3H, $C\underline{H}_3CH_2CH_2$), 1.20 (d, J=7.1 Hz, 3H, $C\underline{H}_3CH$), 1.32–1.70 (m, 4H, $CH_3C\underline{H}_2C\underline{H}_2$), 2.69 (q of d, J=7.1 Hz, 1H, $CH_3C\underline{H}$), 2.88 (br s, 1H, O<u>H</u>), 3.79 (m, 1H, C<u>H</u>OH), 7.00 (m, 1H, Ar<u>H</u>), 7.10–7.23 (m, 4H, Ar<u>H</u>); additional peak for *syn* isomer: 4.03 (m, 1H, C<u>H</u>OH); IR (neat) 3444, 2959, 2873, 1755, 1593, 1493, 1457, 1196, 1163 cm^{-1}; HPLC analysis using Chiralcel OD column (6% ^{i}PrOH/Hexane, 0.5 mL/min): retention times 43.8 (major, *syn*), 60.8 (minor, *syn*), 35.1 (major, *anti*), 39.2 (minor, *anti*) min.[44,75]

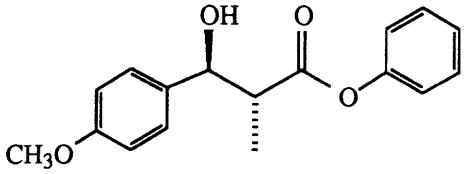

^{1}H NMR (250 MHz, C_6D_6) δ 1.00 (d, J=7.1 Hz, 3H, C<u>H</u>$_3$CH), 2.20 (br s, 1H, O<u>H</u>), 2.99 (d of q, J=7.1 Hz, 1H, CH$_3$C<u>H</u>), 3.29 (s, 3H, OC<u>H</u>$_3$), 4.72 (dd, J=7.5, 5.0 Hz, 1H, C<u>H</u>OH), 6.70–6.80 (m, 3H, Ar<u>H</u>), 6.87–6.95 (m, 2H, Ar<u>H</u>), 6.98–7.25 (m, 4H, Ar<u>H</u>); additional peaks for the *syn* isomer: 1.32 (d, J=7.1 Hz, 3H, C<u>H</u>$_3$CH), 2.90 (d of q, J=1, 7.1 Hz, 1H, CH$_3$C<u>H</u>), 4.95 (m, 1H, C<u>H</u>OH); ^{13}C NMR (75.4 MHz, $CDCl_3$) δ 14.5, 47.5, 55.3, 76.1, 113.9, 121.5, 125.8, 127.8, 129.2, 133.4, 150.4, 159.3, 174.2; additional peaks for the *syn* isomer: 12.0, 47.1, 74.0, 113.7, 121.3, 127.3, 133.5, 150.3, 159.2, 173.7; IR (neat) 3488, 2937, 1755, 1612, 1592, 1514, 1493, 1456, 1304, 1249, 1194, 1163 cm^{-1}; MS (EI) *m/e* calc'd for $C_{17}H_{18}O_4$: 286.1205, found 286.1206; 286 (5), 193 (44), 137 (100), 94 (21); diagnostic peaks in the ^{1}H NMR spectrum of the corresponding (*R*)-MTPA esters: (300 MHz, C_6D_6) δ 6.50 (d, J= 6.9 Hz, PhC<u>H</u>, minor, *syn*), 6.52(d, J= 6.9 Hz, PhC<u>H</u>, major, *syn*), 6.28 (d, J= 10.2 Hz, PhC<u>H</u>, major, *anti*), 6.41 (d, J= 10.2 Hz, PhC<u>H</u>, minor, *anti*).

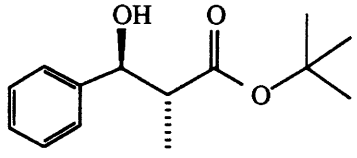

^{1}H NMR (300 MHz, $CDCl_3$) δ 0.97 (d, J=7.2 Hz, 3H, C<u>H</u>$_3$CH), 1.39 (s, 9H, OC(C<u>H</u>$_3$)$_3$), 2.66 (m, 1H, CH$_3$C<u>H</u>), 3.16 (br d, J=4.6 Hz, 1H, O<u>H</u>), 4.66 (dd, J=4.2, 7.8 Hz, 1H, C<u>H</u>OH), 7.19–7.32 (m, 5H, Ar<u>H</u>); additional peaks for the *syn* isomer: 1.06 (d, J=7.2 Hz, 3H, C<u>H</u>$_3$CH), 1.36 (s, 9H, OC(C<u>H</u>$_3$)$_3$), 2.66 (m, 1H, CH$_3$C<u>H</u>), 3.06 (br d, 1H, O<u>H</u>), 4.98 (m, J=4.2, 7.8 Hz, 1H, C<u>H</u>OH); ^{13}C NMR (75.4 MHz, $CDCl_3$) δ 14.8, 28.1, 47.8, 76.3, 81.2, 126.5, 127.7, 128.3, 141.7, 175.1; additional peaks for the *syn* isomer: 11.2, 28.0, 47.1, 73.8, 126.1, 127.3, 128.1; IR (neat) 3458, 2978, 2936,

1727, 1455, 1368, 1253, 1153 cm^{-1}; MS (EI) *m/e* calc'd for $C_{14}H_{20}O_3$: 236.1412, found 236.1410; 236 (4), 180 (29), 163 (20), 107 (100), 74 (32), 57 (63); HPLC analysis using Chiralcel OD column (7% ^{i}PrOH/Hexane, 0.3 mL/min): retention times 47.6 (major, *syn*), 71.9 (minor, *syn*), 38.7 (minor, *anti*), 45.5 (major, *anti*) min.

6.8 Diols and Related Compounds

Optical rotations are not given in cases where the diastereomers are inseparable. Note: To avoid confusion, the numbering system used for the β-hydroxy esters is carried over to the corresponding diols (see the numbering on the structures below).

General Procedure

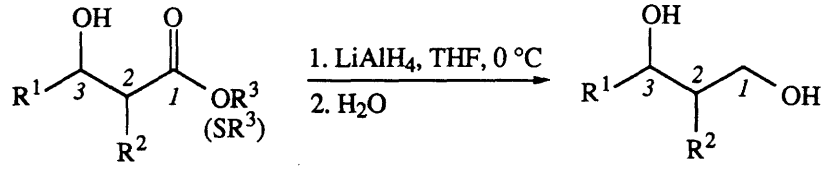

General procedure for the reduction of β-hydroxy esters to 1,3-diols (Procedure D[80]: To a solution of the β-hydroxy ester product (50–100 mg) in THF (2 mL) at 0 °C was slowly added solid lithium aluminum hydride (LAH) until effervescence ceased. The reaction mixture was warmed to room temperature and was allowed to stir for 2 h, then diluted with ether (10 mL) and recooled to 0 °C. Excess LAH was decomposed by sequential dropwise addition of water (ca. 200 μL), 15% NaOH solution (ca. 200 μL), and water (ca. 600 μL). The mixture was stirred for 30 min, then filtered through a Celite bed; the filtered material was washed with ether (3 x 15 mL). Water (5 mL) was added to the filtrate, and the ether layer was separated, dried ($MgSO_4$), and concentrated in vacuo affording the crude diol, which was purified by flash chromatography (50–75% ethyl acetate in hexane).

Diols:

(2*R*, 3*S*)-

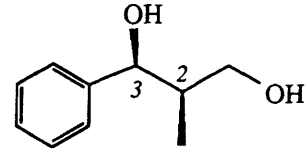

^{1}H NMR (300 MHz, $CDCl_3$) δ 0.82 (d, J=7.2 Hz, 3H, CH_3CH), 2.05 (m, 1H,

$CH_3C\underline{H}$), 2.62 (br s, 1H, O$\underline{H}$), 3.10 (br s, 1H, O$\underline{H}$), 3.65 (m, 2H, C$\underline{H}_2$OH), 4.92 (d, J=3.3 Hz, 1H, C$\underline{H}$OH), 7.20–7.40 (m, 5H, Ar$\underline{H}$); $[\alpha]_D^{20}$ -30.9° (c=1.4, $CHCl_3$) for *syn* (2*R*, 3*S*)-diol of >98% ee.[85]

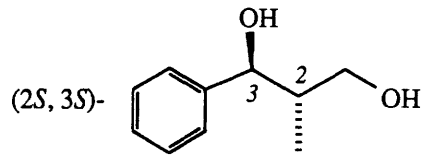

^{1}H NMR (250 MHz, $CDCl_3$) δ 0.69 (d, J=6.9 Hz, 3H, C$\underline{H}_3$CH), 2.05 (m, 1H, $CH_3C\underline{H}$), 3.10 (br m, 2H, O$\underline{H}$), 3.73 (m, 2H, C$\underline{H}_2$OH), 4.52 (d, J=7.8 Hz, 1H, C$\underline{H}$OH), 7.25–7.41 (m, 5H, Ar$\underline{H}$); IR (neat) 3332, 2878, 1454 cm^{-1}; $[\alpha]_D^{20}$ -24.2° (c=0.31, $CHCl_3$) for *anti* (2*S*, 3*S*) diol of 64% ee.[80]

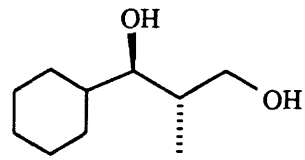

^{1}H NMR (250 MHz, $CDCl_3$) δ 0.89 (d, J=7.0 Hz, 3H, C$\underline{H}_3$CH), 1.00–2.08 (m, 12H, cyclohexyl-$\underline{H}$ and $CH_3C\underline{H}$), 2.42 (br s, 1H, O$\underline{H}$), 2.85 (br s, 1H, O$\underline{H}$), 3.32 (dd, J=2.7, 8.0 Hz, 1H, C$\underline{H}$OH), 3.59–3.80 (m, 2H, C$\underline{H}_2$OH); additional peak for the *syn* isomer: 3.48 (br d, J=8.0 Hz, 1H, C$\underline{H}$OH).[80]

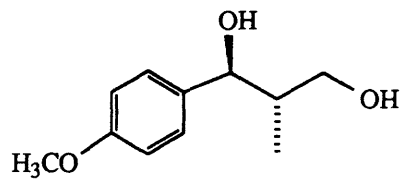

^{1}H NMR (250 MHz, $CDCl_3$) δ 0.64 (d, J=7.1 Hz, 3H, C$\underline{H}_3$CH), 2.00 (m, 1H, $CH_3C\underline{H}$), 2.95 (br s, 2H, O$\underline{H}$), 3.60–3.80 (m, 2H, C$\underline{H}_2$OH), 3.79 (s, 3H, OC$\underline{H}_3$), 4.46 (d, J=8.7 Hz, 1H, C$\underline{H}$OH), 6.85 (d, J=8.8 Hz, 2H, Ar$\underline{H}$), 7.25 (d, J=8.8 Hz, 2H, Ar$\underline{H}$); ^{13}C NMR (75.4 MHz, $CDCl_3$) δ 13.9, 41.8, 55.3, 68.2, 80.6, 113.8, 127.8, 135.5, 159.1; IR (neat) 3355, 2932, 1612, 1514, 1457, 1247, 1176 cm^{-1}; MS (EI) *m/e* calc'd for

$C_{11}H_{16}O_3$: 196.1099, found 196.1098; 196 (7), 137 (100), 109 (22).

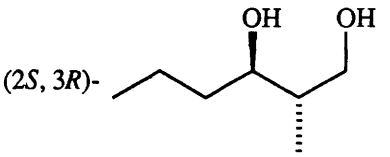

^{1}H NMR (250 MHz, $CDCl_3$) δ 0.87 (d, J=6.9 Hz, 3H, $C\underline{H}_3CH$), 0.93 (t, J=6.9 Hz, 3H, $C\underline{H}_3CH_2$), 1.23–1.85 (m, 5H, $CH_3C\underline{H}_2C\underline{H}_2$ and $C\underline{H}_3CH$), 3.10 (br s, 2H, O<u>H</u>), 3.50–3.85 (m, 3H, C<u>H</u>OH and $C\underline{H}_2OH$); $[\alpha]_D^{20}$ +17.8° (c=1.2, $CHCl_3$) for 88% *anti* (2*S*, 3*R*)-diol of 70% ee.[80]

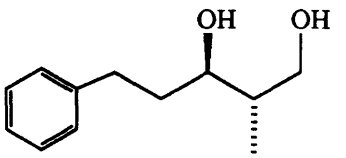

^{1}H NMR (300 MHz, $CDCl_3$) δ 0.93 (d, J=7.2 Hz, 3H, $C\underline{H}_3CH$), 1.85 (m, 3H, $PhCH_2C\underline{H}_2$ and $CH_3C\underline{H}$), 2.65–2.96 (m, 2H, $PhC\underline{H}_2$), 3.60 (br m, 2H, O<u>H</u>), 3.80 (br d, 1H, C<u>H</u>OH), 4.10 (m, 2H, $C\underline{H}_2OH$), 7.20–7.37 (m, 5H, Ar<u>H</u>); IR (neat) 3355, 2956, 1454, 1029 cm^{-1}.[113]

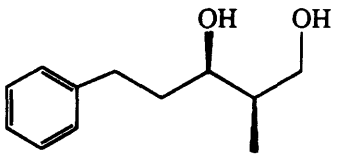

^{1}H NMR (300 MHz, $CDCl_3$) δ 0.91 (d, J=7.2 Hz, 3H, $C\underline{H}_3CH$), 1.80 (m, 3H, $PhCH_2C\underline{H}_2$ and $CH_3C\underline{H}$), 2.62–2.90 (m, 2H, $PhC\underline{H}_2$), 3.68 (m, 4H, O<u>H</u> and $C\underline{H}_2OH$), 3.85 (m, 1H, C<u>H</u>OH), 7.15–7.33 (m, 5H, Ar<u>H</u>).[113]

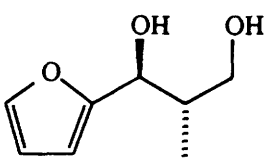

^{1}H NMR (300 MHz, $CDCl_3$) δ 0.81 (d, J=7.0 Hz, 3H, $C\underline{H}_3CH$), 2.25 (m, 1H, $CH_3C\underline{H}$), 3.02 (br s, 1H, O<u>H</u>), 3.23 (br s, 1H, O<u>H</u>), 3.70 (m, 2H, $C\underline{H}_2OH$), 4.63 (d, J=8.5 Hz, 1H, C<u>H</u>OH), 6.30 (t, J=1.5 Hz, 1H, furan-3-<u>H</u>), 6.38 (m, 1H, furan-4-<u>H</u>), 7.41 (m, 1H, furan-5-<u>H</u>); additional peaks for the *syn* isomer: 0.94 (d, J=6.9 Hz, 3H, $C\underline{H}_3CH$), 4.92 (d, J=3.9 Hz, 1H, C<u>H</u>OH); ^{13}C NMR (75.4 MHz, $CDCl_3$) δ 13.6, 39.5, 67.3, 73.2, 107.0, 110.1, 141.9, 155.5; additional peaks for the *syn* isomer: 11.6, 39.8, 66.1, 71.1, 106.5, 141.6, 155.4; IR (neat) 3354, 2965, 2880, 1456, 1150 cm^{-1}; MS (EI) *m/e* calc'd for $C_8H_{12}O_3$: 156.0786, found 156.0787; 156 (8), 138 (8), 97 (100), 69 (12), 41 (22).

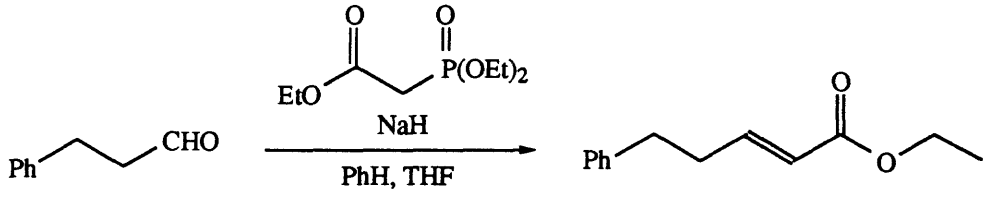

Triethylphosphonoacetate (4.0 mL, 20.2 mmol, 1.3 equiv) was added dropwise to a stirred slurry of sodium hydride (80% dispersion in mineral oil, 0.558 g, 18.6 mmol, 1.2 equiv) suspended in benzene (30 mL) at 0 °C . To the resulting homogeneous solution was added a pre-cooled (0 °C) solution of hydrocinnamaldehyde (2.0 mL, 15.2 mmol, 1 equiv) in THF (20 mL) by cannula over 30 min. The yellow reaction mixture was kept at 0 °C overnight, then allowed to warm to ambient temperature. The reaction was quenched by addition of water, and the organic phase was separated. The aqueous phase was extracted with ether, and the combined organic phases were washed with brine, dried ($MgSO_4$) and concentrated in vacuo. Flash chromatography (5% ethyl acetate in hexane) on the residue afforded the pure unsaturated ester as a colorless oil (2.96 g, 14.5 mmol, 95%): ^{1}H NMR (300 MHz, $CDCl_3$) δ 1.26 (t, J=7.2 Hz, 3H, $OCH_2C\underline{H}_3$), 2.50 (m, 2H, $PhCH_2C\underline{H}_2$), 2.76 (t, J=7.8 Hz, 2H, $PhC\underline{H}_2CH_2$), 4.16 (q, J=7.1 Hz, 2H, $OC\underline{H}_2CH_3$), 5.83 (d of t, J=15.6, 1.6 Hz, 1H, $CH_2C\underline{H}$=CH), 6.98 (d of t, J=15.6, 6.0 Hz, 1H, CH_2CH=C<u>H</u>), 7.15–7.31 (m, 5H, ArH); ^{13}C NMR (75.4 MHz, $CDCl_3$) δ 14.4, 34.0, 34.4, 60.2, 121.8,

126.1, 128.2, 128.4, 140.7, 147.9, 166.4; IR (neat) 3027, 2981, 2936, 1715, 1653, 1604, 1497, 1454, 1367, 1316, 1267, 1198, 1149 cm^{-1}; MS (EI) *m/e* calc'd for $C_{13}H_{16}O_2$: 204.1150, found 204.1150; 204 (8), 158 (19), 130 (41), 91 (100).

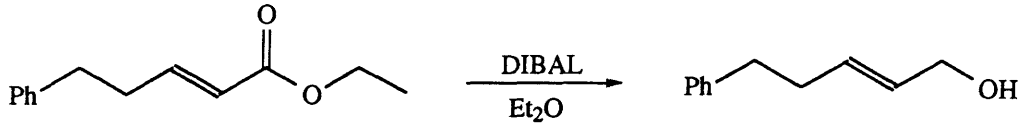

To a solution of the unsaturated ester (0.778 g, 3.81 mmol, 1 equiv) in ether (15 mL) at -78 °C was added dropwise DIBAL (1 M solution in hexane, 9.5 mL, 9.5 mmol, 2.5 equiv). The reaction mixture was stirred for 2 h, then warmed to room temperature and quenched with a saturated aqueous solution of potassium sodium tartrate (Rochelle's salt). The precipitated salts were removed by filtration and washed with ethyl acetate. The organic phase was separated, and the aqueous phase was extracted with ethyl acetate. The combined organic extracts were washed with water and brine, then were dried ($MgSO_4$) and concentrated in vacuo. Flash chromatography on the crude product (10% ethyl acetate in hexane) afforded the pure allylic alcohol as a colorless oil (0.485 mg, 2.99 mmol, 78%): ^1H NMR (300 MHz, $CDCl_3$) δ 2.36 (m, 2H, $PhCH_2C\underline{H}_2$), 2.69 (t, J=7.2 Hz, 2H, $PhC\underline{H}_2CH_2$), 4.05 (br d, J=4.6 Hz, 2H, $C\underline{H}_2OH$), 5.69 (m, 2H, C<u>H</u>=C<u>H</u>), 7.13–7.35 (m, 5H, Ar<u>H</u>); ^{13}C NMR (75.4 MHz, $CDCl_3$) δ 33.9, 35.5, 63.7, 125.9, 128.3, 128.4, 129.6, 132.2, 141.7; IR (neat) 3332, 3026, 2924, 2855, 1496, 1454, 1083 cm^{-1}; MS (EI) *m/e* calc'd for $C_{11}H_{14}O$: 162.1045, found 162.1045; 162 (2), 144 (46), 129 (35), 91 (100), 65 (36).

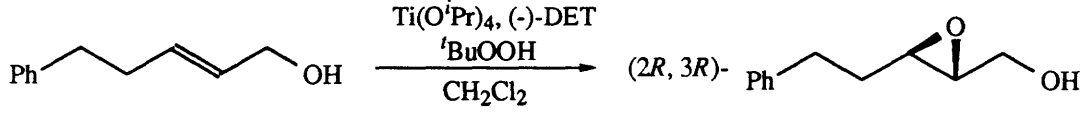

To a solution of titanium(IV) isopropoxide (0.54 mL, 1.8 mmol, 1 equiv) in CH_2Cl_2 (15 mL) at -30 °C was added a solution of (–)-diethyl D-tartrate (0.419 g, 2.03 mmol, 1.1 equiv) in CH_2Cl_2 (5 mL) via cannula. After the mixture was stirred for 15 min,

the allylic alcohol (0.292 g, 1.80 mmol, 1 equiv) was added as a solution in CH_2Cl_2 (5 mL). Stirring was continued for 30 min at -30 °C prior to the introduction of anhydrous *t*-butyl hydroperoxide (1.0 mL of a 5.18 M solution in 2,2,4-trimethylpentane, 5.1 mmol, 2.8 equiv). The reaction was kept at -20 °C overnight, quenched with water (10 mL), and allowed to stir for 45 min at 25 °C. A solution of 30% sodium hydroxide in aqueous saturated NaCl (2 mL) was added, and stirring continued for another hour, after which the layers were separated. The milky aqueous layer was extracted with CH_2Cl_2, and the combined organic layers were dried ($MgSO_4$) and concentrated in vacuo. The crude product was purified by flash chromatography (20–40% ethyl acetate) giving the pure epoxy alcohol as a colorless oil (0.304 g, 1.71 mmol, 95%): ^{1}H NMR (250 MHz, $CDCl_3$) δ 1.60 (br s, 1H, O<u>H</u>), 1.93 (m, 2H, $PhCH_2C\underline{H}_2$), 2.70–2.95 (m, 3H, epoxide-C<u>H</u> and $PhC\underline{H}_2CH_2$), 3.02 (d of t, J=2.5, 7.5 Hz, 1H, epoxide-C<u>H</u>), 3.62 (m, 1H, $C\underline{H}_AH_BOH$), 3.88 (m, 1H, $CH_A\underline{H}_BOH$), 7.20–7.35 (m, 5H, Ar<u>H</u>); ^{13}C NMR (75.4 MHz, $CDCl_3$) δ 32.2, 33.3, 55.3, 58.6, 61.6, 126.1, 128.3, 128.5, 141.0; IR (neat) 3417, 3026, 2928, 2861, 1748, 1603, 1496, 1454, 1260, 1091 cm^{-1}; MS (EI) *m/e* calc'd for $C_{11}H_{14}O_2$: 178.0994, found 178.0995; 178 (0.8), 129 (37), 117 (100), 104 (88), 91 (100); $[\alpha]_D^{20}$ +45.4° (c=0.69, $CHCl_3$) for (2*R*, 3*R*)-epoxide of 91% ee. The ee of the epoxy alcohol was determined by ^{1}H NMR analysis of both the (*R*)- and (*S*)-MTPA esters; diagnostic peaks in the ^{1}H NMR spectrum of the (*R*)-MTPA ester: (300 MHz, C_6D_6) δ 3.97 (dd, J=3.1, 12.1 Hz, 1H, $C\underline{H}_AH_BOH$, (*R*, *R*)-epoxide), 4.12 (dd, J=3.1, 12.1 Hz, 1H, $CH_A\underline{H}_BOH$, (*S*, *S*)-epoxide).

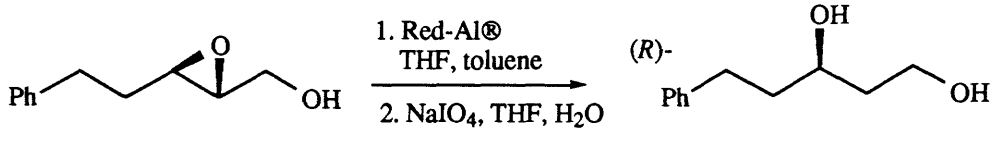

To a solution of the epoxy alcohol (115 mg, 0.644 mmol, 1 equiv) in THF (7 mL) at -20 °C was added dropwise Aldrich Red-Al® (0.60 mL of a 3.4 M solution in toluene, 2.0 mmol, 3.1 equiv). The reaction was allowed to warm to ambient temperature and was

stirred overnight, then quenched by slow cannulation of the reaction mixture into a saturated aqueous solution of Rochelle's salt (10 mL) with vigorous mixing. The mixture was stirred for an additional 20 min, then extracted with ether. The organic layers were evaporated, and the residue was stirred with sodium periodate (137 mg, 0.641 mmol, 1 equiv) in 1:1 THF/H_2O (3 mL) for 1 h at room temperature to remove any 1,2-diol. The reaction mixture was extracted with ether, and the ether layers were dried ($MgSO_4$) and concentrated in vacuo. The crude product was purified by flash chromatography (35–55% ethyl acetate in hexane) affording the 1,3-diol as a colorless oil (90.9 mg, 0.504 mmol, 79%): ^{1}H NMR (300 MHz, $CDCl_3$) δ 1.69–1.90 (m, 4H, $PhCH_2C\underline{H}_2$ and $CH_2C\underline{H}_2OH$), 2.20 (br s, 2H, O<u>H</u>), 2.72 (m, 2H, $PhC\underline{H}_2CH_2$), 3.75–3.93 (m, 3H, C<u>H</u>OH and $C\underline{H}_2OH$), 7.15–7.30 (m, 5H, Ar<u>H</u>); ^{13}C NMR (75.4 MHz, $CDCl_3$) δ 31.9, 38.3, 39.3, 61.7, 71.5, 125.9, 128.3, 128.4, 141.9; IR (neat) 3354, 2939, 1603, 1496, 1454, 1056, 748 cm^{-1}; MS (EI) *m/e* calc'd for $C_{11}H_{16}O_2$: 180.1150, found 180.1151; 180 (0.6), 162 (75), 144 (51), 129 (100), 117 (36), 91 (89); $[\alpha]_D^{20}$ +16.4° (c=1.6, $CHCl_3$) for (*R*)-diol of 91% ee (based on ee of epoxy alcohol).

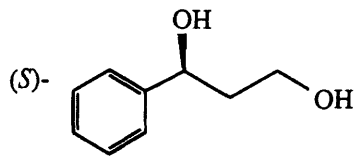

^{1}H NMR (250 MHz, $CDCl_3$) δ 1.24 (m, 2H, $C\underline{H}_2CH_2OH$), 2.31 (br s, 2H, O<u>H</u>), 3.86 (dd, J=5.2, 5.8 Hz, 2H, $CH_2C\underline{H}_2OH$), 4.96 (dd, J=3.9, 8.5 Hz, 1H, C<u>H</u>OH), 7.25–7.36 (m, 5H, Ar<u>H</u>); IR (neat) 3380, 3020, 2940, 1600, 1450, 1040 cm^{-1}; $[\alpha]_D^{20}$ -34.3° (c=0.60, $CHCl_3$) for (*S*)-diol of 93% ee.[80]

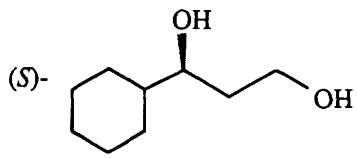

^{1}H NMR (250 MHz, $CDCl_3$) δ 0.93 (m, 13H, cyclohexyl-<u>H</u> and $C\underline{H}_2CH_2OH$),

2.43 (br s, 2H, O<u>H</u>), 3.59 (ddd, J=6.1, 8.8, 10.3 Hz, 1H, C<u>H</u>OH), 3.76–3.90 (m, 2H, C<u>H</u>$_2$OH); IR (neat) 3340, 2920, 2850, 1445, 1040 cm^{-1}; $[\alpha]_D^{20}$ -6.3° (c=0.60, $CHCl_3$) for (*S*)-diol of 84% ee.[80]

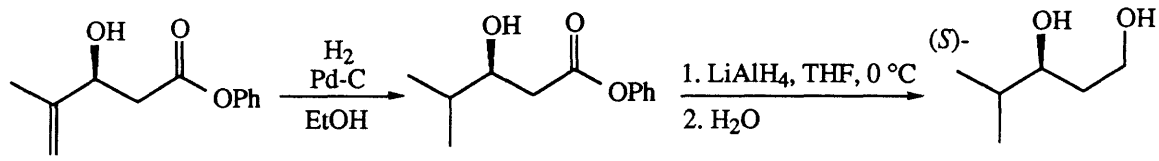

To a solution of 3-hydroxy-4-methylpent-4-enoic acid phenyl ester (72.4 mg, 0.351 mmol, 1 equiv, 70% ee) in ethanol (2 mL) was added 10% palladium on carbon (37.4 mg, 0.0351 mmol, 0.0351 mmol), and the resulting suspension was shaken under 20 psi of hydrogen for 2 h using a Parr hydrogenator. The mixture was filtered through a pad of Celite, and the catalyst was washed with ether. The collected filtrate was concentrated in vacuo, and the crude product was purified by flash chromatography (20% ethyl acetate in hexane) affording 3-hydroxy-4-methylpentanoic acid phenyl ester as a colorless oil (39.4 mg, 0.189 mmol, 54%): ^{1}H NMR (300 MHz, $CDCl_3$) δ 0.94 (d, J=6.9 Hz, 3H, CH(C<u>H</u>$_3$)$_2$), 0.96 (d, J=6.9 Hz, 3H, CH(C<u>H</u>$_3$)$_2$), 1.75 (sept, J=6.9 Hz, 1H, C<u>H</u>(CH$_3$)$_2$), 2.62 (A of ABX, 1H, J_{AB}= 16.5 Hz, J_{AX}= 9.3 Hz, C<u>H</u>$_2$CO), 2.73 (B of ABX, 1H, J_{AB}=16.5, J_{BX}= 3.3 Hz, C<u>H</u>$_2$CO), 3.88 (ddd, J=3.3, 9.3, 5.7 Hz, 1H, C<u>H</u>OH), 7.05 (br d, J=6.9 Hz, 2H, Ar-*ortho*-<u>H</u>), 7.19 (br t, J=6.9 Hz, 1H, Ar-*para*-<u>H</u>), 7.33 (br t, J=6.8 Hz, 2H, Ar-*meta*-<u>H</u>).

This β-hydroxy ester was reduced to the corresponding 1,3-diol with LAH (Procedure I) in 69% yield. ^{1}H NMR (300 MHz, $CDCl_3$) δ 0.89 (d, J=6.6 Hz, 3H, CH(C<u>H</u>$_3$)$_2$), 0.91 (d, J=6.9 Hz, 3H, CH(C<u>H</u>$_3$)$_2$), 1.66 (m, 3H, C<u>H</u>(CH$_3$)$_2$ and C<u>H</u>$_2$CH$_2$OH), 2.53 (br s, 1H, O<u>H</u>), 2.70 (br s, 1H, O<u>H</u>), 3.60 (m, 1H, C<u>H</u>OH), 3.84 (m, 2H, CH$_2$C<u>H</u>$_2$OH); $[\alpha]_D^{20}$ -9.4° (c=0.64, $CHCl_3$) for (*S*)-diol of 70% ee (based on ee of hydroxy ester).[80]

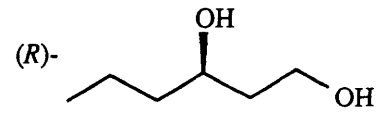

^{1}H NMR (250 MHz, $CDCl_3$) δ 0.91 (t, J=7.0 Hz, 3H, $C\underline{H}_3CH_2CH_2$), 1.30–1.49 (m, 4H, $CH_3C\underline{H}_2C\underline{H}_2$), 1.69–1.72 (m, 2H, $C\underline{H}_2CH_2OH$), 2.43 (br s, 2H, O<u>H</u>), 3.79–3.91 (m, 3H, C<u>H</u>OH and $C\underline{H}_2OH$); $[\alpha]_D^{20}$ -4.2° (c=0.50, $CHCl_3$) for (*R*)-diol of 92% ee (based on ee of hydroxy ester).[80]

6.9 β-Hydroxy Ketones and Related Compounds

Yields and enantiomeric excesses for aldol reactions are given in the text. Racemic samples were used as standards for all ee determinations on optically active material. For the preparation of Mosher's ester derivatives, see Procedure D in Section 6.5.

General Procedures

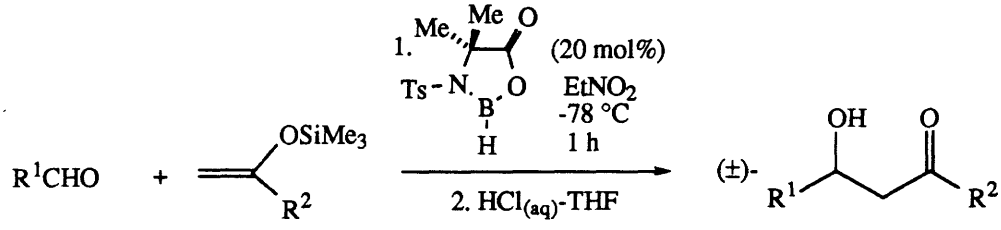

A general procedure for the preparation of racemic β-hydroxy ketones (Procedure J): The achiral ligand *N*-tosyl-2-methylalanine (25.7 mg, 0.100 mmol, 0.2 equiv) in nitroethane (1.5 mL) was treated with BH_3·THF complex (100 μL of a 1 M solution in THF, 0.1 mmol, 0.2 equiv). The solution was warmed to 45 °C for 1 h and cooled to -78 °C before the addition of the silyl enol ether (0.60 mmol, 1.2 equiv) and the aldehyde (0.50 mmol, 1 equiv). The reaction mixture was stirred 1 h at -78 °C, treated with 1:1 aqueous 1 M HCl/THF (1 mL), and allowed to stir for 1 h at room temperature. Following extraction with ether, the organic layers were dried ($MgSO_4$) and concentrated in vacuo, and the crude product was purified by flash chromatography (10–20% ethyl acetate in hexane) giving the racemic β-hydroxy ketone.

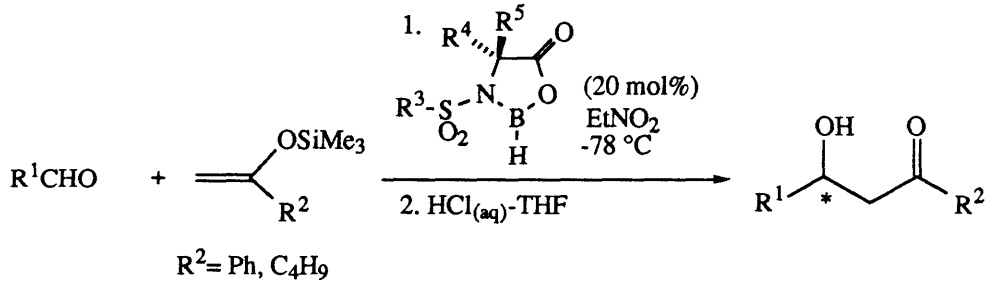

A general procedure for catalytic aldol reactions with silyl enol ethers (Procedure

K): The ligand (0.10 mmol, 0.2 equiv) in nitroethane (1.5 mL) was treated with BH_3·THF complex (100 μL of a 1 M solution in THF, 0.1 mmol, 0.2 equiv). The solution was warmed to 45 °C for 1 h and cooled to -78 °C before the addition of the silyl enol ether (0.60 mmol, 1.2 equiv) and the aldehyde (0.50 mmol, 1 equiv). The reaction was kept at -78 °C overnight and then quenched with 1:1 aqueous 1 M HCl/THF (1 mL). After stirring for 1 h at room temperature, the mixture was extracted with ether, and the organic layers were dried ($MgSO_4$) and concentrated in vacuo. The crude product was purified by flash chromatography (10–20% ethyl acetate in hexane) giving the optically active β-hydroxy ketone.

Aldol Products

(*S*)- 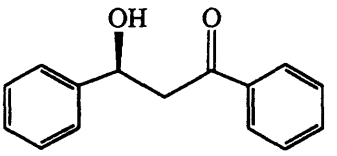

^{1}H NMR (300 MHz, $CDCl_3$) δ 3.34 (AB of ABX, J=6.2 Hz, 2H, C$\underline{H}_2$CO), 3.59 (d, J=2.9 Hz, 1H, O$\underline{H}$), 5.31 (t of d, J=5.9, 2.9 Hz, 1H, C$\underline{H}$OH), 7.24–7.47 (m, 7H, Ar$\underline{H}$), 7.55 (t of d, J=7.2, 1.2 Hz, 1H, Ar$\underline{H}$), 7.92 (dd, J=7.2, 1.2 Hz, 2H, Ar$\underline{H}$); IR (neat) 3472, 3061, 3029, 2963, 2903, 1678, 1597, 1579, 1494, 1449, 1406, 1358, 1269, 1212, 1061 cm^{-1}; $[\alpha]_D^{20}$ -58.7° (c=1.8, $CHCl_3$) for (*S*)-aldol[43,94] of 78% ee; HPLC analysis using a Chiralcel OD column (10% ^{i}PrOH/Hexane, 0.6 mL/min): retention times 24.5 (*S*), 26.6 (*R*) min.

(*S*)- 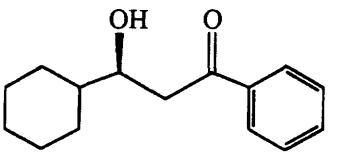

^{1}H NMR (250 MHz, $CDCl_3$) δ 0.82–1.96 (m, 11H, cyclohexyl-$\underline{H}$), 3.02 (A of ABX, 1H, J_{AB}= 17.6 Hz, J_{AX}= 9.2 Hz, C$\underline{H}_2$CO), 3.18 (B of ABX, 1H, J_{AB}=17.6 Hz,

J_{BX}= 2.5 Hz, C$\underline{H}_2$CO), 3.97 (ddd, J=2.5, 6.3, 12.5 Hz, 1H, C$\underline{H}$OH), 7.41–7.59 (m, 3H, Ar-*meta, para*-$\underline{H}$), 7.94 (dd, J=1.5, 8.3 Hz, 2H, Ar-*ortho*-$\underline{H}$); IR (neat) 3483, 2925, 2852, 1678, 1597, 1580, 1449, 1280, 1212, 1101 cm^{-1}; $[\alpha]_D^{20}$ -37.4° (c=0.66, $CHCl_3$) for (*S*)-aldol[94] of 60% ee; HPLC analysis using a Chiralcel OD column (10% ^{i}PrOH/Hexane, 0.6 mL/min): retention times 11.1 (*S*), 14.5 (*R*) min.

(*R*)-

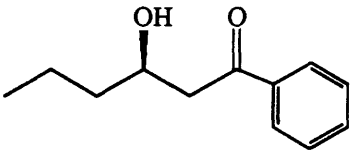

^{1}H NMR (300 MHz, $CDCl_3$) δ 0.99 (t, J=6.9 Hz, 3H, C$\underline{H}_3$CH$_2$), 1.20–1.65 (m, 4H, CH$_3$C$\underline{H}_2$C$\underline{H}_2$), 3.06 (A of ABX, 1H, J_{AB}= 17.6 Hz, J_{AX}= 8.7 Hz, C$\underline{H}_2$CO), 3.20 (B of ABX, 1H, J_{AB}= 17.6 Hz, J_{BX}= 2.7 Hz, C$\underline{H}_2$CO), 3.21 (br s, 1H, O$\underline{H}$), 4.26 (m, 1H, C$\underline{H}$OH), 7.50 (br t, J=7.5 Hz, 2H, Ar$\underline{H}$), 7.62 (br t, J=7.8 Hz, 1H, Ar$\underline{H}$), 7.97 (dd, J=1.8, 7.5 Hz, 2H, Ar$\underline{H}$); IR (neat) 3448, 2958, 2932, 2872, 1679, 1597, 1580, 1449, 1369, 1290, 1211, 1125, 1072 cm^{-1}; $[\alpha]_D^{20}$ -39.5° (c=1.0, $CHCl_3$) for (*R*)-aldol[29,94] of 62% ee; HPLC analysis using a Chiralcel OD column (10% ^{i}PrOH/Hexane, 1.0 mL/min): retention times 6.6 (*R*), 8.1 (*S*) min.

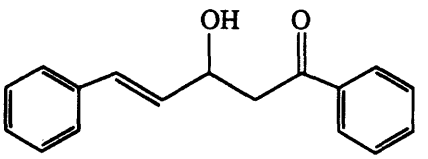

^{1}H NMR (300 MHz, $CDCl_3$) δ 3.21 (A of ABX, 1H, J_{AB}= 12.0 Hz, J_{AX}= 5.4 Hz, C$\underline{H}_2$CO), 3.28 (B of ABX, 1H, J_{AB}= 12.0 Hz, J_{BX}= 2.1 Hz, C$\underline{H}_2$CO), 3.34 (br s, 1H, O$\underline{H}$), 4.91 (ddd, J=2.1, 4.2, 15.0 Hz, 1H, C$\underline{H}$OH), 6.28 (dd, J=6.1, 15.9 Hz, 1H, PhCH=C$\underline{H}$), 6.68 (dd, J=1.2, 16.2 Hz, 1H, PhC$\underline{H}$=CH), 7.17–7.98 (m, 10H, Ar$\underline{H}$); ^{13}C NMR (75.4 MHz, $CDCl_3$) δ 45.2, 68.7, 126.5, 127.7, 128.1, 128.5, 128.7, 130.3, 130.5, 133.6, 136.6, 136.7, 200.0; IR (neat) 3448, 3058, 3026, 1680, 1597, 1579, 1494, 1449, 1357, 1267, 1212 cm^{-1}; MS (EI) *m/e* calc'd for $C_{17}H_{16}O_2$: 252.1150, found

252.1151; 252 (8), 160 (10), 131 (32), 120 (45), 105 (100), 77 (56), 51 (19); $[\alpha]_D^{20}$ -18.7° (c=1.3, $CHCl_3$) for aldol of 74% ee (unassigned); HPLC analysis using a Chiralcel OD column (10% ^{i}PrOH/Hexane, 0.7 mL/min): retention times 36.5 (minor), 40.1 (major) min.

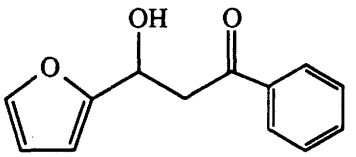

^{1}H NMR (300 MHz, $CDCl_3$) δ 3.45 (A of ABX, 1H, J_{AB}= 17.7 Hz, J_{AX}= 3.5 Hz, C<u>H</u>$_2$CO), 3.58 (B of ABX, 1H, J_{AB}= 17.7 Hz, J_{BX}= 8.4 Hz, C<u>H</u>$_2$CO), 5.35 (X of ABX, 1H, J_{AX}= 3.5 Hz, J_{BX}= 8.4 Hz, C<u>H</u>OH), 6.33 (m, 2H, furan-3,4-<u>H</u>), 7.37 (dd, J=0.9, 1.8 Hz, 1H, furan-5-<u>H</u>), 7.47 (t of d, J=6.0, 1.5 Hz, 2H, Ar-*meta*-<u>H</u>), 7.57 (m, 1H, Ar-*para*-<u>H</u>), 7.97 (dd, J=1.2, 6.9 Hz, 2H, Ar-*ortho*-<u>H</u>); IR (neat) 3454, 2909, 1682, 1597, 1580, 1505, 1449, 1365, 1282, 1213, 1182, 1145, 1065 cm^{-1}; $[\alpha]_D^{20}$ -42.7° (c=1.2, $CHCl_3$) for aldol[94] of 81% ee (unassigned); HPLC analysis using a Chiralcel OD column (10% ^{i}PrOH/Hexane, 0.7 mL/min): retention times 24.6 (major), 26.6 (minor) min..

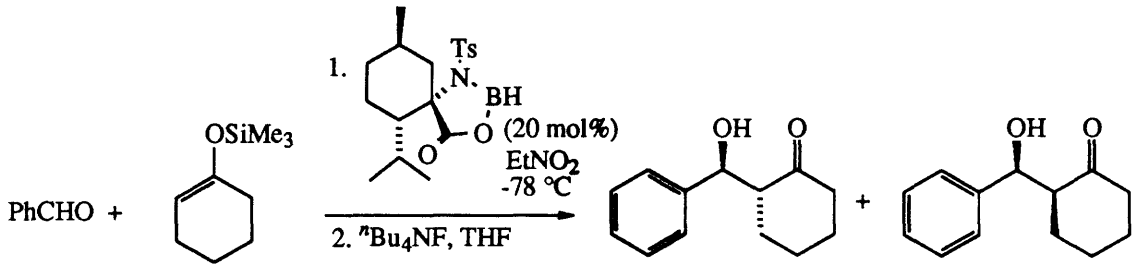

The *N*-tosyl ligand derived from menthone (36.2 mg, 0.102 mmol, 0.2 equiv) in nitroethane (1.5 mL) was treated with BH_3·THF complex (100 μL of a 1 M solution in THF, 0.1 mmol, 0.2 equiv). The solution was warmed to 45 °C for 1 h and cooled to -78 °C before the addition of 1-(trimethylsiloxy)cyclohexene (120 μL, 0.60 mmol, 1.2 equiv) and benzaldehyde (51 μL, 0.50 mmol, 1 equiv). The reaction mixture was kept at -78 °C

overnight before being poured into pH 7 buffer at 0 °C. The aqueous layer was extracted with ether, and the combined organic layers were dried ($MgSO_4$) and concentrated in vacuo, affording the silylated product accompanied by the β-hydroxy ketone. Desilylation was effected by stirring with tetrabutylammonium fluoride (TBAF, 0.5 mL of a 1 M solution in THF, 0.5 mmol, 1 equiv) in THF (1.5 mL) for 10–30 min at 0 °C. The reaction mixture was extracted into ether, and the organic layers were dried ($MgSO_4$) and concentrated in vacuo. The crude product was purified by flash chromatography (10–30% ethyl acetate in hexane) giving first the *syn* and then the *anti* isomers of the β-hydroxy ketone (37.3 mg, 0.183 mmol, 37%, *anti/syn*= 2:1).[43,114]

Anti aldol: ^{1}H NMR (250 MHz, C_6D_6) δ 0.75–1.50 (m, 6H, cyclohexanone ring-H), 1.67 (m, 1H, CHCO), 2.20 (m, 2H, CH_2CO), 4.17 (br s, 1H, OH), 4.77 (d, J=8.5 Hz, 1H, CHOH), 7.08–7.37 (m, 5H, ArH); IR (neat) 3487, 2935, 2860, 1699, 1495, 1449, 1400, 1310, 1203, 1128, 1062 cm^{-1}; $[\alpha]_D^{20}$ -16.3° (c=0.94, $CHCl_3$) for *anti* aldol[114] of 58% ee (unassigned); diagnostic peaks in the ^{1}H NMR spectrum of the corresponding (*R*)-MTPA ester: (300 MHz, C_6D_6) δ 6.31 (d, J= 9.8 Hz, PhCH, minor), 6.52 (d, J= 9.8 Hz, PhCH, major).

Syn aldol: ^{1}H NMR (300 MHz, C_6D_6) δ 0.75–1.60 (m, 6H, cyclohexanone ring-H), 1.73 (m, 1H, CHCO), 2.15 (m, 2H, CH_2CO), 3.04 (br s, 1H, OH), 5.37 (br m, 1H, CHOH), 7.05–7.42 (m, 5H, ArH); $[\alpha]_D^{20}$ -68.1° (c=0.26, $CHCl_3$) for *syn* aldol[114] of 72% ee (unassigned); diagnostic peaks in the ^{1}H NMR spectrum of the corresponding (*R*)-MTPA ester: (300 MHz, C_6D_6) δ 3.43 (br s, OCH_3, major), 3.46 (br s, OCH_3, minor).

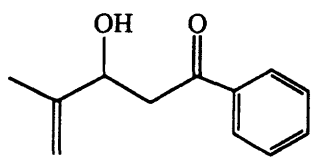

^{1}H NMR (300 MHz, $CDCl_3$) δ 1.78 (s, 3H, CH_3), 3.17 (AB of ABX, 2H, CH_2CO), 4.68 (X of ABX, 1H, CHOH), 4.88 (br d, 1H, $C=CH_2$), 5.04 (br d, 1H,

C=C$\underline{H}_2$), 7.39–7.58 (m, 3H, Ar$\underline{H}$), 7.90 (m, 2H, Ar$\underline{H}$); ^{13}C NMR (75.4 MHz, $CDCl_3$) δ 14.1, 22.6, 31.6, 71.2, 111.3, 128.1, 128.7, 133.5, 136.8, 145.8, 200.0; IR (neat) 3483, 2922, 1681, 1597, 1448, 1275, 1210 cm^{-1}; MS (EI) *m/e* calc'd for $C_{12}H_{14}O_2$: 190.0994, found 190.0993; 190 (5), 162 (31), 147 (13), 120 (83), 105 (100), 77 (89), 51 (23), 41 (15); HPLC analysis using a Chiralcel OD column (10% ^{i}PrOH/Hexane, 0.5 mL/min): retention times 12.8 (major), 14.2 (minor) min.

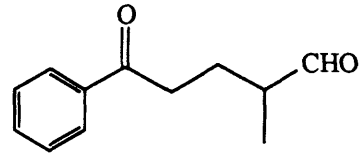

Conjugate addition product: ^{1}H NMR (300 MHz, $CDCl_3$) δ 1.14 (d, J=7.0 Hz, 3H, CH_3), 1.88 (m, 1H, PhC(O)$CH_2C\underline{H}_AH_B$), 2.15 (m, 1H, PhC(O)$CH_2CH_A\underline{H}_B$), 2.45 (m, 1H, C$\underline{H}$CHO), 2.99 (m, 2H, PhC(O)C$\underline{H}_2$), 7.40–7.58 (m, 3H, Ar$\underline{H}$), 7.95 (d, J=8.5 Hz, 2H, Ar-*ortho*-$\underline{H}$), 9.62 (d, J=1.5 Hz, 1H, C$\underline{H}$O); ^{13}C NMR (75.4 MHz, $CDCl_3$) δ 13.8, 24.8, 35.6, 45.7, 127.9, 128.5, 133.0, 136.6; IR (neat) 2972, 2935, 1720, 1685, 1597, 1579, 1449, 1368, 1210, 1180 cm^{-1}; MS (EI) *m/e* calc'd for [M - CHO]$^+$: 161.0966, found 161.0590; 176 (3), 161 (9), 122 (27), 105 (100), 77 (21).

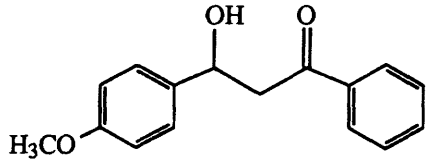

^{1}H NMR (300 MHz, $CDCl_3$) δ 3.33 (AB of ABX, 2H, C$\underline{H}_2$CO), 3.53 (d, J=2.7 Hz, 1H, O$\underline{H}$), 3.77 (s, 3H, OC$\underline{H}_3$), 5.26 (br t, J=6.0 Hz, 1H, C$\underline{H}$OH), 6.88 (dd, J=2.4, 7.5 Hz, 2H, Ar$\underline{H}$), 7.34 (dd, J=2.1, 8.0 Hz, 2H, anisyl-Ar-$\underline{H}$), 7.43 (t of d, J=7.2, 0.6 Hz, 2H, Ar$\underline{H}$), 7.56 (t of d, J=7.5, 1.2 Hz, 1H, Ar$\underline{H}$), 7.93 (dd, J=8.3, 1.5 Hz, 2H, anisyl-Ar-$\underline{H}$); ^{13}C NMR (75.4 MHz, $CDCl_3$) δ 47.3, 55.3, 69.7, 114.0, 127.0, 128.1, 128.7, 133.6, 135.2, 136.6, 159.1, 200.2; IR (neat) 3490, 3059, 2957, 2935, 2836,

1681, 1612, 1596, 1581, 1514, 1449, 1248, 1177 cm^{-1}; MS (EI) *m/e* calc'd for $C_{16}H_{16}O_3$: 256.1099, found 256.1097; 256 (21), 137 (100), 120 (42), 105 (66), 77 (45); $[\alpha]_D^{20}$ -17.0° (c=1.4, $CHCl_3$) for aldol of 32% ee (unassigned); HPLC analysis using a Chiralcel OD column (10% ^{i}PrOH/Hexane, 0.9 mL/min): retention times 17.3 (major), 20.8 (minor) min.

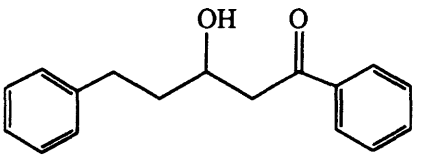

^{1}H NMR (300 MHz, $CDCl_3$) δ 1.72–1.98 (m, 2H, $PhCH_2C\underline{H}_2$), 2.73 (ddd, J=15.0, 9.3, 6.9 Hz, 1H, $PhC\underline{H}_AH_B$), 2.85 (ddd, J=15.0, 9.4, 5.2 Hz, 1H, $PhCH_A\underline{H}_B$), 3.02 (A of ABX, 1H, J_{AB}= 17.5 Hz, J_{AX}= 8.4 Hz, $C\underline{H}_2CO$), 3.13 (B of ABX, 1H, J_{AB}= 17.5 Hz, J_{BX}= 3.2 Hz, $C\underline{H}_2CO$), 3.30 (s, 1H, O<u>H</u>), 4.20 (br m, 1H, C<u>H</u>OH), 7.10–7.29 (m, 5H, ArH), 7.43 (t of d, J=6.9, 1.5 Hz, 2H, Ar<u>H</u>), 7.54 (br t, J=7.2 Hz, 1H, Ar<u>H</u>), 7.89 (dd, J=7.4, 1.3 Hz, 2H, Ar<u>H</u>); ^{13}C NMR (75.4 MHz, $CDCl_3$) δ 31.9, 38.2, 45.1, 67.1, 125.8, 128.0, 128.3, 128.4, 128.6, 133.5, 136.6, 141.8, 200.7; IR (neat) 3474, 3060, 3026, 2926, 1678, 1597, 1580, 1495, 1449, 1370, 1320, 1213, 1150 cm^{-1}; MS (EI) *m/e* calc'd for $C_{17}H_{18}O_2$: 254.1307, found 254.1305; 254 (4), 236 (26), 105 (100), 91 (40); $[\alpha]_D^{20}$ -29.2° (c=1.2, $CHCl_3$) for aldol of 84% ee (unassigned); HPLC analysis using a Chiralcel OD column (10% ^{i}PrOH/Hexane, 0.6 mL/min): retention times 26.2 (major), 33.0 (minor) min.

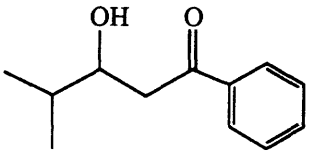

^{1}H NMR (300 MHz, $CDCl_3$) δ 0.99 (d, J=6.7 Hz, 3H, $CH(C\underline{H}_3)_2$), 1.01 (d, J=6.7 Hz, 3H, $CH(C\underline{H}_3)_2$), 1.80 (sept, J=6.7 Hz, 1H, $C\underline{H}(CH_3)_2$), 3.03 (A of ABX, 1H, J_{AB}= 17.1 Hz, J_{AX}= 9.6 Hz, $C\underline{H}_2CO$), 3.17 (B of ABX, 1H, J_{AB}= 17.1 Hz, J_{BX}=

2.4 Hz, C$\underline{H}_2$CO), 3.20 (d, J=4.5 Hz, 1H, O$\underline{H}$), 3.99 (m, 1H, C$\underline{H}$OH), 7.46 (m, 2H, Ar$\underline{H}$), 7.58 (t, J=8.1 Hz, 1H, Ar$\underline{H}$), 7.96 (dd, J=1.2, 8.1 Hz, 2H, Ar$\underline{H}$); ^{13}C NMR (75.4 MHz, $CDCl_3$) δ 17.8, 18.5, 33.1, 42.0, 72.4, 128.1, 128.7, 133.4, 137.0, 201.3; IR (neat) 3478, 2961, 2875, 1681, 1597, 1580, 1470, 1449, 1368, 1281, 1212, 1002 cm^{-1}; MS (EI) *m/e* calc'd for $C_{12}H_{16}O_2$: 192.1150, found 192.1151; 192 (4), 174 (41), 149 (100), 120 (70), 105 (100), 77 (96), 44 (37); $[\alpha]_D^{20}$ -34.7° (c=0.22, $CHCl_3$) for aldol of 63% ee (unassigned); HPLC analysis using a Chiralcel OD column (10% ^{i}PrOH/Hexane, 0.5 mL/min): retention times 13.5 (major), 17.0 (minor) min.

(*S*)-

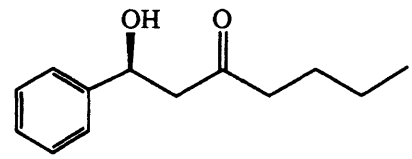

^{1}H NMR (300 MHz, $CDCl_3$) δ 0.85 (t, J=7.0 Hz, 3H, C$\underline{H}_3$), 1.26 (m, 2H, $CH_3C\underline{H}_2$), 1.55 (m, 2H, $CH_3CH_2C\underline{H}_2$), 2.38 (t, J=7.5 Hz, 2H, $CH_2C\underline{H}_2C$(O)), 2.73 (A of ABX, 1H, J_{AB}= 15.0 Hz, J_{AX}= 3.0 Hz, C$\underline{H}_2$CO), 2.82 (B of ABX, 1H, J_{AB}= 15.0 Hz, J_{BX}= 7.2 Hz, C$\underline{H}_2$CO), 3.35 (br s, 1H, O$\underline{H}$), 5.10 (dd, J=4.0, 8.4 Hz, 1H, C$\underline{H}$OH), 7.20–7.32 (m, 5H, Ar$\underline{H}$); IR (neat) 3452, 3062, 2958, 2932, 2872, 1707, 1494, 1454, 1406, 1380, 1201, 1128 cm^{-1}; $[\alpha]_D^{20}$ -52.0° (c=0.76, $CHCl_3$) for (*S*)-aldol[94] of 85% ee; the ee was determined by a chiral shift study (^{1}H NMR) using Eu(hfc)3 in $CDCl_3/CCl_4$.

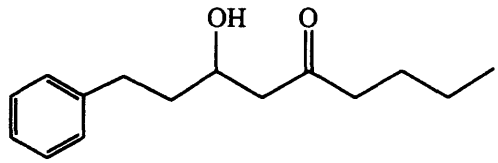

^{1}H NMR (300 MHz, $CDCl_3$) δ 0.89 (t, J=7.2 Hz, 3H, C$\underline{H}_3$), 1.28 (m, 2H, $CH_3C\underline{H}_2$), 1.54 (m, 2H, $CH_3CH_2C\underline{H}_2$), 1.60–1.86 (m, 2H, $PhCH_2C\underline{H}_2$), 2.38 (t, J=7.4 Hz, 2H, $PhC\underline{H}_2$), 2.45–2.85 (m, 4H, $C\underline{H}_2C$(O)$C\underline{H}_2$), 4.03 (m, 1H, C$\underline{H}$OH), 7.13–7.28 (m, 5H, Ar$\underline{H}$); ^{13}C NMR (75.4 MHz, $CDCl_3$) δ 13.9, 22.4, 25.8, 31.9, 38.1, 43.4, 49.0, 66.9, 125.8, 128.3, 128.4, 141.7, 212.2; IR (neat) 3444, 3027, 2957, 2932, 2872, 1704,

1603, 1496, 1455, 1409, 1379, 1100, 1046 cm^{-1}; MS (EI) *m/e* calc'd for $C_{15}H_{22}O_2$: 234.1620, found 234.1620; 234 (6), 216 (38), 117 (22), 91 (42), 85 (100), 57 (31); $[\alpha]_D^{20}$ -8.2° (c=0.87, $CHCl_3$) for aldol of 86% ee (unassigned); HPLC analysis using a Chiralcel OD column (10% ^{i}PrOH/Hexane, 0.5 mL/min): retention times 21.2 (major), 38.3 (minor) min..

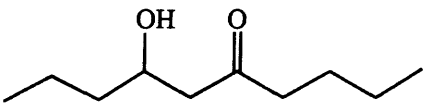

^{1}H NMR (300 MHz, $CDCl_3$) δ 0.88 (t, J=7.5 Hz, 3H, C<u>H</u>$_3$), 0.89 (t, J=7.5 Hz, 3H, C<u>H</u>$_3$), 1.23–1.59 (m, 8H, $CH_3C\underline{H}_2C\underline{H}_2$), 2.41 (t, J=7.5 Hz, 2H, $CH_2C\underline{H}_2C(O)$), 2.47 (A of ABX, 1H, J_{AB}= 15.0 Hz, J_{AX}= 9.0 Hz, C<u>H</u>$_2$CO), 2.58 (B of ABX, 1H, J_{AB}= 15.0 Hz, J_{BX}= 3.6 Hz, C<u>H</u>$_2$CO), 4.03 (m, 1H, C<u>H</u>OH); ^{13}C NMR (75.4 MHz, $CDCl_3$) δ 13.9, 18.8, 22.4, 25.8, 38.6, 43.4, 49.0, 53.0, 67.4, 212.0; IR (neat) 3448, 2958, 2933, 2873, 1707, 1466, 1409, 1379, 1126, 1054 cm^{-1}; MS (EI) *m/e* calc'd for $[M - H]^+$: 171.1385, found 171.1384; 171 (0.1), 154 (4), 129 (14), 97 (28), 85 (68), 58 (70), 44 (100); $[\alpha]_D^{20}$ -31.5° (c=1.0, $CHCl_3$) for aldol of 78% ee (unassigned); diagnostic peaks in the ^{1}H NMR spectrum of the corresponding (*R*)-MTPA ester: (300 MHz, C_6D_6) δ 5.40 (m, C<u>H</u>OC(O), minor), 5.65 (m, C<u>H</u>OC(O), major).

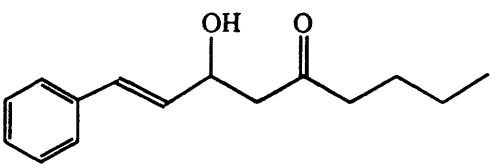

^{1}H NMR (300 MHz, $CDCl_3$) δ 0.93 (t, J=7.5 Hz, 3H, C<u>H</u>$_3$), 1.32 (m, 2H, $CH_3C\underline{H}_2$), 1.58 (m, 2H, $CH_3CH_2C\underline{H}_2$), 2.45 (t, J=7.2 Hz, 2H, $CH_3(CH_2)_2C\underline{H}_2$), 2.72 (m, AB of ABX, 2H, C<u>H</u>$_2$CO), 3.15 (br s, 1H, O<u>H</u>), 4.75 (ddd, J=0.9, 6.0, 12.0 Hz, 1H, C<u>H</u>OH), 6.20 (dd, J=6.1, 15.6 Hz, 1H, PhCH=C<u>H</u>), 6.64 (dd, J=1.1, 15.6 Hz, 1H, PhC<u>H</u>=CH), 7.20–7.39 (m, 5H, Ar<u>H</u>); ^{13}C NMR (75.4 MHz, $CDCl_3$) δ 13.9, 22.4, 25.8, 43.6, 49.0, 68.6, 126.4, 127.6, 128.5, 130.1, 130.2, 136.5, 211.3; IR (neat)

3425, 3026, 2958, 2932, 2872, 1708, 1494, 1449, 1406, 1380, 1127 cm^{-1}; MS (EI) *m/e* calc'd for $C_{15}H_{20}O_2$: 232.1463, found 232.1463; 232 (25), 190 (29), 133 (69), 104 (63), 91 (39), 85 (100), 57 (59); $[\alpha]_D^{20}$ -16.1° (c=1.1, $CHCl_3$) for aldol of 80% ee (unassigned); HPLC analysis using a Chiralcel OD column (10% ^iPrOH/Hexane, 0.5 mL/min): retention times 42.2 (major), 48.9 (minor) min.

(*S*)-

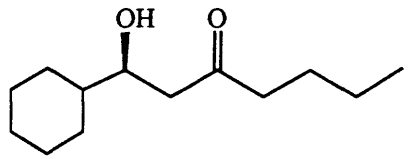

^1H NMR (250 MHz, $CDCl_3$) δ 0.89 (t, J=7.5 Hz, 3H, $C\underline{H}_3$), 0.92–1.88 (m, 15H, cyclohexyl-H and $CH_3C\underline{H}_2C\underline{H}_2$), 2.42 (t, J=7.0 Hz, 2H, $CH_2C\underline{H}_2C(O)$), 2.46 (A of ABX, 1H, J_{AB}= 16.5 Hz, J_{AX}= 9.5 Hz, $C\underline{H}_2CO$), 2.58 (B of ABX, 1H, J_{AB}= 16.5 Hz, J_{BX}= 2.4 Hz, $C\underline{H}_2CO$), 2.98 (br s, 1H, O<u>H</u>), 3.77 (m, 1H, C<u>H</u>OH); IR (neat) 3358, 2917, 2850, 1703, 1445, 1406, 1351 cm^{-1}; $[\alpha]_D^{20}$ -29.2° (c=0.85, $CHCl_3$) for (*S*)-aldol[94] of 75% ee; diagnostic peaks in the ^1H NMR spectrum of the corresponding (*R*)-MTPA ester: (300 MHz, C_6D_6) δ 3.47 (br s, $OC\underline{H}_3$, major), 3.49 (br s, $OC\underline{H}_3$, minor).

6.10 Silyl Ketene Acetals and Silyl Enol Ethers

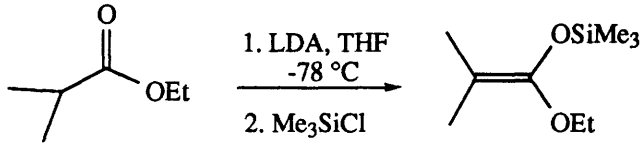

To a solution of diisopropylamine (15.4 mL, 0.110 mol, 1.1 equiv) in THF (100 mL) at 0 °C was slowly added *n*-butyllithium (44.0 mL of a 2.5 M solution in hexane, 0.110 mol, 1.1 equiv) After 15 min, the mixture was cooled to -78 °C and ethyl isobutyrate (13.3 mL, 11.6 g, 0.100 mol, 1 equiv) was added, dropwise, over a period of 15 min. The solution was stirred for 1 h at the same temperature before the gradual addition of trimethylsilyl chloride (14.0 mL, 0.110 mol, 1.1 equiv). The reaction mixture was warmed to room temperature and stirred overnight before concentrating in vacuo, adding hexane (25 mL), and filtering through a layer of Celite to remove precipitated lithium salts. The solution was concentrated with a rotary evaporator to a pale yellow oil. The crude product was distilled through a Vigreux column under reduced pressure to afford, after a short fore-run, the pure ketene acetal[74] as a colorless liquid (15.9 g, 84.4 mmol, 84%): b.p. 61–62 °C/ 16 mm Hg; ^{1}H NMR (300 MHz, $CDCl_3$) δ 0.23 (s, 9H, $Si(C\underline{H}_3)_3$), 1.25 (t, J=7.2 Hz, 3H, $OCH_2C\underline{H}_3$), 1.56 (s, 3H, $C\underline{H}_3C{=}C$), 1.61 (s, 3H, $C\underline{H}_3C{=}C$), 3.80 (q, J=7.2 Hz, 2H, $OC\underline{H}_2CH_3$); d 0.897.

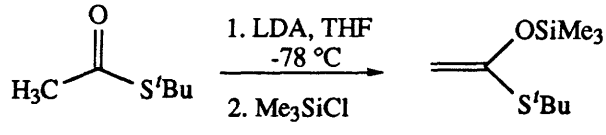

To a solution of diisopropylamine (8.22 mL, 58.7 mmol, 1.5 equiv) in THF (40 mL) at 0 °C was slowly added *n*-butyllithium (24.4 mL of a 2.40 M solution in hexane, 58.7 mmol, 1.5 equiv) After 20 min, the mixture was cooled to -78 °C and *S*-*t*-butyl ethanethioate (5.1719 g, 39.116 mmol, 1 equiv) in THF (10 mL) was added, dropwise, over a period of 15 min. The solution was stirred for 1 h at the same temperature before

the gradual addition of trimethylsilyl chloride (11.9 mL, 93.9 mmol, 2.4 equiv). After an additional hour at -78 °C the reaction mixture was warmed to room temperature and concentrated in vacuo. Pentane (25 mL) was added to the residue, and the mixture was filtered through a layer of Celite to remove precipitated lithium salts (this step may need to be repeated). The solution was concentrated with a rotary evaporator providing a turbid orange oil. This crude product was distilled through a Vigreux column under reduced pressure to afford, after a short fore-run, the pure ketene acetal[36] as a colorless liquid (5.04 g, 24.7 mmol, 63%): b.p. 68–78 °C/ 20 mm Hg; ^{1}H NMR (250 MHz, C_6D_6) δ 0.16 (s, 9H, $Si(C\underline{H}_3)_3$), 1.38 (s, 9H, $SC(C\underline{H}_3)_3$), 4.62 (s, 1H, $C{=}C\underline{H}_2$), 4.85 (s, 1H, $C{=}C\underline{H}_2$); d 0.95.

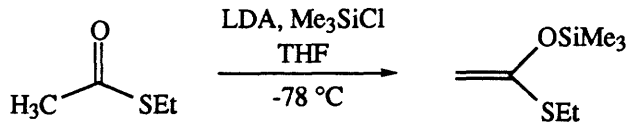

To a solution of diisopropylamine (6.7 mL, 48 mmol, 1.5 equiv) in THF (30 mL) at 0 °C was slowly added *n*-butyllithium (19.2 mL of a 2.5 M solution in hexane, 48 mmol, 1.5 equiv) After 15 min, the mixture was cooled to -78 °C and a precooled (-78 °C) solution of *S*-ethyl ethanethioate (3.3 g, 32 mmol, 1 equiv) and trimethylsilyl chloride (9.6 mL, 76 mmol, 2.4 equiv) in THF (15 mL) was added via cannula over 1 h. The solution was stirred for 30 min at the same temperature and then warmed to room temperature over a 1 h period before concentrating in vacuo, adding pentane (25 mL), and filtering through a layer of Celite to remove precipitated lithium salts. The filtrate was concentrated with a rotary evaporator providing a pale yellow oil. The crude product was distilled through a Vigreux column under reduced pressure to afford, after a short fore-run, the pure ketene acetal[36] as a colorless liquid (4.23 g, 24.0 mmol, 75%): b.p. 35 °C/ 1.2 mm Hg; ^{1}H NMR (250 MHz, $CDCl_3$) δ 0.25 (s, 9H, $Si(C\underline{H}_3)_3$), 1.15 (t, J=7.5 Hz, 3H, $SCH_2C\underline{H}_3$), 2.54 (q, J=7.5 Hz, 2H, $SC\underline{H}_2CH_3$), 4.51 (d, J=2.0 Hz, 1H, $C\underline{H}_2{=}C$), 4.59 (d, J=2.0 Hz, 1H, $C\underline{H}_2{=}C$).

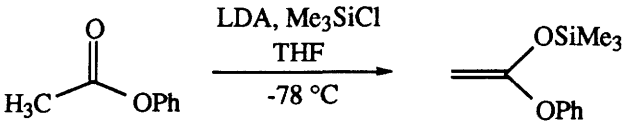

To a solution of diisopropylamine (10.5 mL, 75.0 mmol, 1.5 equiv) in THF (40 mL) at 0 °C was slowly added *n*-butyllithium (31.0 mL of a 2.40 M solution in hexane, 75.0 mmol, 1.5 equiv). After 15 min, the mixture was cooled to -78 °C and a precooled (0 °C) solution of phenyl acetate (6.3 mL, 50 mmol, 1 equiv) and trimethylsilyl chloride (15.2 mL, 120 mmol, 2.4 equiv) in THF (15 mL) was added via cannula over 30 min. The solution was stirred for 1 h at the same temperature and then warmed to room temperature before concentrating in vacuo, adding pentane (25 mL), and filtering through a layer of Celite to remove precipitated lithium salts. The filtrate was concentrated with a rotary evaporator leaving a pale yellow oil. The crude product was distilled through a Vigreux column under reduced pressure to afford, after a short fore-run, the pure ketene acetal as a colorless liquid (6.98 g, 33.5 mmol, 67%): b.p. 35–37 °C/ 0.05 mm Hg (lit.[17c] 50–52 °C/ 0.1 mm Hg); ^{1}H NMR (300 MHz, C_6D_6) δ 0.13 (s, 9H, $Si(C\underline{H}_3)_3$), 3.50 (d, J=3.0 Hz, 1H, $C\underline{H}_2$=C), 3.68 (d, J=3.0 Hz, 1H, $C\underline{H}_2$=C), 6.78-7.08 (m, 5H, Ar<u>H</u>); d 0.89.

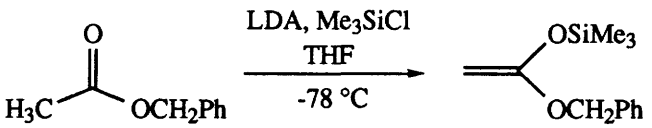

To a solution of diisopropylamine (7.70 mL, 54.9 mmol, 1.1 equiv) in THF (125 mL) at 0 °C was slowly added *n*-butyllithium (34.0 mL of a 1.6 M solution in hexane, 54.4 mmol, 1.1 equiv). After 15 min, the mixture was cooled to -78 °C and a precooled (0 °C) solution of benzyl acetate (7.2 mL, 50 mmol, 1 equiv) and trimethylsilyl chloride (7.0 mL, 55 mmol, 1.1 equiv) in THF (25 mL) was added via cannula over 10 min. The solution was stirred for 1 h at the same temperature and then warmed to room temperature overnight before concentrating in vacuo, adding pentane (25 mL), and filtering through a layer of Celite to remove precipitated lithium salts. The filtrate was concentrated with a rotary

evaporator leaving a pale yellow oil. The crude product was distilled through a Vigreux column under reduced pressure to afford, after a short fore-run, the pure ketene acetal as a colorless liquid (6.50 g, 29.2 mmol, 59%): b.p. 88–89 °C/ 0.3 mm Hg; ^{1}H NMR (250 MHz, $CDCl_3$) δ 0.23 (s, 9H, $Si(C\underline{H}_3)_3$), 3.20 (d, J=3.5 Hz, 1H, $C\underline{H}_2$=C), 3.31 (d, J=3.5 Hz, 1H, $C\underline{H}_2$=C), 4.78 (s, 2H, $OC\underline{H}_2Ph$), 7.26–7.40 (m, 5H, Ar$\underline{H}$).

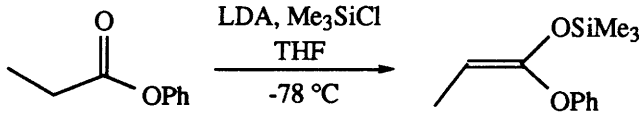

87% *E*(*O*)

To a solution of diisopropylamine (7.10 mL, 50.7 mmol, 1.5 equiv) in THF (27 mL) at 0 °C was slowly added *n*-butyllithium (42.0 mL of a 1.20 M solution in hexane, 50.4 mmol, 1.5 equiv). After 15 min, the mixture was cooled to -78 °C and a precooled (-78 °C) solution of phenyl propionate (4.80 mL, 33.6 mmol, 1 equiv) and trimethylsilyl chloride (10.2 mL, 80.4 mmol, 2.4 equiv) in THF (10 mL) was added via cannula over 30 min. The solution was stirred for 30 min at the same temperature and then warmed to room temperature before it was concentrated in vacuo, diluted with pentane (25 mL), and filtered through a layer of Celite to remove precipitated lithium salts. The filtrate was concentrated with a rotary evaporator leaving a pale yellow oil. The crude product was distilled twice through a Vigreux column under reduced pressure to afford, after a short fore-run, the ketene acetal[44] as an 87:13 mixture of *E*(*O*) and *Z*(*O*) isomers (5.23 g, 23.5 mmol, 70%). *E*(*O*) isomer: b.p. 38–43 °C/ 0.025 mm Hg; ^{1}H NMR (300 MHz, C_6D_6) δ 0.08 (s, 9H, $Si(C\underline{H}_3)_3$), 1.57 (d, J=6.9 Hz, 3H, $C\underline{H}_3CH$), 4.38 (q, J=6.6 Hz, 1H, $CH_3C\underline{H}$), 6.81 (m, 1H, Ar$\underline{H}$), 7.05-7.13 (m, 4H, Ar$\underline{H}$). *Z*(*O*) isomer: 1.61 (d, J=6.9 Hz, 3H, $C\underline{H}_3CH$), 4.18 (q, J=6.6 Hz, 1H, $C\underline{H}_3CH$).

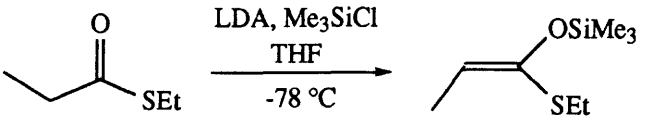

94% *E*(*O*)

To a solution of diisopropylamine (6.7 mL, 48 mmol, 1.5 equiv) in THF (30 mL) at 0 °C was slowly added *n*-butyllithium (30 mL of a 1.6 M solution in hexane, 48 mmol, 1.5 equiv). After 15 min, the mixture was cooled to -78 °C and a precooled (-78 °C) solution of *S*-ethyl propanethioate (3.8 mL, 32 mmol, 1 equiv) and trimethylsilyl chloride (9.6 mL, 76 mmol, 2.4 equiv) in THF (15 mL) was added via cannula over 30 min. The solution was stirred for 1 h at the same temperature and then warmed to room temperature before it was concentrated in vacuo, diluted with pentane (25 mL), and filtered through a layer of Celite to remove precipitated lithium salts. The filtrate was concentrated with a rotary evaporator and the residue was vacuum distilled through a Vigreux column to afford, after a short fore-run, the ketene acetal[36] as an 94:6 mixture of *E*(*O*) and *Z*(*O*) isomers (3.96 g, 20.8 mmol, 65%). *E*(*O*) isomer: b.p. 44–46 °C/ 1.5 mm Hg ; ^{1}H NMR (250 MHz, C_6D_6) δ 0.18 (s, 9H, $Si(C\underline{H}_3)_3$), 1.13 (t, J=7.3 Hz, 3H, $SCH_2C\underline{H}_3$), 1.77 (d, J=6.5 Hz, 3H, $C\underline{H}_3CH$), 2.58 (q, J=7.3 Hz, 2H, $SC\underline{H}_2CH_3$), 5.10 (q, J=6.5 Hz, 1H, $CH_3C\underline{H}$).

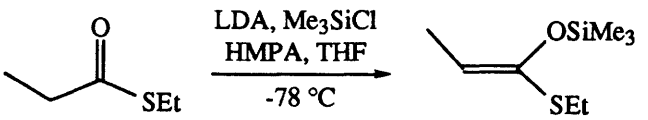

89% *Z*(*O*)

To a solution of diisopropylamine (5.12 mL, 36.6 mmol, 1.3 equiv) in THF (67 mL) at 0 °C was slowly added *n*-butyllithium (14 mL of a 2.4 M solution in hexane, 34 mmol, 1.3 equiv). After 10 min, the mixture was cooled to -78 °C and a solution of HMPA in THF (23% by volume, 15 mL) was added. A precooled (-78 °C) solution of *S*-ethyl propanethioate (3.2 mL, 26 mmol, 1 equiv), triethylamine (1.3 mL, 9.3 mmol, 0.4 equiv), and trimethylsilyl chloride (6.0 mL, 47 mmol, 1.8 equiv) was then slowly added

via cannula over 1 h. The solution was stirred for 30 min at -78 °C and warmed to room temperature before it was diluted with cold (-30 °C) pentane (100 mL) and washed with ice-cold saturated aqueous $NaHCO_3$ (50 mL) and water (100 mL). The layers were separated, and the pentane layer was dried ($MgSO_4$) and concentrated with a rotary evaporator. The oil thus obtained was vacuum distilled through a Vigreux column to afford, after a short fore-run, the ketene acetal[36] as an 11:89 mixture of *E*(*O*) and *Z*(*O*) isomers (3.6 g, 19 mmol, 73%). *Z*(*O*) isomer: b.p. 54–56 °C/ 1.5 mm Hg ; ^1H NMR (250 MHz, C_6D_6) δ 0.23 (s, 9H, $Si(C\underline{H}_3)_3$), 1.12 (t, J=7.3 Hz, 3H, $SCH_2C\underline{H}_3$), 1.56 (d, J=6.5 Hz, 3H, $C\underline{H}_3CH$), 2.49 (q, J=7.3 Hz, 2H, $SC\underline{H}_2CH_3$), 5.15 (q, J=6.5 Hz, 1H, $CH_3C\underline{H}$).

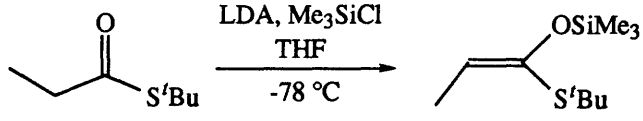

>98% *E*(*O*)

To a solution of diisopropylamine (6.7 mL, 48 mmol, 1.5 equiv) in THF (30 mL) at 0 °C was slowly added *n*-butyllithium (30 mL of a 1.6 M solution in hexane, 48 mmol, 1.5 equiv). After 15 min, the mixture was cooled to -78 °C and a precooled (-78 °C) solution of *S*-*t*-butyl propanethioate (4.7 mL, 32 mmol, 1 equiv) and trimethylsilyl chloride (9.6 mL, 76 mmol, 2.4 equiv) in THF (15 mL) was added via cannula over 30 min. The solution was stirred for 1 h at the same temperature and then warmed to room temperature before it was concentrated in vacuo, diluted with pentane (25 mL), and filtered through a layer of Celite to remove precipitated lithium salts. The filtrate was concentrated with a rotary evaporator and the crude product was distilled under reduced pressure through a Vigreux column to afford, after a short fore-run, the purified *E*(*O*) ketene acetal[115] with only a trace of the *Z*(*O*) isomer (4.82 g, 22.1 mmol, 69%). *E*(*O*) isomer: b.p. 60 °C/ 1.5 mm Hg; ^1H NMR (300 MHz, $CDCl_3$) δ 0.26 (s, 9H, $Si(C\underline{H}_3)_3$), 1.44 (s, 9H, $SC(C\underline{H}_3)_3$), 1.84 (d, J=7.3 Hz, 3H, $C\underline{H}_3CH$), 5.38 (q, J=7.3 Hz, 1H, $CH_3C\underline{H}$).

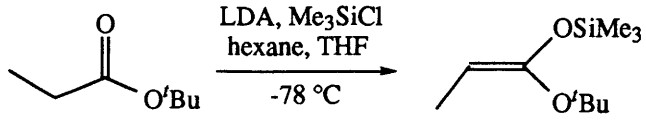

91% *E*(*O*)

To a solution of diisopropylamine (3.5 mL, 25 mmol, 1.5 equiv) in THF (70 mL) at 0 °C was slowly added *n*-butyllithium (10.4 mL of a 2.4 M solution in hexane, 25 mmol, 1.5 equiv). After 20 min, the mixture was cooled to -78 °C and diluted with hexane (40 mL). A precooled (-78 °C) solution of *t*-butyl propionate (2.4 mL, 16 mmol, 1 equiv) and trimethylsilyl chloride (17.6 mL of a 2.0 M solution in hexane, 35.2 mmol, 2.2 equiv) in hexane (20 mL) was then added over a 3 h period. The solution was stirred for 20 min at -78 °C and warmed to room temperature before it was concentrated in vacuo, diluted with cold pentane (60 mL), and filtered through a layer of Celite to remove precipitated lithium salts (the filtration may need to be repeated). The filtrate was concentrated in vacuo and the crude product thus obtained was fractionally distilled through a Vigreux column to afford, after a short fore-run, the ketene acetal as a 10:1 mixture of *E*(*O*) and *Z*(*O*) isomers (1.36 g, 6.72 mmol, 42%). *E*(*O*) isomer: b.p. 37–39 °C/ 1.6 mm Hg; ^{1}H NMR (250 MHz, C_6D_6) δ 0.18 (s, 9H, Si($C\underline{H}_3$)$_3$), 1.33 (s, 9H, OC($C\underline{H}_3$)$_3$), 1.65 (d, J=7.3 Hz, 3H, $C\underline{H}_3$CH), 4.04 (q, J=7.3 Hz, 1H, $CH_3C\underline{H}$); d 0.842.

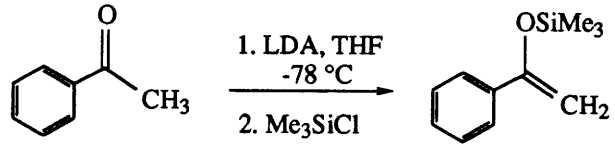

The silyl enol ether was prepared by a modification of the literature procedure.[24] To a solution of diisopropylamine (7.7 mL, 55 mmol, 1.1 equiv) in THF (100 mL) at 0 °C was slowly added *n*-butyllithium (22 mL of a 2.5 M solution in hexane, 55 mol, 1.1 equiv) After 15 min, the mixture was cooled to -78 °C and acetophenone (6.01 g, 5.83 mL, 50 mmol, 1 equiv) was added, dropwise, over a period of 15 min. The solution was stirred for 1 h at the same temperature before the gradual addition of trimethylsilyl chloride (6.98

mL, 55.0 mmol, 1.1 equiv). The reaction mixture was warmed to room temperature and stirred for 2 h before it was concentrated in vacuo, diluted with hexane (25 mL), and filtered through a layer of Celite to remove precipitated lithium salts. The solution was concentrated with a rotary evaporator to a pale yellow oil. The crude product was distilled through a Vigreux column under reduced pressure to afford, after a short fore-run, the pure ketene acetal as a colorless liquid (8.76 g, 45.5 mmol, 91%): b.p. 83–84 °C/ 4.0 mm Hg; ^{1}H NMR (300 MHz, C_6D_6) δ 0.13 (s, 9H, Si($C\underline{H}_3$)$_3$), 4.41 (d, J=1.7 Hz, 1H, C=$C\underline{H}_2$), 4.87 (d, J=1.7 Hz, 1H, C=$C\underline{H}_2$), 7.01–7.14 (m, 3H, Ar$\underline{H}$), 7.62 (dd, J=7.5, 1.2 Hz, 2H, Ar$\underline{H}$); d 0.948.

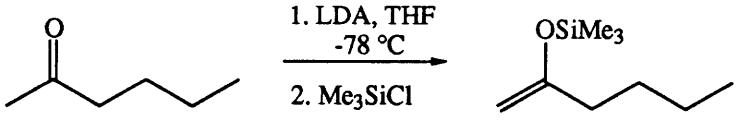

To a solution of diisopropylamine (7.0 mL, 50 mmol, 1 equiv) in THF (100 mL) at 0 °C was slowly added *n*-butyllithium (18.0 mL of a 2.75 M solution in hexane, 49.5 mmol, 1 equiv) After 15 min, the mixture was cooled to -78 °C and 2-hexanone (6.0 mL, 49 mmol, 1 equiv) was added, dropwise, over a period of 15 min. The solution was stirred for 1 h at the same temperature before the gradual addition of trimethylsilyl chloride (7.5 mL, 59 mmol, 1.2 equiv). The reaction mixture was warmed to room temperature before it was concentrated in vacuo, diluted with pentane (25 mL), and filtered through a layer of Celite to remove precipitated lithium salts. The solution was concentrated with a rotary evaporator to a yellow oil. The crude product was distilled through a Vigreux column under reduced pressure to afford, after a short fore-run, the pure silyl enol ether[43] (6.76 g, 39.2 mmol, 80%): b.p. 45–60 °C/ 20 mm Hg; ^{1}H NMR (300 MHz, C_6D_6) δ 0.18 (s, 9H, Si($C\underline{H}_3$)$_3$), 0.86 (t, J=7.3 Hz, 3H, $C\underline{H}_3$), 1.28 (m, 2H, $CH_3C\underline{H}_2$), 1.50 (m, 2H, $CH_3CH_2C\underline{H}_2$), 2.07 (t, J=7.6 Hz, 2H, $CH_3(CH_2)_2C\underline{H}_2$), 4.13 (br s, 1H, $C\underline{H}_2$=C), 4.18 (br s, 1H, $C\underline{H}_2$=C); d 0.79.

6.11 Miscellaneous Compounds (Chapter Five)

Yields and enantiomeric excesses for aldol reactions are given in the text. Racemic samples were used as standards for all ee determinations on optically active material.

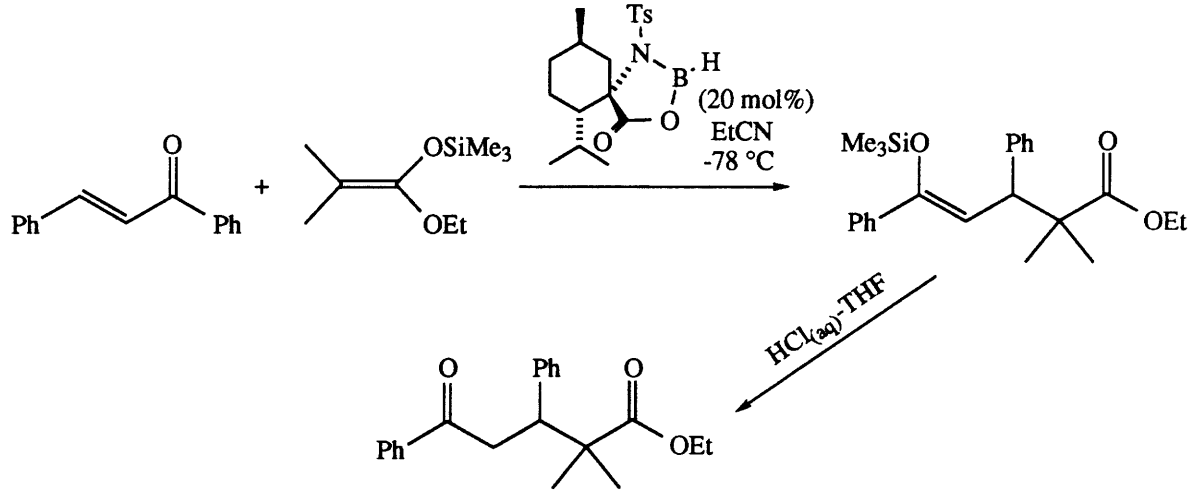

The *N*-tosyl ligand derived from menthone (35.6 mg, 0.101 mmol, 0.2 equiv) in propionitrile (1.5 mL) was treated with BH_3·THF complex (100 μL of a 1 M solution in THF, 0.1 mmol, 0.2 equiv). The solution was warmed to 45 °C for 1 h and cooled to -78 °C before the addition of the ketene acetal (126 μL, 0.6 mmol, 1.2 equiv). Chalcone (104.5 mg, 0.5018 mmol, 1.0 equiv) was then added as a solution in propionitrile (1 mL) over 3.5 h (syringe pump) and the reaction mixture was stirred overnight at the same temperature before being poured into pH 7 buffer. The aqueous layer was extracted with ether, and the combined organic layers were dried ($MgSO_4$) and concentrated in vacuo, affording predominantly the silyl enol ether derivative of the Michael product. Desilylation was effected by stirring with 1:1 aqueous 1 M HCl/THF (4 mL) for 1 h. Following extraction with ether, drying ($MgSO_4$), and concentration in vacuo, the residue was purified by flash chromatography (5–15% ethyl acetate in hexane) giving the keto ester as a white solid (87.4 mg, 0.269 mmol, 54%): m.p. 82–84°; ^{1}H NMR (300 MHz, $CDCl_3$) δ 1.09 (s, 3H, $C\underline{H}_3$), 1.16 (s, 3H, $C\underline{H}_3$), 1.18 (t, J=6.9 Hz, 3H, $OCH_2C\underline{H}_3$), 3.21 (X of ABX, 1H, J_{AX}= 16.8 Hz, J_{BX}= 3.3 Hz, PhC$\underline{H}$), 3.57 (A of ABX, 1H, J_{AX}= 16.8 Hz,

J_{AB}= 10.5 Hz, PhC(O)C$\underline{H}_2$), 3.75 (B of ABX, 1H, J_{BX}= 3.3 Hz, J_{AB}= 10.5 Hz, PhC(O)C$\underline{H}_2$), 4.08 (q, J=6.9 Hz, 2H, OC$\underline{H}_2$CH$_3$), 7.12–7.22 (m, 5H, Ar$\underline{H}$), 7.37 (t, J=7.7 Hz, 2H, Ar$\underline{H}$), 7.48 (t of m, J=7.7 Hz, 1H, Ar$\underline{H}$), 7.83 (dd, J=8.7 Hz, 1.2H, Ar$\underline{H}$); ^{13}C NMR (75.4 MHz, $CDCl_3$) δ 14.2, 21.6, 24.9, 40.1, 46.1, 48.0, 60.6, 126.8, 127.9, 128.0, 128.5, 129.5, 132.9, 137.2, 140.1, 177.3, 198.3; IR (neat) 2988, 1720, 1686, 1597, 1448, 1365, 1298, 1126, 1026 cm^{-1}; MS (EI) *m/e* calc'd for $C_{21}H_{24}O_3$: 324.1725, found 324.1722; 324 (6), 209 (100), 105 (100); HPLC analysis using a Chiralcel OD column (7% ^{i}PrOH/Hexane, 0.3 mL/min): retention times 20.8, 22.1 min.

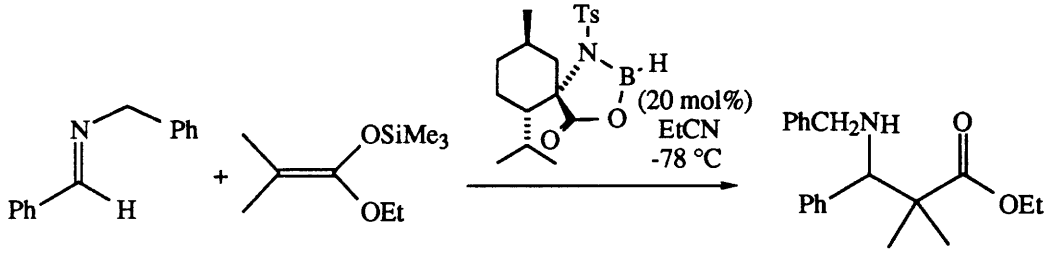

The *N*-tosyl ligand derived from menthone (36.1 mg, 0.102 mmol, 0.2 equiv) in propionitrile (1.5 mL) was treated with BH_3·THF complex (100 μL of a 1 M solution in THF, 0.1 mmol, 0.2 equiv). The solution was warmed to 45 °C for 1 h and cooled to -78 °C before the addition of the ketene acetal (126 μl, 0.6 mmol, 1.2 equiv). *N*-benzylidenebenzylamine (93.0 μL, 0.500 mmol, 1.0 equiv) was then added as a solution in propionitrile (1 mL) over 3.5 h (syringe pump) and the reaction mixture was stirred overnight at -78 °C before being poured into pH 7 buffer. The aqueous layer was extracted with ether, and the combined organic layers were dried ($MgSO_4$) and concentrated in vacuo. The residue was purified by flash chromatography (5–10% ethyl acetate in hexane) affording the amino ester as a white solid (38.6 mg, 0.124 mmol, 25%). The balance was unreacted starting materials: ^{1}H NMR (250 MHz, $CDCl_3$) δ 1.01 (s, 3H, 2-C$\underline{H}_3$), 1.09 (s, 3H, 2-C$\underline{H}_3$), 1.18 (t, J=7.5 Hz, 3H, OCH$_2$C$\underline{H}_3$), 1.73 (br s, 1H, N$\underline{H}$), 3.51 (AB q, 2H, J_{AB}= 13.8 Hz, Δν= 56.7 Hz, PhC$\underline{H}_2$), 3.89 (s, 1H, PhC$\underline{H}$), 4.08 (m, 2H, OC$\underline{H}_2$CH$_3$), 7.16–7.37 (m, 10H, Ar$\underline{H}$); ^{13}C NMR (75.4 MHz, $CDCl_3$) δ 13.7, 18.9, 23.7, 46.8, 51.1,

60.0, 67.4, 126.3, 126.8, 127.3, 127.7, 128.6, 138.7, 140.1, 176.7; IR (neat) 2978, 2930, 1724, 1454, 1386, 1249, 1131, 1028 cm^{-1}; MS (EI) *m/e* calc'd for [M - OCH_2CH_3]$^+$: 266.1545, found 266.1543; 266 (6), 196 (100), 91 (100); chiral shift study (^1H NMR) using Eu(hfc)$_3$ in $CDCl_3/CCl_4$ indicated 0% ee.

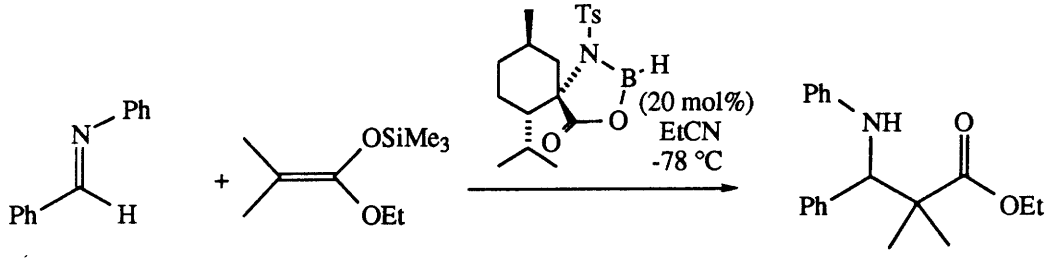

The *N*-tosyl ligand derived from menthone (35.6 mg, 0.101 mmol, 0.2 equiv) in propionitrile (1.5 mL) was treated with BH_3·THF complex (100 μL of a 1 M solution in THF, 0.1 mmol, 0.2 equiv). The solution was warmed to 45 °C for 1 h and cooled to -78 °C before the addition of the ketene acetal (126 μL, 0.6 mmol, 1.2 equiv). *N*-benzylideneaniline (91.4 mg, 0.504 mmol, 1.0 equiv) was then added as a solution in propionitrile (1 mL) over 3.5 h (syringe pump) and the reaction mixture was stirred overnight at -78 °C before being poured into pH 7 buffer. The aqueous layer was extracted with ether, and the combined organic layers were dried ($MgSO_4$) and concentrated in vacuo. The residue was purified by flash chromatography (5–10% ethyl acetate in hexane) affording the amino ester as a white solid (133.3 mg, 0.4482 mmol, 90%): m.p. 115–117 °C; ^1H NMR (300 MHz, $CDCl_3$) δ 1.11 (s, 3H, 2-C$\underline{H}_3$), 1.13 (t, J=7.2 Hz, 3H, $OCH_2C\underline{H}_3$), 1.23 (s, 3H, 2-C$\underline{H}_3$), 4.08 (q of d, J=7.2, 1.5 Hz, 2H, $OC\underline{H}_2CH_3$), 4.46 (s, 1H, PhC$\underline{H}$), 4.78 (br s, 1H, N$\underline{H}$), 6.46 (d, J=7.2 Hz, 2H, Ar$\underline{H}$), 6.56 (t, J=7.2 Hz, 1H, Ar$\underline{H}$), 7.01 (t, J=7.2 Hz, 2H, Ar$\underline{H}$), 7.15–7.34 (m, 5H, Ar$\underline{H}$); ^{13}C NMR (75.4 MHz, $CDCl_3$) δ 13.6, 20.1, 24.1, 46.4, 60.4, 63.9, 112.8, 116.7, 126.9, 127.4, 127.9, 128.5, 138.8, 146.5, 176.0; IR (neat) 3406, 2979, 1718, 1602, 1506, 1317, 1249, 1135, 1026 cm^{-1}; MS (EI) *m/e* calc'd for $C_{19}H_{23}NO_2$: 297.1729, found 297.1730; 297 (23), 182 (100), 104 (13); chiral shift study (^1H NMR) using Eu(hfc)$_3$ in $CDCl_3/CCl_4$ indicated 0%

ee.

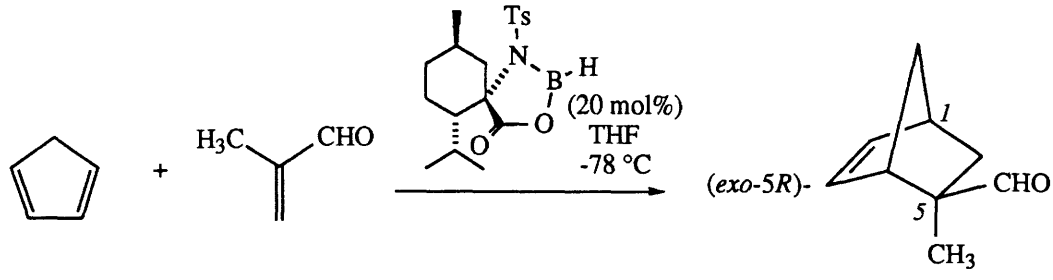

The *N*-tosyl ligand derived from menthone (35.3 mg, 0.100 mmol, 0.2 equiv) in THF (1.5 mL) was treated with BH_3·THF complex (100 μL of a 1 M solution in THF, 0.1 mmol, 0.2 equiv). The solution was warmed to 45 °C for 1 h and cooled to -78 °C before the dropwise addition of methacrolein (130 μL, 1.55 mmol, 3 equiv) and freshly cracked cyclopentadiene (42 μL, 0.51 mmol, 1 equiv). The reaction mixture was stirred for 3 h at -78 °C before being poured into ice-water. The solution was shaken with ether, and the combined organic layers were dried ($MgSO_4$) and concentrated in vacuo (Note: The neat adduct is volatile and can tolerate only brief exposure to heat or high vacuum). Purification was accomplished by flash chromatography (3% ether in pentane) affording the adduct[105,116] (*exo/endo*= 99/1 by ^1H NMR) as an oily colorless solid (57.6 mg, 0.423 mmol, 83%): ^1H NMR (300 MHz, $CDCl_3$) δ 0.74 (d, J=12.0 Hz, 1H, 6-*endo*-H), 0.99 (s, 3H, CH_3), 1.37 (d, J=1.5 Hz, 2H, methano-CH_2), 2.23 (dd, J=12.2, 4.2 Hz, 1H, 6-*exo*-H), 2.80 (br s, 1H, C(4)-H), 2.87 (br s, 1H, C(1)-H), 6.09 (dd, J=3.0, 5.7 Hz, 1H, C=CH), 6.28 (dd, J=3.0, 6.0 Hz, 1H, C=CH), 9.67 (s, 1H, CHO); $[\alpha]_D^{20}$ -14.3° (c=2.6, EtOH) for 99% *exo* isomer of 76% ee {lit.[116] $[\alpha]_D^{20}$ -15.3° (EtOH) for (5*R*)-isomer}.

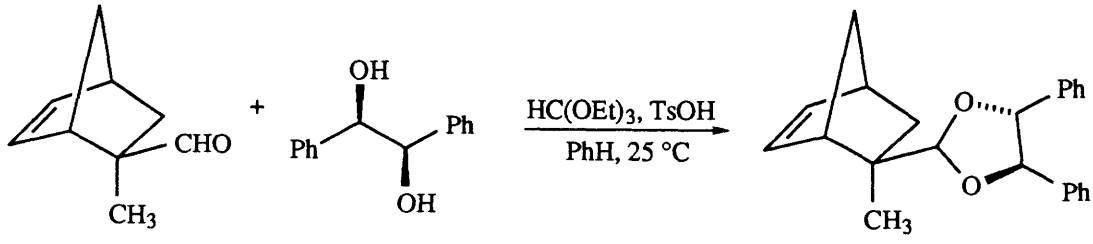

Determination of ee: a solution of the Diels–Alder adduct (11.1 mg, 0.0815 mmol,

1 equiv), (*R*,*R*)-stilbene diol[119] (1,2-diphenyl-1,2-ethanediol) (26.2 mg, 0.122 mmol, 1.5 equiv), triethylorthoformate (15 μL, 0.090 mmol, 1.1 equiv), and tosic acid monohydrate (spatula-tip) in benzene (1 mL) was stirred at room temperature overnight at which point TLC analysis indicated the complete conversion of the adduct to a new product. The reaction mixture was diluted with ether and shaken with saturated aqueous $NaHCO_3$ and water. The accumulated aqueous phases were back-extracted into ether, and the combined ethereal solutions were washed with brine, dried ($MgSO_4$) and concentrated in vacuo to give the crude acetal (54.1 mg, >100%); diagnostic peaks in the ^1H NMR spectrum of the acetal derived from the *exo* Diels-Alder adduct and (*R*, *R*)-stilbene diol: (300 MHz, $CDCl_3$) δ 0.85 (m, 1H, methano-C<u>H</u>), 1.01 (s, 3H, C<u>H</u>$_3$), 1.32 (m, 1H, 6-*endo*-H), 1.72 (br t, J=9.4 Hz, 1H, 6-*exo*-H), 1.88 (t of d, J=3.0, 9.4 Hz, 1H, methano-C<u>H</u>), 2.78 (m, 2H, C(1)-<u>H</u>, C(4)-<u>H</u>), 4.65 (m, 2H, PhC<u>H</u>), 5.38 (s, 1H, C<u>H</u>(OR)$_2$, (5*R*)-adduct), 5.40 (s, 1H, C<u>H</u>(OR)$_2$, (5*S*)-adduct), 6.12 (m, 2H, alkene-<u>H</u>), 7.12–7.27 (m, 10H, Ar<u>H</u>).

References and Notes

(1) (a) Kane, R. *Ann. Physik. Chem.* **1838**, [2] *44*, 475. (b) Kane, R. *J. Prakt. Chem.* **1838**, *15*, 129.

(2) For reviews of the aldol reaction, see: (a) Mukaiyama, T. *Org. React.* **1982**, *28*, 203. (b) Heathcock, C. H. In *Asymmetric Synthesis*; Morrison, J. D., Ed.; Academic Press: New York, 1984; Vol. 3, Chapter 2.

(3) Masamune, S.; Choy, W.; Kerdesky, F. A. J.; Imperiali, B. *J. Am. Chem. Soc.* **1981**, *103*, 1566.

(4) Evans, D. A.; Bartroli, J.; Shih, T.L. *J. Am. Chem. Soc.* **1981**, *103*, 2127.

(5) Bonner, M. P.; Thornton, E. R. *J. Am. Chem. Soc.* **1991**, *113*, 1299.

(6) Oppolzer, W.; Blagg, J.; Rodriguez, I.; Walther, E. *J. Am. Chem. Soc.* **1990**, *112*, 2767.

(7) Masamune, S.; Sato, T.; Kim, B. M.; Wollmann, T. A. *J. Am. Chem. Soc.* **1986**, *108*, 8279.

(8) Paterson, I.; McClure, C. K. *Tetrahedron Lett.* **1987**, *28*, 1229.

(9) Corey, E. J.; Kim, S. S. *J. Am. Chem. Soc.* **1990**, *112*, 4976.

(10) Duthaler, R. O.; Herold, P.; Lottenbach, W.; Oertle, K.; Riediker, M. *Angew. Chem. Int. Ed. Engl.* **1989**, *28*, 495.

(11) Kim, B. M.; Williams, S. F.; Masamune, S. In *Comprehensive Organic Synthesis, Selectivity, Strategy & Efficiency in Modern Organic Chemistry*; Trost, B. M., Fleming, I., Heathcock, C. H., Eds.; Pergamon: Oxford, 1991; Vol. 2, Chapter 1.7.

(12) Masamune, S. *Pure & Appl. Chem.* **1988**, *60*, 1587.

(13) (a) Mukaiyama, T.; Narasaka, K.; Banno, K. *Chem Lett.* **1973**, 1011. (b) Mukaiyama, T.; Banno, K.; Narasaka, K. *J. Am. Chem. Soc.* **1974**, *96*, 7503.

(14) Recently, several reports have appeared concerning silyl enol ethers and ketene acetals that react with aldehydes in the absence of a Lewis acid: (a) Myers, A. G.; Kephart, S. E.; Chen, H. *J. Am. Chem. Soc.* **1992**, *114*, 7922 and references therein. (b) Denmark, S. E.; Griedel, B. D.; Coe, D. M. *J. Org. Chem.* **1993**, *58*, 988. (c) Kobayashi, S.; Nishio, K. *J. Org. Chem.* **1993**, *58*, 2647.

(15) Saigo, K.; Osaki, M.; Mukaiyama, T. *Chem. Lett.* **1975**, 989.

(16) For example, (a) Mazza, S. M.; Lal, K.; Salomon, R. G. *J. Org. Chem.* **1988**, *53*, 3681. (b) Gennari, C.; Cozzi, P. G. *J. Org. Chem.* **1988**, *53*, 4015. (c) Smith, A. B. III; Lupo, Jr., A. T.; Ohba, M.; Chen, K. *J. Am. Chem. Soc.* **1989**, *111*, 6648. (d) Evans, D. A.; Gage, J. R.; Leighton, J. L. *J. Am. Chem. Soc.* **1992**, *114*, 9434.

(17) (a) Slougui, N.; Rousseau, G. *Synth. Commun.* **1987**, *17(1)*, 1. (b) Ireland, R. E.; Wipf, P.; Armstrong , III, J. D. *J. Org. Chem.* **1991**, *56*, 650. (c) Colvin, E. W. *Silicon Reagents in Organic Synthesis*; Academic Press: London, 1988; Chapter 15.

(18) Ojima, I.; Kogure, T. *Organometallics* **1982**, *1*, 1390.

(19) Corey, E. J.; Gross, A. W. *Tetrahedron Lett.* **1984**, *25*, 495.

(20) For a review of aldol reactions using silyl enolates, see: Gennari, C. In *Comprehensive Organic Synthesis, Selectivity, Strategy & Efficiency in Modern Organic Chemistry*; Trost, B. M., Fleming, I., Heathcock, C. H., Eds.; Pergamon: Oxford, 1991; Vol. 2, Chapter 2.4 and references therein.

(21) (a) Denmark, S. E.; Almstead, N. G. *J. Am. Chem. Soc.* **1993**, *115*, 3133 and references therein. (b) Childs, R. F.; Mulholland, D. L.; Nixon, A. *Can. J. Chem.* **1982**, *60*, 801.

(22) Kuwajima, I.; Nakamura, E. *Acc. Chem. Res.* **1985**, *18*, 181.

(23) Masamune, S.; Kaiho, T.; Garvey, D. S. *J. Am. Chem. Soc.* **1982**, *104*, 5521.

(24) Heathcock, C. H.; Davidsen, S. K.; Hug, Kathleen T.; Flippin, L. A. *J. Org. Chem.* **1986**, *51*, 3027.

(25) Kuwajima, I.; Nakamura, E.; Hashimoto, K. *Org. Synth.* **1983**, *61*, 122.

(26) Mukaiyama, T.; Kobayashi, S.; Murakami, M. *Chem. Lett.* **1985**, 447.

(27) Hong, Y.; Norris, D. J.; Collins, S. *J. Org. Chem.* **1993**, *58*, 3591.

(28) Kobayashi, S.; Hachiya, I. *Tetrahedron Lett.* **1992**, *33*, 1625.

(29) Wada, M.; Takeichi, E.; Matsumoto, T. *Bull. Chem. Soc. Jpn.* **1991**, *64*, 990.

(30) Kawai, M.; Onaka, M.; Izumi, Y. *Chem. Lett.* **1986**, 1581.

(31) Murata, S.; Suzuki, M.; Noyori, R. *Tetrahedron* **1988**, *44*, 4259 and references therein.

(32) (a) Noyori, R.; Yokoyama, K.; Sakata, J.; Kuwajima, I.; Nakamura, E.; Shimizu, M. *J. Am. Chem. Soc.* **1977**, *109*, 1265. (b) Noyori, R.; Nishida, I.; Sakata, J. *J. Am. Chem. Soc.* **1981**, *103*, 2106.

(33) (a) Gennari, C.; Bernardi, A.; Colombo, L.; Scolastico, C. *J. Am. Chem. Soc.* **1985**, *107*, 5812. (b) Gennari, C.; Colombo, L.; Bertolini, G.; Schimperna, G. *J. Org. Chem.* **1987**, *52*, 2754.

(34) Helmchen, G.; Leikauf, U.; Taufer-Knöpfel, I. *Angew. Chem. Int. Ed. Engl.* **1985**, *24*, 874.

(35) Oppolzer, W.; Marco-Contelles, J. *Helv. Chim. Acta* **1986**, *69*, 1699.

(36) (a) Kobayashi, S.; Uchiro, H.; Fujishita, Y.; Shiina, I.; Mukaiyama, T. *J Am. Chem. Soc.* **1991**, *113*, 4247. (b) Kobayashi, S.; Mukaiyama, T. *Chem. Lett.* **1989**, 297. (c) Mukaiyama, T.; Uchiro, H.; Kobayashi, S. *Chem. Lett.* **1989**, 1001. (d) Mukaiyama, T.; Kobayashi, S.; Uchiro, H.; Shiina, I. *Chem. Lett.* **1990**, 129. (e)

Mukaiyama, T.; Kobayashi, S.; Sano, T. *Tetrahedron* **1990**, *46*, 4653. (f) Kobayashi, S.; Ohtsubo, A.; Mukaiyama, T. *Chem. Lett.* **1991**, 831.

(37) Braun, M. *Angew. Chem. Int. Ed. Engl.* **1987**, *26*, 24.

(38) (a) Kobayashi, S.; Fujishita, Y.; Mukaiyama, T. *Chem. Lett.* **1990**, 1455. (b) Kobayashi, S.; Furuya, M.; Ohtsubo, A.; Mukaiyama, T. *Tetrahedron: Asymmetry* **1991**, *2*, 635. (c) Kobayashi, S.; Uchiro, H.; Shiina, I.; Mukaiyama, T. *Tetrahedron* **1993**, *49*, 1761.

(39) Mukaiyama, T.; Inubushi, A.; Suda, S.; Hara, R.; Kobayashi, S. *Chem. Lett.* **1990**, 1015.

(40) Mukaiyama, T.; Takashima, T.; Kusaka, H.; Shimpuku, T. *Chem. Lett.* **1990**, 1777.

(41) Cotton, F. A.; Wilkinson, G. *Advanced Inorganic Chemistry*, 5th ed.; Wiley: New York, 1988; p 656.

(42) Reetz, M. T.; Kyung, S.-H.; Bolm, C.; Zierke, T. *Chem. Ind. (London)* **1986**, 824.

(43) Furuta, K.; Maruyama, T.; Yamamoto, H. *J. Am. Chem. Soc.* **1991**, *113*, 1041.

(44) Furuta, K.; Maruyama, T.; Yamamoto, H. *Synlett* **1991**, 439.

(45) Reetz, M. T.; Kunisch, F.; Heitmann, P. *Tetrahedron Lett.* **1986**, *27*, 4721.

(46) Reetz, M. T.; Vougioukas, A. E. *Tetrahedron Lett.* **1987**, *28*, 793.

(47) Ando, A.; Miura, T.; Tatematsu, T.; Shioiri, T. *Tetrahedron Lett.* **1993**, *34*, 1507.

(48) For conceptually different catalytic aldol reactions, see: (a) Ito, Y.; Sawamura, M.; Hayashi, T. *J. Am. Chem. Soc.* **1986**, *108*, 6405. (b) Ito, Y.; Sawamura, M.; Shirakawa, E.; Hayashizaki, K.; Hayashi, T. *Tetrahedron Lett.* **1988**, *29*, 235. (c) Slough, G. A.; Bergman, R. G.; Heathcock, C. H. *J. Am. Chem. Soc.* **1989**, *111*, 938. (d) Sasai, H.; Suzuki, T.; Arai, S.; Arai, T.; Shibasaki, M. *J. Am. Chem. Soc.* **1992**,

114, 4418. (e) Sasai, H.; Suzuki, T.; Itoh, N.; Tanaka, K.; Date, T.; Okamura, K.; Shibasaki, M. *J. Am. Chem. Soc.* **1993**, *115*, 10372.

(49) Dr. Kou Hiroya, Dr. John C. Roberts, Mr. Hiroaki Suga, and the author performed the work described in Section 2.1.

(50) (a) Bloodworth, A. J.; Davies, A. G. In *Organotin Compounds*; Sawyer, A. K., Ed.; Marcel Dekker: New York, 1971; Vol. 1, Chapter 4. (b) Yoshino, N.; Akutsu, H. *Nippon Kagaku Kaishi* **1978**, 742.

(51) (a) Chandler, C. D.; Fallon, G. D.; Koplick, A. J.; West, B. O. *Aust. J. Chem.* **1987**, *40*, 1427. (b) Thomas, I. M. U. S. Patent 3 946 056, 1976.

(52) Bradley, D. C.; Caldwell, E. V.; Wardlaw, W. *J. Chem. Soc.* **1957**, 4775.

(53) Sawyer, A. K.; Frey, C. *Synth. React. Inorg. Met.-Org. Chem.* **1983**, *13(2)*, 259.

(54) Piekos, R.; Radecki, A. *Roczniki Chem.* **1965**, *39(5)*, 765.

(55) Takasu, M.; Yamamoto, H. *Synlett* **1990**, 194.

(56) Sartor, D.; Saffrich, J.; Helmchen, G. *Synlett* **1990**, 197.

(57) (a) Carey, F. A.; Sundberg, R. J. *Advanced Organic Chemistry, Part B: Reactions and Synthesis*, 2nd Ed.; Plenum: New York, 1983; p 207. (b) Furuta, K.; Miwa, Y.; Iwanaga, K.; Yamamoto, H. *J. Am. Chem. Soc.* **1988**, *110*, 6254.

(58) Cotton, F. A.; Stokely, P. F. *J. Am. Chem. Soc.* **1970**, *92*, 294.

(59) (a) Jung, M. E.; Gervay, J. *J. Am. Chem. Soc.* **1991**, *113*, 224 and references therein. (b) Kirby, A. *J. Adv. Phys. Org. Chem.* **1980**, *17*, 183.

(60) (a) Beesley, R. M.; Ingold, C. K.; Thorpe, J. F. *J. Chem. Soc.* **1915**, *107*, 1080. (b) Ingold, C. K. *J. Chem. Soc.* **1921**, *119*, 305.

(61) For general and specific synthetic procedures, see: Williams, R. M. *Synthesis of Optically Active α-Amino Acids*; Pergamon: Oxford, 1989.

(62) Steiger, R. E. In *Org. Synth. Coll. Vol. III*; Horning, E. C., Ed.; Wiley: New York, 1955; p 88.

(63) (a) Cram, D. J.; Gaston, L. K.; Jäger, H. *J. Am. Chem. Soc.* **1961**, *83*, 2183. (b) McKenzie, A.; Clough, G. W. *J. Chem. Soc.* **1912**, *101*, 390.

(64) March, J. *Advanced Organic Chemistry*, 3rd Ed.; Wiley: New York, 1985; pp 370, 445.

(65) Slates, H. L.; Taub, D.; Kuo, C. H.; Wendler, N. L. *J. Org. Chem.* **1964**, *29*, 1424.

(66) With the exception of the 2,3-dichlorophenyl derivative, the ligands in Table 2.8 were synthesized in enantiomerically pure form by Dr. A. Abiko and the aldol reactions were carried out by Dr. H. Sajiki. The 2,3-dichlorophenyl derivative was prepared by the author from an optically pure amino acid kindly provided by Dr. D. Depernet of SIPSY (Avrillé Cedex, France); the aldol reaction with this ligand was carried out by the author.

(67) Reference 64, p 855.

(68) Bucherer, H. T.; Leib, V. A. *J. Prakt. Chem.* **1934**, *141*, 5.

(69) Munday, L. *J. Chem. Soc.* **1961**, 4372.

(70) (a) Cremlyn, R. J. W.; Chisholm, M. *J. Chem. Soc. (C)* **1967**, 1762. (b) Cremlyn, R. J. W.; Chisholm, M. *J. Chem. Soc. (C)* **1967**, 2269.

(71) Edward, J. T.; Jitrangsri, C. *Can. J. Chem.* **1975**, *53*, 3339.

(72) (a) Matta, M. S.; Rohde, M. F. *Tetrahedron Lett.* **1972**, *41*, 4157. (b) Ansell, J.; Morgan, P.; Price, H. C. *Tetrahedron Lett.* **1978**, *47*, 4615. (c) Trigo, G. G.; Avendaño, C.; Santos, E.; Edward, J. T.; Wong, S. C. *Can. J. Chem.* **1979**, *57*, 1456. (d) Sacripante, G.; Edward, J. T. *Can. J. Chem.* **1982**, *60*, 1982. (e) Galdecki, Z.; Karolak-Wojciechowska, M. *J. Crystallogr. Spectrosc. Res.* **1986**, *16*, 467. (f) Haroutounian, S. A.; Georgiadis, M. P.; Polissiou, M. G. *J. Heterocyclic Chem.* **1989**, *26*, 1283.

(73) Dr. Emma Parmee prepared the enantiomerically pure ligands **A**[117] and **B**[118] and tested the activity of their borane complexes in the Mukaiyama reaction; the results are shown below.

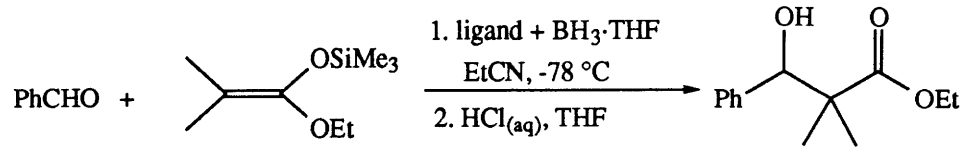

Entry	Ligand	Amount of Promoter/ mol %	Yield/ %	ee/ %
1	A	100	98	73
2	A	20	60	50
3	B	20	67	85

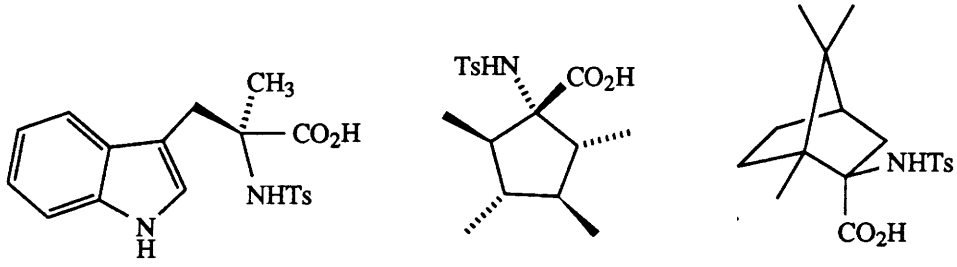

A **B** **C**

The borane complex of ligand **C**, prepared by Dr. Atsushi Abiko from (+)-camphor, did not promote the Mukaiyama aldol reaction or the Diels-Alder reaction of cyclopentadiene and methacrolein.

(74) Kiyooka, S.; Kaneko, Y.; Komura, M.; Matsuo, H.; Nakano, M. *J. Org. Chem.* **1991**, *56*, 2276 and Supplementary Material.

(75) Kiyooka, S.; Kaneko, Y.; Kume, K. *Tetrahedron Lett.* **1992**, *33*, 4927.

(76) *Chiral Liquid Chromatography*; Lough, W. J., Ed.; Blackie: London, 1989.

(77) *Asymmetric Synthesis*; Morrison, J. D., Ed.; Academic Press: New York, 1984; Vol. 1.

(78) Dale, J. A.; Dull, D. L.; Mosher, H. S. *J. Org. Chem.* **1969**, *34*, 2543.

(79) Kende, A. S.; Kawamura, K.; Orwat, M. J. *Tetrahedron Lett.* **1989**, *30*, 5821 and references therein.

(80) Kim, B. M. Ph.D. Thesis, Massachusetts Institute of Technology, Feb. 1988.

(81) Gao, Y.; Hanson, R. M.; Klunder, J. M.; Ko, S. Y.; Masamune, H.; Sharpless, K. B. *J. Am. Chem. Soc.* **1987**, *109*, 5765.

(82) Ma, P.; Martin, V. S.; Masamune, S.; Sharpless, K. B.; Viti, S. M. *J. Org. Chem.* **1982**, *47*, 1378.

(83) Burgess, K.; Ohlmeyer, M. J. *Tetrahedron Lett.* **1989**, *30*, 395.

(84) The ketene acetal shown below gives *anti* aldol products in tin(II)-promoted asymmetric aldol reactions: Mukaiyama, T.; Uchiro, H.; Shiina, I.; Kobayashi, S. *Chem. Lett.* **1990**, 1019. For an application to total synthesis, see: Kanda, Y.; Fukuyama, T. *J. Am. Chem. Soc.* **1993**, *115*, 8451.

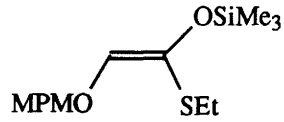

(85) Masamune, S.; Sato, T.; Kim, B. M.; Wollmann, T. A. *J. Am. Chem. Soc.* **1986**, *108*, 8279 and Supplementary Material.

(86) Sartor, D.; Saffrich, J.; Helmchen, G.; Richards, C. J.; Lambert, H. *Tetrahedron: Asymmetry* **1991**, *2*, 639.

(87) Corey, E. J.; Sarshar, S.; Bordner, J. *J. Am. Chem. Soc.* **1992**, *114*, 7938.

(88) One modeling study suggests that the aldehyde carbonyl carbon is activated toward nucleophilic attack by one of the sulfonyl oxygens: Nevalainen, V. *Tetrahedron: Asymmetry* **1993**, *4*, 1565.

(89) Reetz, M. T.; Hüllmann, M.; Massa, W.; Berger, S.; Rademacher, P.; Heymanns, P. *J. Am. Chem. Soc.* **1986**, *108*, 2405.

(90) Hoffmann, R. W. *Angew. Chem. Int. Ed. Engl.* **1992**, *31*, 1124.

(91) Tanimoto, N.; Gerritz, S. W.; Sawabe, A.; Noda, T.; Filla, S. A.; Masamune, S., submitted for publication in *Angew. Chem. Int. Ed. Engl.*

(92) Masamune, S.; Choy, W.; Petersen, J. S.; Sita, L. R. *Angew. Chem. Int. Ed. Engl.* **1985**, *24*, 1.

(93) Duplantier, A. J.; Nantz, M. H.; Roberts, J. C.; Short, R. P.; Somfai, P.; Masamune, S. *Tetrahedron Lett.* **1989**, *30*, 7357.

(94) Corey, E. J.; Cywin, C. L.; Roper, T. D. *Tetrahedron Lett.* **1992**, *33*, 6907.

(95) (a) Corey, E. J.; Loh, T.-P. *J. Am. Chem. Soc.* **1991**, *113*, 8966. (b) Corey, E. J.; Loh, T.-P.; Roper, T. D.; Azimioara, M. D.; Noe, M. C. *J. Am. Chem. Soc.* **1992**, *114*, 8290.(c) Corey, E. J.; Loh, T.-P. *Tetrahedron Lett.* **1993**, *34*, 3979.

(96) Mikami, K.; Matsukawa, S. *J. Am. Chem. Soc.* **1993**, *115*, 7039.

(97) Gao, Q.; Maruyama, T.; Mouri, M.; Yamamoto, H. *J. Org. Chem.* **1992**, *57*, 1951.

(98) Ishihara, K.; Gao, Q.; Yamamoto, H. *J. Am. Chem. Soc.* **1993**, *115*, 10412.

(99) (a) Brown, H. C.; Ravindran, N.; Kulkarni, S. U. *J. Org. Chem.* **1980**, *45*, 384. (b) Brown, H. C.; Salunkhe, A. M.; Argade, A. B. *Organometallics* **1992**, *11*, 3094.

(100) (a) Furuta, K.; Mouri, M.; Yamamoto, H. *Synlett* **1991**, 561. (b) Ishihara, K.; Mouri, M.; Gao, Q.; Maruyama, T.; Furuta, K.; Yamamoto, H. *J. Am. Chem. Soc.* **1993**, *115*, 11490.

(101) Costa, A. L.; Piazza, M. G. Tagliavini, E.; Tromboni, C.; Umani-Ronchi, A. *J. Am. Chem. Soc.* **1993**, *115*, 7001.

(102) (a) Keck, G. E.; Tarbet, K. H.; Geraci, L. S. *J. Am. Chem. Soc.* **1993**, *115*, 8467. (b) Keck, G. E.; Krishnamurthy, D.; Grier, M. C. *J. Org. Chem.* **1993**, *58*, 6543.

(103) (a) Ojima, I.; Inaba, S.; Yoshida, K. *Tetrahedron Lett.* **1977**, *18*, 3643. (b) Guanti, G.; Narisano, E.; Banfi, L. *Tetrahedron Lett.* **1987**, *28*, 4331. (c) Colvin, E. W.; McGarry, D.; Nugent, M. J. *Tetrahedron* **1988**, *44*, 4157. (d) Corey, E. J.; Decicco, C. P.; Newbold, R. C. *Tetrahedron Lett.* **1991**, *32*, 5287. (d) Hattori, K.; Miyata, M.; Yamamoto, H. *J. Am. Chem. Soc.* **1993**, *115*, 1151.

(104) Mukaiyama, T.; Hara, R. *Chem. Lett.* **1989**, 1171 and references therein.

(105) (a) Furuta, K.; Shimizu, S.; Miwa, Y.; Yamamoto, H. *J. Org. Chem.* **1989**, *54*, 1481. (b) Ishihara, K.; Gao, Q.; Yamamoto, H. *J. Org. Chem.* **1993**, *58*, 6917.

(106) Bao, J.; Wulff, W. D.; Rheingold, A. L. *J. Am. Chem. Soc.* **1993**, *115*, 3814.

(107) Maruoka, K.; Murase, N.; Yamamoto, H. *J. Org. Chem.* **1993**, *58*, 2938.

(108) Seerden, J.-P. G.; Scheeren, H. W. *Tetrahedron Lett.* **1993**, *34*, 2669.

(109) Seebach, D. *Angew. Chem. Int. Ed. Engl.* **1990**, *29*, 1320.

(110) Watson, S. C.; Eastham, J. F. *J. Organomet. Chem.* **1967**, *9*, 165.

(111) Still, W. C.; Kahn, M.; Mitra, A. *J. Org. Chem.* **1978**, *43*, 2923.

(112) Colombo, L.; Ulgheri, F.; Prati, L. *Tetrahedron Lett.* **1989**, *30*, 6435.

(113) NMR comparison spectra kindly provided by Professor Kevin Burgess of Texas A & M University.

(114) Maruoka, K.; Hirayama, N.; Yamamoto, H. *Polyhedron* **1990**, *9*, 223.

(115) Gennari, C.; Beretta, M. G.; Bernardi, A.; Moro, G.; Scolastico, C.; Todeschini, R. *Tetrahedron* **1986**, *42*, 893.

(116) Hashimoto, S.; Komeshima, N.; Koga, K. *J. Chem. Soc., Chem. Commun.* **1979**, 437.

(117) Bourne, G. T.; Crich, D.; Davies, J. W.; Horwell, D. C. *J. Chem. Soc. Perkin Trans. I* **1991**, 1693.

(118) Hoffmann, N.; Scharf, H.-D. *Tetrahedron: Asymmetry* **1991**, *2*, 977.

(119) McKee, B. H.; Gilheany, D. G.; Sharpless, K. B. *Org. Synth.* **1992**, *70*, 47.

Appendix One

NMR Spectra of Key Compounds

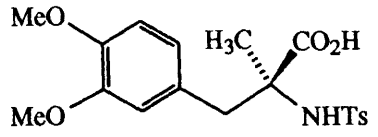

Spectrum 1: 300 MHz ^{1}H NMR, $CDCl_3$

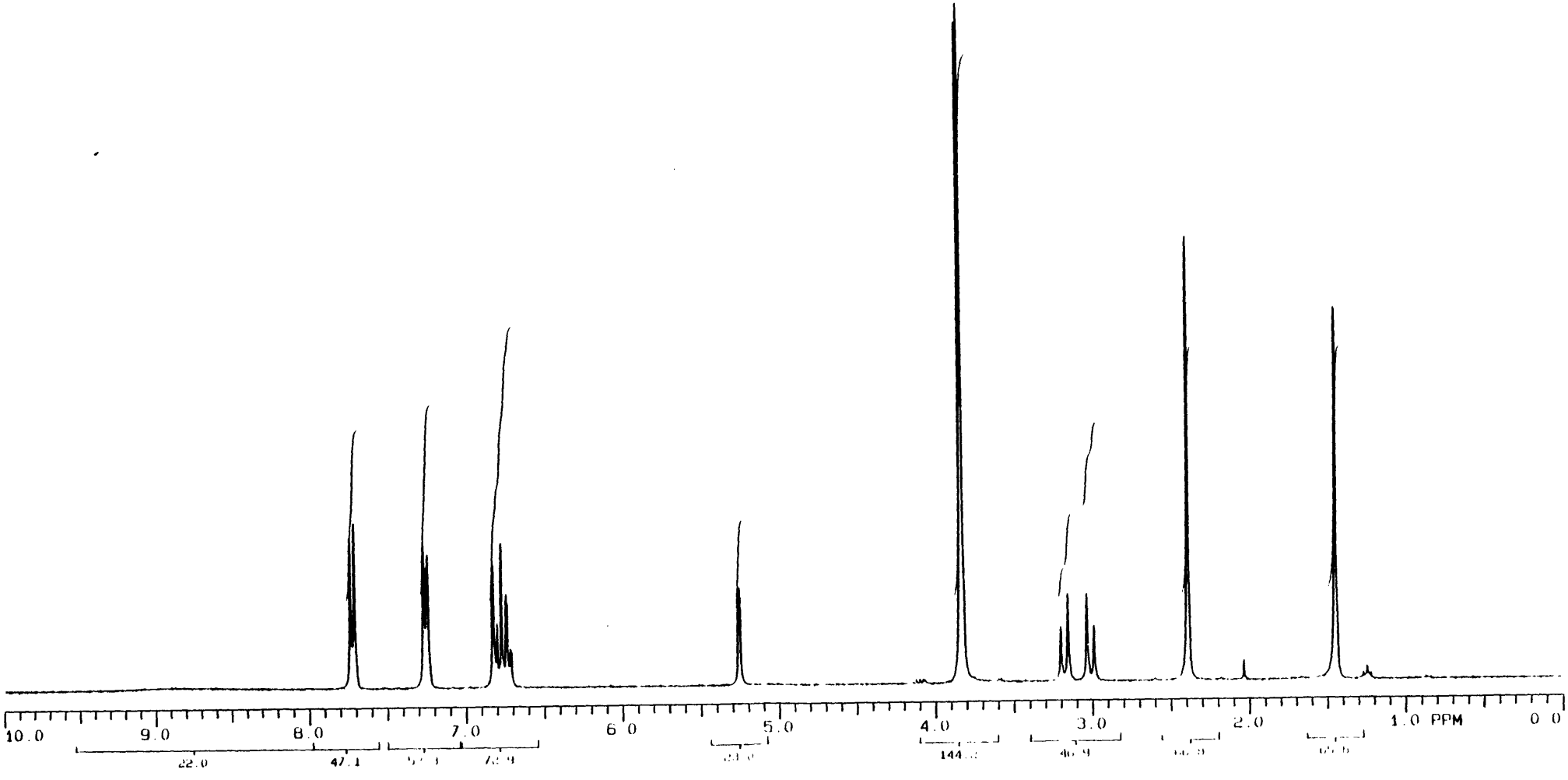

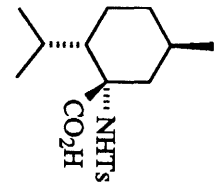

Spectrum 2: 300 MHz ^{1}H NMR, $CDCl_3$

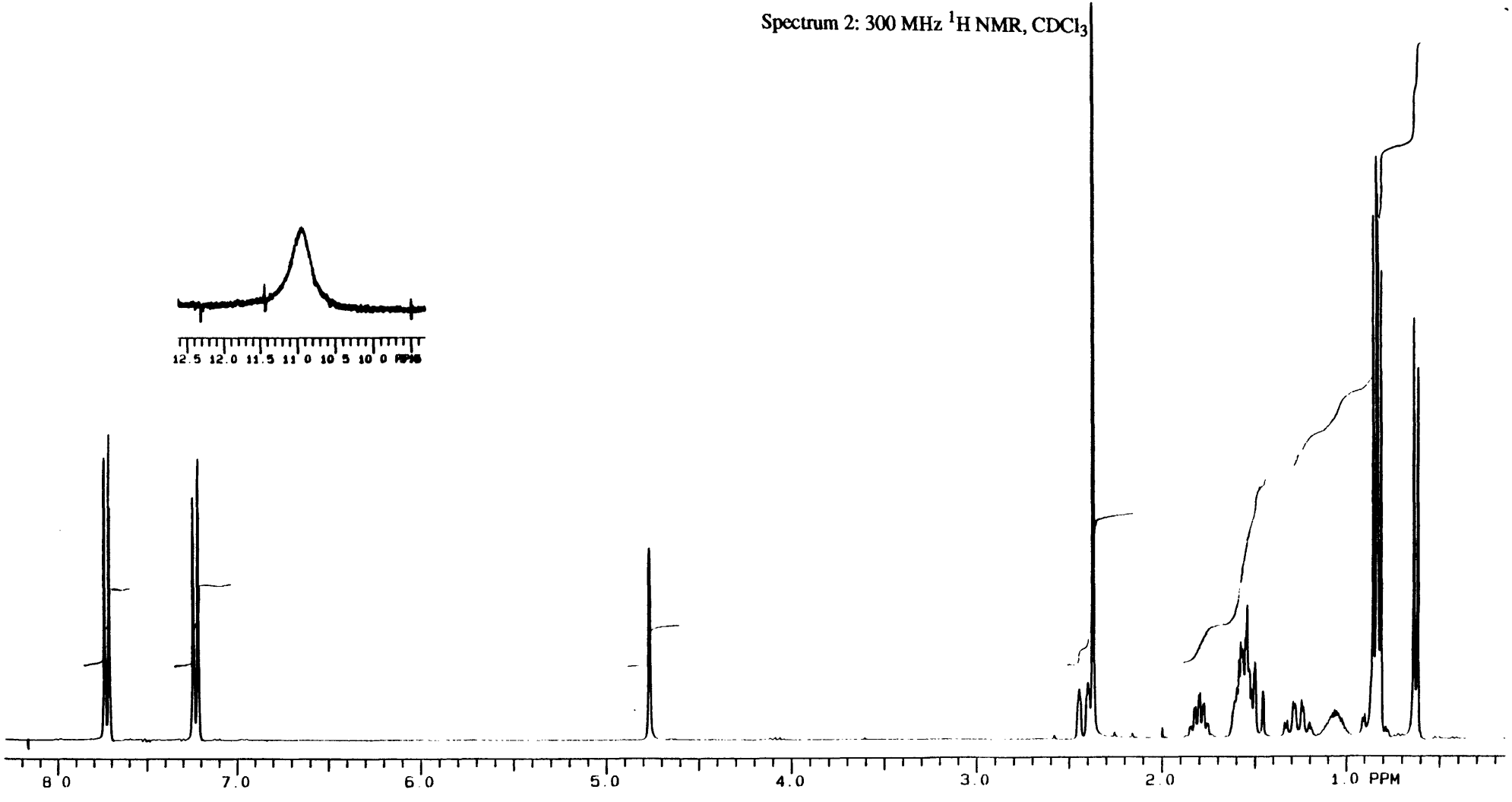

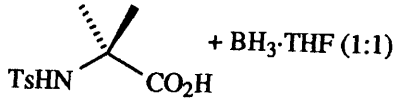

+ BH_3·THF (1:1)

Spectrum 3: ^{11}B NMR, CD_2Cl_2

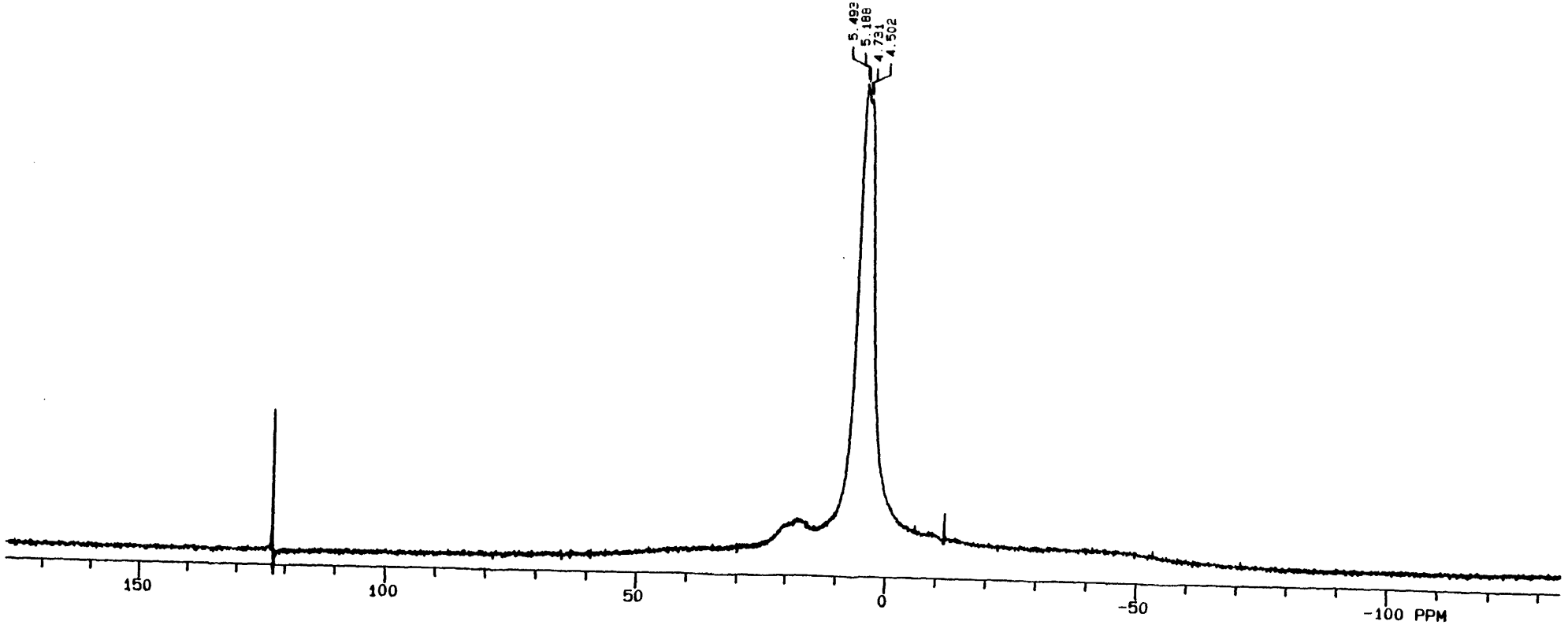

11.000 96 1.500 429.4 B --- ---
30030.0 4100 YYY 0 --- --- ---
0.100 0 S 6000 30030.0 -12935.4
5.0 240 84.0 N

S2PUL

CD2Cl2

XL-300 OBSERVE B11 -50 TO 100 PP
M. BF3 AT 0PPM

B
09-04-91
300

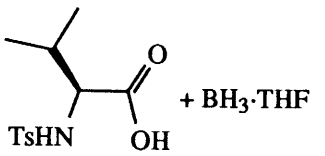

Spectrum 4: ^{11}B NMR, CH_2Cl_2

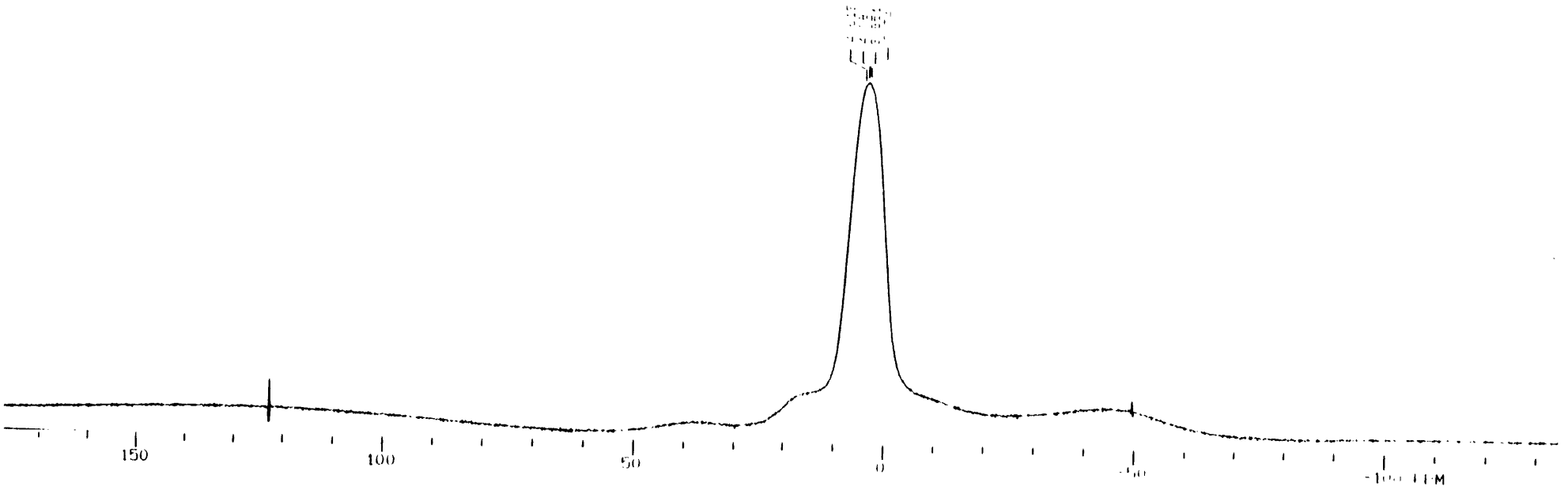

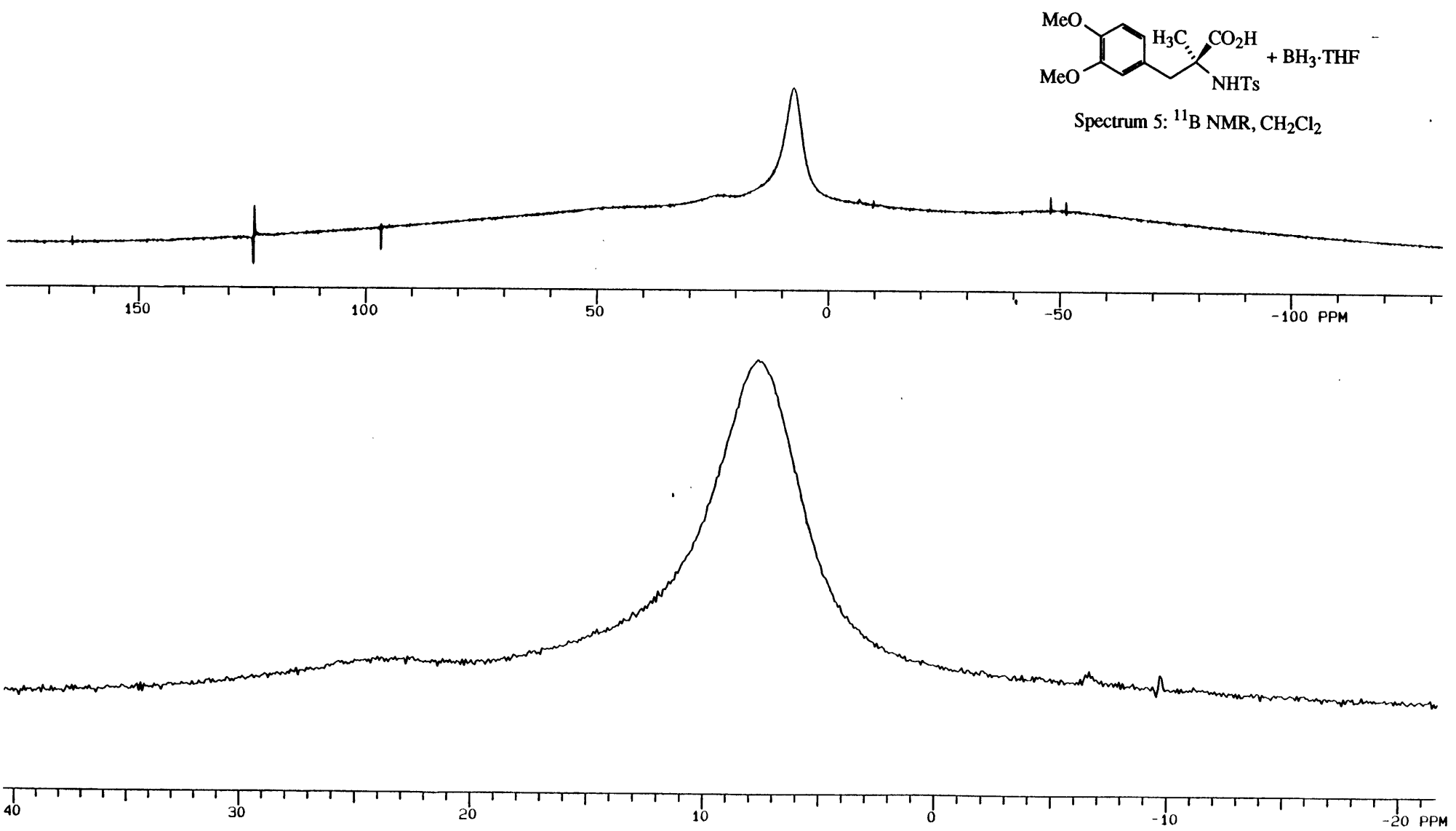

Spectrum 5: ^{11}B NMR, CH_2Cl_2

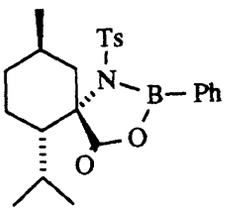

Spectrum 6: 300 MHz ^{1}H NMR, C_6D_6

Appendix Two

X-Ray Crystal Structure of

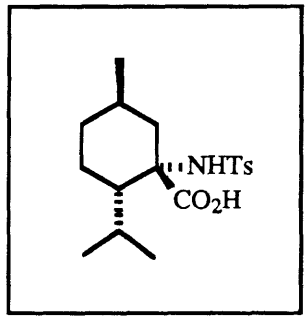

Crystal prepared by Dr. Y. Hong; structure solved by Dr. W. M. Davis.

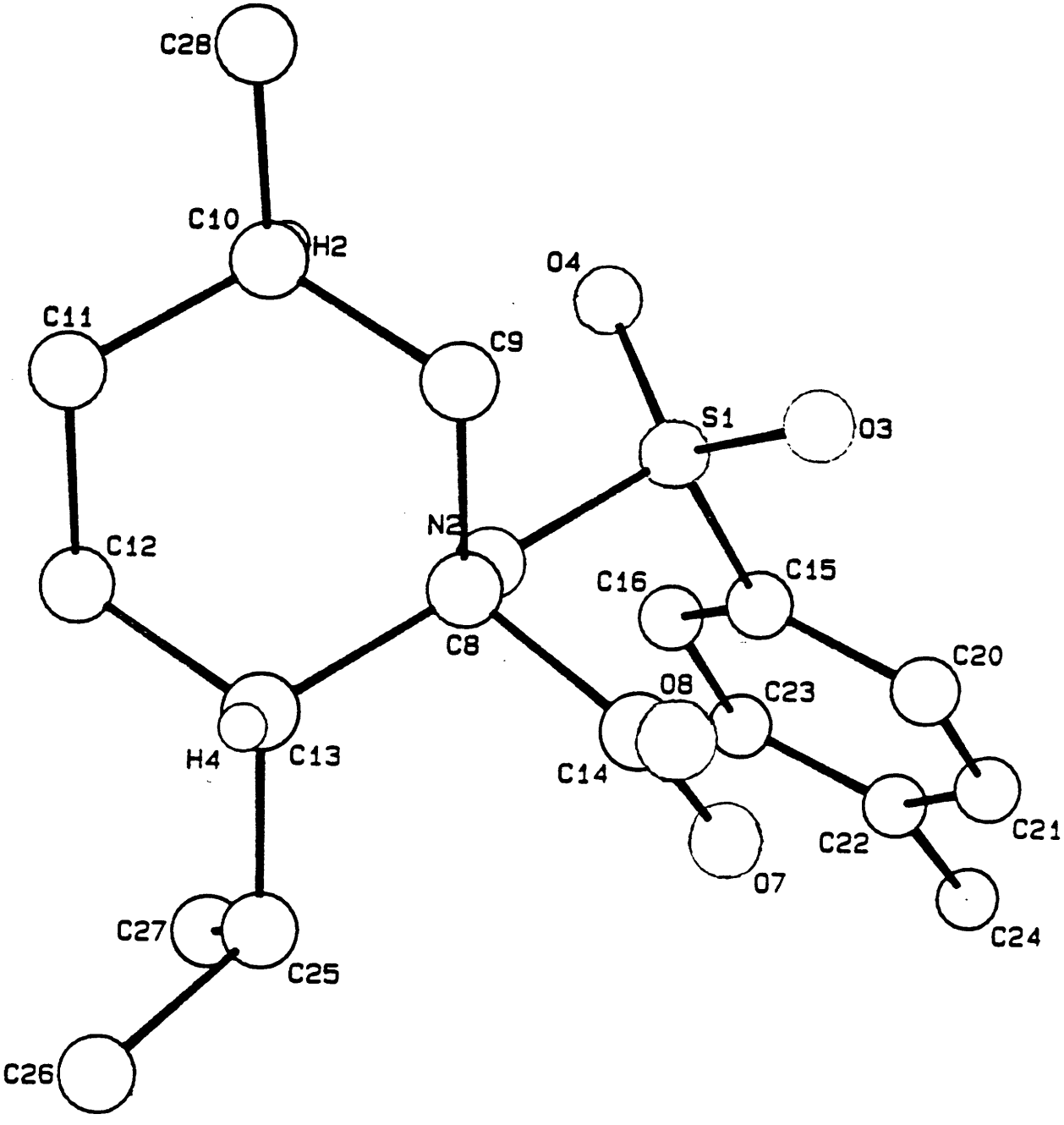
C28
C10
H2
C11
C9
O4
S1
O3
N2
C12
C15
C16
C8
C20
O8
C23
H4
C13
C14
C21
C22
O7
C27
C24
C25
C26

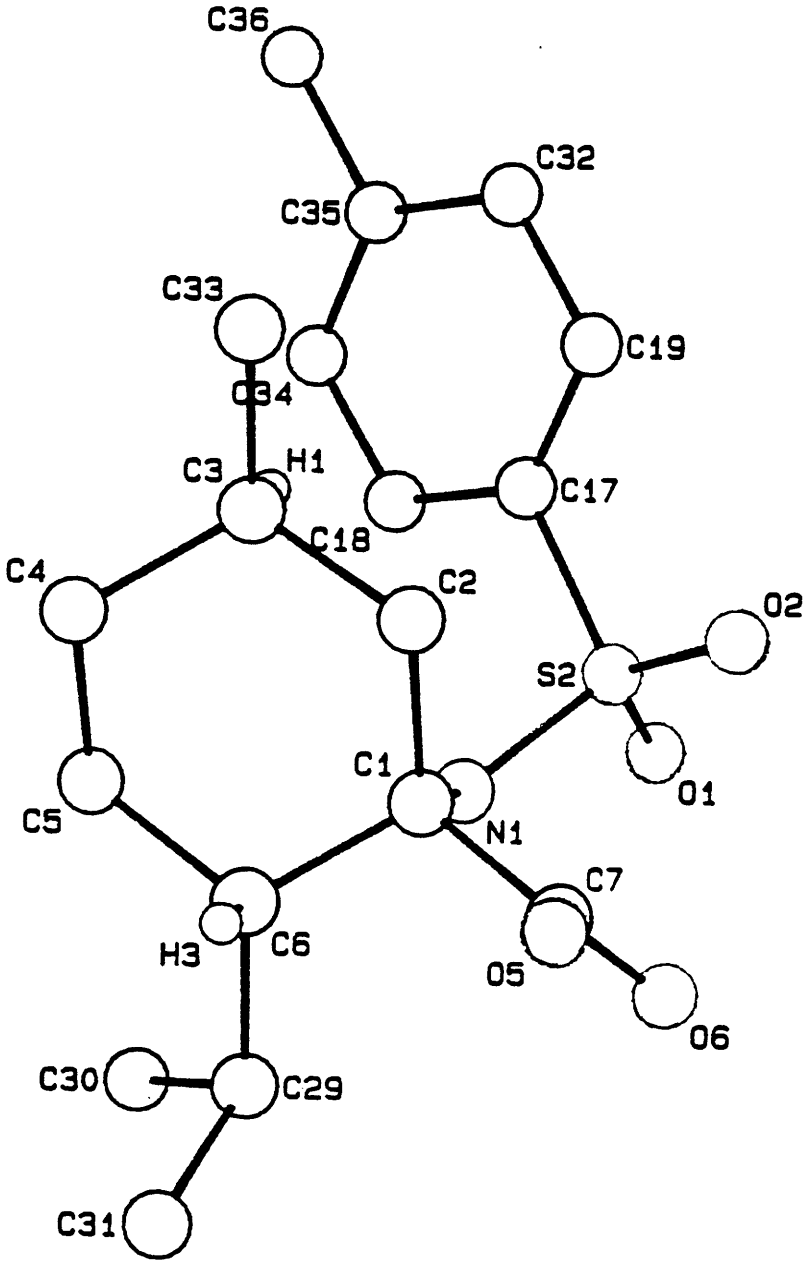
C36
C32
C35
C33
C19
C34
C3
H1
C17
C18
C4
C2
O2
S2
O1
C1
C5
N1
C7
H3
C6
O5
O6
C30
C29
C31

EXPERIMENTAL

DATA COLLECTION

A colorless prismatic crystal of $C_{18}H_{24}N_4OS$ having approximate dimensions of 0.290 X 0.180 X 0.150 mm was mounted on a glass fiber. All measurements were made on an Enraf-Nonius CAD-4 diffractometer with graphite monochromated Mo Kα radiation.

Cell constants and an orientation matrix for data collection, obtained from a least-squares refinement using the setting angles of 25 carefully centered reflections in the range $16.00 < 2\theta < 22.00°$ corresponded to an orthorhombic cell with dimensions:

a = 8.695 (1)Å
b = 19.949 (2)Å
c = 22.333 (2)Å
V = 3874 (1)Å^3

For Z = 8 and F.W. = 344.47, the calculated density is 1.181 g/cm^3. Based on the systematic absences of:

h00: h ≠ 2n
0k0: k ≠ 2n
00l: l ≠ 2n

and the successful solution and refinement of the structure, the space group was determined to be:

$P2_12_12_1$ (#19)

The data were collected at a temperature of 23 ± 1°C using the ω-2θ scan technique to a maximum 2θ value of 54.9°. Omega scans of several intense reflections, made prior to data collection, had an average width at half-height of 0.27° with a take-off angle of 2.8°. Scans of (0.80 + 0.35 tan θ)° were made at speeds ranging from 0.9 to 8.0°/min (in omega). Moving-crystal moving counter background measurements were made by scanning an additional 25% above and below the scan range. The counter aperture consisted of a variable horizontal slit with a width ranging from 2.0 to 2.5 mm and a vertical slit set to 2.0 mm. The diameter of the incident beam collimator was 0.7 mm and the crystal to detector distance was 21 cm. For intense reflections an attenuator was automatically inserted in front of the detector.

DATA REDUCTION

A total of 4989 reflections was collected. The intensities of three representative reflections which were measured after every 60 minutes of X-ray exposure time remained constant throughout data collection indicating crystal and electronic stability (no decay correction was applied).

The linear absorption coefficient for Mo Kα is 1.7 cm^{-1}. An empirical absorption correction, using the program DIFABS[3], was applied which resulted in transmission factors ranging from 0.67 to 1.11. The data were corrected for Lorentz and polarization effects.

STRUCTURE SOLUTION AND REFINEMENT

The structure was solved by direct methods[4]. The non-hydrogen atoms were refined either anisotropically or isotropically. The final cycle of full-matrix least-squares refinement[5] was based on 2317 observed reflections ($I > 3.00\sigma(I)$) and 433 variable parameters and converged (largest parameter shift was 0.12 times its esd) with unweighted and weighted agreement factors of:

$$R = \Sigma \; ||Fo| - |Fc|| \; / \; \Sigma \; |Fo| = 0.079$$

$$R_w = [(\; \Sigma \; w \; (|Fo| - |Fc|)^2 \; / \; \Sigma \; w \; Fo^2 \;)]^{1/2} = 0.080$$

The standard deviation of an observation of unit weight[6] was 2.12. The weighting scheme was based on counting statistics and included a factor ($p = 0.03$) to downweight the intense reflections. Plots of $\Sigma \; w \; (|Fo| - |Fc|)^2$ versus $|Fo|$, reflection order in data collection, $\sin\theta/\lambda$, and various classes of indices showed no unusual trends. The maximum and minimum peaks on the final difference Fourier map corresponded to 0.32 and -0.32 $e^-/Å^3$, respectively.

Neutral atom scattering factors were taken from Cromer and Waber[7]. Anomalous dispersion effects were included in Fcalc[8]; the values for $\Delta f'$ and $\Delta f''$ were those of Cromer[9]. All calculations were performed using the TEXSAN[10] crystallographic software package of Molecular Structure Corporation.

References

(1) PLUTO:
Motherwell,S. & Clegg,W.; PLUTO. Program for plotting molecular and crystal structures. Univ. of Cambridge, England (1978).

(2) ORTEP:
Johnson,C.K.; ORTEPII. Report ORNL-5138. Oak Ridge National Laboratory, Oak Ridge, Tennessee (1976).

(3) DIFABS:
Walker & Stuart, Acta Cryst. A39, 158-166, (1983).

(4) Structure Solution Methods:
MITHRIL
Gilmore,C.J.; MITHRIL - an integrated direct methods computer program. J. Appl. Cryst. 17, 42-46, Univ. of Glasgow, Scotland, (1984).
DIRDIF
Beurskens,P.T.; DIRDIF: Direct Methods for Difference Structures - an automatic procedure for phase extension and refinement of difference structure factors. Technical Report 1984/1 Crystallography Laboratory, Toernooiveld, 6525 Ed Nijmegen, Netherlands.

(5) Least-Squares:
Function minimized: $\Sigma\, w\,(|Fo| - |Fc|)^2$
where: $w = 4Fo^2/\sigma^2(Fo^2)$
$\sigma^2(Fo^2) = [S^2(C+R^2B) + (pFo^2)^2]/Lp^2$
S = Scan rate
C = Total Integrated Peak Count
R = Ratio of Scan Time to background counting time.
B = Total Background Count
Lp = Lorentz-polarization factor
p = p-factor

(6) Standard deviation of an observation of unit weight:

$$[\Sigma\, w(|Fo| - |Fc|)^2/(No - Nv)]^{1/2}$$

where: No = number of observations
Nv = number of variables

(7) Cromer,D.T. & Waber,J.T.; "International Tables for X-ray Crystallography", Vol. IV, The Kynoch Press, Birmingham, England, Table 2.2 A (1974).

(8) Ibers,J.A. & Hamilton,W.C.; Acta Crystallogr., 17, 781 (1964).

(9) D.T. Cromer, "International Tables for X-ray

Crystallography", Vol/ IV, The Kynoch Press, Birmingham, England, Table 2.3.1 (1974).

(10) TEXSAN - TEXRAY Structure Analysis Package, Molecular Structure Corporation (1985).

EXPERIMENTAL DETAILS

A. Crystal Data

Empirical Formula	$C_{18}H_{24}N_4OS$
Formula Weight	344.47
Crystal Color, Habit	colorless, prismatic
Crystal Dimensions (mm)	0.290 X 0.180 X 0.150
Crystal System	orthorhombic
No. Reflections Used for Unit Cell Determination (2θ range)	25 (16.0 - 22.0°)
Omega Scan Peak Width at Half-height	0.27
Lattice Parameters:	a = 8.695 (1)Å b = 19.949 (2)Å c = 22.333 (2)Å V = 3874 (1)Å^3
Space Group	$P2_12_12_1$ (#19)
Z value	8
D_{calc}	1.181 g/cm^3
F_{000}	1472
$\mu_{(MoK\alpha)}$	1.70 cm^{-1}

B. Intensity Measurements

Diffractometer	Enraf-Nonius CAD-4
Radiation	MoKα (λ = 0.71069 Å)
Temperature	23°C
Attenuator	Zr foil, (factor = 17.9)
Take-off Angle	2.8°

Detector Aperture	2.0 - 2.5 mm horizontal 2.0 mm vertical
Crystal to Detector Distance	21 cm
Scan Type	ω-2θ
Scan Rate	0.9 - 8.0°/min (in omega)
Scan Width	(0.80 + 0.35 tanθ)°
$2\theta_{max}$	54.9°
No. of Reflections Measured	Total: 4989
Corrections	Lorentz-polarization Absorption (trans. factors: 0.67 - 1.11)

C. Structure Solution and Refinement

Structure Solution	Direct Methods
Refinement	Full-matrix least-squares
Function Minimized	Σ w (|Fo| - |Fc|)^2
Least-squares Weights	$4Fo^2/\sigma^2(Fo^2)$
p-factor	0.03
Anomalous Dispersion	All non-hydrogen atoms
No. Observations (I>3.00σ(I))	2317
No. Variables	433
Reflection/Parameter Ratio	5.35
Residuals: R; R_w	0.079; 0.080
Goodness of Fit Indicator	2.12
Max Shift/Error in Final Cycle	0.12
Maximum Peak in Final Diff. Map	0.32 $e^-/Å^3$
Minimum Peak in Final Diff. Map	-0.32 $e^-/Å^3$

Positional parameters for 91059 HONG/SM

atom	x	y	z
S(1)	0.8843(4)	0.0524(2)	0.7760(1)
S(2)	0.4562(4)	0.0695(2)	0.4425(1)
O(1)	0.4127(9)	0.0125(4)	0.4066(3)
O(2)	0.366(1)	0.1290(4)	0.4409(4)
O(3)	0.782(1)	0.1005(4)	0.7493(3)
O(4)	0.823(1)	0.0036(4)	0.8170(3)
O(5)	0.671(1)	0.2591(4)	0.3797(3)
O(6)	0.557(1)	0.1719(4)	0.3376(3)
O(7)	1.069(1)	0.1711(4)	0.7132(3)
O(8)	0.973(1)	0.2607(4)	0.7574(3)
N(1)	0.636(1)	0.0839(4)	0.4230(4)
N(2)	1.025(1)	0.0921(4)	0.8106(4)
C(1)	0.703(1)	0.1538(6)	0.4280(5)
C(2)	0.672(1)	0.1897(5)	0.4890(5)
C(3)	0.759(2)	0.1566(5)	0.5418(5)
C(4)	0.932(1)	0.1534(6)	0.5293(5)
C(5)	0.959(1)	0.1145(6)	0.4720(4)
C(6)	0.876(1)	0.1471(6)	0.4170(5)
C(7)	0.636(1)	0.1952(6)	0.3772(5)
C(8)	1.014(1)	0.1652(6)	0.8201(4)
C(9)	0.871(1)	0.1876(6)	0.8567(5)
C(10)	0.886(2)	0.1591(7)	0.9207(5)
C(11)	1.027(2)	0.1814(7)	0.9530(5)
C(12)	1.174(2)	0.1613(7)	0.9168(6)
C(13)	1.164(1)	0.1904(6)	0.8523(6)
C(14)	1.018(1)	0.1991(6)	0.7586(6)
C(15)	0.974(1)	0.0060(6)	0.7178(5)
C(16)	1.053(2)	-0.0512(7)	0.7322(6)
C(17)	0.465(1)	0.0430(6)	0.5174(5)
C(18)	0.566(2)	-0.0127(7)	0.5294(5)
C(19)	0.376(2)	0.0782(8)	0.5586(7)
C(20)	0.950(2)	0.0279(7)	0.6591(5)
C(21)	1.012(2)	-0.0111(8)	0.6136(6)
C(22)	1.099(2)	-0.0711(8)	0.6243(8)
C(23)	1.123(2)	-0.0902(7)	0.6839(8)
C(24)	1.159(2)	-0.1122(8)	0.5722(7)
C(25)	1.316(2)	0.1831(9)	0.8157(7)
C(26)	1.432(2)	0.2406(8)	0.8375(8)
C(27)	1.393(2)	0.1147(8)	0.823(1)
C(28)	0.744(2)	0.1781(8)	0.9569(6)
C(29)	0.923(2)	0.1156(6)	0.3544(5)
C(30)	0.998(2)	0.0455(9)	0.3632(7)
C(31)	1.045(2)	0.156(1)	0.3239(7)
C(33)	0.721(2)	0.1969(6)	0.5992(5)
C(34)	0.581(2)	-0.0343(9)	0.5917(8)
C(35)	0.492(3)	-0.001(1)	0.6342(8)
C(36)	0.511(2)	-0.024(1)	0.7007(6)
C(32)	0.390(2)	0.057(1)	0.6209(8)
H(1)	0.721	0.111	0.547

Positional parameters for 91059 HONG/SM

atom	x	y	z
H(2)	0.887	0.109	0.918
H(3)	0.914	0.194	0.416
H(4)	1.147	0.240	0.858

Positional parameters and B(eq) for 91059 HONG/SM

atom	x	y	z	B(eq)
S(1)	0.8843(4)	0.0524(2)	0.7760(1)	4.2(2)
S(2)	0.4562(4)	0.0695(2)	0.4425(1)	3.6(1)
O(1)	0.4127(9)	0.0125(4)	0.4066(3)	4.3(4)
O(2)	0.366(1)	0.1290(4)	0.4409(4)	5.1(5)
O(3)	0.782(1)	0.1005(4)	0.7493(3)	4.7(4)
O(4)	0.823(1)	0.0036(4)	0.8170(3)	5.8(5)
O(5)	0.671(1)	0.2591(4)	0.3797(3)	4.5(4)
O(6)	0.557(1)	0.1719(4)	0.3376(3)	5.0(5)
O(7)	1.069(1)	0.1711(4)	0.7132(3)	4.4(4)
O(8)	0.973(1)	0.2607(4)	0.7574(3)	5.8(5)
N(1)	0.636(1)	0.0839(4)	0.4230(4)	2.9(4)
N(2)	1.025(1)	0.0921(4)	0.8106(4)	3.4(4)
C(1)	0.703(1)	0.1538(6)	0.4280(5)	3.2(5)
C(2)	0.672(1)	0.1897(5)	0.4890(5)	3.9(6)
C(3)	0.759(2)	0.1566(5)	0.5418(5)	3.8(6)
C(4)	0.932(1)	0.1534(6)	0.5293(5)	4.0(6)
C(5)	0.959(1)	0.1145(6)	0.4720(4)	3.9(6)
C(6)	0.876(1)	0.1471(6)	0.4170(5)	4.3(6)
C(7)	0.636(1)	0.1952(6)	0.3772(5)	3.2(5)
C(8)	1.014(1)	0.1652(6)	0.8201(4)	3.1(5)
C(9)	0.871(1)	0.1876(6)	0.8567(5)	4.6(6)
C(10)	0.886(2)	0.1591(7)	0.9207(5)	4.9(7)
C(11)	1.027(2)	0.1814(7)	0.9530(5)	5.9(8)
C(12)	1.174(2)	0.1613(7)	0.9168(6)	5.3(8)
C(13)	1.164(1)	0.1904(6)	0.8523(6)	4.9(7)
C(14)	1.018(1)	0.1991(6)	0.7586(6)	3.8(6)
C(15)	0.974(1)	0.0060(6)	0.7178(5)	3.9(6)
C(16)	1.053(2)	-0.0512(7)	0.7322(6)	6.2(8)
C(17)	0.465(1)	0.0430(6)	0.5174(5)	4.3(6)
C(18)	0.566(2)	-0.0127(7)	0.5294(5)	5.5(8)
C(19)	0.376(2)	0.0782(8)	0.5586(7)	8(1)
C(20)	0.950(2)	0.0279(7)	0.6591(5)	5.9(8)
C(21)	1.012(2)	-0.0111(8)	0.6136(6)	7(1)
C(22)	1.099(2)	-0.0711(8)	0.6243(8)	7(1)
C(23)	1.123(2)	-0.0902(7)	0.6839(8)	7(1)
C(24)	1.159(2)	-0.1122(8)	0.5722(7)	9(1)
C(25)	1.316(2)	0.1831(9)	0.8157(7)	7(1)
C(26)	1.432(2)	0.2406(8)	0.8375(8)	9(1)
C(27)	1.393(2)	0.1147(8)	0.823(1)	10(1)
C(28)	0.744(2)	0.1781(8)	0.9569(6)	7(1)
C(29)	0.923(2)	0.1156(6)	0.3544(5)	4.9(7)
C(30)	0.998(2)	0.0455(9)	0.3632(7)	10(1)
C(31)	1.045(2)	0.156(1)	0.3239(7)	12(1)
C(33)	0.721(2)	0.1969(6)	0.5992(5)	4.7(7)
C(34)	0.581(2)	-0.0343(9)	0.5917(8)	8(1)
C(35)	0.492(3)	-0.001(1)	0.6342(8)	9(1)
C(36)	0.511(2)	-0.024(1)	0.7007(6)	13(1)
C(32)	0.390(2)	0.057(1)	0.6209(8)	10(1)
H(1)	0.721	0.111	0.547	4.5

Positional parameters and B(eq) for 91059 HONG/SM

atom	x	y	z	B(eq)
H(2)	0.887	0.109	0.918	6.1
H(3)	0.914	0.194	0.416	5.1
H(4)	1.147	0.240	0.858	6.2

ATOM	U11	U22	U33	U12	U13	U23
S(1)	0.053(2)	0.056(2)	0.049(2)	-0.010(2)	-0.005(2)	0.013(2)
S(2)	0.038(2)	0.048(2)	0.052(2)	-0.002(2)	-0.001(2)	0.002(2)
O(1)	0.052(6)	0.056(5)	0.057(5)	-0.012(5)	-0.003(4)	-0.014(4)
O(2)	0.048(5)	0.056(6)	0.089(7)	0.008(5)	0.011(6)	-0.006(5)
O(3)	0.048(5)	0.077(6)	0.055(5)	-0.000(5)	-0.009(4)	0.008(5)
O(4)	0.068(6)	0.097(7)	0.054(5)	-0.040(6)	-0.003(5)	0.026(5)
O(5)	0.085(7)	0.036(5)	0.049(5)	-0.000(5)	-0.008(5)	0.001(4)
O(6)	0.075(6)	0.062(6)	0.052(5)	-0.019(5)	-0.020(5)	0.009(4)
O(7)	0.054(6)	0.047(5)	0.065(5)	0.001(5)	0.016(5)	0.006(4)
O(8)	0.096(7)	0.059(6)	0.067(6)	0.021(6)	0.014(6)	0.011(5)
N(1)	0.023(5)	0.026(5)	0.059(6)	-0.005(4)	-0.001(4)	0.000(4)
N(2)	0.039(6)	0.041(6)	0.048(5)	-0.010(5)	-0.002(5)	-0.002(5)
C(1)	0.033(7)	0.043(7)	0.045(7)	-0.006(6)	-0.004(6)	0.010(6)
C(2)	0.065(9)	0.046(7)	0.036(6)	0.015(7)	-0.008(6)	0.004(6)
C(3)	0.07(1)	0.023(6)	0.050(7)	-0.002(6)	-0.013(7)	0.003(6)
C(4)	0.039(8)	0.07(1)	0.044(7)	0.002(7)	0.002(6)	-0.009(7)
C(5)	0.049(7)	0.060(8)	0.038(6)	0.010(7)	-0.014(6)	0.001(6)
C(6)	0.048(8)	0.055(8)	0.060(8)	-0.001(7)	-0.002(7)	-0.004(7)
C(7)	0.043(7)	0.043(7)	0.037(6)	-0.003(7)	-0.002(6)	-0.000(6)
C(8)	0.041(8)	0.046(7)	0.032(6)	-0.015(6)	-0.014(6)	0.007(5)
C(9)	0.058(8)	0.08(1)	0.040(6)	0.019(8)	0.021(7)	0.016(7)
C(10)	0.07(1)	0.07(1)	0.045(7)	0.019(9)	0.014(8)	0.003(7)
C(11)	0.11(1)	0.08(1)	0.040(7)	-0.00(1)	-0.023(9)	-0.007(7)
C(12)	0.09(1)	0.07(1)	0.050(8)	0.004(9)	-0.022(9)	0.002(7)
C(13)	0.058(9)	0.06(1)	0.067(9)	-0.020(8)	-0.012(8)	-0.011(8)
C(14)	0.042(8)	0.038(7)	0.065(8)	-0.001(7)	0.008(7)	0.002(7)
C(15)	0.062(8)	0.033(7)	0.054(8)	-0.016(7)	0.003(8)	-0.003(6)
C(16)	0.09(1)	0.048(8)	0.10(1)	0.01(1)	-0.00(1)	0.007(9)
C(17)	0.047(7)	0.059(9)	0.056(8)	-0.030(8)	-0.006(7)	0.009(7)
C(18)	0.08(1)	0.07(1)	0.060(9)	-0.02(1)	-0.022(8)	0.017(8)
C(19)	0.08(1)	0.14(1)	0.07(1)	-0.04(1)	0.03(1)	-0.04(1)
C(20)	0.10(1)	0.08(1)	0.040(8)	-0.01(1)	-0.002(9)	-0.010(7)
C(21)	0.11(1)	0.09(1)	0.06(1)	-0.03(1)	-0.00(1)	0.01(1)
C(22)	0.09(1)	0.06(1)	0.11(1)	-0.03(1)	-0.00(1)	0.01(1)
C(23)	0.13(2)	0.05(1)	0.10(1)	-0.01(1)	0.02(1)	0.00(1)

ATOM	U11	U22	U33	U12	U13	U23
C(24)	0.13(2)	0.10(1)	0.09(1)	0.01(1)	0.04(1)	-0.05(1)
C(25)	0.06(1)	0.11(1)	0.09(1)	-0.02(1)	-0.004(9)	0.00(1)
C(26)	0.08(1)	0.08(1)	0.18(2)	-0.02(1)	-0.04(1)	0.03(1)
C(27)	0.07(1)	0.08(1)	0.22(2)	0.01(1)	0.02(1)	-0.05(1)
C(28)	0.11(1)	0.11(1)	0.053(9)	0.03(1)	0.028(9)	0.014(9)
C(29)	0.08(1)	0.047(8)	0.064(8)	-0.001(8)	0.008(8)	-0.021(7)
C(30)	0.15(2)	0.12(1)	0.11(1)	0.07(1)	-0.03(1)	-0.04(1)
C(31)	0.18(2)	0.19(2)	0.09(1)	-0.14(2)	0.08(1)	-0.06(1)
C(33)	0.09(1)	0.043(8)	0.049(7)	-0.003(8)	0.003(8)	-0.017(6)
C(34)	0.11(2)	0.11(2)	0.08(1)	-0.04(1)	-0.03(1)	0.04(1)
C(35)	0.13(2)	0.16(2)	0.07(1)	-0.09(2)	-0.01(1)	0.05(1)
C(36)	0.18(2)	0.26(2)	0.05(1)	-0.07(2)	-0.03(1)	0.04(1)
C(32)	0.12(2)	0.17(2)	0.07(1)	-0.08(2)	0.01(1)	-0.01(1)
H(1)	0.057					
H(2)	0.078					
H(3)	0.065					
H(4)	0.078					

(1)	(2)	(3)	(4)	angle
S(1)	N(2)	C(8)	C(9)	59(1)
S(1)	N(2)	C(8)	C(13)	-178.5(7)
S(1)	N(2)	C(8)	C(14)	-65(1)
S(1)	C(15)	C(16)	C(23)	179(1)
S(1)	C(15)	C(20)	C(21)	-176(1)
S(2)	N(1)	C(1)	C(2)	47(1)
S(2)	N(1)	C(1)	C(6)	170.4(7)
S(2)	N(1)	C(1)	C(7)	-74(1)
S(2)	C(17)	C(18)	C(34)	177(1)
S(2)	C(17)	C(19)	C(32)	-178(1)
O(1)	S(2)	N(1)	C(1)	153.1(7)
O(1)	S(2)	C(17)	C(18)	56(1)
O(1)	S(2)	C(17)	C(19)	-125(1)
O(2)	S(2)	N(1)	C(1)	22.5(9)
O(2)	S(2)	C(17)	C(18)	-173.5(9)
O(2)	S(2)	C(17)	C(19)	6(1)
O(3)	S(1)	N(2)	C(8)	11.4(9)
O(3)	S(1)	C(15)	C(16)	-167(1)
O(3)	S(1)	C(15)	C(20)	8(1)
O(4)	S(1)	N(2)	C(8)	-119.3(8)
O(4)	S(1)	C(15)	C(16)	-38(1)
O(4)	S(1)	C(15)	C(20)	137(1)
O(5)	C(7)	C(1)	N(1)	173.0(9)
O(5)	C(7)	C(1)	C(2)	48(1)
O(5)	C(7)	C(1)	C(6)	-72(1)
O(6)	C(7)	C(1)	N(1)	-8(1)
O(6)	C(7)	C(1)	C(2)	-132(1)
O(6)	C(7)	C(1)	C(6)	107(1)
O(7)	C(14)	C(8)	N(2)	-20(2)
O(7)	C(14)	C(8)	C(9)	-146(1)
O(7)	C(14)	C(8)	C(13)	96(1)
O(8)	C(14)	C(8)	N(2)	164(1)
O(8)	C(14)	C(8)	C(9)	38(1)
O(8)	C(14)	C(8)	C(13)	-80(1)
N(1)	S(2)	C(17)	C(18)	-54(1)
N(1)	S(2)	C(17)	C(19)	125(1)
N(1)	C(1)	C(2)	C(3)	69(1)
N(1)	C(1)	C(6)	C(5)	-74(1)
N(1)	C(1)	C(6)	C(29)	58(1)
N(2)	S(1)	C(15)	C(16)	75(1)
N(2)	S(1)	C(15)	C(20)	-109(1)
N(2)	C(8)	C(9)	C(10)	65(1)
N(2)	C(8)	C(13)	C(12)	-66(1)
N(2)	C(8)	C(13)	C(25)	65(1)
C(1)	N(1)	S(2)	C(17)	-93.8(8)
C(1)	C(2)	C(3)	C(4)	56(1)
C(1)	C(2)	C(3)	C(33)	179(1)
C(1)	C(6)	C(5)	C(4)	-57(1)
C(1)	C(6)	C(29)	C(30)	-112(1)
C(1)	C(6)	C(29)	C(31)	132(1)
C(2)	C(1)	C(6)	C(5)	52(1)
C(2)	C(1)	C(6)	C(29)	-176.2(9)

The sign is positive if when looking from atom 2 to atom 3 a clockwise motion of atom 1 would superimpose it on atom 4.

Torsion or Conformation Angles (cont)

(1)	(2)	(3)	(4)	angle
C(2)	C(3)	C(4)	C(5)	-58(1)
C(3)	C(2)	C(1)	C(6)	-52(1)
C(3)	C(2)	C(1)	C(7)	-171(1)
C(3)	C(4)	C(5)	C(6)	59(1)
C(4)	C(5)	C(6)	C(29)	170(1)
C(5)	C(4)	C(3)	C(33)	-178.9(8)
C(5)	C(6)	C(1)	C(7)	171.4(9)
C(5)	C(6)	C(29)	C(30)	19(2)
C(5)	C(6)	C(29)	C(31)	-97(1)
C(7)	C(1)	C(6)	C(29)	-56(1)
C(8)	N(2)	S(1)	C(15)	127.9(8)
C(8)	C(9)	C(10)	C(11)	59(1)
C(8)	C(9)	C(10)	C(28)	-178(1)
C(8)	C(13)	C(12)	C(11)	-57(1)
C(8)	C(13)	C(25)	C(26)	152(1)
C(8)	C(13)	C(25)	C(27)	-86(2)
C(9)	C(8)	C(13)	C(12)	60(1)
C(9)	C(8)	C(13)	C(25)	-170(1)
C(9)	C(10)	C(11)	C(12)	-58(1)
C(10)	C(9)	C(8)	C(13)	-58(1)
C(10)	C(9)	C(8)	C(14)	-173(1)
C(10)	C(11)	C(12)	C(13)	55(1)
C(11)	C(12)	C(13)	C(25)	171(1)
C(12)	C(11)	C(10)	C(28)	179(1)
C(12)	C(13)	C(8)	C(14)	179(1)
C(12)	C(13)	C(25)	C(26)	-78(1)
C(12)	C(13)	C(25)	C(27)	43(2)
C(14)	C(8)	C(13)	C(25)	-51(1)
C(15)	C(16)	C(23)	C(22)	-5(2)
C(15)	C(20)	C(21)	C(22)	0(2)
C(16)	C(15)	C(20)	C(21)	-1(2)
C(16)	C(23)	C(22)	C(21)	4(2)
C(16)	C(23)	C(22)	C(24)	-176(1)
C(17)	C(18)	C(34)	C(35)	2(2)
C(17)	C(19)	C(32)	C(35)	-2(2)
C(18)	C(17)	C(19)	C(32)	2(2)
C(18)	C(34)	C(35)	C(36)	-180(1)
C(18)	C(34)	C(35)	C(32)	-3(3)
C(19)	C(17)	C(18)	C(34)	-2(2)
C(19)	C(32)	C(35)	C(34)	3(3)
C(19)	C(32)	C(35)	C(36)	179(2)
C(20)	C(15)	C(16)	C(23)	3(2)
C(20)	C(21)	C(22)	C(23)	-1(2)
C(20)	C(21)	C(22)	C(24)	178(1)

The sign is positive if when looking from atom 2 to atom 3 a clockwise motion of atom 1 would superimpose it on atom 4.

Intramolecular Distances Involving the Nonhydrogen Atoms

atom	atom	distance	atom	atom	distance
S(1)	O(3)	1.436(8)	C(8)	C(14)	1.53(1)
S(1)	O(4)	1.440(8)	C(9)	C(10)	1.55(2)
S(1)	N(2)	1.648(9)	C(10)	C(11)	1.49(2)
S(1)	C(15)	1.78(1)	C(10)	C(28)	1.52(2)
S(2)	O(1)	1.442(7)	C(11)	C(12)	1.57(2)
S(2)	O(2)	1.425(8)	C(12)	C(13)	1.56(2)
S(2)	N(1)	1.644(8)	C(13)	C(25)	1.57(2)
S(2)	C(17)	1.76(1)	C(15)	C(16)	1.37(2)
O(5)	C(7)	1.31(1)	C(15)	C(20)	1.40(2)
O(6)	C(7)	1.21(1)	C(16)	C(23)	1.47(2)
O(7)	C(14)	1.24(1)	C(17)	C(18)	1.44(2)
O(8)	C(14)	1.29(1)	C(17)	C(19)	1.39(2)
N(1)	C(1)	1.52(1)	C(18)	C(34)	1.46(2)
N(2)	C(8)	1.48(1)	C(19)	C(32)	1.46(2)
C(1)	C(2)	1.56(1)	C(20)	C(21)	1.39(2)
C(1)	C(6)	1.52(2)	C(21)	C(22)	1.43(2)
C(1)	C(7)	1.52(1)	C(22)	C(23)	1.40(2)
C(2)	C(3)	1.55(1)	C(22)	C(24)	1.52(2)
C(3)	C(4)	1.53(2)	C(25)	C(26)	1.60(2)
C(3)	C(33)	1.55(1)	C(25)	C(27)	1.53(2)
C(4)	C(5)	1.52(1)	C(29)	C(30)	1.55(2)
C(5)	C(6)	1.57(1)	C(29)	C(31)	1.50(2)
C(6)	C(29)	1.59(2)	C(34)	C(35)	1.39(2)
C(8)	C(9)	1.56(1)	C(35)	C(36)	1.56(2)
C(8)	C(13)	1.57(1)	C(35)	C(32)	1.49(3)

Distances are in angstroms. Estimated standard deviations in the least significant figure are given in parentheses.

Intramolecular Distances Involving the Hydrogen Atoms

atom	atom	distance	atom	atom	distance
C(3)	H(1)	0.982	C(10)	H(2)	1.003
C(6)	H(3)	0.993	C(13)	H(4)	1.005

Distances are in angstroms. Estimated standard deviations in the least significant figure are given in parentheses.

Intermolecular Distances Involving the Nonhydrogen Atoms

atom	atom	distance	ADC(*)	atom	atom	distance	ADC(*)
O(1)	N(2)	3.04(1)	65402	O(6)	O(8)	2.62(1)	45603
O(1)	O(4)	3.06(1)	65402	O(6)	O(7)	3.33(1)	45603
O(1)	C(12)	3.56(2)	65402	O(6)	C(14)	3.37(1)	45603
O(4)	N(1)	2.96(1)	65502	O(6)	C(16)	3.50(2)	65402
O(4)	C(30)	3.13(2)	65502	O(7)	C(7)	3.39(1)	55603
O(4)	C(29)	3.31(1)	65502	O(8)	C(23)	3.36(2)	75604
O(5)	O(7)	2.65(1)	45603	O(8)	C(7)	3.44(1)	55603
O(5)	C(4)	3.39(1)	45603	C(21)	C(32)	3.56(2)	65501
O(5)	C(14)	3.47(1)	45603	C(22)	C(32)	3.60(2)	65501
O(5)	O(8)	3.54(1)	45603	C(27)	C(30)	3.45(2)	75502

Contacts out to 3.60 angstroms. Estimated standard deviations in the least significant figure are given in parentheses.

atom	atom	distance	ADC(*)	atom	atom	distance	ADC(*)
O(1)	H(2)	2.997	65402	C(20)	H(1)	3.597	1
C(18)	H(2)	3.177	65402	C(33)	H(3)	3.460	45603

Contacts out to 3.60 angstroms. Estimated standard deviations in the least significant figure are given in parentheses.

(*)footnote

The ADC (atom designator code) specifies the position of an atom in a crystal. The 5-digit number shown in the table is a composite of three one digit numbers and one two digit number: TA(1st digit) + TB(2nd digit) + TC(3rd digit) + SN(4th and 5th digit). TA, TB, & TC are the crystal lattice translation digits along cell edges a, b, and c. A translation digit of 5 indicates the origin unit cell. If TA=4, this indicates a translation of one unit cell length along the a axis in the negative direction. Each translation digit can range in value from 1 to 9 and thus (+/-)4 lattice translations from the origin (TA=5,TB=5,TC=5) can be represented.

The SN or symmetry operator number refers to the number of the symmetry operator used to generate the coordinates of the target atom. A list of the symmetry operators relevant to this structure are given below.

For a given intermolecular contact, the first atom (origin atom) is located in the origin unit cell (TA=5,TB=5,TC=5) and its position can be generated using the identity operator (SN=1). Thus, the ADC for an origin atom is always ADC=55501. The position of the second atom (target atom) can be generated using the ADC and the coordinates of that atom in the parameter table. For example, an ADC of 47502 refers to the target atom moved through operator two, then translated -1 cell translations along the a axis, +2 cell translations along the b axis, and 0 cell translations along the c axis.

An ADC of 1 indicates an intermolecular contact between two fragments (i.e.cation and anion) that reside in the same asymmetric unit.

Symmetry Operators:

(	1)		+X	,	+Y	,	+Z	(	2)	1/2-X	, -Y , 1/2+Z
(	3)	1/2+X	, 1/2-Y	,	-Z	(	4)			-X	, 1/2+Y , 1/2-Z

Part Two:

Synthesis and *E–Z* Isomerization Kinetics of a New Disilene*

A.1 Introduction

Chemists have been intrigued with the synthesis of a compound containing a double bond between two silicon atoms for nearly a century.[1,2,3] In 1911, Kipping synthesized a compound thought to be a disilene ($R_2Si{=}SiR_2$) by the reductive Wurtz-type coupling of a tetravalent dichlorosilane derivative[4]; however, the products of this and related reactions were later shown to be cyclic oligosilanes containing only single bonds.[5] Such results raised serious doubt as to whether stable disilenes could exist. Other unfruitful efforts directed toward the synthesis of compounds containing doubly bonded silicon, phosphorus, and arsenic contributed to a widely held belief that elements of the second and subsequent rows of the periodic table did not participate in $p\pi$–$p\pi$ bonding (the so-called "double bond rule"[2]). Disilenes remained in the class of "nonexistent compounds" until the late 1960s.[6] In 1969, Roark and Peddle provided evidence for the existence of a disilene as a reactive intermediate in the thermolysis of the compounds shown in Scheme A.1 with anthracene, isolating a Diels–Alder adduct of tetramethyldisilene.[7] This result was corroborated by several other reports in the 1970s on the trapping of transient disilenes.[8]

---

*This section describes work carried out by the author in 1989 and 1990. Abbreviations used in the text for substituent groups: 1-Ad= 1-adamantyl; Dep= 2,6-diethylphenyl; Dip= 2,6-diisopropylphenyl; Dis= bis(trimethylsilyl)methyl; Dmp= 2,6-dimethylphenyl; Mes= mesityl (2,4,6-trimethylphenyl); Np= naphthalenide; Tip= 2,4,6-triisopropylphenyl; TMS= trimethylsilyl.

Scheme A.1

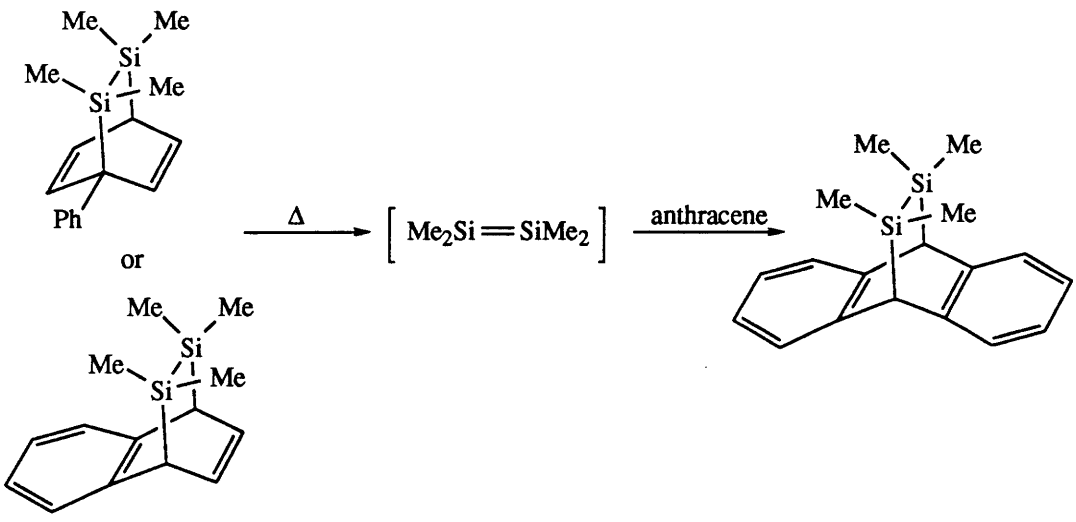

The independent isolations of the first stable disilenes reported by West[9] in late 1981 and by Masamune[10] in early 1982 led to an extensive exploration of the chemistry of Group 14 dimetallenes. In the last decade, a number of disilene derivatives have yielded to synthesis, and their spectroscopic properties, molecular structures, and reactions have been studied in detail. The isolated disilenes possess bulky aromatic or aliphatic substituents which shield the double bond from polymerization. The West synthesis involved the ultraviolet irradiation of linear trisilane **1** (Scheme A.2) while the approach developed in the

Scheme A.2

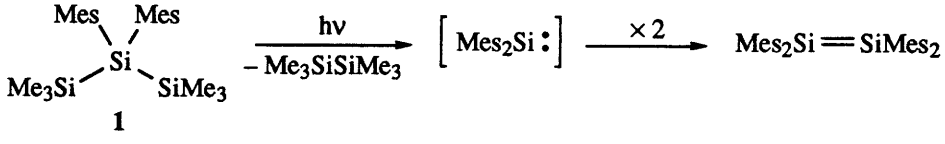

Masamune group employed cyclotrisilane **2** (the first three-membered cyclosilane) as a photolytic disilene precursor (Scheme A.3). Both methods involved the dimerization of divalent silicon intermediates (carbene analogues, or silylenes). Photolysis of one equivalent of the cyclotrisilane presumably produced one equivalent each of the disilene **3**,

Scheme A.3

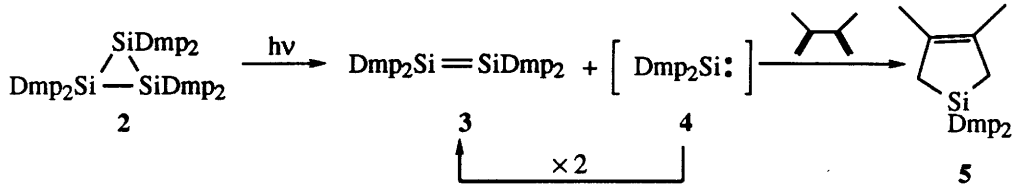

and silylene **4**, which dimerized to give another equivalent of **3**. The formation of a silylene was confirmed by trapping with 2,3-dimethyl-1,3-butadiene, yielding the cycloadduct **5**.

The development of digermene and distannene chemistry followed suit. In 1972 and 1976 (before the disilene syntheses described above), Lappert and co-workers described in preliminary form the preparations of the first distannene, **8**, and digermene, **9** (Scheme A.4), formed by dimerization of divalent intermediates **6** and **7** which were in

Scheme A.4

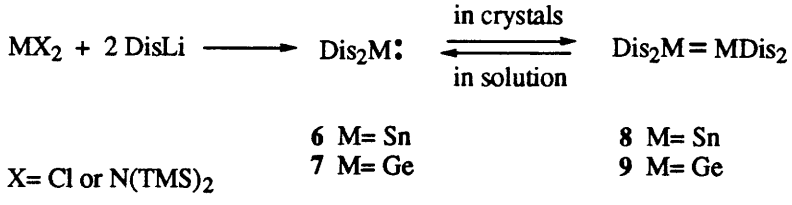

turn constructed from stable divalent tin and germanium compounds.[11] X-Ray crystallographic analysis confirmed the dimeric nature of Lappert's dimetallenes, but in solution, dissociation to the (monomeric) metallylenes **6** and **7** was observed. In 1982, the same year the near-quantitative photoconversion of a cyclotrisilane to a disilene was published, Masamune also reported the analogous synthesis of a three-membered cyclogermane and evidence for its photochemical cleavage to a digermene (Scheme A.5).[12] Although this digermene, **10**, bearing 2,6-dimethylphenyl substituents, could not be completely purified, its *solution* ^{1}H NMR and UV spectra were consistent with a dimeric structure.

Scheme A.5

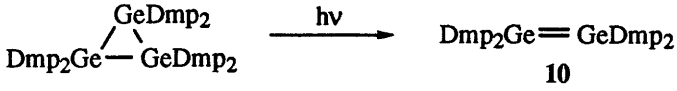

The first molecular structure of a digermene that retained its structural integrity in solution was obtained for tetrakis(2,6-diethylphenyl)digermene (**11**) in 1984.[13] This digermene was also synthesized by photolysis of a cyclotrigermane and exhibited spectral properties consistent with a double bond formulation. The reactions of both **10** and **11** with methanol to afford 1-methoxydigermane derivatives **12** and **13** provided additional evidence for their retention of structural integrity in solution (Scheme A.6). This result

Scheme A.6

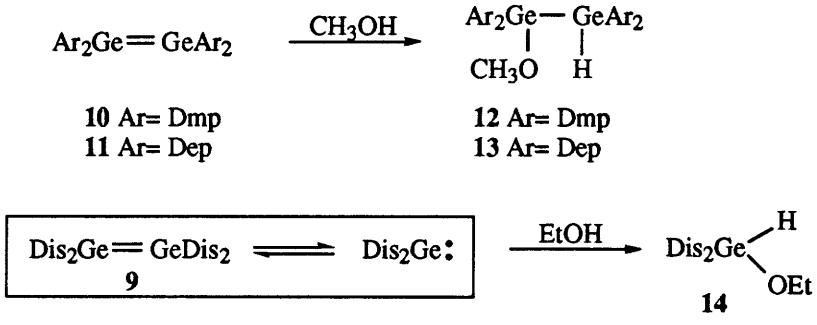

contrasts with the ethanolysis of Lappert's digermene **9**, which gave bis[bis(trimethylsilyl)methyl]germane ethoxide **14**, presumably arising from an insertion reaction of the corresponding singlet germylene.

In 1985, Masamune and Sita reported the synthesis of **16**, a new distannene

Scheme A.7

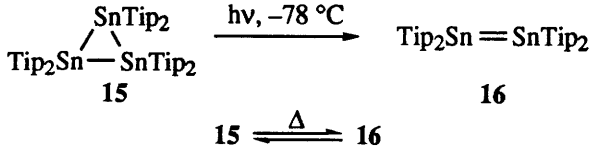

(Scheme A.7).[14] This compound exhibited a facile thermal rearrangement back to the cyclotristannane (**15**) from which it was photolytically derived, precluding X-ray crystallographic analysis. More importantly, **16** yielded to spectral characterization in solution and was shown to fully retain its dimeric structure.

The cyclotrimetallanes possessed unique molecular frameworks in their own right and had clearly proven to be valuable precursors to dimetallenes for the silicon, germanium, and tin cases. These three-membered rings were synthesized via the reductive coupling and cyclization of tetravalent dichloro(mono)metallanes by lithium naphthalenide in DME (Scheme A.8), a variation of the original method for the synthesis of

Scheme A.8

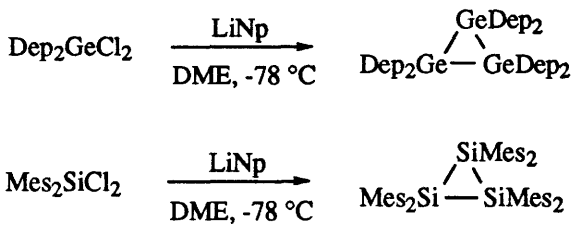

cyclopolysilanes developed by Kipping. This reaction is sensitive to the nature of the organic substituents on the metal: for both silicon and germanium, one of the substituents on the dichloro(mono)metallane precursor must be either a 2,6-dimethylphenyl-, a mesityl-, or a 2,6-diethylphenyl- moiety for successful cyclotrimerization. Smaller substituents, such as phenyl, lead to the formation of larger cyclooligomers.

Interestingly, the use of bulkier groups such as 2,6-diisopropylphenyl- or 2,4,6-triisopropylphenyl- on the dihalo(mono)silanes and -germanes leads directly to the

Scheme A.9

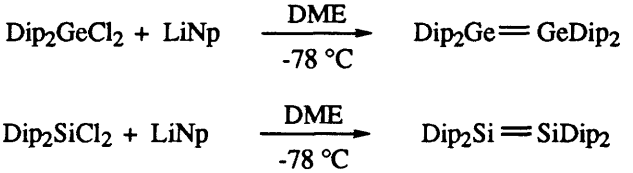

formation of disilenes and digermenes, without detection of the intermediate cyclotrimetallanes (Scheme A.9). The syntheses of a tetraaryldisilene[15] and two new tetraaryldigermenes[16,17] by the reductive coupling of dichloro(mono)metallanes were documented in 1987 and 1989 respectively. In 1987, workers in the Masamune group prepared the first stable tetraalkyldisilene, tetrakis[bis(trimethylsilyl)methyl]disilene, from the direct reductive coupling of the substituted diiodo(mono)silane derivative using lithium naphthalenide.[18]

Scheme A.10

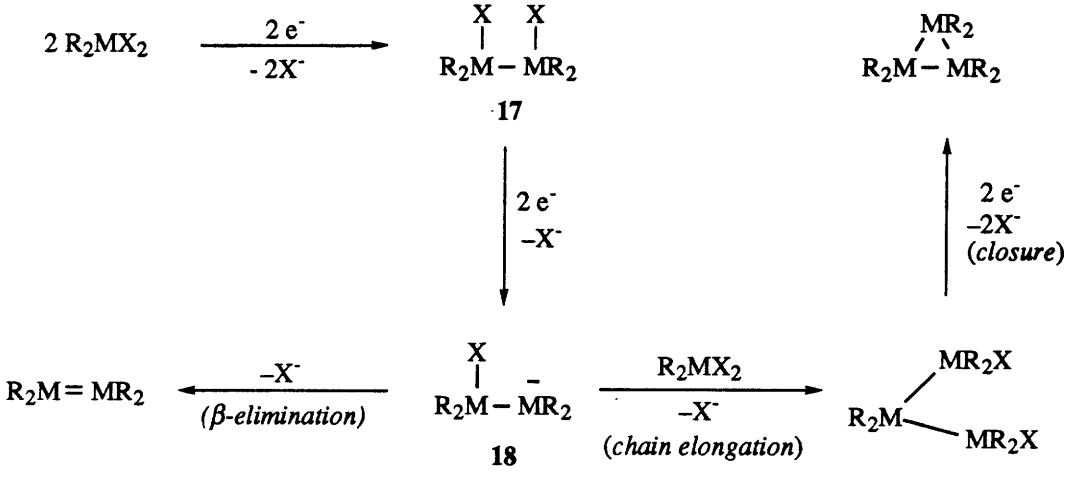

The reductive coupling method has provided a useful pathway to some exceptionally hindered dimetallenes, for which the analogous three-membered rings were not accessible. Assuming a linear chain elongation mechanism, the outcome of these reactions may be explained in terms of the steric bulk of the ligands attached to the metal atoms.[16] The likely intermediate **18** resulting from further reduction of a 1,2-dihalodimetallane **17** may follow one of two pathways (Scheme A.10): (1) β-elimination, or (2) chain elongation by reaction with another molecule of dihalo(mono)metallane. β-elimination is preferred in the reductive coupling of dichloro[bis(2,6-diisopropylphenyl)]germane, and chain elongation occurs with dichloro[bis(2,6-

diethylphenyl)]germane. For the latter compound, cyclization is apparently enforced at the trimetallane stage and cyclotrimetallanes are formed (Thorpe–Ingold effect).[19]

Disilenes and digermenes are isolated as highly air- and moisture-sensitive yellow to orange crystals, some of which exhibit thermochromicity. Maximum electronic absorptions are observed at 420–430 nm for tetraaryldisilenes and 410–420 nm for tetraaryldigermenes; hypsochromic shifts are observed upon alkyl substitution. X-Ray crystal structures have been solved for several disilenes and digermenes (Table A.1). The

Table A.1 Selected Structural Parameters of Double-Bond Systems ($R^1R^2M{=}MR^1R^2$)

Cpd.	M	R^1	R^2	d(M=M)/ Å	Fold angle α/ °	Twist angle θ/ °	Ref.
19[a]	Si	Mes	Mes	2.16	18	12	35
19	Si	Mes	Mes	2.14	10, 13	3	35
20[b]	Si	Mes	^{t}Bu	2.14	0	0	36
21[b]	Si	Mes	1-Ad	2.14	3	0	31
22	Si	Dep	Dep	2.14	0	10	36
23	Si	Tip	Tip	2.14	0	3	15
11	Ge	Dep	Dep	2.21	12	10	13
24[c,d]	Ge	Mes	Dip	2.30	36	7	30
9	Ge	Dis	Dis	2.35	32	0	21
8	Sn	Dis	Dis	2.77	41	0	21

[a]The crystal contains toluene. [b]*E*-isomer. [c]The crystal contains THF. [d]*Z*-isomer.

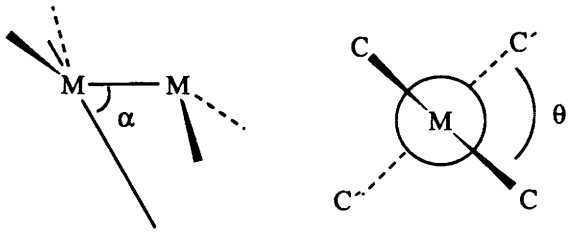

Fold angle Twist angle

Si=Si distances for compounds **19–23** are all close to 2.14 Å, representing an approximately 8.5% compression from the normal Si-Si single bond distance. In **20**, **22**, and **23**, each silicon atom and the three atoms directly attached to it are coplanar, much like

the structural arrangement around each sp^2-hybridized carbon in alkenes. The silicon atoms in **19** and **21**, however, exhibit small pyramidal distortions, as evidenced by fold (or "*trans*-bent") angles from the plane of about 10° and 3° respectively. Another type of distortion is apparent in **19**, **22**, and **23**, in which all four Si-Ar bonds are not coplanar and small dihedral "twist" angles exist between the C-Si-C and C′-Si′-C′ planes. In those cases where geometrical isomerism was possible, the *E*-disilenes were more thermally stable.

Germanium-germanium bond distance in the digermenes listed in Table A.1 range from 2.21 Å to 2.35 Å, corresponding to bond shortenings of 4 to 10% from typical Ge-Ge single bond distances. The germanium atoms in the digermenes are pyramidalized, with fold angles ranging from 12° for **11**, the germanium analogue of **22**, to 36° for **24**, a considerably distorted digermene. Additionally, dihedral twist angles exist for **24** (7°) and **11** (10°) but not for **9**. Although **24** is somewhat more *trans*-bent than Lappert's digermene **9** (fold angle= 32°), it does not dissociate in solution. Surprisingly, the thermodynamic isomer of **24** is the *Z*-isomer; this unexpected preference is probably a phenomenon of its *trans*-bent geometry.

The existence of nonplanar *trans*-bent structures for certain dimetallenes indicates that the orbital description of the metal-metal double bond is not the same as that for carbon-carbon double bonds. In a valence bond approach, Trinquier and Malrieu[20] assume

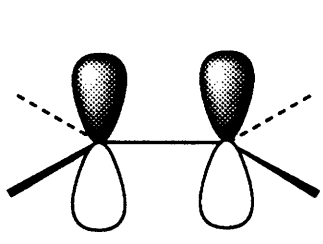

25

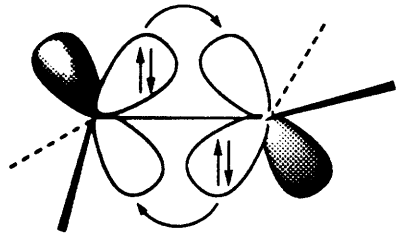

26

that the distorted dimetallene is built from interacting singlet metallylenes with dative bent bonds. The n_σ pair of one species is partially delocalized into the empty p_π atomic orbital

of the other (**26**). The deviation from planarity was shown to depend on the singlet–triplet energy separation (ΔE_{ST}) of the metallylene. A classical planar $\sigma + \pi$ double bond (**25**), which requires the interaction of triplet states, cannot be formed when the singlet configuration is much more stable than the triplet configuration. For a symmetrical homopolar system $R_2M{=}MR_2$, the *trans*-bent geometry occurs when $1/4\ E_{\sigma+\pi} \leq \Delta E_{ST} < 1/2\ E_{\sigma+\pi}$, where $E_{\sigma+\pi}$ represents the $\sigma + \pi$ energy of the double bond. Beyond the critical value of $1/2\ E_{\sigma+\pi}$, no double bond would exist. This prediction is borne out for SiF_2 and GeF_2, which have very large singlet–triplet separations and adopt doubly bridged dimeric structures rather than M=M double bonds. Table A.2 presents the expected structures of

Table A.2 Singlet-Triplet Separations in XH_2 versus X=X Bond Energies[a]

	ΔE_{ST}	$1/4\ E_{\sigma+\pi}$	$1/2\ E_{\sigma+\pi}$	expected structure
$H_2C{=}CH_2$	–9	43	86	planar
$H_2Si{=}SiH_2$	18–21	18–19	35–38	*trans* bent (borderline)
$H_2Ge{=}GeH_2$	22	15–17	30–35	*trans* bent
$H_2Sn{=}SnH_2$	23	15–17	30–35	*trans* bent
$H_2Pb{=}PbH_2$	41	12–15	25–30	doubly bridged

[a]In kcal/mol. This Table is taken from: Trinquier, G. *J. Am. Chem. Soc.* **1990**, *112*, 2130.

ethene and the parent dimetallenes based on estimates of ΔE_{ST} and $E_{\sigma+\pi}$. The *trans*-bent geometry is slightly favored for disilene. It is likely that the planar Si=Si bonds observed in disilenes **20**, **22**, and **23** arise from preferences due to packing in the crystal lattice or steric repulsion of the bulky ligands in the *trans*-bent geometry.

In a molecular orbital scheme, bending introduces two opposing effects: a weakening of the σ and π MOs and a stabilizing mixing of orbitals: σ with π^* and π with σ^*. If the latter interactions are large, the stabilizing effect will outweigh the weakening of the σ and π bonds.[20b,21] This is apparently the case for digermenes **9**, **11**, and **24**. The π–σ^* energy separation is much smaller in parent digermene ($H_2Ge{=}GeH_2$) than in ethene

owing to (1) the larger $n\sigma$–$p\pi$ separation in the germylene (which is proportional to its larger ΔE_{ST}) and (2) weaker π-bonding in digermene.[20a] Other researchers contend that disilene and digermene have such small π–σ^* separations that substituent electronegativity plays the major role in determining the degree of orbital mixing and hence the double bond geometry.[22] Modifications of these arguments are necessary when larger and π-conjugating substituents are considered.

Disilenes and digermenes readily take part in 1,2-addition and cycloaddition reactions, many of which afford novel three- and four-membered ring systems containing two silicon or germanium atoms (Scheme A.11).[1] The course of dimetallene oxidation has

Scheme A.11

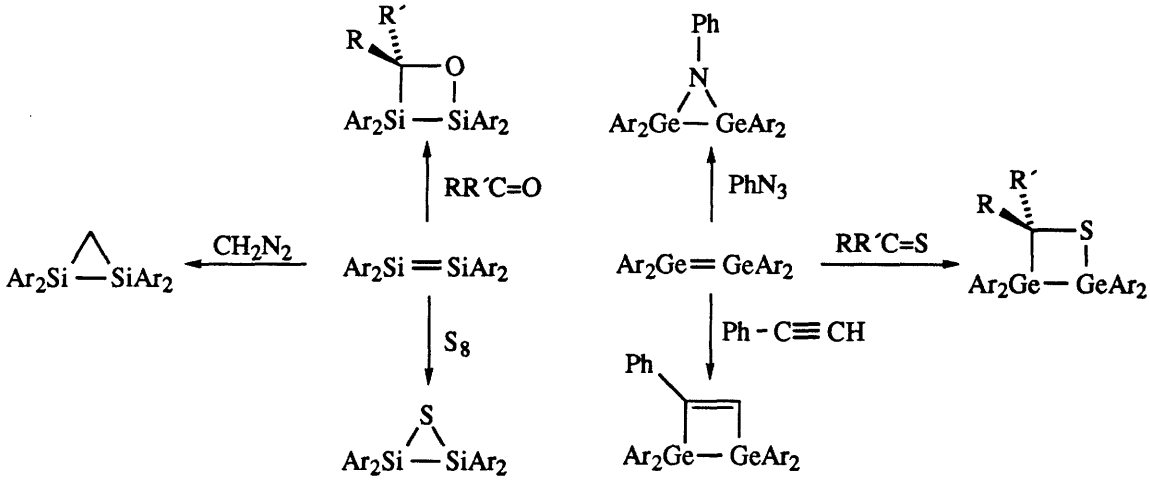

in particular received much attention.[3] η^2-Disilene complexes of platinum, molybdenum, and tungsten have also recently been prepared.[23]

The areas of dimetallene synthesis, characterization, crystallographic structure elucidation, and reactivity have provided many challenges since the early 1980s. Another important objective that has merited significant efforts in the Masamune group and others is the evaluation of the activation energy required for thermal *E*–*Z* isomerization, which is normally equated to the so-called π-energy of the M=M bond. To date, several disilene and digermene derivatives of the type $R^1R^2M{=}MR^1R^2$ ($R^1{\neq}R^2$) have been isolated, and the

rates for some of their *E–Z* thermal interconversions have been measured. When the work for this thesis was begun in October 1989, workers in the Masamune group had already completed the *E–Z* isomerization kinetics experiments for two disilenes and a digermene, and obtained activation parameters for the barrier to rotation in these compounds. Section A.2 includes a presentation of the theory behind the kinetics experiments and a reinvestigation of the isomerization kinetics for one of the disilenes. Section A.3 is devoted to the synthesis and isomerization kinetics of a new disilene, which bears the same substituents as the digermene isomers already examined. These efforts were directed towards drawing some generalizations about the strength of the π-bond in disilenes and digermenes.

A.2 Background and New Kinetics Results for Disilene 29

In 1984, the Masamune[24] and West[25] groups independently carried out the first *E–Z* isomerization kinetics experiments for a pair of disilenes, *E*- and *Z*-**20**, in order to evaluate the strength of the π bond (i.e., the barrier to rotation). The isomer concentrations were determined by ^{1}H NMR spectroscopy. The experiments for **20** indicated a first order

Table A.3 Kinetics Parameters for the *E–Z* Isomerization of **20**

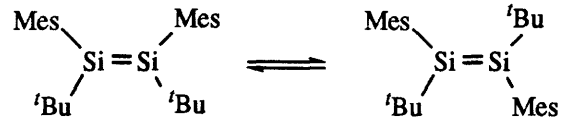

Z-**20** ⟷ *E*-**20**

Source	$\Delta H^{\ddagger}_{Z\rightarrow E}$[a]	$\Delta S^{\ddagger}_{Z\rightarrow E}$[b]	$\Delta H^{\ddagger}_{E\rightarrow Z}$[a]	$\Delta S^{\ddagger}_{E\rightarrow Z}$[b]
Masamune[24]	23	−8 to −12	28	−13 to −17
West[25]	31	+11		
	(33)[c]	(+19)[c]		

[a]In kcal/mol. [b]In eu. [c]Data from West recalculated according to the Eyring formula, using the rate constants measured at the highest and lowest temperatures.

E–Z isomerization mechanism, but the West and Masamune groups derived different values for some of the activation parameters (Table A.3). An analogous isomerization experiment was desired for a tetraaryl-substituted disilene, since it had been decided that the digermene *E–Z* kinetics experiments to follow would also be performed on tetraaryl-substituted derivatives. In 1987, disilenes *E*- and *Z*-**29** were synthesized by the photolysis of *cis,cis*- or *cis,trans*-cyclotrisilanes **27** and **28** (Scheme A.12).[17] Photolysis of the *cis,cis*-

Scheme A.12

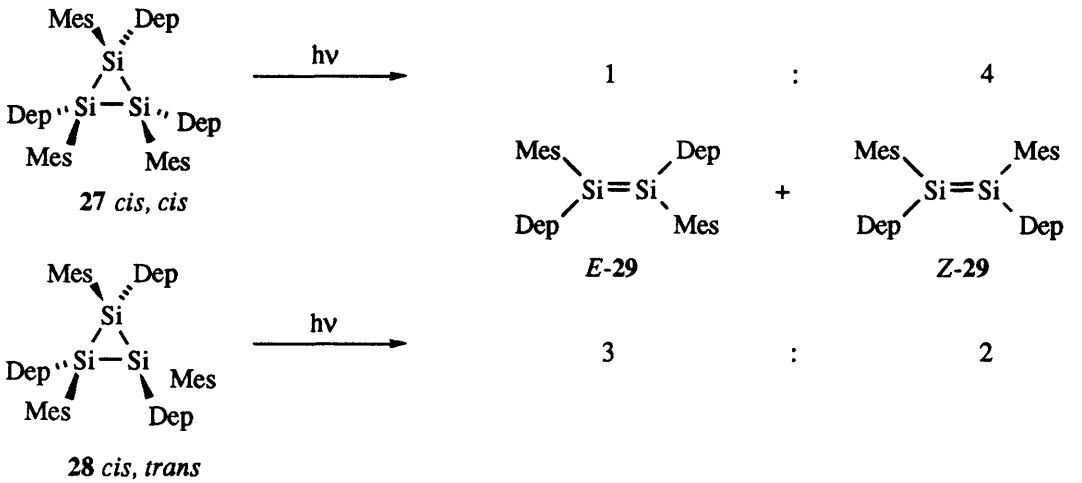

cyclotrisilane **27** produced a ca. 4:1 ratio of isomeric disilenes, whereas the *cis,trans* isomer **28** generated the same two disilenes in a ratio of about 2:3. Based on straightforward stereochemical arguments concerning the cleavage patterns of *cis,cis*- and *cis,trans*-cyclotrisilanes, the initial major disilene isomer produced from **27** was presumed to be the *Z* isomer of **29**, and the other isomer, produced in slight excess from photolysis of **28**, was presumed to be *E*-**29**.

The results of the first isomerization kinetics experiments on disilene **29**, summarized in Table A.4, did not correspond well with either of the two determinations for the interconversion of *E*- and *Z*-**20** (see Table A.3). The values for the enthalpies of activation in Table A.4 were closer to 30 kcal/mol; the entropy terms were small positive

quantities, which differed from the negative values reported from the Masamune experiments, and were not as large as the positive values reported by West.

Table A.4 Original Kinetics Results[17] for Disilene **29**[a]

Temp./ K	K	Presumed $Z \rightarrow E$	Presumed $E \rightarrow Z$
337.1	0.97	$k_1 = (1.04 \pm 0.03) \cdot 10^{-5}$ s^{-1} $\Delta G^{\ddagger} = 27.5 \pm 0.1$ kcal mol^{-1}	$k_{-1} = (1.07 \pm 0.03) \cdot 10^{-5}$ s^{-1} $\Delta G^{\ddagger} = 27.5 \pm 0.1$ kcal mol^{-1}
359.8	0.83	$k_1 = (1.57 \pm 0.04) \cdot 10^{-4}$ s^{-1} $\Delta G^{\ddagger} = 27.5 \pm 0.1$ kcal mol^{-1}	$k_{-1} = (1.89 \pm 0.05) \cdot 10^{-4}$ s^{-1} $\Delta G^{\ddagger} = 27.3 \pm 0.1$ kcal mol^{-1}
		$\Delta H^{\ddagger} = 28.1 \pm 0.6$ kcal mol^{-1} $\Delta S^{\ddagger} = 1.9 \pm 1.6$ eu	$\Delta H^{\ddagger} = 29.8 \pm 0.6$ kcal mol^{-1} $\Delta S^{\ddagger} = 6.8 \pm 1.6$ eu
		$\Delta H^{\circ} = 1.6 \pm 0.3$ kcal mol^{-1} $\Delta S^{\circ} = -0.3 \pm 0.1$ eu	

[a]Errors in rate constants were obtained from the standard deviations of the slopes of the lines when plotting Eq. 5.

The isomerization kinetics for disilenes *E*- and *Z*-**29** were investigated again in early 1990 under improved conditions. Notably, a purified disilene was used instead of a photolyzed mixture. The crude disilenes (obtained from the photolysis of *trans*-cyclotrisilane **28**) were recrystallized from methylcyclohexane to afford a 20:1 mixture favoring the the thermodynamically more stable isomer of **29**, presumably the *E* isomer. The crystals were about 95% pure, with the cyclotrisilane as a minor impurity. The earlier experiment involved photolysis of the *cis,cis*-cyclotrisilane **27**, which generated a 4:1 mixture of disilenes favoring the thermodynamically *less* stable isomer, presumably *Z*-**29**.

A second advantage of the new experiments was the use of the Varian VXR500 (500 MHz) NMR spectrometer instead of the 300 MHz instrument. A major requirement of the kinetics experiment is that the two isomers of each dimetallene pair be clearly distinguishable from each other and from the background to the extent that their concentrations in solution can be accurately calculated. The concentrations of the disilene

isomers were followed by integration of the strong and sharp *meta*-hydrogen singlets of the mesityl group. The 500 MHz spectrometer provided the greatest resolution of the very similar chemical shifts arising from the two isomers of the disilene.

Toluene-d_8 was chosen as a solvent for the present study. In the earlier experiment[17], methylcyclohexane-d_{14} had been used because of its transparency to ultraviolet radiation. Unexpectedly, toluene drew the isomer peaks closer together in all regions of the spectrum; nevertheless, the 500 MHz spectrometer was able to sufficiently resolve the peaks in the mesityl-*meta*-hydrogen region of the spectrum. It seems unlikely that any considerable differences between the two determinations would arise solely on the basis of solvation effects of toluene vs. methylcyclohexane.

The new kinetics experiments closely followed a standard procedure developed earlier.[17] Two kinetics runs were performed at approximately 64 °C and 87 °C, with periods of 50% equilibration (hitherto referred to as *equilibration half-time*) of about 8 h and 40 min, respectively. After the initial ratio of isomers was measured by ^{1}H NMR at room temperature, the sample (in a sealed NMR tube with degassed toluene-d_8 and 1 μL of hexamethyldisilane as an internal standard) was completely immersed into an ethylene glycol constant temperature bath as a stopwatch was simultaneously started. When a data point was required, the disilenes were removed from the hot bath and flash-cooled as quickly as possible in an ice–water bath as the timer was stopped. The sample was subsequently equilibrated to room temperature and placed in the NMR probe. The heating periods were repeated as described above. About fifteen timed data measurements were taken in each run until equilibrium was achieved. The integrations were carefully measured from the mesityl-*meta*-hydrogen region (6.5–6.7 ppm)[26] on an expanded scale spectrum, giving the ratio of isomer concentrations for each data point. Fewer data measurements (ca. 10 to 12) were taken during the first four isomerization half-times in order to minimize the error introduced by the repeated cooling and heating of the sample. We assumed that equilibrium had been established when (1) three consecutive isomer ratios taken at least 0.5

equilibration half-times apart were approximately equal and (2) at least ten equilibration half-times, representing a 99.9% degree of completion for a first-order equilibration process, had passed since the commencement of the experiment.

The kinetic description of the equilibrium between *E* and *Z* disilene isomers is given in Eq. 1, and this relationship generates the rate expression in Eq. 2.[27] The total concentration of disilenes, which remains constant throughout the equilibration, is

$$\mathbf{Z} \underset{k_{-1}}{\overset{k_1}{\rightleftharpoons}} \mathbf{E} \qquad \text{(Eq. 1)}$$

$$\frac{d[\mathbf{Z}]}{dt} = -k_1[\mathbf{Z}] + k_{-1}[\mathbf{E}] \qquad \text{(Eq. 2)}$$

$$N = [\mathbf{Z}] + [\mathbf{E}] \qquad \text{(Eq. 3)}$$

$$K = \frac{k_1}{k_{-1}} \qquad \text{(Eq. 4)}$$

$$\ln([\mathbf{Z}] - [\mathbf{Z}]_\infty) - \ln([\mathbf{Z}]_0 - [\mathbf{Z}]_\infty) = -(k_1 + k_{-1})t \qquad \text{(Eq. 5)}$$

represented by *N* (Eq. 3). The equilibrium constant *K* for the overall process in Eq. 1 is defined in Eq. 4. The rate expression in Eq. 2 can be integrated and further simplified to give the first-order equilibration function in Eq. 5. In this equation, $[\mathbf{Z}]_0$ and $[\mathbf{Z}]_\infty$ represent the initial and equilibrium concentrations, respectively, of the *Z* isomer. Eq. 5 shows the linear relationship between elapsed time and the natural logarithm of a function of the concentration. If the experimental data are plotted with time as the abscissa and $\ln([\mathbf{Z}] - [\mathbf{Z}]_\infty)$ as the ordinate, the data should approximate a straight line if the mechanism is first order. The slope of the line, *m*, is given in Eq. 6, and by combining this expression with the definition of the equilibrium constant in Eq. 4, an equation can be derived that permits the calculation of the actual rate constants (Eq. 7).

$$m = -(k_1 + k_{-1}) \qquad \text{(Eq. 6)}$$

$$k_1 = \frac{-mK}{K+1} \qquad \text{(Eq. 7)}$$

According to transition state theory, a rate constant may be translated into the free energy of activation $\Delta G^{\ddagger}$ by Eyring's formula (Eq. 8).[28] This equation contains

$$\Delta G^{\ddagger} = -RT \ln\left(\frac{kh}{\kappa k_B T}\right) \qquad \text{(Eq. 8)}$$

$$\Delta G^{\ddagger} = \Delta H^{\ddagger} - T\Delta S^{\ddagger} \qquad \text{(Eq. 9)}$$

$$\Delta S^{\ddagger} = \frac{\Delta H^{\ddagger}}{T} + R \ln\left(\frac{kh}{\kappa k_B T}\right) \qquad \text{(Eq. 10)}$$

$$\Delta H^{\ddagger} = R \frac{T_1 T_2}{T_2 - T_1} \ln\left(\frac{k_2 T_1}{k_1 T_2}\right) \qquad \text{(Eq. 11)}$$

four important physical constants—the Boltzmann constant k_B, Planck's constant h, the gas constant R and a transmission coefficient κ. This last value is specific to the process being followed, and is generally assumed to be equal to one.[28] When two different values of $\Delta G^{\ddagger}$ for the same reaction are determined (*via* two different rate constants) at two different temperatures, the definition of $\Delta G^{\ddagger}$ (Eq. 9) permits values to be calculated for $\Delta H^{\ddagger}$ and $\Delta S^{\ddagger}$, which are assumed to be independent of temperature. The entropy of activation can be calculated via Eq. 10, which may be derived by replacing $\Delta G^{\ddagger}$ in Eq. 8 with the argument of Eq. 9 and solving for $\Delta S^{\ddagger}$. If the two values for $\Delta G^{\ddagger}$, their corresponding rate constants (k_1 and k_2), and values of temperature (T_1 and T_2) are incorporated into Eqs. 8 and 9, the system can be solved for $\Delta H^{\ddagger}$ in terms of the rate constants and temperatures (Eq. 11), which are obtained directly from the experimental data. The evaluation of errors for these thermodynamic activation parameters is discussed in detail in other works and will not be addressed here.[17,28]

Plots of [**E**]/*N* vs. *t* for both runs are shown in Figures A.1 and A.2. These plots are both apparently logarithmic as expected, and do not indicate the presence of any

Figure A.1 Concentrations of *Z*- and *E*-**29** vs. *t* at 63.9 °C

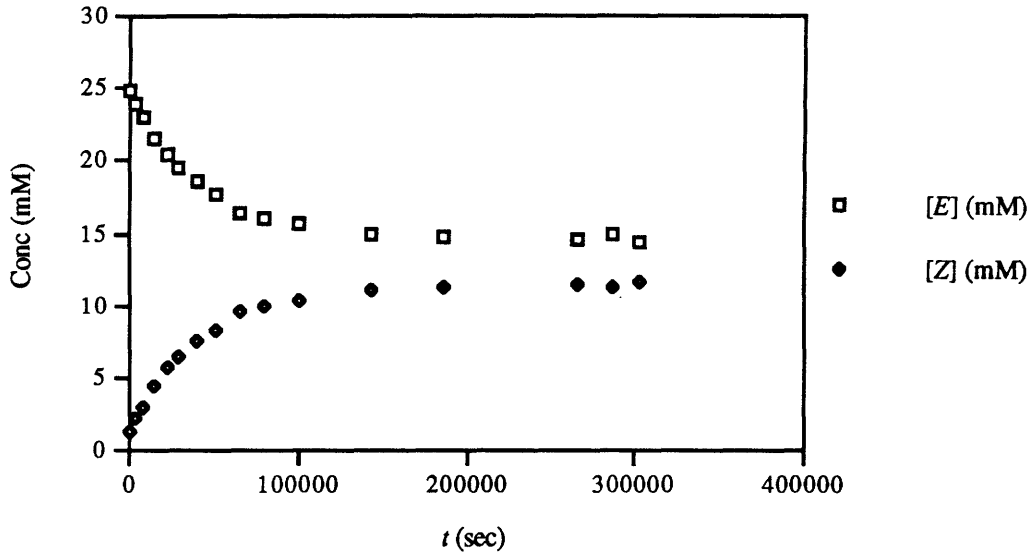

Figure A.2 Concentrations of *Z*- and *E*-**29** vs. *t* at 86.5 °C

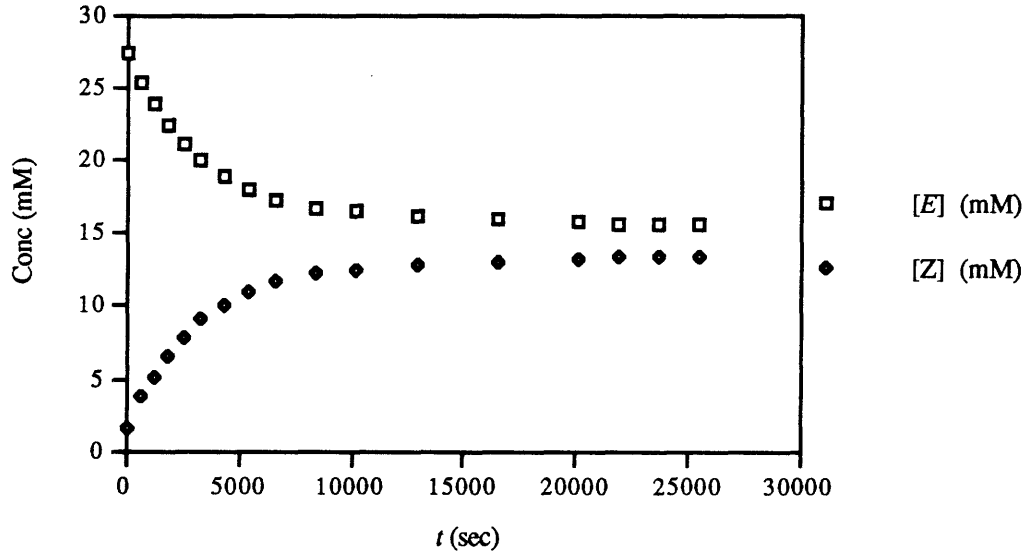

unusual phenomena. Plots of the data as calculated according to Eq. 5 ($\ln([\mathbf{E}] - [\mathbf{E}]_\infty)$ vs. *t*) for both runs are given in Figures A.3 and A.4, showing the expected linear relationship between these functions and verifying the apparent first order behavior of this

Figure A.3 First Order Plot for *E*-**29** vs. *t* at 63.9 °C

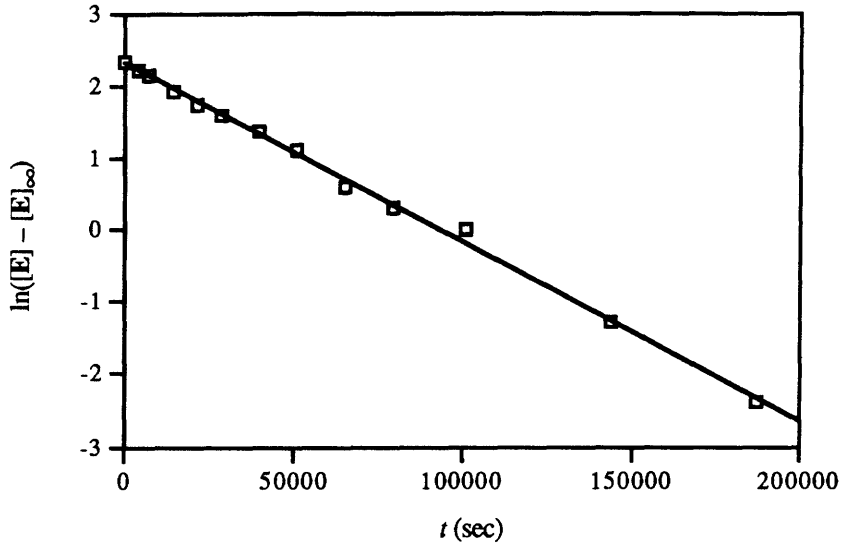

Figure A.4 First Order Plot for *E*-**29** vs. *t* at 86.5 °C

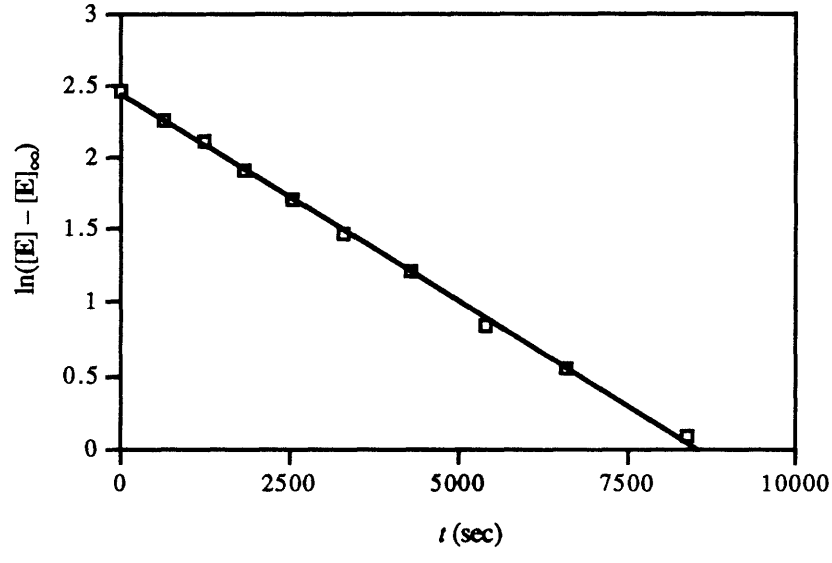

isomerization. In creating these latter two plots, data points at or near equilibrium have been omitted because errors in the values of the ordinate function become extremely high as [**E**]/*N* approaches [**E**]$_\infty$/*N*, where [**E**]$_\infty$ represents the equilibrium concentration of the *E*-disilene. The activation parameters and other values derived from the plots and further calculations are presented in Table A.5. Also included are values for the free energies of

reaction $\Delta G°$ at both temperatures, which can be calculated from the equilibrium constant K according to Eq. 12, and the enthalpy and entropy of reaction, $\Delta H°$ and $\Delta S°$, as calculated from Eqs. 13 and 14. The raw data from this kinetics experiment is provided in the Experimental section.

$$\Delta G° = -RT\ln K \qquad \text{(Eq. 12)}$$

$$\Delta H° = R\frac{T_1 T_2}{T_2 - T_1}\ln\left(\frac{K_{T_2}}{K_{T_1}}\right) \qquad \text{(Eq. 13)}$$

$$\Delta S° = \frac{\Delta H°}{T_1} + R\ln K_{T_1} \qquad \text{(Eq. 14)}$$

Table A.5 New Kinetics Results for Disilene **29**[a]

Temp./ K	K	Presumed $Z \rightarrow E$	Presumed $E \rightarrow Z$
337.1	1.29	$k_1 = (1.35 \pm 0.05)\cdot 10^{-5}$ s^{-1}	$k_{-1} = (1.05 \pm 0.03)\cdot 10^{-5}$ s^{-1}
		$\Delta G^{\ddagger} = 27.3 \pm 0.1$ kcal mol^{-1}	$\Delta G^{\ddagger} = 27.5 \pm 0.1$ kcal mol^{-1}
359.7	1.17	$k_1 = (1.59 \pm 0.03)\cdot 10^{-4}$ s^{-1}	$k_{-1} = (1.37 \pm 0.02)\cdot 10^{-4}$ s^{-1}
		$\Delta G^{\ddagger} = 27.4 \pm 0.1$ kcal mol^{-1}	$\Delta G^{\ddagger} = 27.5 \pm 0.1$ kcal mol^{-1}
		$\Delta H^{\ddagger} = 25.6 \pm 0.8$ kcal mol^{-1}	$\Delta H^{\ddagger} = 26.7 \pm 0.8$ kcal mol^{-1}
		$\Delta S^{\ddagger} = -5.0 \pm 2.5$ eu	$\Delta S^{\ddagger} = -2.4 \pm 2.5$ eu
		$\Delta H° = -1.1$ kcal mol^{-1}	$\Delta G°_{337.1} = -0.17$ kcal mol^{-1}
		$\Delta S° = -2.8$ eu	$\Delta G°_{359.7} = -0.11$ kcal mol^{-1}

[a]Errors in rate constants were obtained from the standard deviations of the slopes of the lines in Figures A.3 and A.4 and the calculated errors in K.

The values of $\Delta G^{\ddagger}$ obtained in this experiment are very similar to those from the earlier experiment (see Table A.4). The new $\Delta H^{\ddagger}$ parameters are approximately 3 to 4 kcal/mol smaller than the earlier values. Most interesting, however, are the new $\Delta S^{\ddagger}$ parameters: these are small negative numbers, differing from the earlier small positive

values. These new parameters for entropy of activation, however, have the same *sign* as the $\Delta S^{\ddagger}$ results for disilene **20**, although the new ones are somewhat smaller. They also share the same sign with and are close to the $\Delta S^{\ddagger}$ values from the isomerization kinetics of digermene **24** (Table A.6).

Table A.6 Kinetics Parameters[17,30] for the *E*–*Z* Isomerization of **24**

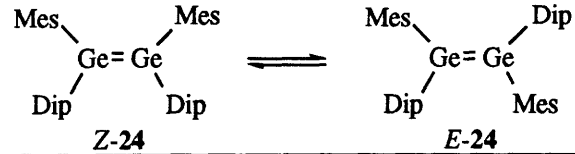

Z-**24** ⇌ *E*-**24**

$\Delta H^{\ddagger}_{Z\rightarrow E}$[a]	$\Delta S^{\ddagger}_{Z\rightarrow E}$[b]	$\Delta H^{\ddagger}_{E\rightarrow Z}$[a]	$\Delta S^{\ddagger}_{E\rightarrow Z}$[b]
22	–5	20	–10

[a]In kcal/mol. [b]In eu.

Additional experiments have also proven that the error introduced by the frequent heating and cooling of the sample during the high temperature kinetics run is negligible, and that the activation parameters obtained from this run are reproducible.[29] Because these experiments were carried out on the 500 MHz NMR spectrometer, used purified disilene, and featured fewer measurements during the first several isomerization half-times, we believe that the new results are more accurate than the earlier ones. The new entropy of activation parameters are more consistent with those from earlier dimetallene kinetics experiments.

A.3 Synthesis of a New Disilene

In late 1989 we planned to synthesize and perform *E*–*Z* isomerization kinetics experiments on a new disilene, **32**. This would provide the first opportunity to compare

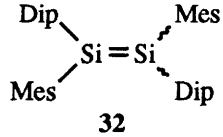

32

the activation barriers to isomerization for a disilene and digermene with the same substituents. A comparison of the activation parameters for disilene **32** with those of the previously studied disilenes **20** and **29** might also provide further insight into the consistency of the kinetics results, particularly with regard to the entropy of activation.

The synthesis and isomerization kinetics of digermene **24** was achieved by Scott Batcheller in 1987 (Table A.6); in May 1990 the crystal structure of that compound was solved by Dr. William Davis.[30] The *Z*-isomer of **24** was synthesized by reductive coupling of the substituted dichloro(mono)germane, and the synthesis of the silicon analogue **32** was expected to proceed in a similar manner. The preparation of disilenes by direct reductive coupling of the dihalo(mono)silanes was known (Section A.1).

After several troublesome attempts to synthesize the possible disilene precursor **31** starting with tetrachlorosilane, a higher-yielding route was chosen beginning with the

Scheme A.13 Synthesis of Disilene **32**

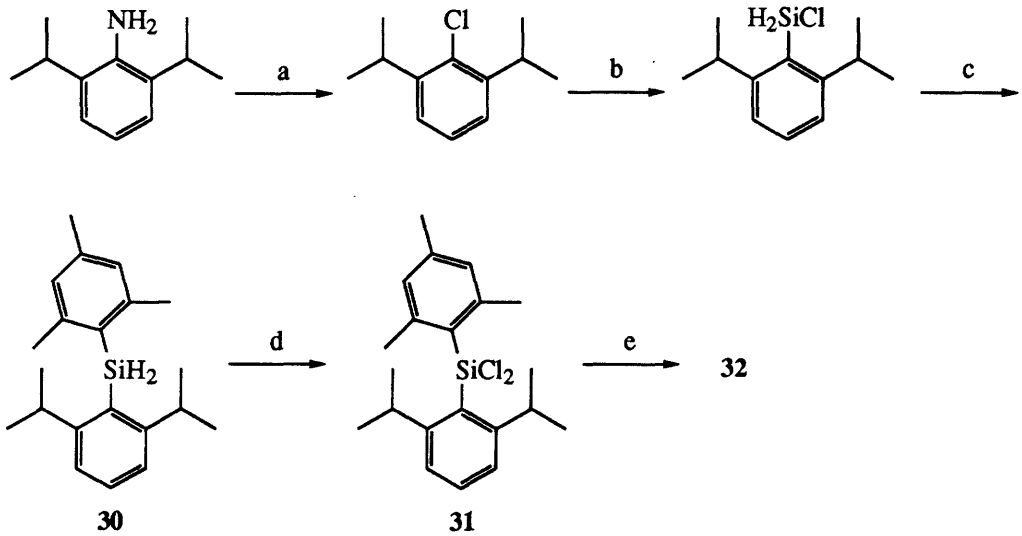

(a) $NaNO_2$, HCl, 0 °C then Cu, Δ, 40%; (b) i. Mg, THF, Δ; ii. H_2SiCl_2, Et_2O, -78 °C, 75%; (c) Mesityllithium, THF, -78 °C, 75%; (d) CCl_4, cat. $(PhCO_2)_2$, 93%; (e) Lithium naphthalenide, DME, -78 °C, 20%.

reaction of 2,6-diisopropylphenylmagnesium chloride with dichlorosilane (Scheme A.13). Mesityllithium, formed from 2-bromomesitylene and *t*-butyllithium, reacted smoothly with

the resulting 2,6-diisopropylphenylchlorosilane to give silane **30**, which was purified by column chromatography. **30** was successfully chlorinated in refluxing carbon tetrachloride with a catalytic amount of benzoyl peroxide, affording dichlorosilane **31**. When a solution of **31** in DME was added to two equivalents of lithium naphthalenide at –78 °C, a yellow-orange solid was obtained after removal of naphthalene and lithium salts. The mass and ^{1}H NMR spectra of this product indicated the presence of disilene **32**. This material also displayed a characteristic disilene electronic absorption at 430 nm. Disilene **32** was isolated as an orange solid in about 20% yield as a ca. 60:1 mixture of isomers. The major component was tentatively assigned as the *Z*-isomer for reasons that will become clear in Section A.4.

A.4 *E–Z* Isomerization Kinetics for Disilene 32

The isomerization kinetics experiments for new disilene **32** were expected to proceed in a similar fashion to those for disilene **29**, and this expectation was realized. The new disilene was washed with methylcyclohexane and brought very close to 100% purity. Again, the 500 MHz NMR spectrometer was employed to procure the best resolution and the most accurate results possible. A preliminary kinetics run indicated that the isomerization proceeded with an equilibrium half-time of two hours at 80 °C, so the actual experimental temperatures were planned to be about 70 °C and 90 °C, anticipating half-times of 400 and 40 minutes, respectively. The initial ratio of disilene isomers was about 60:1, and the equilibrium ratio of the same isomers was 1:1.2. The initially less abundant isomer was slightly *favored* in the equilibrium mixture, and we assumed this one to be the *E*-isomer. The kinetically preferred, isolated disilene isomer was presumed to be the *Z*-isomer, in analogy to its digermene counterpart. Because of the large difference between the initial and equilibrium ratios, the isomerization could be followed through a large range of isomer concentrations.

The kinetics experiment was carried out essentially as described in Section A.2, using toluene-d_8 as the solvent. In this experiment, the highest resolution was obtained from the mesityl-*para*-methyl proton resonances (1.99–2.06 ppm). The integrations were carefully measured from this region on an expanded scale spectrum, giving the ratio of isomer concentrations for each data point.

Figure A.5 Concentrations of *Z*- and *E*-**32** vs. *t* at 68.9 °C

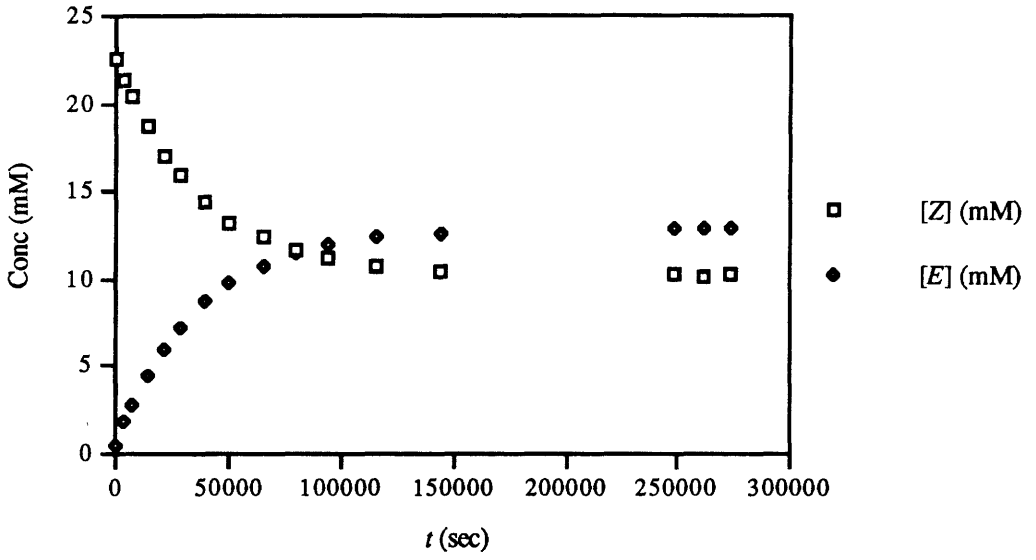

Figure A.6 Concentrations of *Z*- and *E*-**32** vs. *t* at 90.8 °C

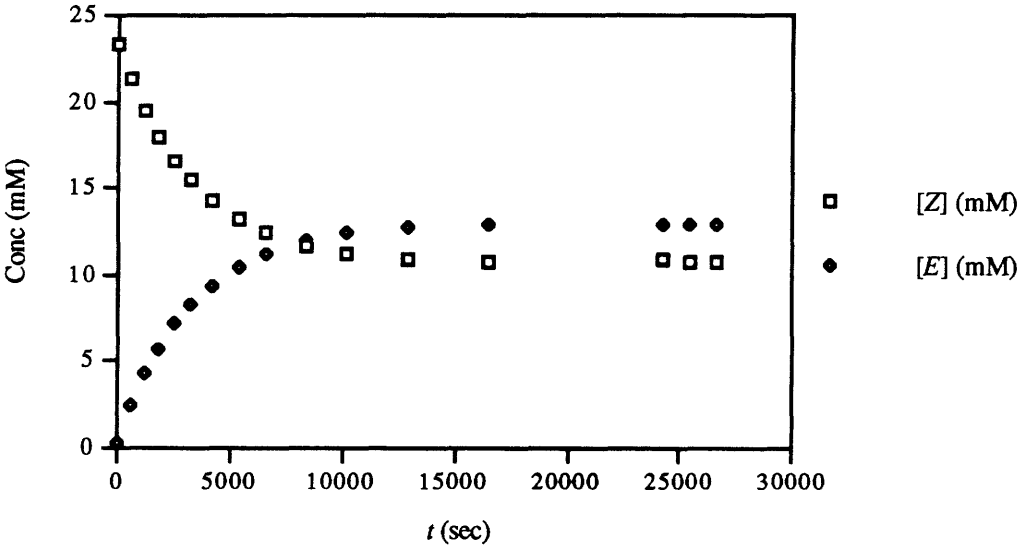

Plots of [**E**]/*N* and [**Z**]/*N* vs. *t* for both runs are shown in Figures A.5 and A.6. These plots are both logarithmic as expected, and do not indicate the presence of any unusual phenomena. Plots of the data as calculated according to Eq. 5 for both runs are given in Figures A.7 and A.8; the clean linearity verifies the first order behavior of this

Figure A.7 First Order Plot for *Z*-**32** vs. *t* at 68.9 °C

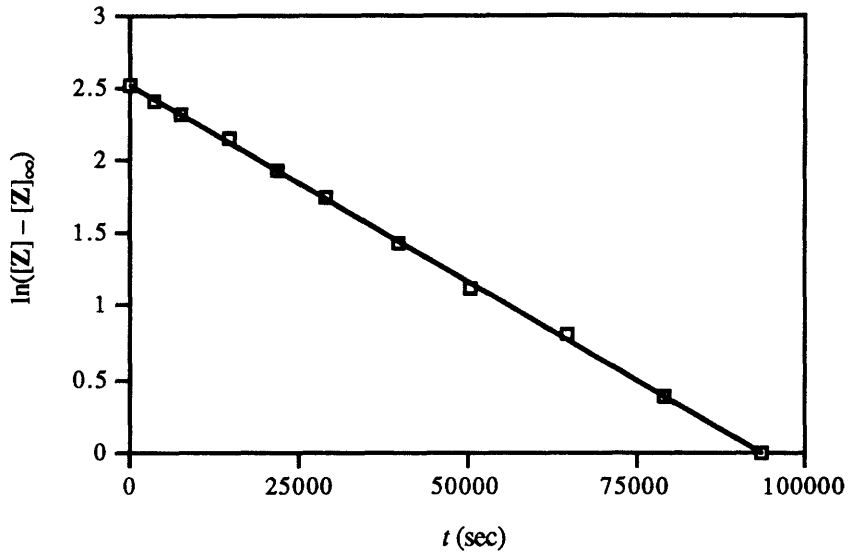

Figure A.8 First Order Plot for *Z*-**32** vs.*t* at 90.8 °C

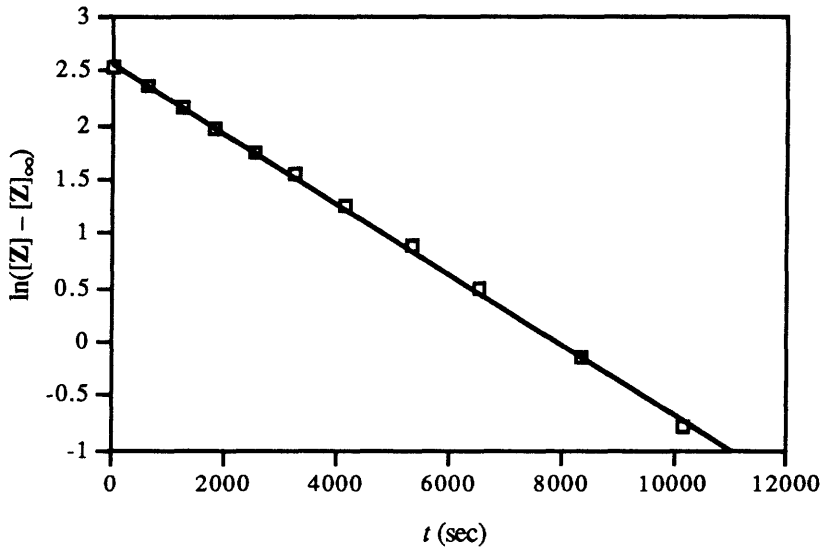

isomerization. In creating these latter two plots, data points at or near equilibrium have been omitted because errors in the values of the ordinate function become extremely high as $[\mathbf{Z}]/N$ approaches $[\mathbf{Z}]_\infty/N$, where $[\mathbf{Z}]_\infty$ represents the equilibrium concentration of the *Z*-disilene. The activation parameters and other values derived from the plots and further calculations are presented in Table A.7. The raw data from this kinetics experiment as well as other pertinent information are provided in the Experimental section.

Table A.7 Kinetics Results for Disilene **32**[a]

Temp./ K	*K*	Presumed $Z \rightarrow E$	Presumed $E \rightarrow Z$
342.1	1.26	$k_1 = (1.53 \pm 0.03) \cdot 10^{-5}$ s^{-1}	$k_{-1} = (1.21 \pm 0.02) \cdot 10^{-5}$ s^{-1}
		$\Delta G^{\ddagger} = 27.7 \pm 0.1$ kcal mol^{-1}	$\Delta G^{\ddagger} = 27.8 \pm 0.1$ kcal mol^{-1}
364.0	1.19	$k_1 = (1.67 \pm 0.04) \cdot 10^{-4}$ s^{-1}	$k_{-1} = (1.41 \pm 0.02) \cdot 10^{-4}$ s^{-1}
		$\Delta G^{\ddagger} = 27.7 \pm 0.1$ kcal mol^{-1}	$\Delta G^{\ddagger} = 27.9 \pm 0.1$ kcal mol^{-1}
		$\Delta H^{\ddagger} = 26.3 \pm 0.5$ kcal mol^{-1}	$\Delta H^{\ddagger} = 27.0 \pm 0.5$ kcal mol^{-1}
		$\Delta S^{\ddagger} = -4.0 \pm 2.0$ eu	$\Delta S^{\ddagger} = -2.4 \pm 2.0$ eu
		$\Delta H^{\circ} = -0.65$ kcal mol^{-1}	$\Delta G^{\circ}_{342.1} = -0.16$ kcal mol^{-1}
		$\Delta S^{\circ} = -1.4$ eu	$\Delta G^{\circ}_{364.0} = -0.13$ kcal mol^{-1}

[a]Errors in rate constants were obtained from the standard deviations of the slopes of the lines in Figures A.7 and A.8 and the calculated errors in *K*.

This set of data is in very good agreement with that reported for **29**. Indeed, the enthalpy and entropy values are within experimental error of each other for the two experiments. This is reasonable, as disilenes **29** and **32** only differ in the substitution of a 2,6-diisopropylphenyl- for a 2,6-diethylphenyl- group. The derived $\Delta S^{\ddagger}$ parameters are again small, negative numbers, which are slightly outside the range of the larger negative numbers obtained for disilene **20**.

Several of the kinetics experiments performed to date on dimetallenes are summarized in Table A.8. The mechanism of these isomerizations exclusively involves rotation about the M=M bond and not a thermal dissociation–recombination pathway: the

presence of 2,3-dimethyl-1,3-butadiene, an efficient metallylene trapping agent, did not affect the rates of isomerization or produce trapping products even after prolonged exposure at temperatures where the isomerization is completed within a few hours.[30]

Table A.8 Comparison of Activation Parameters for Dimetallene *E*–*Z* Pairs

Cpd.	M	Ligands	$\Delta H^{\ddagger}_{Z\rightarrow E}$[a]	$\Delta S^{\ddagger}_{Z\rightarrow E}$[b]	$\Delta H^{\ddagger}_{E\rightarrow Z}$[a]	$\Delta S^{\ddagger}_{E\rightarrow Z}$[b]	Ref.
20	Si	Mes, ^{t}Bu	23	–8 to –12	28	–13 to –17	24
20	Si	Mes, ^{t}Bu	31	+11			25
20			(33)[c]	(+19)[c]			
29	Si	Mes, Dep	26	–5	27	–2	new
32	Si	Mes, Dip	26	–4	27	–2	new
	Si	Mes, 1-Ad	28	+5	27	–4	31
			(27)[c]	(+3)[c]	(27)[c]	(–4)[c]	
	Si	Mes, $NTMS_2$	25	0			25
24	Ge	Mes, Dip	22	–5	20	–10	17

[a]In kcal/mol. [b]In eu. [c]Data from West recalculated according to the Eyring formula, using the rate constants measured at the highest and lowest temperatures.

For the first time, the activation parameters for an identically substituted disilene (**32**) and digermene (**24**) can be compared. Both dimetallenes exhibit first order isomerization kinetics. The enthalpy of activation for the Ge=Ge bond isomerization is somewhat (4–7 kcal/mol) lower than that of the disilene isomerization. Most recent calculations arrive at an estimate of about 25 kcal/mol for the double bonds of both parent disilene and digermene.[32] Considering the sizable ligands used in the present study, one concludes that theory and experiment are in reasonable agreement.

A.5 Experimental

General

All reactions were carried out in flame-dried glassware under an inert atmosphere of argon. Solvents and reagents were purified according to known procedures.[33] In particular, THF was double-distilled from sodium–benzophenone ketyl and/or LAH prior to use. DME was dried over anhydrous $MgSO_4$, then distilled from CaH_2 and again from dark blue ketyl immediately before use. Solvents used for disilene synthesis and kinetics were freshly vacuum transferred from potassium mirror at 10^{-4} mm Hg. The high-vacuum manipulations were carried out on a vacuum line equipped with an Edwards Series 63 Diffstak oil-diffusion pump, an Edwards E2M2 two-stage rotary vacuum forepump, and a Varian 843 vacuum ionization gauge. Vacuum transfers and degassings were performed on the high vacuum line employing cryogenic trap-to-trap techniques. Manipulations requiring an inert atmosphere were performed in a Vacuum Atmospheres Co. dry box with a nitrogen atmosphere and an HE-63-P Pedatrol unit . Oxygen content inside the dry box was rated at 5 ppm or less.

Purifications by standard flash chromatography employed E. Merck Kieselgel 60 (230–400 mesh). Thin layer chromatography was performed on E. Merck Kieselgel 60 F_{254} silica gel-coated plates of thickness 0.25 mm. Boiling points for compounds which were kugelrohr distilled refer to a maximum oven temperature.

^1H NMR spectra were recorded on either a Bruker WM250 (250 MHz), a Bruker AC250 (250 MHz), a Varian XL300 (300 MHz), a Varian Gemini (300 MHz), or a Varian VXR500 (500 MHz) spectrometer. Chemical shifts are reported in units of parts per million (ppm) from standard solvent peaks, usually benzene-d_6 (7.15 ppm), chloroform-*d* (7.24 ppm), or toluene-d_8 (2.09 ppm). Splitting patterns are designated as "s" for singlet, "d" for doublet, "t" for triplet, "q" for quartet, "sept" for septet, "dd" for doublet of doublets, "m" for multiplet, and "b" for broad. Positions in aryl groups are designated by the prefixes "*ortho*," "*meta*," and "*para*" relative to the position bearing the heteroatom.

Low resolution electron impact (EI) mass spectra were obtained on a Finnegan MAT System 8200 mass spectrometer operated by Ed Takach. Ultraviolet/visible spectra were recorded on a Hewlett-Packard 8450A Diode Array spectrophotometer in 1-mm path length quartz UV cells. Sonications were performed with a Bransonic 220 ultrasonic bath.

E–*Z* Isomerization Kinetics Determinations

The Isomerization Kinetics of the 1,2-Bis(2,6-diethylphenyl)-1,2-dimesityldisilenes *Z*- and *E*-**29**

In a dry box, 10 mg (0.018 mmol) of an isomeric mixture of disilenes *E*- and *Z*-**29**[17] (ca. 20:1 favoring the *E* isomer), was dissolved in toluene-d_8. 1 μL of hexamethyldisilane was added as an internal reference. This solution, of total volume 0.7 mL, was filtered through an oven-dried Kimwipe into a thin-walled 500 MHz NMR tube with a joint. This apparatus was then attached to a closed Teflon high-vacuum stopcock and removed from the dry box. The solution was degassed on the high-vacuum line *via* four freeze–evacuate–thaw cycles, flame-sealed at 10^{-4} torr, and stored at 0 °C until the start of the experiment.

The sample was warmed to room temperature, and a ^{1}H NMR spectrum was taken of it on a Varian VT500 500 MHz spectrometer. The optimum FID acquisition and processing parameters were found to be as follows: sweep width (SW) = 8000 Hz, acquisition time (AT) = 1.892 s, number of points (NP) = 30272, pulse width (PW) = 5.5 ms, pre- and post-acquisition delays (P1, D1, D2) = 0 s, transmitter offset (TOF) = 0 Hz, number of pulses (NT) = 64, double precision (DP) selected, line broadening (LB) = –0.6, Fourier number (FN) = 65536. The optimum spectrum display was obtained by (1) phasing the spectrum between 0 and 8 ppm, (2) applying drift correction (DC), which makes the baseline parallel to the horizontal axis, (3) closing the observation window to include only the peaks of interest for integration, and (4) fine tuning the phasing and

balancing the integrals for that window. The mesityl-*meta*-hydrogen region (6.50–6.80 ppm) was chosen for monitoring the isomerization. This region included only the desired signals, had wide areas of flat baseline on each side of the window, and gave sufficient resolution of the two peaks to be integrated (after the resolution enhancement described above). The 0.3 ppm regions of interest were plotted out across 20 cm, and the integrals above the expanded peaks were carefully measured. This procedure was followed for every data point.

After the initial data acquisition was stored on tape, the sample was immersed completely into an ethylene glycol constant temperature bath at the appropriate temperature, 63.9 °C for the low-temperature run and 86.5 °C for the high-temperature run. As the sample was immersed, a stopwatch was simultaneously started to record the time interval. The isomerizations were halted by removal of the sample from the bath and immediate immersion into an ice–water bath as the stopwatch was stopped. The cooled sample was then equilibrated to room temperature and subjected to NMR analysis as before. At the beginning of each run, spectra were taken at a rate of approximately five per half-time, with this frequency decelerated as the samples approached equilibrium. The half-times were determined to be about 40 min for the high-temperature run and about 8 h for the low-temperature run. Spectra were taken over a period of 3–4 half-times.

After the conclusion of each data collection, the samples were left in their constant temperature baths for a total of about ten half-times to achieve equilibrium. At this point, they were subjected to at least three separate NMR analyses, and the values thus obtained for each run were averaged to give the experimental equilibrium concentrations. The initial and equilibrium spectra were compared and found to have demonstrated no changes other than the isomerization of the disilenes. The ratio of disilenes to hexamethyldisilane (reference compound), monitored during each NMR analysis, remained constant within experimental error.

The concentrations of the isomers were calculated by dividing the integral over one peak by the sum of the entire area of interest for a given spectrum. These percentages were multiplied by the total actual concentration of disilenes in the sample, giving the

Table A.9 Experimental Data from the 63.9 °C Kinetics Determination for the Isomerization of *Z*- and *E*-**29**

Point	*t*/ s	[E]/ mM	[Z]/ mM	ln ([E] – $[E]_\infty$)[a]
1	0	24.78	1.22	2.316
2	3603	23.86	2.14	2.221
3	7200	23.09	2.91	2.134
4	14401	21.54	4.46	1.932
5	21601	20.36	5.64	1.744
6	28796	19.60	6.40	1.601
7	39600	18.53	7.47	1.358
8	50400	17.67	8.33	1.109
9	64800	16.43	9.57	0.582
10	79200	16.00	10.00	0.307
11	100800	15.65	10.35	0.010
12	144000	14.92	11.08	–1.273
13	187200	14.73	11.27	–2.408
14	265500	14.62	11.38	*b*
15	287100	14.83	11.17	*b*
16	303296	14.37	11.63	*b*

[a]*K*= 1.289 (as defined in Eq. 4). $[E]_\infty$= 14.64 mM; $[E]_0$= 24.78 mM. [b]Late points were omitted from use in Eq. 5 due to the high errors associated with these points.

concentrations of *E*- and *Z*-**29**. These data are presented in Tables A.9 and A.10. The plots of these concentrations versus time are given in Figures A.1 and A.2 in the text. The data were plotted according to equation 5, and gave plots that were apparently linear (see

Table A.10 Experimental Data from the 86.5 °C Kinetics Determination for the Isomerization of *Z*- and *E*-**29**

Point	*t*/ s	[E]/ mM	[Z]/ mM	ln ([E] – $[E]_\infty$)[a]
1	0	27.31	1.68	2.460
2	610	25.27	3.74	2.268
3	1200	23.85	5.16	2.109
4	1800	22.40	6.61	1.915
5	2520	21.14	7.86	1.710
6	3300	19.93	9.08	1.463
7	4290	18.96	10.03	1.209
8	5400	17.95	11.05	0.850
9	6600	17.34	11.66	0.548
10	8400	16.70	12.30	0.086
11	10200	16.44	12.56	–0.186
12	12900	16.12	12.88	–0.673
13	16502	16.04	12.96	–0.844
14	20102	15.75	13.25	–1.967
15	21902	15.66	13.34	*b*
16	23732	15.57	13.43	*b*
17	25532	15.57	13.43	*b*

[a]*K*= 1.165 (as defined in Eq. 4). $[E]_\infty$= 15.61 mM; $[E]_0$= 27.31 mM. (b) Late points were omitted from use in Eq. 5 due to the high errors associated with these points.

Figures A.3 and A.4 in the text). The first eight data points provided the best straight line and were used to calculate the activation parameters. The rate constants and activation parameters were calculated as shown in the text.

The Isomerization Kinetics of the 1,2-Bis(2,6-diisopropylphenyl)-1,2-dimesityldisilenes *Z*- and *E*-**32**

This experiment followed the previous one very closely. In a dry box, 10 mg (0.016 mmol) of an isomeric mixture of disilenes *Z*- and *E*-**32** (ca. 60:1 presumably favoring the *Z* isomer) was dissolved in toluene-d_8. 1 μL of hexamethyldisilane was added as an internal reference. This solution, of total volume 0.7 mL, was filtered through oven-dried glass wool into a thin-walled 500 MHz NMR tube with a joint. This apparatus was then attached to a closed Teflon high-vacuum stopcock and removed from the dry box. The solution was degassed on the high-vacuum line via several freeze–evacuate–thaw cycles, flame-sealed at 10^{-4} torr, and stored at 0 °C until the start of the experiment.

The sample was warmed to room temperature, and a ^{1}H NMR spectrum was taken on a Varian VT500 500 MHz spectrometer. The optimum FID acquisition and processing parameters were found to be as follows: sweep width (SW) = 8000 Hz, acquisition time (AT) = 1.892 s, number of points (NP) = 30272, pulse width (PW) = 5.5 ms, pre- and post-acquisition delays (P1, D1, D2) = 0 s, transmitter offset (TOF) = 0 Hz, number of pulses (NT) = 64, double precision (DP) selected, line broadening (LB) = –0.7, Fourier number (FN) = 65536, and Gaussian function (GF) = 0.568. The optimum spectrum display was obtained by (1) phasing the spectrum between 0 and 8 ppm, (2) applying drift correction (DC), which makes the baseline parallel to the horizontal axis, (3) closing the observation window to include only the peaks of interest for integration, and (4) fine tuning the phasing and balancing the integrals for that window. The mesityl-*para*-methyl region (1.99–2.06 ppm) was chosen for monitoring the isomerization. This region included only the desired signals, had wide areas of flat baseline on each side of the window, and gave sufficient resolution of the two peaks to be integrated (after the resolution enhancement described above). The regions of interest were plotted out across 20 cm, and the integrals above the expanded peaks were carefully measured. This procedure was followed for every data point from both experiments.

The procedure for heating, cooling, and measuring spectra was identical to that for disilene **29**. The experimental temperatures were 68.9 °C and 90.8 °C, giving equilibrium half times of about 6.5 h and 40 min, respectively. A comparison of the initial and

Table A.11 Experimental Data from the 68.9 °C Kinetics Determination for the Isomerization of *Z*- and *E*-**32**

Point	*t*/ s	[Z]/ mM	[E]/ mM	ln ([Z] – $[Z]_\infty$)[a]
1	0	22.59	0.508	2.52
2	3601	21.32	1.78	2.41
3	7199	20.35	2.75	2.32
4	14400	18.67	4.44	2.14
5	21599	17.07	6.03	1.93
6	28800	15.89	7.21	1.74
7	39600	14.37	8.73	1.43
8	50400	13.26	9.84	1.12
9	64800	12.43	10.67	0.801
10	79200	11.67	11.43	0.382
11	93600	11.20	11.90	0.003
12	115200	10.72	12.38	–0.657
13	144600	10.49	12.61	–1.25
14	248400	10.21	12.89	*b*
15	261000	10.19	12.91	*b*
16	273600	10.21	12.89	*b*

[a]*K*= 1.26 (as defined in Eq. 4). $[Z]_\infty$= 10.2 mM; $[Z]_0$= 22.6 mM. [b]Late points were omitted from use in Eq. 5 due to the high errors associated with these points.

equilibrium spectra demonstrated no apparent changes other than disilene isomerization. There were no detectable new compounds in the samples, and the ratio of disilenes to hexamethyldisilane (reference compound), monitored during each NMR analysis, remained

constant within experimental error. It was therefore assumed that the direct isomerization between *E*- and *Z*-**32** was the only transformation occurring.

The concentrations of *E*- and *Z*-**32** over the course of the experiments are presented in Tables A.11 and A.12. The relevant plots and data are given in the text. Only the first eight data points were used to calculate the activation parameters, as these provided the best straight line.

Table A.12 Experimental Data from the 90.8° C Kinetics Determination for the Isomerization of *Z*- and *E*-**32**

Point	*t*/ s	[Z]/ mM	[E]/ mM	ln ([Z] – $[Z]_\infty$)[a]
1	0	23.37	0.33	2.53
2	600	21.26	2.44	2.35
3	1200	19.43	4.27	2.16
4	1800	17.97	5.74	1.97
5	2520	16.54	7.16	1.75
6	3240	15.45	8.25	1.54
7	4140	14.29	9.41	1.25
8	5340	13.23	10.48	0.89
9	6540	12.44	11.26	0.50
10	8340	11.66	12.04	–0.15
11	10140	11.26	12.44	–0.78
12	12840	10.95	12.75	*b*
13	16440	10.81	12.89	*b*
14	24240	10.86	12.85	*b*
15	25440	10.81	12.89	*b*
16	26640	10.74	12.96	*b*

[a]K= 1.19 (as defined in Eq. 4). $[Z]_\infty$= 10.8 mM; $[Z]_0$= 23.4 mM. [b]Late points were omitted from use in Eq. 5 due to the high errors associated with these points.

Synthesis of a New Disilene

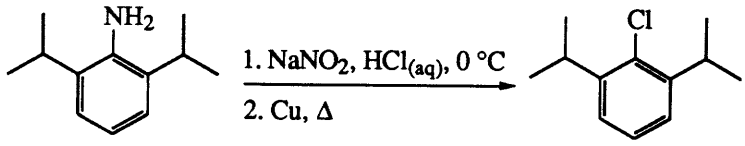

A 2-L three-neck round-bottom flask equipped with a thermometer, mechanical stirrer, and addition funnel was charged with concentrated hydrochloric acid (352 mL), and cooled to 0 °C with an ice bath. 2,6-Diisopropylaniline (146 g, 0.824 mol, 1 equiv) was slowly added with efficient stirring. The reaction mixture was cooled to –10 °C with an ice/NaCl bath, and a solution of $NaNO_2$ (70 g, 1.0 mol, 1.2 equiv) in water (120 mL) was added through the addition funnel over 2 hr. The temperature of the reaction mixture must be maintained near –10 °C for efficient absorption of the orange-brown gas produced. Copper powder (5.25 g, 82.6 mmol, 0.1 equiv) was then added in small amounts, and the reaction mixture was allowed to warm up to room temperature. The addition funnel was replaced with a reflux condenser, and the solution was brought to reflux for 2 hr.

After cooling, the black homogeneous reaction mixture was extracted into hexane. The organic layers were washed with 1 M HCl, 1 M NaOH, and saturated NaCl solution, then dried ($MgSO_4$) and evaporated under vacuum, leaving a rust-colored oil. This was purified by column chromatography on silica gel (1000 g) using hexane and short path distillation to give the title compound as a colorless oil (65 g, 0.33 mol, 40%): bp 70 °C, 0.025 mm Hg; ^1H NMR (250 MHz, C_6D_6) δ 1.11 (d, 12H, $CH(C\underline{H}_3)_2$, J= 7.7 Hz), 3.55 (sept, 2H, $C\underline{H}(CH_3)_2$, J= 7.7 Hz), 6.95–7.07 (m, 3H, Ar$\underline{H}$).

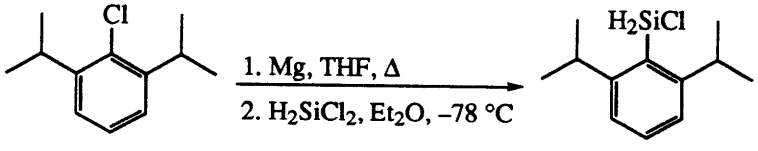

To a solution of condensed dichlorosilane (ca. 14.4 g, 143 mmol, 5.5 equiv) in ether (40 mL) at –78 °C in a 250-mL three-neck round-bottom flask was added a filtered

solution of 2,6-diisopropylphenylmagnesium chloride (25.7 mmol, 1 equiv) in THF (35 mL) at –78° C, prepared from the reaction of 2,6-diisopropylchlorobenzene in refluxing THF with magnesium (caution: dichlorosilane is a pyrophoric, corrosive gas). The resulting mixture was stirred at –78 °C for two hours, warmed to room temperature, and stirred overnight.

The reaction mixture was cannulated into a 1-L one-neck round-bottom flask and diluted with dry pentane (400 mL). The precipitated magnesium salts were removed by filtration through a layer of Celite under inert atmosphere, employing either standard Schlenk glassware or a nitrogen-filled glove bag. The solvents were then removed by distillation (with methanol and aqueous sodium hydroxide traps attached to the distillation apparatus to neutralize excess dichlorosilane vapors) leaving a yellow oil, which was kugelrohr-distilled to provide the title compound as a colorless oil (4.37 g, 19.3 mmol, 75%): bp 80–90 °C/ 0.005 mm Hg; ^{1}H NMR (250 MHz, C_6D_6) δ 1.12 (d, $CH(C\underline{H}_3)_2$, 12H, J= 6.6 Hz), 3.37 (sept, $C\underline{H}(CH_3)_2$, 2H, J= 6.6 Hz), 5.42 (s, Si$\underline{H}$, 2H), 6.99–7.25 (m, Ar$\underline{H}$, 3H).

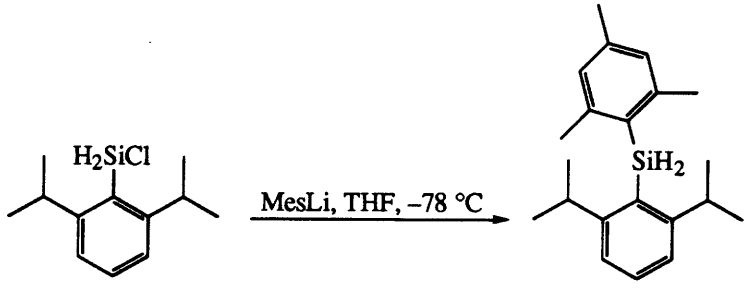

To a solution of (2,6-diisopropylphenyl)chlorosilane (1.56 g, 6.89 mmol, 1 equiv) of in THF (3 mL) and pentane (5 mL) at –78 °C was added a solution of mesityllithium (7.83 mmol, 1.1 equiv) in THF (10 mL) at 0 °C via cannula over 10 min. [The mesityllithium was prepared by adding a 1.65 M solution of *t*-butyllithium in pentane (9.3 mL, 15 mmol) dropwise to 2-bromomesitylene (1.56 g, 7.83 mmol) in THF (10 mL) at –78 °C, and stirring for 2 h]. The reaction mixture was allowed to warm up to room

temperature and was stirred overnight. After extraction into pentane and washing with water, the organic layers were dried ($MgSO_4$) and evaporated to a colorless oil. The product was purified by flash chromatography on silica gel (175 g), eluting with hexane, providing a white solid after evaporation. This was kugelrohr distilled to give the pure silane as a white solid (1.86 g, 5.99 mmol, 87%): mp 47–48° C; bp 120–140 °C, 0.45 mm Hg; ^{1}H NMR (250 MHz, C_6D_6) δ 1.13 (d, $CH(C\underline{H}_3)_2$, 12 H, J= 6.6 Hz), 2.07 (s, Mes-*para*-$C\underline{H}_3$, 3H), 2.37 (s, Mes-*ortho*-$C\underline{H}_3$, 6H), 3.49 (sept, $C\underline{H}(CH_3)_2$, 2H, J= 6.9 Hz), 5.40 (s, $Si\underline{H}$, 2H), 6.71 (s, Mes-*meta*-$Ar\underline{H}$, 2H), 7.10 (d, Dip-*meta*-$Ar\underline{H}$, 2H, J= 7.5 Hz), 7.28 (t, Dip-*para*-$Ar\underline{H}$, 1H, J= 7.5 Hz); MS [EI] (relative intensity) *m/z* 310.2 (17, M^+), 190 (60), 175 (76), 147 (100).

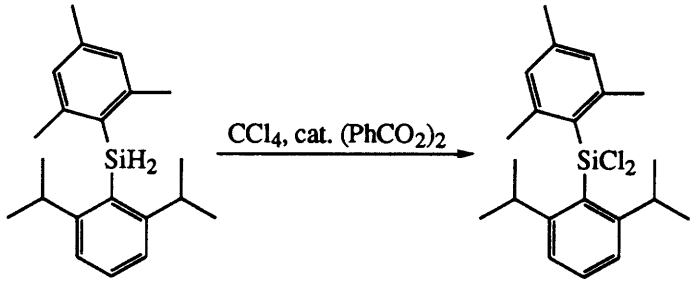

The diarylsilane (1.86 g, 5.99 mmol, 1 equiv), CCl_4 (50 mL), and benzoyl peroxide (0.19 g, 0.78 mmol, 0.1 equiv) were combined in a 100–mL one-neck round-bottom flask with a reflux condenser. The solution was brought to reflux for 24 h (at which point the reaction was complete by GC analysis) then cooled and evaporated to give a light yellow oil. Kugelrohr distillation at low temperature removed a low-boiling side product and then afforded the dichlorosilane (2.10 g, 5.53 mmol, 92%) as a colorless oil which crystallized to a white solid: mp 78–84 ° C; bp 105–115° C/ 0.005 mm Hg; ^{1}H NMR (250 MHz, C_6D_6) δ 1.08 (d, $CH(C\underline{H}_3)_2$, 12H, J= 6.6 Hz), 1.97 (s, Mes-*para*-$C\underline{H}_3$, 3H), 2.43 (s, Mes-*ortho*-$C\underline{H}_3$, 6H), 3.90 (sept, $C\underline{H}(CH_3)_2$, 2H, J= 6.6 Hz), 6.58 (s, Mes-*meta*-$Ar\underline{H}$, 2H), 7.04 (d, Dip-*meta*-$Ar\underline{H}$, 2H, J= 7.8 Hz), 7.20 (t, Dip-*para*-$Ar\underline{H}$, 1H, J= 8.1 Hz); MS [EI] (relative intensity) *m/z* 378 (M^+, 4), 245 (28), 243 (41), 120 (100).

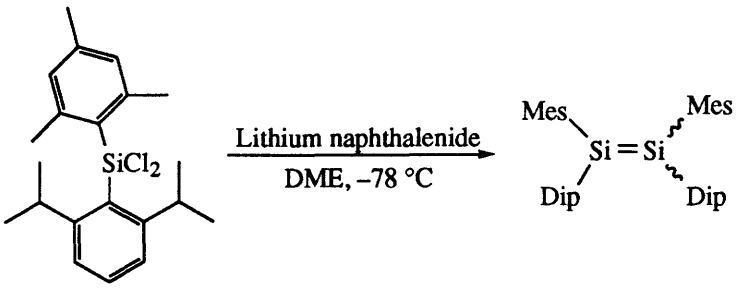

A mixture of of lithium powder (46.0 mg, 6.63 mmol, 2.3 equiv) containing 0.5% sodium, freshly sublimed naphthalene (90 mg, 7.0 mmol, 2.4 equiv), and dry, degassed 1,2-dimethoxyethane (DME, 6 mL) was stirred at room temperature under argon for 1.5 h to give a homogeneous, dark green solution of lithium naphthalenide. This was cooled to –78 °C, and a solution of the diaryldichlorosilane (1.09 g, 2.88 mmol, 1 equiv) in DME (10 mL), also at –78 °C, was added via cannula over 5 min. The reaction mixture was stirred at –78 °C for 1 h, warmed to room temperature, and stirred an additional 2.5 h. The dark brown solution was concentrated by removal of the solvent in vacuo, followed by sublimation of the naphthalene (60 °C/ 0.005 mm Hg). In a dry box, the resulting orange oil was suspended in toluene (5 mL) and filtered through a layer of Celite to remove lithium salts. After removal of solvent in vacuo, the residual orange oil slowly crystallized. The bright yellow-orange crystals were washed with methylcyclohexane and collected, affording the disilene (170 mg, 0.280 mmol, 19%), as a ca. 60:1 mixture of isomers.[34] The major isomer was tentatively assigned as the *Z*-isomer (see text): mp 185.5–186.5 °C; ^{1}H NMR (500 MHz, toluene-d_8) *Z* -isomer (presumed): δ 0.60 (br s, CH(C$\underline{H}_3$)$_2$, 12H), 1.31 (br s, CH(C$\underline{H}_3$)$_2$, 12H), 2.03 (s, Mes-*para*-C$\underline{H}_3$, 6H), 2.44 (br s, Mes-*ortho*-C$\underline{H}_3$, 6H), 2.54 (br s, Mes-*ortho*-C$\underline{H}_3$, 6H), 3.76 (br s, C$\underline{H}$(CH$_3$)$_2$, 2H), 4.55 (br s, C$\underline{H}$(CH$_3$)$_2$, 2H), 6.64 (s, Mes-*meta*-H, 4H), 6.95–7.04 (m, Dip-*meta*-Ar$\underline{H}$, 4H), 7.18 (t, Dip-*para*-Ar$\underline{H}$, 2H, J = 8.0 Hz); *E*-isomer (presumed): ^{1}H NMR (500 MHz, toluene-d_8) δ 0.60 (d, CH(C$\underline{H}_3$)$_2$, 6H, J= 6.5 Hz), 0.65 (d, CH(C$\underline{H}_3$)$_2$, 6 H, J= 6.5 Hz), 1.33 (d, CH(C$\underline{H}_3$)$_2$, 6H, J= 6.5 Hz), 1.40 (d, CH(C$\underline{H}_3$)$_2$, 6H, J= 6.5 Hz), 2.01 (s, Mes-*para*-

$C\underline{H}_3$, 6H), 2.42 (s, Mes-*ortho*-$C\underline{H}_3$, 6H), 2.51 (s, Mes-*ortho*-$C\underline{H}_3$, 6H), 3.80 (sept, $C\underline{H}(CH_3)_2$, 2H, J= 6.5 Hz), 4.52 (sept, $C\underline{H}(CH_3)_2$, 2H, J= 6.5 Hz), 6.65 (s, Mes-*meta*-H, 2H), 6.67 (s, Mes-*meta*-H, 2H), 6.94–7.07 (m, Dip-*meta*-Ar$\underline{H}$, 4H), 7.18 (t, Dip-*para*-Ar$\underline{H}$, 2H, J= 7.5 Hz); UV [isolated mixture] (methylcyclohexane) λ (log ε) 430 (4.3), 336 (4.0), 280 (4.2); MS [EI] (relative intensity) *m/z* 616 (M^+, 43), 307 (100), 188 (30).

A.6 References

(1) For a recent, comprehensive review of Group 14 chemistry, see: Tsumuraya, T.; Batcheller, S. A.; Masamune, S. *Angew. Chem. Int. Ed. Engl.* **1991**, *30*, 902.

(2) For a review of multiple bonding in the heavier Group 14 and 15 elements, see: Norman, N. C. *Polyhedron* **1993**, *12*, 2431.

(3) For a review on disilenes, see: West, R. *Angew. Chem. Int. Ed. Engl.* **1987**, *26*, 1201.

(4) Kipping, F. S. *Proc. Chem. Soc. London* **1911**, *27*, 143.

(5) (a) Kipping, F. S.; Sands, J. E. *J. Chem. Soc. Trans.* **1921**, *119*, 830. (b) Kipping, F. S.; Sands, J. E. *J. Chem. Soc. Trans.* **1921**, *119*, 848. (c) Kipping, F. S. *J. Chem. Soc.* **1927**, 2719. (d) Gilman, H.; Schwebke, G. L. *J. Am. Chem. Soc.* **1964**, *86*, 2693.

(6) Dasent, W. E. *Nonexistent Compounds*; Marcel Dekker: New York, 1965.

(7) (a) Peddle, G. J. D.; Roark, D. N.; Good, A. M.; McGeachin, S. G. *J. Am. Chem. Soc.* **1969**, *91*, 2807. (b) Roark, D. N.; Peddle, G. J. D. *J. Am. Chem. Soc.* **1972**, *94*, 5837.

(8) (a) Nakadaira, Y.; Kobayashi, T.; Otsuka, T.; Sakurai, H. *J. Am. Chem. Soc.* **1979**, *101*, 486. (b) Sakurai, H.; Nakadaira, Y.; Kobayashi, T. *J. Am. Chem. Soc.* **1979**, *101*, 487.

(9) West, R.; Fink, M. J.; Michl, J. *Science* **1981**, *214*, 1343.

(10) Masamune, S.; Hanzawa, Y.; Murakami, S.; Bally, T.; Blount, J. F. *J. Am. Chem. Soc.* **1982**, *104*, 1150.

(11) (a) Goldberg, D. E.; Harris, D. H.; Lappert, M. F.; Thomas, K. M. *J. Chem. Soc. Chem. Commun.* **1976**, 261. (b) Davidson, P. J.; Harris, D. H.; Lappert, M. F. *J. Chem. Soc. Dalton Trans.* **1976**, 2268. (c) Davidson, P. J.; Lappert, M. F. *J. Chem. Soc. Chem. Commun.* **1973**, 317.

(12) Masamune, S.; Hanzawa, Y.; Williams, D. J. *J. Am. Chem. Soc.* **1982**, *104*, 6136.

(13) (a) Snow, J. T.; Murakami, S.; Masamune, S.; Williams, D. J. *Tetrahedron Lett.* **1984**, *25*, 4191. (b) Masamune, S.; Murakami, S.; Snow, J. T.; Tobita, H.; Williams, D. J. *Organometallics* **1984**, *3*, 333.

(14) Masamune, S.; Sita, L. R. *J. Am. Chem. Soc.* **1985**, *107*, 6390.

(15) Watanabe, H.; Takeuchi, K.; Fukawa, N.; Kato, M.; Goto, M.; Nagai, Y. *Chem. Lett.* **1987**, 1341.

(16) Park, J.; Batcheller, S. A.; Masamune, S. *J. Organomet. Chem.* **1989**, *367*, 39.

(17) Batcheller, S. A., Ph.D. Thesis, Massachusetts Institute of Technology, Feb. 1990.

(18) Masamune, S.; Eriyama, Y.; Kawase, T. *Angew. Chem. Int. Ed. Engl.* **1987**, *26*, 6.

(19) (a) Beesley, R. M.; Ingold, C. K.; Thorpe, J. F. *J. Chem. Soc.* **1915**, *107*, 1080. (b) Ingold, C. K. *J. Chem. Soc.* **1921**, *119*, 305. (c) Kirby, A. *J. Adv. Phys. Org. Chem.* **1980**, *17*, 183.

(20) (a) Trinquier, G.; Malrieu, J.-P. *J. Am. Chem. Soc.* **1987**, *109*, 5303. (b) Malrieu, J.-P.; Trinquier, G. *J. Am. Chem. Soc.* **1989**, *111*, 5916. (c) Trinquier, G. *J. Am. Chem. Soc.* **1990**, *112*, 2130.

(21) Goldberg, D. E.; Hitchcock, P. B.; Lappert, M. F.; Thomas, K. M.; Thorne, A. J.; Fjeldberg, T.; Haaland, A.; Schilling, B. E. R. *J. Chem. Soc. Dalton Trans.* **1986**, 2387.

(22) Liang, C.; Allen, L. C. *J. Am. Chem. Soc.* **1990**, *112*, 1039.

(23) (a) Pham, E. K.; West, R. *Organometallics* **1990**, *9*, 1517. (b) Pham, E. K.; West, R. *J. Am. Chem. Soc.* **1989**, *111*, 7667. (c) Berry, D. H.; Chey, J. H.; Zipin, H. S.; Carroll, P. J. *J. Am. Chem. Soc.* **1990**, *112*, 452.

(24) Murakami, S.; Collins, S.; Masamune, S. *Tetrahedron Lett.* **1984**, *25*, 2131.

(25) Michalczyk, M. J.; West, R.; Michl, J. *Organometallics* **1985**, *4*, 826.

(26) In the previous experiment, the mesityl-*para*-methyl region (2.00–2.15 ppm) was monitored.

(27) The kinetics discussion is adapted from reference 17.

(28) (a) Peterson, R. C.; Markgraf, J. H.; Ross, S. D. *J. Am. Chem. Soc.* **1961**, *83*, 3819. (b) Wiberg, K. B. *Physical Organic Chemistry*; Wiley: New York, 1964; pp 374–379.

(29) In a separate determination, we found that the isomer distribution in a disilene sample that had been heated for 54 min *continuously* was within experimental error of a sample that had been immersed and withdrawn from the heating bath five times over the course of 54 min.

In a repeat high-temperature (86.5 °C) kinetics experiment on disilene **29**, the rate constants (k_1 = 1.67·10^{-4}, k_{-1} = 1.37·10^{-4} s^{-1}) were within experimental error of those reported in Table A.5.

(30) Batcheller, S. A.; Tempkin, O.; Tsumuraya, T.; Davis, W. M.; Masamune, S. *J. Am. Chem. Soc.* **1990**, *112*, 9394 and Supplementary Material.

(31) Shepherd, B. D.; Powell, D. R.; West, R. *Organometallics* **1989**, *8*, 2664.

(32) Grev, R. S.; Schaefer, H. F. III.; Baines, K. M. *J. Am. Chem. Soc.* **1990**, *112*, 9458.

(33) Perrin, D. D.; Armarego, W. L. F. *Purification of Laboratory Chemicals*, 3rd Ed.; Pergamon: Oxford, 1988.

(34) The conditions for this step were optimized by Dr. T. Tsumuraya.

(35) Shepherd, B. D.; Campana, C. F.; West, R. *Heteroat. Chem.* **1990**, *1*, 1.

(36) Fink, M. J.; Michalczyk, M. J.; Haller, R. J.; West, R. *Organometallics* **1984**, *3*, 793.

Publications

Some of the work in this thesis has appeared in the following publications:

1. Parmee, E. R.; Hong, Y.; Tempkin, O.; Masamune, S., "The Catalytic Asymmetric Aldol Reaction of Aldehydes with Unsubstituted and Monosubstituted Silyl Ketene Acetals: Formation of *Anti*-β-Hydroxy-α-Methyl Esters", *Tetrahedron Lett.* **1992**, *33*, 1729.

2. Parmee, E. R.; Tempkin, O.; Masamune, S.; Abiko, A., "New Catalysts for the Asymmetric Aldol Reaction: Chiral Boranes Prepared from α,α-Disubstituted Glycine Arenesulfonamides", *J. Am. Chem. Soc.* **1991**, *113*, 9365.

3. Batcheller, S. A.; Tsumuraya, T.; Tempkin, O.; Davis, W. M.; Masamune, S., "(Z)-1,2-Bis(2,6-diisopropylphenyl)-1,2-dimesityldigermene: Synthesis, Crystal Structure, and π-Bond Energy", *J. Am. Chem. Soc.* **1990**, *112*, 9394.

Biographical Note

Orin Tempkin was born on July 4, 1967, in Brooklyn, NY and raised in Brooklyn and Queens. After graduation from Benjamin N. Cardozo High School in 1984, he enrolled at Columbia College where he majored in chemistry, served as a teaching assistant, and carried out undergraduate research in the laboratories of Professor Thomas J. Katz. During the summer of 1987 he was a laboratory technician at American Cyanamid (now Cytec) in Stamford, CT. He received the BA in Chemistry from Columbia in May 1988 and the following fall entered the graduate program at the Massachusetts Institute of Technology. Shortly after, he joined the research group of Professor Satoru Masamune where he developed new reagents for catalytic asymmetric synthesis and studied the behavior of Group 14 dimetallenes. Orin Tempkin is the recipient of a graduate fellowship from the Merck Manufacturing Division and will begin a one year postdoctoral appointment at Merck in early 1994. He is also a theater enthusiast, and has performed major roles in four plays with the Shakespeare Ensemble at MIT.